System Identification of Offshore Platforms

Jensen, Jakob Laigaard

Publication date:
1990

Document Version
Early version, also known as pre-print

INSTITUTTET FOR BYGNINGSTEKNIK
DEPT. OF BUILDING TECHNOLOGY AND STRUCTURAL ENGINEERING
AALBORG UNIVERSITETSCENTER • AUC • AALBORG • DANMARK

FRACTURE & DYNAMICS
PAPER NO. 22

Ph.D.-Thesis defended publicly at the University of Aalborg, February 26, 1990

JAKOB LAIGAARD JENSEN
SYSTEM IDENTIFICATION OF OFFSHORE PLATFORMS
APRIL 1990 ISSN 0902-7513 R9011

The FRACTURE AND DYNAMICS papers are issued for early dissemination of research results from the Structural Fracture and Dynamics Group at the Department of Building Technology and Structural Engineering, University of Aalborg. These papers are generally submitted to scientific meetings, conferences or journals and should therefore not be widely distributed. Whenever possible reference should be given to the final publications (proceedings, journals, etc.) and not to the Fracture and Dynamics papers.

PREFACE

The present thesis *System Identification of Offshore Platforms* has been prepared as a part of my Ph.D. study during the period from March 1987 to January 1990 at the Department of Building Technology and Structural Engineering, University of Aalborg, Denmark.

My supervisors have been Associate Professor, Ph.D. Lars Pilegaard Hansen and Senior Lecturer Ph.D. Rune Brincker, both the Department of Building Technology and Structural Engineering, University of Aalborg. Their support and guidance during the years are greatly appreciated.

The proofreading has been performed by senior secretary Mrs. Kirsten Aakjær and the figures has been carried out by draughtsman Mr. Poul Skørbæk Sørensen. Their careful work is greatly appreciated.

Thanks are also given to the staff in the labortory, led by engineer assistant Mr. Henning Andersen, for the experimental work performed in connection with my Ph.D. study.

Finally, the Danish tax-payers' support through the Danish Technical Research Council is greatfully acknowledged.

Aalborg, April 1990 Jakob Laigaard Jensen

LIST OF CONTENTS

1. INTRODUCTION

The subject of this thesis is to investigate system identification methods for determination of the dynamic characteristics of offshore platforms. This includes estimation of eigenfrequencies, damping ratios, mode shapes and, furthermore, a general assessment of the structural performance.

The thesis has been made in relation to an offshore test program, "Integrated Experimental/Numerical Analysis of Dynamic Properties of Offshore Structures", which has been performed at the Department of Building Technology and Structural Engineering of the University of Aalborg since 1987. The main purpose of this thesis has been to provide a basic knowledge of system identification of structures which has been needed in the offshore test program mentioned. This has been accomplished by a survey of literature and by developing and testing different approaches on simulated as well as experimental data.

1.1 Background and Motives

System identification is a discipline with a very wide range of application. The tradition of applying of system identification is not very common in civil engineering, whereas in areas such as electrical engineering, geophysics and aircraft and spacecraft industry there is a long tradition in the field. The concept of system identification in civil engineering is especially related to experiences from the aircraft and spacecraft industry where the development of system identification of vibrating structures was initiated after the Second World War, see e.g. the classical paper by Kennedy and Pancu [1]. During the sixties and seventies there was an increasing interest of measuring the dynamic performance of tall buildings. After the price shock of the oil prices in 1973 the industrial countries began to exploit their own oil resources which led to offshore structures at increasing water depths. At an early stage it became clear that the dynamic performance of offshore structures could not be ignored in the design phase. This led to an interest of system identification of offshore structures which accelerated in the middle of the seventies and lasted up to the date of this thesis.

The interest of system identification of offshore structures can be divided into two subjects:

- An interest for improving the knowledge of the dynamic performance with the purpose of reducing the prizes on offshore platforms.

- An interest of monitoring the structural integrity by evaluation of the dynamic performance and thus reducing the inspection costs.

Besides those motives, which are related to cost-benefit analysis within the private sphere there are also some authority requirements with respect to a minimum instrumentation of offshore structures. This is e.g. the case in Norway where the Norwegian Petroleum Directorate in 1978 issued at set of regulations with regard to minimum instrumentation, see Holand et al. [2]. The purpose was twofold:

- Platform data and environmental data in the vicinity of the platforms must be collected in order to assess the safety of the load-carrying structure of the platforms and their foundation. This is done by checking the design assumptions and by a semi-continuous registration of the behaviour of the platforms.
- Environmental data must be collected for a systematic statistical mapping of the physical environment.

Thus, in the case of Norway, the public authority gives some minimum requirements with respect to collecting knowledge of the structural performance and structural integrity monitoring. While there are specific requirements for instrumentation in Norway there are only general regulations with respect to structural inspection in the United Kingdom, USA and Denmark (accordingly to the author's knowledge).

1.2 Reader's Guide

In the subsequent part of the present chapter it is argued that system identification of offshore platforms is an important subject within structural engineering of offshore platforms.

A thesis on system identification involves theoretical as well as practical considerations. Since it has not been possible to obtain real records of the response of offshore platforms, the practical experience referred to in this thesis is related to references and an experiment which in this thesis is referred to as **the experimental case**. The experimental set-up of this experiment is described at the end of this chapter.

With respect to the practical offshore experience a review of the practical experience obtained from references is given in chapter 2. The review concerns the performed measurings and identification results of offshore platforms during the seventies and the eighties.

After the introduction given in chapter 1 and 2, in chapter 3 a theoretical introduction to the principles of system identification is given in general, emphasizing the importance of structural modelling and experimental considerations. The latter subjects are concretized in chapter 4 and 5, respectively.

After giving the base of system identification in chapters 3 to 5, three groups of methods for system identification are considered in chapters 6,7 and 8, respectively. The methods have been divided into the groups with respect to the formulation of the structural model applied. Finally, chapter 9 rounds off with a discussion and a conclusion.

1.3 Are Offshore Structures Dynamically Excited ?

The dynamic behaviour of structures can be characterized by a set of eigenfrequencies, damping ratios and a mode shape matrix. However, whether the structure responds dynamically towards the excitation, i.e. the waves is a question about the proximity of the eigenfrequencies and the frequencies at which the energy in the waves is concentrated. The excitation frequency where most energy is located is called the peak frequency of the excitation. The peak frequency of the excitation will depend on the significant wave height, H_s, the water depth and in general the geographic location, while the eigenfrequency will depend upon the type of structure and be strongly correlated with the water depth. The latter point will be clearly demonstrated in the next chapter.

In the Danish part of the North Sea the wave energy will be concentrated in a narrow band of frequencies with a typical peak frequency, f_p in the range $0.05-0.3$ Hz, while the lowest eigen frequency will be somewhat higher. The peak frequency will be strongly correlated with the significant wave height. The fundamental correlation is given in figure 1.1 corresponding to the recommendation of the Danish offshore code, [3]. It is seen that the most severe sea states give relatively small peak frequencies, while the weak sea states may give relatively high peak frequencies. Thus, the risk of dynamic excitation of an offshore platform will typically be largest for the weak sea states.

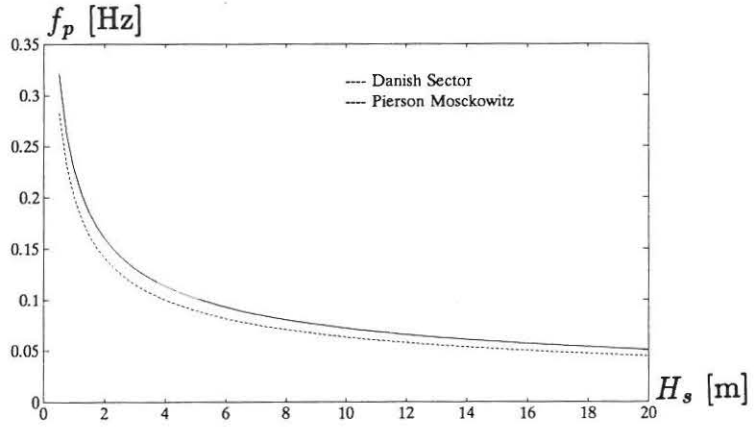

Figure 1.1. The peak frequency of the wave elevation spectrum as a function of the significant wave height, H_s according to the Danish Code of Practice for the Design and Construction of Pile Supported Offshore Steel Structures, [3].

The typical lowest eigenfrequency of existing jacket platforms lies in the range of $0.6-1$. Hz for the water depths in the Danish sector. In the Norwegian part and the British part of the North Sea, the lowest eigenfrequency can be as low as 0.40 Hz. In Norway certain measurings have shown that the effect of structural resonance is less than 5 % in the root mean square (r.m.s.) sense for a jacket platform at 70 m water depth, ($f_1 = 0.55$ Hz) and a gravity platform at 150 m depth, ($f_1 = 0.42$ Hz), Spidsøe and Langen [4]. On the other hand, it seems that some excitation of the two lowest bending modes and the lowest torsional mode always exists ,Robberstad and Agnello [5], Nataraja [6]. Thus, even though offshore platforms at existing

water depths may behave quasi statically the dynamic characteristics seems to be present in the structural response. Two situations will lead to increased dynamic behaviour of offshore structures:

- New design concepts.
- Structures at increasing water depths.

1.3.1 New Design Concepts

Figure 1.2 show some of the existing and some new design concepts of offshore platforms. The conventional design concepts are jacket and Condeep platforms which, at moderate water depths, will behave quasi statically. However, due to the exploitation of marginal oil fields cheaper concepts have been considered and developed. E.g. in the Danish North Sea the monopile (mono-tower) concept has been considered for unmanned production platforms during the last 5 years. This has now resulted in a new concept called a tripod platform which is expected to be realized before 1991. This platform is expected to have a first eigenfrequency about 0.40 Hz. In general the monopile concept gives first eigenfrequencies about $0.3-0.5$ Hz, see e.g. Kirkegaard [7], Cook [8] who have considered platforms at water depths about $30-40$m. Thus, this new concept at moderate water depths obviously leads to less stiff structures, and thus to increased importance of the dynamic structural properties. At larger water depths alternative concepts such as guided towers and semi-submersible platforms have also been developed with the same consequences. Thus, new design concepts are in general likely to increase the need for assessing the dynamic behaviour of offshore platforms.

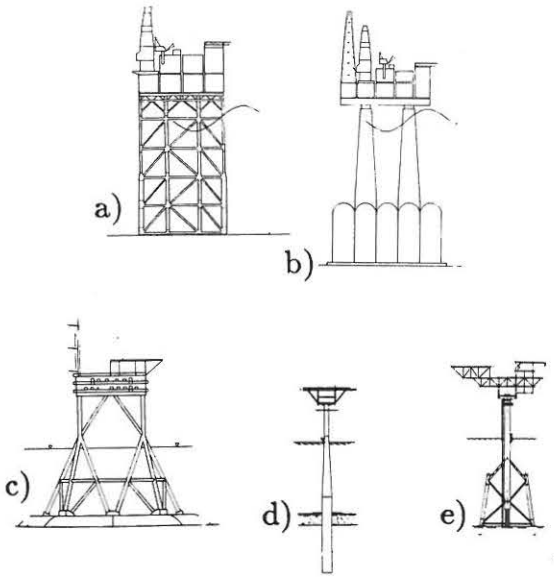

Figure 1.2. a) Jacket platform, b) Condeep platform, c) Hybrid platform d) Monopile platform, e) Tripod platform.

1.3.2 The Effect of Increasing Water Depth

As it has been pointed out the lowest eigenfrequencies will decrease with increasing water depth. In Vugts [9] sensitivity studies indicate that design of structures at increasing water depths is more controlled by stiffness than strength requirements. This can be illustrated by the characteristics of a clamped beam which can be considered to be a simple model of an offshore platform. In figure 1.3 the principle correlation is shown for the static maximum moment, the static maximum displacement and the first eigenfrequency with respect to the beam length. It is seen that, while the moment varies linearly with the beam length, the displacement increases with the beam length raised to the 3rd power. Thus, for a given beam length it will be the stiffness and not the strength which will prescribe the beam dimension. The effect of the beam length will accelerate because the eigenfrequency will be inversely proportional to the square of the beam length which will increase the resonance behaviour and thus give a dynamic amplification of the static maximum moment and displacement.

Vugts [9] concludes through his sensitivity study that for water depths of jacket structures over 150 m in the North Sea the dynamic behaviour will be of significance while for depths under 150 m the structure will behave quasi statically with respect to the wave excitation.

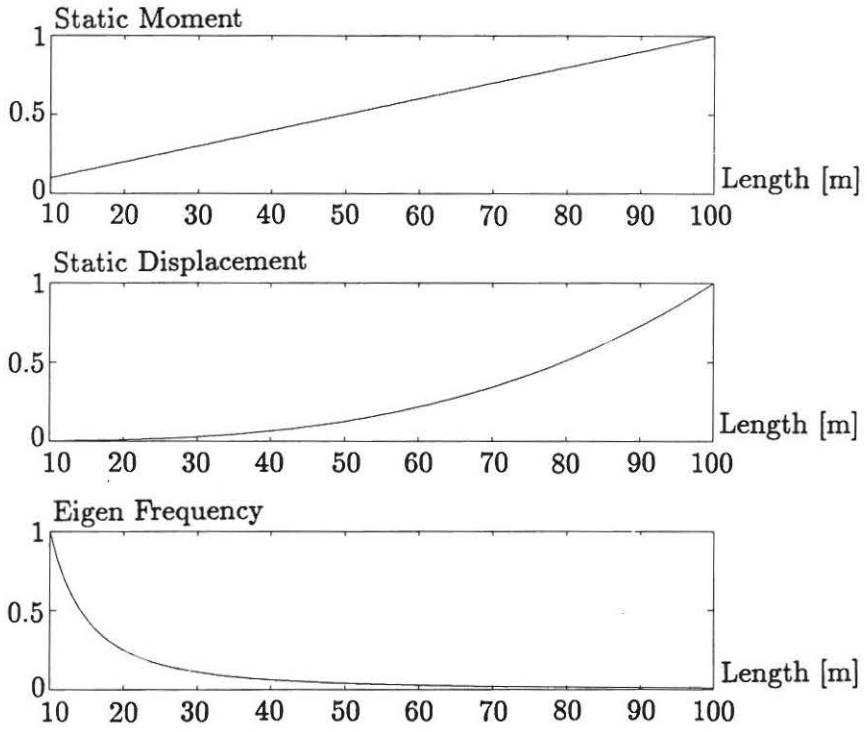

Figure 1.3 The maximum moment, the maximum static displacement and the eigenfrequency as a function of the beam length of a clamped beam with a single force at the beam end (all ordinates have been normalized to one).

1.4 Consequences of Dynamical Performance

The dynamic performance will depend upon the sea state and it will have several consequences:

- Vibrations can be a problem for occupants on the platforms.
- Dynamical amplification of the response can significant increase the ultimative loads the structure has to resist.
- The fatigue damage will increase due to dynamical performance.
- Dynamical amplification will mean that structural information can be evaluated from the response. This means that structural integrity monitoring can be performed.

1.4.1 Human Tolerances with Regard to Vibrations

In the code ISO 6897 [10] maximum limits of the r.m.s.-value of the acceleration response is given for the frequency interval $[0.063 - 1]$ Hz corresponding to the occupants not being bothered by structural vibrations. If e.g. the code is applied to a platform described by a single degree-of-freedom (SDOF) system vibrating in resonance with an eigenfrequency of 0.4 Hz, the code prescribes that the platform must have a dynamic horizontal acceleration with a magnitude less than 0.68 m/s^2 for events of more than of 10 min. At resonance this means that the damping becomes of vital importance to the magnitude of the dynamic response, which will be inversely proportional with respect to the damping ratio:

$$x^{dyn} = \frac{x^{static}}{2\zeta_0} \tag{1.1}$$

see Thomson [21]. Thus, with a damping ratio of 0.01 it is found that the static displacement (without dynamic amplification) should be less than 0.002 m. This clearly illustrates an important aspect of knowing the damping and the eigenfrequencies.

1.4.2 Dynamic Amplification of Ultimate Loads

Figure 1.4 shows the dynamic amplification factor of an SDOF system for different damping ratios. It is seen that the dynamic amplification becomes very large in the region of resonance depending on the magnitude of the damping. This means that if any structure is dynamically excited due to ultimate loads such as waves with a return period of 50 years then the necessary strength of the structure is increased manyfold. However, in general the peak frequency of the wave excitation spectrum of such sea state will lie far apart from the lowest eigenfrequency compared with the peak frequencies of weaker sea states. Consequently, the dynamic amplification will in general be smaller for the severe sea states and thus less important.

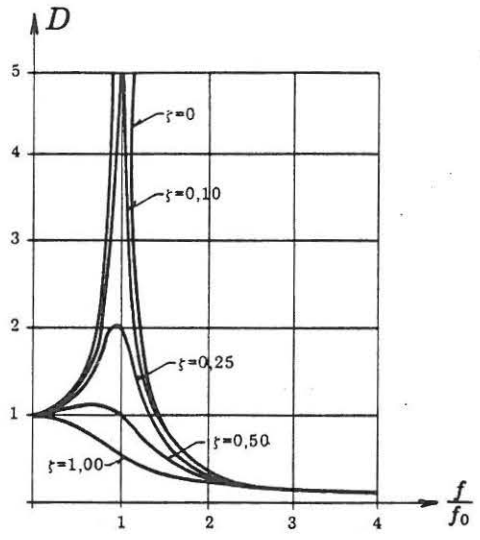

Figure 1.4. Dynamic amplification factor for an SDOF system, $D=\frac{x^{dynamic}}{x^{static}}=\frac{1}{\sqrt{(1-(f/f_0)^2)^2+(2\zeta_0 f/f_0)^2}}$, see e.g. Thomson [21].

1.4.3 Fatigue

The effect upon the fatigue life of tubular joints of jacket structures has been investigated by Vandiver [11] for a wave excitation causing both a quasi-static and a dynamic response contribution. He found that the fatigue life T was extremely sensitive to variation in the eigenfrequency f_0 and the damping ratio ζ_0:

$$\bullet \quad T^{true} \propto \left(\frac{f_0^{true}}{f_0^{pred}}\right)^{18} T^{pred} \tag{1.2}$$

$$\bullet \quad T^{true} \propto \left(\frac{\zeta_0^{true}}{\zeta_0^{pred}}\right)^{2} T^{pred} \tag{1.3}$$

The work was based upon the approach to fatigue damage given by Wirshing [12]. A similar approach has been applied by Kirkegaard et al. [7] in evaluation of sensitivity of the reliability index β with respect to the eigenfrequency and the damping ratio. The reliability index β is a measure of the probability of failure, Madsen [14]. In figure 1.5a. is shown how the reliability index varies with the damping and the natural period. The calculated fatigue life variation with the damping ratio is shown in figure 1.5b for a very similar monopile platform.

It is seen from Vandiver's results as well as from figure 1.5 that the damping ratio and the eigenperiod are of vital importance when fatigue is a design criterion. When the stiffness of the structure becomes sufficiently small it is the fatigue due to the overall dynamic performance of the structure that is vital. For jacket structures

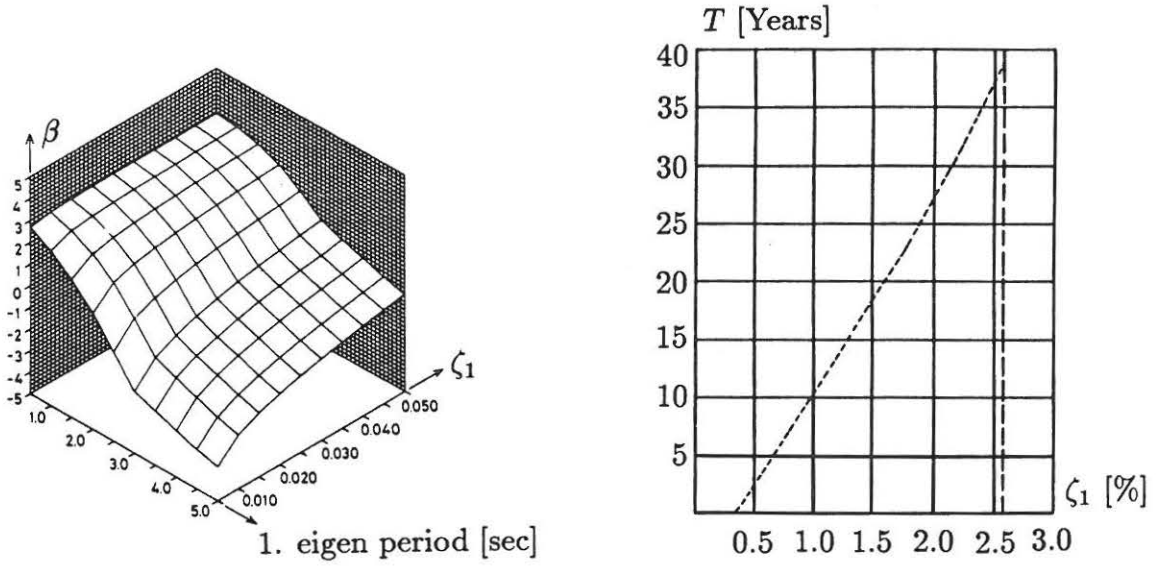

Figure 1.5. a) The variation of the reliability index β with respect to the eigenperiod and the damping ratio for an analysis of a monopile structure at 33.7 m in the Danish part of the North Sea, Kirkegaard et al. [7]. b) The variation of fatigue life T with respect to damping ratio for an analysis of a monopile structure at 32 m water depth and f_0=0.38 Hz in the Netherlands, Peters and Boonstra [13].

without any global dynamic performance it is typically local fatigue due to wave slamming at the splash zone which is important. Thus, when there is no overall dynamic performance of the structure, the magnitude of the damping becomes unimportant as expected, see e.g. Sunder and Connor [15].

1.4.4 Integrity Monitoring

A positive effect of the latent dynamic problem is that it makes it possible to take advantage of the information hidden in the response of the structure. The response will contain information about the eigenfrequencies, the damping ratios and the mode shapes of the excited eigenmodes. Since a change in those parameters reveals some kind of change in the structure it will in principle be possible continuously to check the structural integrity by vibration monitoring. This is also sometimes called damage detection since a change in the structure is often associated with a damage. The eigenfrequencies will decrease if the stiffness is reduced due to a crack or an accident and the mode shapes will change. Similarly it can be expected that the damping will increase due to friction in cracks or other nonlinear mechanisms. Changes in the foundations or modifications of the structure will also affect the parameters. Besides the continuous check of the integrity of the structure the design basis can also be continuously checked with e.g. reestimation of the fatigue

damage as a consequence. A survey of the aspect of integrity monitoring has been given in Ting and Sunder [16] and Richardson [17].

The investigations during the late seventies and the eighties of the concept of assessing the structural integrity by vibration monitoring seems uniquely to lead to the conclusion:

1. In general the success of the approach has been limited in practice. Primarily because the eigen modes associated with damage has not been sufficiently excited. E.g. in practice Kenley and Dodds [18] found that only complete failure of braces of an jacket structures could be identified through changes in eigenfrequencies.
2. Most investigations indicates that the best indication of structural changes is obtained from changes in the mode shapes and the eigenfrequencies , see Robberstad and Agnello [5], Coppolino and Rubin [19].

In spite of limited success in practice the interest of integrity monitoring from the global structural response has not decreased. This is probably due to the large economic perspectives of the principle. If platform inspection to some degree can be performed by vibration monitoring, a large amount of money can be saved, see Brown and Huckvale [20].

1.5 The Experimental Case

Since no full-scale measurements of offshore structures have been available in this study simple experimental investigations have been performed to get a proper insight into the practical problems of system identification.

The experimental model throughout the study has been a 4 m high monopile model excited by displacement of the base, see figure 1.6. Due to the excitation and the box profile of the monopile only two modes have in general been considered corresponding to 2 DOF system with a first eigenfrequency about 1.1 Hz and a second eigenfrequency about 7.2 Hz. The dynamic performance of 2 DOF system is relatively simple to understand and yet it is sufficiently complicated to contain the aspects of multi-degrees-of-freedom (MDOF) systems to which offshore structures in general should be expected to be related.

The experimental monopile is in fact quite similar to a simple offshore structure in spite of its simplicity. The excitation of an offshore structure will often be highly spatially correlated with respect to the elevation, and the force spectrum will in certain sea states be proportional to wave elevation which can be measured. Thus, in certain cases, it will be possible to describe the wave force as a random force process where the intensity is dependent on the elevation.

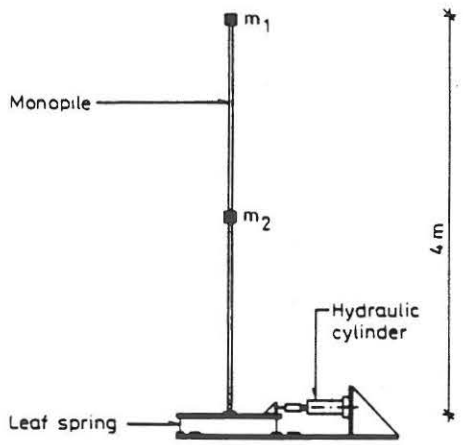

Figure 1.6. Monopile model (the experimental case).

Due to the base excitation of the monopile the force distribution will be quite analog. Due to Langranges equations, see e.g. Thomson [21], it can be shown that the force distribution will correspond to the mass distribution and will be described by the acceleration process going on at the base $\ddot{x}_b$:

$$\overline{p}(t) = - \begin{pmatrix} m_1 \\ m_2 \\ \vdots \\ m_n \end{pmatrix} \ddot{x}_b(t) \tag{1.4}$$

which in the frequency domain is equivalent to a force p_i at the ith mass with a spectral density function:

$$S_{pp}(f) = (2\pi f)^4 m_{(i)}^2 S_{x_b x_b}(f) \tag{1.5}$$

m_i is the lumped mass at the ith degree of freedom with $i = 1, 2, \ldots n$ and $S_{x_b x_b}(f)$ is the spectral density function of $x_b(t)$.

Thus, obviously, the excitation is in fact quite analog so the experimental cases with the monopile throughout this thesis will be quite relevant in the study of system identification methods of offshore structures. A detailed description of the performance of the monopile is given in Jensen [22].

1.6 References

[1] Kennedy, C. C. and C. D. P. Pancu, "Use of Vectors in Vibration Measurement and Analysis", J. Aeronautical Sciences, vol. 14, no. 11, 1947.

[2] Holand, I., S. Berg and G. Beck, "Environmental And Structural Instrumentation Of Platforms

On the Norwegian Continental Shelf", 2nd Int. Conf. on Behaviour Of Offshore Structures, BOSS 79, London,UK, 1979.

[3] Dansk Ingeniørforening's "Code of Practice for the Design and Construction of Pile Supported Offshore Steel Structures", DS 449, (NP-166-N) Denmark, 1983.

[4] Spidsøe, N. and I. Langen, "Damping of Fixed Offshore Platforms", Behaviour of Offshore Structures, BOSS85, Elsevier Science Publishers B.V., 1985.

[5] Robberstad, L. and G. Agnello, "New Structural Monitoring Using Movable Sensors", Instrumentert Overvåking av Offshore Konstruksjoner, Norske Sivilingeniørers Forening, Dr.Holms Hotel, Geilo, Norway, 1985.

[6] Nataraja, R., "Structural Integrity Monitoring in Real Seas", OTC 4538, Offshore Technology Conference, Houston, USA, 1983.

[7] Kirkegaard, P. H., J. D. Sørensen and R. Brincker, "Fatigue of a Mono-tower Platform", Paper no. 9 in Fracture & Dynamics, Institute of Building Technology and Structural Engineering, University of Aalborg, Denmark, 1988.

[8] Cook, M. F., "Damping Estimations, Response Prediction and Fatigue Calculation of an Operational Single Pile Platform", Ms.S. Thesis, Department of Ocean Engineering, Massachusetts Institute of Technology, USA, 1982.

[9] Vugts, J., H., "Dynamic Response and Fatigue Damage with Increasing Water Depths", Conference on Safety of Deepwater Oil and Gas Production, Det Norske Veritas, Norway, Nov 1981.

[10] International Standard, ISO 6897, first edition 1984-08-15, 1984.

[11] Vandiver, J. K., "The Sensitivity of Fatigue Life Estimates to Variations in Structural Natural Periods, Modal Damping Ratios, and Directional Spreading of The Seas", Proc. of the 3rd Int. Conf. on the Behaviour of Offshore Structures, BOSS 82, Massachusetts Institute of Technology, USA, 1982.

[12] Wirsching, P., "Fatigue Reliability for Offshore Structures", J. Structural Engineering, Vol. 110,No. 10, Oct., 1984.

[13] Peters, H. and H. Boonstra, "Fatigue Loading on a Single Pile Platform Due to Combined Action of Waves and Currents", Behaviour of Offshore Structures, BOSS 88, 1988.

[14] Madsen, H. O., S. Krenk & N. C. Lind, "Methods of Structural Safety", Prentice-Hall, 1986.

[15] Sunder, S. S. and J. J. Connor, "Sensitivity Analysis for Steel Jacket Offshore Platforms", Applied Ocean Research, 1981, vol. 3, no. 1, CML Publications, 1981.

[16] Ting, S.-K. and S. Shyam Sunder, "Testing and Monitoring of Offshore Structures: A State of the ART Review", Report No. 1 in Monitoring of Offshore Structures, Researh report R82-48, Massachusetts Institute of Technology, USA, July 1982.

[17] Richardson, M. H., "Detection of Damage in Structures from Changes in Their Dynamic (Modal) Properties - a Survey", U.S. Nuclear Regularity, NUREC/CR-1431,UCRL-15103, USA, 1980.

[18] Kenley, R. M. and C. J. Dodds, "West Sole WE Platform: Detection of Damage by Structural

Response Measurements", OTC 3866, Offshore Technology Conference, Houston, USA, 1980.

[19] Coppolino, R. N. and S. Rubin, "Detectability of Structural Failures in Offshore Platforms by Ambient Vibration Monitoring", OTC 3865, Offshore Technology Conference, Houston, USA, 1980.

[20] Brown, D. R. and S. A. Huckvale, "Monitoring and Structural Response of Steel Offshore Structures", European Offshore Petroleum Conference and Exhibition, London, UK, 1979.

[21] Thomson, W. T., "Theory of Vibration with Applications", 2nd Edition, George Allen & Unwin, 1981.

[22] Jensen, J. L., "Dynamical Analysis of a Monopile Model", Paper No.10 in Fracture & Dynamics, Institute of Building Technology and Structural Engineering, University of Aalborg, Denmark, 1988.

2. STATE-OF-THE-ART

During the seventies and the eighties the number of performed measurings and subsequent system identifications increased with the explosive increase in the number of offshore platforms. A survey has been performed to obtain information about how system identification is performed in practice and what practical results have been obtained. The survey which has been based on international journals and conference proceedings includes offshore structures which have been experimentally investigated during the seventies and the eighties.

An extensive survey of the available literatures on the topic has been performed on the basis of more than 40 references corresponding to the experimental investigation of 34 offshore platforms. The number of investigated platforms are no doubt much larger, but a lot of the obtained information is not publicly available. E.g. the major part of all Norwegian platforms are instrumented due to authority regulations, but the number of references on those has been limited.

The performed survey is believed to reveal the typical results which can be expected from a system identification. It has not been possible to give an extensive final conclusive comment on the survey because the purpose of each instrumentation and analysis has been varying. The quality and quantity of the available references has also been very different, and furthermore, the presentation of the practical experiences varies considerably in form.

The survey has resulted in two sets of tables, the first set, tables 2.1 to 2.3, concerns the instrumentation and general information while the second set, tables 2.4 to 2.6, deals with the performed system identification methods and the obtained results. The two sets of tables are closely related but it has been necessary to divide the results of the survey into two sets of tables due to practical considerations. Anyway in the following, section 2.1 contains comments on mainly the first set of tables while the second set of tables is considered in section 2.2. A general discussion on the estimates of eigenfrequencies and damping ratios is given in sections 2.3 and 2.4, respectively.

2.1 The Performed Measurings: Tables 2.1-2.3

In tables 2.1a and 2.1b the performed instrumentations of jacket structures are given, and in table 2.2 and 2.3 the reported instrumentations of gravity and other platforms types are shown. The latter includes monopiles (monotower, tripod etc.)

Structure / Water Depth	Instr. Period	Ref.	H_s / Excitation	Sensors	Data Rec.	Comment
West Sole WE,4 legs 25m, N.Sea (UK)	1978 Aug	1	0.67m ambient	16 acc.	A	removal of struct. subj:damage detect.
Ekofisk, 8 legs 70m, N.Sea (N)	1979 Jun	2	1-2m ambient/ exciters	4 points acc,str.gau.	A	authority requirements /research
Ekofisk 2/4H,4 legs 70m, N.Sea (N)	1980- 83	3	11.3m ambient	10 acc. 84 str.gau. wave radar etc	D+A	authority requirements
Valhall QP,4 legs 70m, N.Sea (N)	1980- 83	3	10.8m ambient	?	?	
Frigg DP2, 8 legs 98m, N.Sea (N)	1978- permanent	4,5	1-13m ambient	8 acc str.gau. wave-radar	A+D /research	authority requirements
SP65A, 8 legs 103m, Me.Gulf (US) SP62C, 8 legs 103m, Me.Gulf (US) WD152A, 8 legs 124m, Me.Gulf (US) Eugene Island 331B, 8 legs, 82m, Me.Gulf (US)	1975- 76	6	2-3m ambient/ Snap-Back /Impulse	acc. vel. wave staff water particle velocities were measured	A	research for ambient as well as forced excitation
MP296A , 8 legs 71m, Me.Gulf (US) SP62B, 8 legs 125m, Me.Gulf(US) SS274, 8legs 71m, Me.Gulf (US)	1978 + 1979	7,8,9	ambient	acc. at 7 variating points	D	Joint Industry Resarch Project case of damage detection
Forties Alpha,4 legs 133m,N.Sea(UK)	1980- 82	13	ambient	8 acc.	D	integrity monitoring
Amorco Montrore Alpha,8 legs 100m,N.Sea (UK)	1980- 82	13	ambient	10 acc. curr.m. wave staff	A	integrity monitoring

Table 2.1A. Performed measurings of jacket platforms with respect to the dynamic characteristic behaviour.

Structure / Water Depth	Instr. Period	Ref.	H_s / Excitation	Sensors	Data rec.	Comment
Occ.Claymero,8 legs 127m,N.Sea (UK)	1982 May-Aug	13	ambient	55 acc. 10 str.gau. 8 wave-pres.tr.	D	integrity - monotoring
4 legs 23m, (US)	1974 visites	14	ambient	3 acc.	A	damage detection due to impact
Light Station,4 legs 25m, NY Harb. (US)	1973 temporary	15	ambient	acc.	A	structural integrity
Bullwinkle, 16 legs, 450m (US)	permanent	16	ambient	10 mov.acc. 11 str.gau. wave staffs	D (T)	
SP62C, 8 legs 100m, Me.Gulf (US)	temporary temporary	10 11	4.5-5.5m /0.5-1m ambient ambient	17 acc. 2 acc.	A A	damage detection research on damping
Ocean Test Struct. 22m, Me.Gulf (US)	1976- permanent	12	3m ambient	92 sensors str.gau.,wave staff,curr.m.	D	research platform subject: hydrodynamic loading
4 legs 28m Abr.Gulf	1980 April	29	Exciter	mov.acc.	D	detection of of progressive damage(research)
Platform Hope 210m Cal.coast(US)	1969- permanent	30	ambient	6 acc.	A	earthquake instrumentation
Platfrom Grace,8legs 106m Cal.coast (US)	1981- permanent	31	ambient	23 acc.	D (T)	earthquake instrumentation
Midle Ground Shoal, Platform A,Alaska(US) ditto,Platform B West Delta,124m, Me.Gulf (US)	1971 (visites)	47	ambient	9 vel. (moveable)	A	research

Table 2.1B. Performed measurings of jacket platforms with respect to the dynamic characteristic behaviour.

Structure / Water Depth	Instr. Period	Ref.	H_s / Excitation	Sensors	Data	Comment
Gullfaks A,Condeep 134m,N.Sea (N)	1986- permanent	32,33	-9.5m ambient	16 acc.	D	authority requir. design verification, monitor. during. installation
TCP2,Frigg field 103m,N.Sea (N)	1979- permanent	34,35, 36,39	13.8m ambient	56 sensors: acc. str.gau. wave-radar 32 shock tr.	D	design verification, integrity, waves
Brent B,Condeep 140m,N.Sea (N)	1975- 77	37	10.3m ambient	10 acc., 24 str.gau. 3D-wave staff	D+A	integrity, design verification
Statfjord A,Condeep 145m,N.Sea (N)	1979- permanent	38,39	ambient	8 acc. (?) 16 shock tr. 2 wave staffs + more	D+A	authority req., design verification,
Statfjord Alp N.Sea (N)		39	ambient	acc,memb.forces		

Table 2.2. Performed measurings of concrete gravity platforms with respect to the dynamic characteristic behaviour.

Structure / Water Depth	Instr.	Ref. Period	H_s / Excitation	Sensors	Data rec.	Comment
Amoco, Monopile 30m, Me.Gulf (US) (single well)	1980 Mar 1 week visite	17-22	0.3 -2.7m ambient	2 mov.acc. 1 wave staff 1 anom. 1 curr.m.	A	research authority requir. ?
Europlatf.,Monopile 32m, N.Sea (NL) (meterological st.)	1983 +1985 (2months)	23	ambient	4 acc. Wave staffs anom.,Curr.m.	D (T)	vibration problems
Monopile 18m,Cameroon Africa,(conduct)	1982 Jun-Jul	24	<2m ambient	3 acc. 4 str.gau. wave staff,curr.m.	D	verification of design
Lena Guyed Tower 193m Me.Gulf (US) (guided tower)	1984- permanent	25	ambient	41 load cells,13 acc. 3 displ.,16 anom. 2 wave staffs	D+A (T)	installation, integrity monotor., research
Nordsee 30m,N.Sea (D) (hybrid)	1975 Nov. + ?	26,27	Shaker, Snap-Back with H=1.4m	> 6 acc. 18 str.gau.	A	structure for research
Christchurch Bay Tow. 8m, S.Coast (UK) (hybrid)	visites	28	Exciter	acc.	-	research struct., tested offshore and onshore

Table 2.3. Performed measurings of other platform types with respect to the dynamic characteristic behaviour.

and different sort of hybrid platforms. The typical instrumentation consists of $10 - 20$ sensors which measure the ambient excitation and the response due to ambient excitation.

The first column of the tables refers to the instrumented structure, the name of the structure, the number of legs in the case of jacket structures, the water depth and the location of the structure are given. The locations considered are mostly the North Sea and the Mexican Gulf.

The second column refers to the period in which the structure has been instrumented. From the references attempts have been made to determine whether the structure is permanently instrumented or whether it just includes a short period. Permanent platform instrumentation is typically due to authority regulations while short periods often are directed in relation to research projects organized in joint industrial and research programmes. A short period may mean just a couple of days.

The third column gives the reference from which the information has been obtained.

The fourth column gives the reported ambient excitation H_s for which measurements have been analyzed and also tells whether an external excitation has been applied (forced vibration or initial displacement etc.). The ambient excitation is the most frequently applied excitation source for the measured response since it is cheaper than applying an external excitation . Furthermore there will always be an extra risk with respect to the structural integrity when external excitation is applied.

The fifth column gives information about the sensors applied, the numbers and the principal types. This information is quite uncertain due to unprecise references. The following abbreviations have been applied:

- acc: accelerometers.
- mov.acc.: movable accelerometers.
- vel: velocity transducers/geophones (relative).
- displ: displacement transducers (relative).
- str.gau.: strain gauges.
- memb.forces.: strain gauges set-up to measure member forces.
- shock.tr.: shock transducers (typical for the response due to wave slamming).
- pres.trans.: pressure transducers (wave load).
- curr.m.: current meter.
- anom.: anometers (wind).

The sixth column refers to the recording of the data: D for digital records, A for analog records and (T) for transmission of data from the platform to the main centre, typical onshore. Transmission of data has only been applied in the case of instrumentation over a long period. Transportable equipment has usually been applied when the measurings were performed during short visits. In the case of long periods of instrumentation, minicomputers are applied to control the sampling, i.e.

when and for how long to sample. A current check of the sea state is applied in the case of automatic sampling. In the case of permanent instrumentation a typical sampling rule in the Norwegian sector of the North Sea seems according to Holand et al. [39] to be something like:

- Storm: Complete set of records of 20 minutes every 3 hours plus a reduced set of records of 20 minutes every hour.
- Normal sea: Complete set of records of 20 minutes every 24 hours plus a reduced set of records of 20 minutes every 3 hours.

A reduced set of records means here enough data to obtain a set of key numbers such as mean values, variance, maxima, minima, check of trends in data, etc. obtained from measured signals of the response and environmental data.

The minicomputer usually also includes an A/D-conversion and subsequent storage. However, it is not unusual also to let the minicomputer control a synchronous analog sampling since information is lost forever by the digitalization, and as backup copy which can be sampled and filtered in alternative ways.

The seventh column includes the main purpose of the instrumentation according to the given references. The purpose of the instrumentation has typically been the motives given in the previous chapter, namely an interest to improve the general knowledge about the dynamic performance and/or to monitor the integrity of the structure by observing any changes in its response. In USA permanent vibration monitoring has especially been used due to risk of earthquakes. Besides monitoring the structural behaviour it has also been a general purpose to improve the knowledge of the wave and wind loading.

2.2 The Performed Identifications: Tables 2.4-2.6

The results of the identification and interpretation of the measured data are shown in tables 2.4 to 2.6. The tables provide important structural knowledge of offshore platforms and they give a review of the possibilities of system identification.

The first column gives the information of the given structure, the water depth, d and the applied excitation either being ambient excitation or a kind of external excitation. The reference of the performed measurement and identification is given by the number in the brackets. From the platform name it is possible to compare the instrumentation of the platform described in tables 2.1 to 2.3 with the identification results.

The second column gives the two lowest estimated eigenfrequencies plus the highest eigenfrequency which has been identified corresponding to three rows per performed identification session. The number of the mode is given in brackets. This presentation shows how close the two lowest eigenfrequencies were located, and further, the highest identifiable eigenfrequency. At a fourth row the magnitude of the coefficient

Struct./d/ref. excitation	f_i Hz	ζ_i	$\overline{\Phi}_i$ no.	T/f_s min./Hz.	Analysis type	Comment
West Sole WE,25m (1)	1.365 (1)	-	none	20-45	FFT	peak
ambient,H_s=0.7m	1.44 (2)	-		/ ?		frequencies
1978	3.95 (6)	-				
	±1%					
West Sole WE,25m ( )	1.375 (1)	-				
ambient	1.375 (2)	-				
1975	4.00 (6)	-				
Ekofisk,70m (2)	0.66 (1)	0.035(1)	none	? /	FFT	peak freq.
shakers	0.70 (2)	0.028(2)		f_{max}=15		damping by
1979	5.41(13)	0.026(3)				peak value
		±43%				
ditto	-	0.018(1)				damping by
	-	0.011(2)				bw.
	-	0.028(3)				
	-	±9%				damping by
ambient H_s=1−2m	-	0.014(1)				bw.
Ekofisk 2/4H,70m (3)	0.51(1)	-	none	-	FFT	peak freq.
ambient H_s=11m	0.55(2)	-				no influence
	0.67(3)	-				of sea state
Frigg DP2,98m (4)	0.625(1)	-	none	20	FFT	response
ambient H_s=1−13m	0.68 (2)	-		/6.25		vs. waves, peak
	0.90 (3)	-				frequencies
	-	0.01		40/	FFT	damping vs.
ditto (5)	-	-0.03		16.67		wave height
SP65A,103m(6)	0.56(1)	0.027(1)	none	20/	FFT	zero cross.
snapback/impulse	0.59(2)	0.022-			50 av.	freq. +log.
	0.83(3)	0.027(2)			0.0037Hz	dec.
SP62C,103m (6)	0.66(1)	0.026-0.029(1)	none	ditto	ditto	ditto
snapback/impulse	0.66(2)	0.034-0.042(2)				
	0.96(3)					
ambient		0.010(1)				damp. by bw.
ambient		0.021-0.051				damp. by sp.mom.
WD152A,124m (6)	0.61(1)	0.022(1)	none	ditto	ditto	zero cross.
snapback/impulse	0.62(2)	-				freq. +log.
	1.03(3)	-				dec.
ambient		0.031(1)				damp. by bw.
ambient		0.024-0.049(1)				damp. by sp.mom.
Eugene Isl.,82m (6)			none	ditto	ditto	
	0.52(1)					
	0.54(2)					

Table 2.4A. Performed analysis of jacket platforms with respect to the dynamic characteristic behaviour.

Struct.,d,ref excitation	f_i Hz	ζ_i	$\overline{\Phi}_i$ no.	T/f_s min./Hz	Analysis type	Comment
SS274,71m (7) ambient ditto (8,9)	0.65-0.66(1) 0.68-0.70(2) 4.57-4.60(10)	-	(1)- (10) (1) -(12)	240/ ? 	FFT 60 av. 	peak freq. shape vect.
Amorco Mont.Alpha 100m (13) ambient	0.516(1) 0.535(2) 0.666(5) ±1%	-	none	15-50 /7.66- 61.3	FFT (1024) /MEM	peak freq. MEM equals FFT results
Forties Alpha 133m (13) ambient	0.486(1) 0.569(2) 2.562(8) ±1−2%	-	none	60/ 10.24	FFT (1024) /MEM	peak freq. MEM equals FFT results
?(US),23m (14) ambient	0.985(1) ±0.5%	0.01	none		FFT	
Light St.,25m,(15) ambient	1.12(1) 1.46(3)	- -	none		FFT	
SP62C,100m,(10) ambient H_s=0.5−5.5m ditto,(11)	0.646(1) 0.658(2) 2.62(11) ? (24) ±0.8%	- 0.0114(1) 0.0045(2) 0.0027(3) 0.020(1) 0.021(2) 0.013(3) ±15%	none	 32 / 6.4 	FFT FFT MEM	peak freq. f_i : ±1−2% due to sea state damp. by bw. damp. by bw.
ditto,(42) (41)	0.642(1)	0.0322(1) ±62% 0.0165(1) 0.0172(2) 0.0120(3)	none	16.7/ 6.4	Ran. dec. Time	zero cross., log.dec. damp. by log.dec.

Table 2.4B. Performed analysis of jacket platforms with respect to the dynamic characteristic behaviour.

of variation of the eigenfrequencies is given. The uncertainty includes in general the statistical uncertainty on the data, uncertainty of the identification method, and uncertainty due to time-varying characteristics of the structure, e.g. correlation with the sea state.

In analogy with the second column the third column gives the estimated damping ratios corresponding to the two lowest eigenmodes plus the ratio for the highest identified mode. At the fourth row the coefficient of variation is given if it has been estimated.

The fourth column gives the number of mode shapes which has been estimated. In general it is seen from the tables that eigenfrequencies are almost always identified while mode shapes rarely seem to be estimated. However, the interest in estimating the damping ratios and the mode shapes seems to be increasing. The typical case is that the three lowest eigenmodes have been identified since only those modes are sufficiently excited. In a single case up to 40 modes have been claimed to have been identified but, this is an exception where external excitation due to a shaker was applied.

Struct./d/ref. excitation	f_i Hz	ζ_i	$\overline{\Phi}_i$ no.	T/f_s min./Hz.	Analysis type	Comment
Midle Grou.Sh.Pl. A (47), ambient	0.90(1) 1.00(2) 1.20(3) ±2–3%	0.037(1) 0.037(2) 0.036(3) ±5%	none	? / 31.25	FFT 15 av.	peak freq. damping by bw.
Midle Grou.Sh.Pl. B (47), ice	0.98(1) 1.09(2) 1.41(5) ±1%	0.037(1) 0.033(2) 0.035(5) ± 5%	none	? / 31.25	FFT 15 av.	peak freq. damping by bw.
West Delta ,124m (47), ambient	0.24(1) 0.25(2) 0.40(3) ±2–3%	0.038(1) 0.038(2) 0.035(3) ±-5%		? / 31.25	FFT 15 av.	peak freq. damping by bw.
Ocean Test Struct. 22m, (12) ambient	-	-	-	-	-	estimation of C_D and C_M, member forces etc.
Abr.Gulf,28m,(29) shaker	0.85- 5.0		(1)- (40)		FFT	
Platf. Hope,210m, (30),earthquake	0.59(1) 0.61(2) ±1%	0.020-0.037(1) 0.026-0.028(2) ±10–25%	none		FFT	peak freq. damp. by. sp.mom.

Table 2.4C. Performed analysis of jacket platforms with respect to the dynamic characteristic behaviour.

If possible the fifth column gives the basic length of the applied time series plus the sampling frequency or alternatively the maximum frequency kept in digitally converted signals.

The most typical record length seems to be 20 minutes. This record length is thought to be due to the need for limiting the amount of data when measurings are performed over a longer period. Furthermore, the record length is also limited by the fact that system identification in general assumes data due to stationary random processes. The wave excitation process will only be quasi stationary within shorter periods of time. The sampling frequency has to be sufficiently high to ensure an accurate representation of the continuous signals on digital form. On the other hand, the amount of data must be limited. The result is that filtering and synchro-

Struct.,d,ref. Excitation	f_i Hz	ζ_i	$\overline{\Phi}_i$ no.	T/f_s sec./Hz	Analysis type	Comment
Gullfaks A,134m,(33)	0.438(1)	0.015(1)	(1)-	20/	ARMA	identific.
ambient	0.533(2)	0.014(2)	(4)	2.3-11.4		from
	0.753(4)	0.021(4)				ARMA-
	±2%	±8−30%				model
TCP2,103m,(34)	0.647(1)	-	none	20/	FFT	peak freq.
ambient,H_s<13.8m	0.760(2)					+
1979	1.07(3)					response
	±2−3%					vs.
						waves
extra deck mass(31%)	0.593(1)					
	0.675(2)					
ditto, (35)	0.605(1)	-		20/	MEM	peak freq.
1980,storm	0.645(2)					
	0.765(3)					identific. of
ditto, (35)	0.605(1)			20/	MEM	stiffness
1981,storm	0.600(2)					and
extra deck mass(31%)	0.670(3)					mass
(36)				20/	FFT	member force
H_s<12m				4		vs. waves
Brent B,140m,(37)	0.56(1)	-	(1)-	20/	FFT	peak freq.
ambient,H_s<10.3m	0.58(2)		(3)			+identfic. of
	0.84(3)					stiffness
Statfjord A,145m,(38)	0.43(1)	0.015(1)	(1)-	20/	ARMA	identific. by
ambient,H_s<10.7m	0.43(2)	0.02(2)	(3)	8		ARMA, estimates
	1.58(8)					vs. waves
		±50%				stifn. identific.

Table 2.5. Performed analysis of concrete gravity platforms with respect to the dynamic characteristic behaviour.

Struct.,d,ref. Excitation	f_i Hz	ζ_i	$\overline{\Phi}_i$ no.	T/f_s sec./Hz	Analysis type	Comment
Monopile,30m,(19)	0.3234(1)	0.0104(1)	none	32/	MEM	curvefit
ambient	0.3237(1)	0.0111(1)		6.4		peak freq.+
						damp.by bw.
ditto	0.3228(1)	0.0227(1)		32/	FFT	curvefit
	0.3234(1)	0.0244(1)		6.4		peak freq.+
						damp.by bw.
ditto, (18,21)	0.32(1)		(1)-	80/	MEM	peak freq.
	1.20(2)		(2)	6.4		
	3.06(3)					
ditto, (17,20)	0.325(1)	0.011(1)	none		MEM	peak freq.,
H_s=0.3−1m	0.327(2)	0.013(2)				damp. by
		±<14%				bw.
ditto, (17,20)	0.323(1)	0.010(1)	none		MEM	ditto
H_s=1.7−2.7m	0.328(2)	0.014(2)				
		±<20%				
ditto, (17,20)	0.323(1)	0.009(1)	none		MEM	ditto
H_s=0.7−1.3m	0.327(2)	0.011(2)				
		±<27%				
ditto, (22)						identific. of
						mass+stiffness
ditto, (43)	0.326(1)	0.0095(1)	none		Ran.-	Ibrahim time
		±<9%			dec.	domain method
Monopile(NL),32m	0.382(1)	0.015(1)	none		FFT	peak freq.,
(23),ambient						damp. by bw.
Monopile(Africa)	0.41(1)	-	(1)-	40/	FFT	shape vect.
18m,Cameroon	2.58(2)		(5)	20		
ambient,H_s=2m	5.00(5)					C_D and C_M
						estimated
Nordsee,hybrid ,30m	2.22(1)	0.028(1)	none	75	FFT	curvefit,
(26,27)	3.34(2)	-			(0.02Hz)	also mass
shakers and	4.03(3)	0.023(3)				estimation
H=1.4m	±<3.5%	±<30%				
Christch.Bay,hybrid	2.3-2.4(1)	0.02-0.04(1)	none		FFT	peak freq.,
8m,(28)	3.3-4.9(2)	0.01-0.03(2)				damp. by bw.
shakers						off-/onshore

Table 2.6. Performed analysis of other platform types with respect to the dynamic characteristic behaviour.

nous sampling with different sampling frequencies are widely applied for the purpose of getting information about a given frequency region in the measured response and excitation processes.

The sixth column shows the kind of signal analysis which has been reported in each reference:

- FFT (Fast Fourier Transformation) which is further described in chapter 5 and partly also in chapter 7.
- MEM (Maximum Entrophy Method) which is described in chapter 8.
- Random dec. (random decrement technique) which is described in chapter 5 and partly in chapters 6 and 7.
- ARMA (Auto-Regresssive Moving Average) which is described in chapter 8.

The first two kinds of analysis are usually applied in the frequency domain while two latter are methods in the time domain. The first and the third method are methods which in system identification are combined with some kind of curvefitting algorithm, while the second and the fourth method are methods which provide parametric expressions for e.g. the eigenfrequencies and the damping ratios.

In the case of a performed FFT analysis any available information of the number of averages, the resolution or the number of frequency points is also given in the sixth column.

In the seventh column comments have been made on the system identification and any applied curvefitting algorithm. The applied curvefitting algorithms include:

- Peak freq. (frequency) which is identification of the eigenfrequencies from the peak frequencies of the measured response spectra.
- Damping by bw. (bandwidth) which is identification of the damping ratio from the width of the resonance peak in the measured response spectra, see chapter 7.
- Zero cross. freq. (zero crossing frequency) which is identification of the eigenfrequency from the zero crossing period of the measured response process, see chapter 7.
- Log. dec. (logarithmic decrement) which is identification of the damping from a free decay, see chapter 7.
- Damp. by sp.mom. (damping by spectral moments) which is identification of the damping ratio from the three lowest spectral moments of the response spectrum, see chapter 7.
- Shape vect. (shape vectors) which is identification of the eigenfrequencies and the mode shapes from a curvefit on a measured response spectrum, see chapter 7.
- Ibrahim time domain method which is a method for identification of the modal parameters from a free decay, see chapter 7.

The more general curvefitting algorithms which have been applied in some references are discussed in chapter 7.

2.3 The Eigenfrequency Estimates

From the estimated eigenfrequencies of jacket platforms it is seen that the first eigenfrequency is clearly correlated with the water depth, see figure 2.1. The first eigenfrequency decreases with increasing water depth just as it was the case with the clamp beam in figure 1.3. A similar observation can be made for tall buildings. Ellis [44] observed from a review of experimental and numerical analysis of 163 buildings that the most reliable calculated estimate of the first eigenfrequency was obtained from the expression $f_1 = \frac{46}{h}$ Hz obtained from a fit of the experimental estimated eigenfrequencies with h as the height of the building. It was reported that the uncertainty of estimates obtained by numerical analysis by finite element methods were about 50%. The uncertainty of the identified eigenfrequency from measurements typical lie in the range of $1-2\%$. This case for tall buildings clearly illustrates the importance of the concept of system identification in structural design.

One reason for the uncertain prediction of eigenfrequency is probably that the mass distribution of structures is more uncertain than commonly expected. Snedden [45] has reported that already at the construction site of offshore structures there is an uncertainty of the masses of construction elements about $10-15\%$ in spite of a performed weight control. This source of uncertainty will tend to give an underestimation the total mass since modification of the design during construction will in general tend to give an increase of the steel consumption because steel is relatively inexpensive. This source plus the uncertainty of structural modification during the structural lifetime may mean an uncertain of the mass distribution of about 20% leading to an uncertainty prediction of the eigenfrequencies.

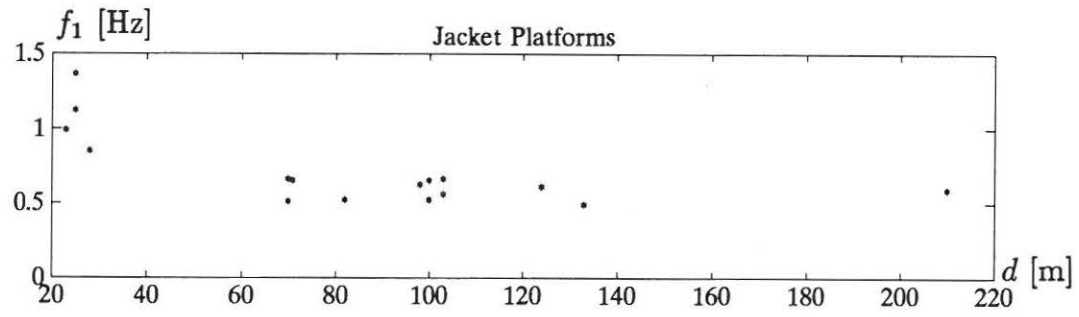

Figure 2.1. Identified first eigenfrequency of jacket platforms versus the water depth.

Only a small number of identified eigenfrequencies has been found on gravity platforms. However, the same correlation w.r.t. the water depth is expected to exist. The first eigenfrequency seems to lie in the range $0.30 - 0.65$ Hz for water depths $100 - 150$ m.

Offshore structures such as monopiles (monotowers, single standing conductors, tripods etc.) are becoming increasingly popular structural concepts for unmanned platforms, however, the number of such platforms are still small and thus also the number of performed measurings. However, some cases of system identification of such platforms have been found. At a water depth about $30 - 40$ m, the first eigenfrequency will typically lie in the range $0.30 - 0.40$ Hz.

Structural changes will also affect the eigenfrequencies. A practical example was given by the TCP2 condeep platform in the Norwegian part of the North Sea, see tables 2.5 and 2.3. Here, a 31% increase in the deck mass led to a 13% decrease in some of the lowest eigenfrequencies. Furthermore, during a period of 5 years some eigenfrequencies dropped about 10%. Thus an offshore structure cannot be considered to be a time independent system over several years.

For an SDOF system the first eigenfrequency is given by $f_0 = 2\pi\sqrt{\frac{k}{m}}$ which leads to the sensitivity relations of the eigenfrequency with respect to the mass and the stiffness:

$$\frac{df_0}{f_0} = -\frac{1}{2}\frac{dm}{m} \tag{2.1}$$

$$\frac{df_0}{f_0} = \frac{1}{2}\frac{dk}{k} \tag{2.2}$$

The observed decrease in the eigenfrequency in the Norwegian case is seen to have the same magnitude which was to be expected for an SDOF system. Thus, since it is the lowest eigenmodes which are excited in practice, significant stiffness and mass changes associated with the lowest eigenmodes will be observed as significant changes in the lowest eigenfrequencies, while structural changes affecting the performance of the higher modes will in general not be possible to detect, since those modes are not dynamically excited.

2.4 The Damping Estimates

The estimated damping ratios in the tables 2.4 to 2.6 do not seem to be correlated with the water depth. Instead they seem to depend upon the type of structure. Neither does the damping ratio seem to depend upon the eigenmode considered. This means that in general offshore structures will not be proportionally damped. This latter aspect is further discussed in chapter 4.

An analysis of all identified damping ratios of jacket platforms for all modes shows

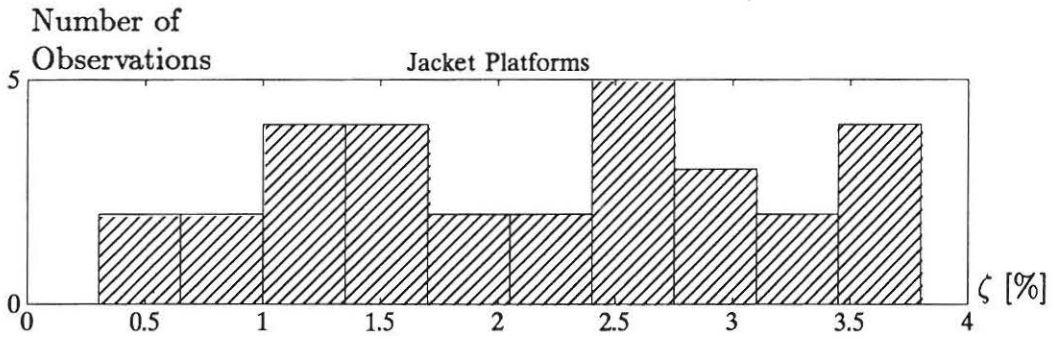

Figure 2.2. Histogram of identified damping ratios for jacket platforms including all identified modes.

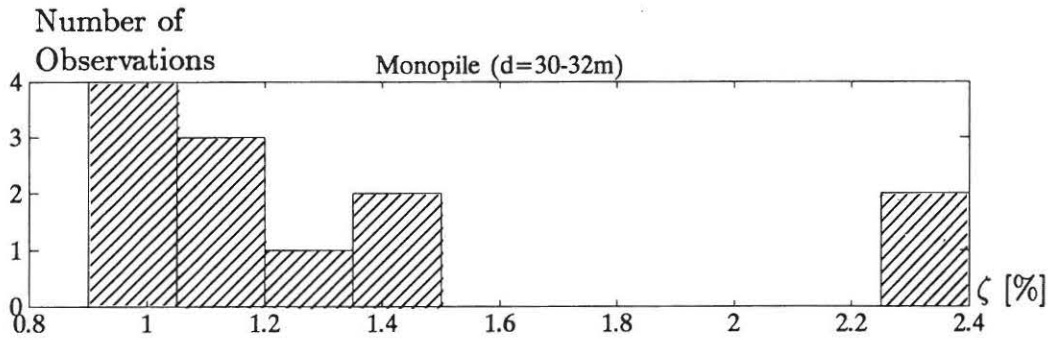

Figure 2.3. Histogram of the identified damping ratios of all modes for investigated monopile structures.

that the damping typically lies between $1-3\%$ with a mean of 2.1% and a coefficient of variation of 46%, see figure 2.2.

For monopile structures the damping may be a little smaller with a mean of 1.3% and a coefficient of variation of 37%, see figure 2.3. For gravity platforms the damping seems to lie in the range $1.4 - 2.1\%$. However, only a few structures of the two structural types have been included in the survey.

The estimated magnitude of the damping ratios can be compared with the recommendation of Det Norske Veritas [48] as shown in table 2.7. The damping values from the Det Norske Veritas include only structural damping. A contribution of the magnitude $0.005 - 0.02$ may be added due to the surrounding water. The damping in the foundation is not explicit evaluated in the reference. It is seen that the obtained damping from the review is in general larger than the given values for the structural damping. The damping contribution from the foundation and wa-

ter seems to be rather uncertain according to the rules of Det Norske Veritas and it is clear that the damping is in general underestimated if the design basis only includes the structural damping given by e.g. Det Norske Veritas. This will be a conservative element in the design basis and thus lead to less optimal structures.

Estimates due to	Jacket platforms	Monopile platforms	Gravity platforms
Review	2.1%	1.3%	1.4-2.1%
D.N.V.	1%	1%	1-2 %

Table 2.7. Damping ratios from the review and from the rules of Det Norske Veritas (D.N.V.) [48].

The review has shown that a priori knowledge of the damping ratios based upon the tables is coupled with a coefficient of variation of the damping ratio in the range of 50% while a performed identification on a given structure may reduce the uncertainty of the damping ratio down to a magnitude of about 10%. E.g. the case with a monopile platform shows that if a single analysis is disregarded the coefficient of variation due to different analysis is as low as 7% for the first damping ratio and 12% for the second damping ratio. Thus, a substantial reduction in the uncertainty of damping can be obtained by identification of a given structure.

2.5 Conclusion

The performed survey has revealed the existing practice and stage of system identification of offshore platforms.

The results of the survey of performed system identifications show that the eigenfrequencies and the damping ratios can be estimated of a certain accuracy for a given offshore platform which will provide a much better basis than the general a priori knowledge that e.g. Det Norske Veritas' rules represent. The latter will typically be the knowledge which can be extracted from a survey of the performed kind which clearly illustrates how uncertain the a priori knowledge of especially damping is, and it is thus also pointed out how conservative the design basis must be to ensure the reliability of the structures.

The aspect has been illustrated by Jeary and Ellis [46] who have investigated the effect of reducing the uncertainty of predicted response by employing results of system identification. Considering an SDOF system harmonically excited with an excitation frequency equal to its eigenfrequency f_0 and the force amplitude $F(f_0)$, the displacement amplitude is given by:

$$X(f_0) = \frac{F(f_0)}{4\pi^2 f_0^2 m 2\zeta_0} \tag{2.3}$$

which leads to a simple relation between the uncertainty of the predicted response and sources of uncertainty:

$$\frac{dX(f_0)}{X(f_0)} = \frac{dF(f_0)}{F(f_0)} - \frac{dm}{m} - \frac{d\zeta_0}{\zeta_0} - \frac{2df_0}{f_0} \tag{2.4}$$

Assuming the following uncertainties at the design stage:

$$f_0 : \pm 50\% \quad m : \pm 20\% \quad \zeta_0 : \pm 100\% \quad F(f_0) : \pm 20\%$$

the uncertainty of displacement amplitude at resonance becomes: $\pm 240\%$, while a performed system identification, if it has led to the following reduced uncertainties:

$$f_0 : \pm 0.1\% \quad m : \pm 20\% \quad \zeta_0 : \pm 10\% \quad F(f_0) : \pm 20\%$$

leads to an uncertainty of $\pm 50\%$ of the predicted response.

This example illustrates together with the discussion in the this and the previous chapter, what can be gained by system identification of offshore structures.

2.6 References

[1] Kenley, R. M. and C. J. Dodds, "West Sole WE Platform: Detection of Damage By Structural Response Measurements", OTC 3866, Offshore Technology Conference, Houston, USA, 1980.

[2] Gundy, W. E., T. D. Schartcon and R. L. Thomas, "Damping Measurements of An Offshore PLatform", OTC 3863, Offshore Technology Conference, Houston, USA, 1980.

[3] Langen, I. ,N. Spidsøe, R. L. Bruce and J. W. Heaver, "Measured Dynamic Behaviour of North Sea Jacket Platform", OTC 4655, Offshore Technology Conference, Houston, USA, 1984.

[4] Ansquer, P. F. and R. S. Carton, "Field Measurements of Correlation Between Waves and Platform Response Versus Signigicant Wave Height and Wave Direction", OTC 3797, Offshore Technology Conference, Houston, USA, 1980.

[5] Olagnon, M. and M. Prevosto, "The Variation of Damping Ratios with Sea Conditions for Offshore Structures Under Natural Excitation", OTC 4654, Offshore Technology Conference, Houston, USA, 1984.

[6] Ruhl, J. A., "Observed Platforms: Observed Behavior and Comparaisons with Theory", OTC 2553, Offshore Technology Conference, Houston, USA, 1976.

[7] Duggan, D. M., E. R. Wallace and S. R. Caldwell, "Measured and Predicted Vibrational Behaviour of Gulf of Mexico Platforms", OTC 3864, Offshore Technology Conference, Houston, USA, 1980.

[8] Burke, B. G. and N. R. Sosaian, "Analysis of Ambient Vibration Data By Multiple Shape Vectors", OTC 4284, Offshore Technology Conference, Houston, USA, 1982.

[9] Burke, B. G. and P. M. Safaie, "Characterization of Ambient Vibration Data By Response Shape Vectors", OTC 3862, Offshore Technology Conference, Houston, USA, 1980.

[10] Coppolino, R. N. and S. Rubin, "Detectability of Structural Failures in Offshore Platforms By Ambient Vibration Monitoring", OTC 3865, Offshore Technology Conference, Houston, USA, 1980.

[11] Cambell, R. B. and J. K. Vandiver, "The Estimation of Natural Frequencies and Damping Ratios of Offshore Structures", OTC 3861, Offshore Technology Conference, Houston, USA, 1980.

[12] Haring, R. E., "Status of the Ocean Test Structure Program", in Safety of Structures Under Dynamic Loading, vol. 2, ed I.Holand et al. Tapir, 1978.

[13] Nataruja, R., "Structural Integrity Monitoring in Real Seas", OTC 4538, Offshore Technology Conference, Houston, USA, 1983.

[14] Vandiver, J. K., "Detection of Structural Failures of Fixed Platforms By Measurements of Dynamic Response", J. of Petroleum Technology, Mar. 1977.

[15] Wojnarowski, M. E. , S. G. Stiansen and N. E. Reddy, "Structural Integrity Evaluation of A Field Platform Using Vibration Criteria", OTC 2909, Offshore Technology Conference, Houston, USA, 1977.

[16] Swanson, R. C. and G. D. Baker, "The Bullwinkle Platform Instrumentation System", OTC 6052, Offshore Technology Conference, Houston, USA, 1989.

[17] Cook, M. F., "Damping Estimation, Response Prediction and Fatigue Calculation of An Operational Single Pile Platform", M.Sc. Thesis, Massachusetts Inst. of Techn.., USA, 1982.

[18] Briggs, M. J., "Multichannel Maximum Entropy Method of Spectral Analysis Applied To Offshore Structures", Thesis, Massachusetts Inst. of Techn.., USA, 1981.

[19] Xinsen, L. and J. K. Vandiver, "Damping and Natural Frequency Estimation Using the Least Pth Optimization Technique", OTC 4283, Offshore Technology Conference, Houston, USA, 1982.

[20] Cook, M. F. and J. K. Vandiver, "Measured and Predicted Dynamic Response of A Single Pile", OTC 4285, Offshore Technology Conference, Houston, USA, 1980.

[21] Briggs, M. J. and J. K. Vandiver, "Multichannel Maximum Entropy Method of Spectral Analysis Applied To Offshore Platforms", OTC 4286, Offshore Technology Conference, Houston, USA, 1982.

[22] Sunder, S. S. and R. A. Sanni, "Foundation Stiffness Identification for Offshore Structures", Applied Ocean Research 1984, vol. 6, no. 3, CML Publisher, 1984.

[23] Peters, H. and H. Boonstra, "Fatigue Loading On A Single Pile Platform Due To Combined

Action of Waves and Currents", Behaviour of Offshore Structures, BOSS 88, 1988.

[24] Barnouin, B., M. Olagnon, O. Guillermin, R. Nerzic and M. Cahg, "Comparison of the Prediction with Full Scale Measurements On A Free Standing Conductor Pile", Proc. of the 3rd Int. Offshore Mechanics and Artic Eng. Symp., vol.2 , American Society of Mechanical Engineers, New Orleans, USA, 1984.

[25] Lamb, W. C. Jr., H. C. Hibbard, A. L. Jansen, W. A. Koorner and R. H. Rothberg, "Instrumentation for Monitoring Behaviour of Lena Guyrf Tower", OTC 4684, Offshore Technology Conference, Houston, USA, 1984.

[26] Kolb, M., W., D. Longree and A. Westram, "Untersuchungen von Eigenschwingungen der Forschungsplattform Nordsee bei naturlicher und kunstlicher Anregung", VDI-Schwingungstagung, VDI-Berichte 269, Verein Deutche Ingenieure, Germany, 1976.

[27] Natke, H. G. and H. Schulze, "Parameter Adjustment of A Model of An Offshore Platform From Estimated Eigen Frequencies Data", J.Sound and Vibration, vol. 77 (2), 1981.

[28] Ellis, B. R., "The Dynamic Characteristics of An Offshore Structure, Both Before, and After A Structural Failure", in Safety of Structures Under Dynamic Loading, vol.2, ed. I.Holand et al., Tapir, 1978

[29] Crohas, H. and P. Lepert, "Damage Detection Monitoring Method for Offshore Platforms Is Field Tested", Oil & Gas Journal, Feb. 22, OGJ Report, 1982.

[30] Vanmarcke, E. H. and R. N. Iascone, "Estimation of Dynamic Characteristics of Deep Water Ocean Tower Structures", Report no. MITSG72-12, Massachusetts Inst. of Techn., USA, 1972.

[31] Chen, J., R. R. Ullmann and A. B. Mason, "Measurement of Earthquake Ground Acceleration and Structural Response", OTC 6172, Offshore Technology Conference, Houston, USA, 1989.

[32] Lokna, T. and K. A. Nyhus, "Damping and Natural Frequencies During Towout and Installation of the Gullfaks A Platform", OTC 5786, Offshore Technology Conference, Houston, USA, 1988.

[33] Hoeklie, M. and O. E. Hansteen, "Measured and Predicted Dynamic Behaviour of the Gullfaks A Platform", OTC 5785, Offshore Technology Conference, Houston, USA, 1988.

[34] Ansquer, P. F., S. A. Antaleusky, E. Hjelde and G. Agnello, "Field Measurement of Platform Behaviour, Comparison with Design, and Long Term Monitoring of Response Stability After Three Years of Service", J.Energy Resources Technology vol.106, Dec., American Society of Mechanical Engineers, Dec. 1984.

[35] Thebault, J., L. Robberstad, I. Langen, G. Agnello, I. Doucet and R. Nerlic, "in Service Response Analysis of Two Fixed Offshore Platforms", Behaviour of Offshore Structures BOSS84, Elsevier Science Publishers, 1984.

[36] Spidsøe, N. and B. A. Leite, "Statistical Properties of Measured Wave-Induced Section Forces in Gravity Platform Shaft", OTC 5415, Offshore Technology Conference, Houston, USA, 1986.

[37] Hansteen, O. E., E. Dibiago and K. H. Andersen, "Performance of the Brent B Offshore Platform", Proc. 10th Int. Conf. On Soil Mechanics and Foundation Engineering, vol. 1, Stockholm, Sweeden, 1981.

[38] Spidsøe, N. and O. Skjaastad, "Measured Storm-Induced Variations of the Soil- Structure Interaction Properties of A Gravity Platform", OTC 5410, Offshore Technology Conference, Houston, USA, 1987.

[39] Holand, I., S. Berg and G. Beck, "Environmental and Structural Instrumentation of Platforms On the Norwegian Continental Shelf", 2nd Int. Conf. On Behaviour of Offshore Structures, BOSS79, London, UK, 1979.

[40] Eide, O., K. H. Andersen and T. Cunne, "Observed Foundation Behaviour of Concrete Gravity Platforms Installed in the North Sea 1973-1978", Appl. Ocean Research vol.3, no.3, 1981.

[41] Ruhl, J. A., "Forced Vibration Tests of A Deepwater Platform", OTC3514, Offshore Technology Conferecne, Houston, USA, 1979.

[42] Nasir, J. and S. S. Sunder, "An Evaluation of the Random Decrement Technique of Vibration Signature Analysis for Monitoring Offshore Platforms", Research Report R82-52,Dept. of Civil Eng.,Massachusetts Inst. of Techn.., USA, 1982.

[43] Longo, P., "Vibration Monitoring of Offshore Platforms Using the Ibrahim Time Domain Modal Identification Technique", M.Sc. Thesis,Dept. of Ocean Eng.,Massachusetts Inst. of Techn.., USA, 1982.

[44] Ellis, B. R., "An Assessment of the Accuracy of Predicting the Fundamental Natural Frequencies of Buildings and the Implification Concerning The Dynamic Analysis of Structures", Proc. of the Institution of Civil Engineers, part 2, vol. 69 Sept., UK., 1980.

[45] Snedden, C. N., "Weight Control of Offshore Structures", Offshore Research Focus, no. 25, June 1981.

[46] Jeary, A. P. and B. R. Ellis, "The Accuracy of Mathematical Models of Structural Dynamics", in Design for Dynamic Loading - the Use of Model Analysis, ed. G.S.T.Armer and F.K.Garus Construction Press, London, UK, 1982.

[47] Earle, E. N and W. L. Mandery, "Deterministic of Dynamic Characteristics of Offshore Platforms From Random Vibrations", OTC 1840, Offshore Technology Conference, Houston, USA, 1973.

[48] "Rules for the Design, Construction and Inspection of Offshore Structures, 1977, Appendix G, Dynamic Analysis", (reprint with corrections) , Det Norske Veritas, OSLO, 1982.

3. PRINCIPLES OF SYSTEM IDENTIFICATION

The purpose of this chapter is to give an introduction to the general principles of system identification. System identification is a general discipline which has application to all sorts of problems where a model is needed for the description of phenomena in such fields such as chemical processes, biological systems, electrical engineering, astronautics and mechanical and civil engineering.

The principles of system identification have especially been studied and developed in the field of electrical engineering while the research has only been modest in the field of civil engineering. However, since the models in electrical and civil engineering are often quite analogous (the same differential equations) it is possible to benefit from the long tradition for system identification in electrical engineering and other fields.

The system identification process for a structural dynamic system can be divided into four different steps:

- Proper modelling of the structural dynamic system.
- Obtaining informative data about the system.
- Estimation of the model: Parameter estimation.
- Evaluation and validation of the estimated model.

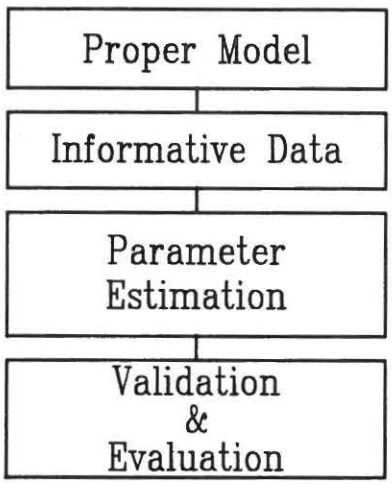

Figure 3.1 The system identification process.

In the strict sense the word system identification must not be confused with pa-

rameter estimation since this is only one step of the system identification process. However, in other chapters a less strict attitude will be applied since the meaning of the word will be clear.

3.1 Proper Modelling of the Structural Dynamic Systems

The word dynamic system refers to systems having a response which depends upon the past. The system is defined as the mechanism which due, to one or several input processes has one or several output processes. This means that when the input and the output is defined, then the system is defined but yet unknown. Hence, the first step is to define what is the input process and the output process. Furthermore, it must be expected that there will exist other unknown inputs to the system which will be defined as noise since they will distort the relation between the assumed input and output.

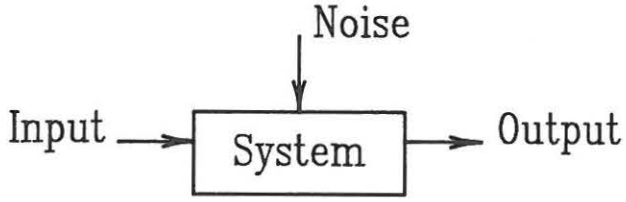

Figure 3.2 System model.

After the system has been defined it is possible to seek for a proper model. The proper model is usually assumed to belong to one of the following mathematical formulations:

A. A set of linear time invariant (lumped parameter) ordinary 2nd order linear differential equations.
B. A set of linear time invariant (distributed parameter) partial differential equations.
C. A set of time variant and/or nonlinear differential equations (lumped or distributed parameters).

In this thesis the models are mostly type A models with a few examples of type C models. Type B and C can only be applied in practice to very simple structures. The models can be divided into several general types of formulations:

1. Non-parametric measured input output relation: Transfer function model, e.g. obtained by sinus excitation where the excitation frequency is varied.
2. Model with physical parameters (parametric).
3. Model with modal parameters (parametric).
4. Model of the black box type (parametric), e.g. a model of a measured time series.

The word parametric refers to whether the model is described by a general class of models with a set of parameters or by a case dependent array of measured numbers presented graphically e.g. as a transfer function. The transfer function model will usually not be used as a final model but as a preliminary rough model followed by some sort of parametric model fit due to some curvefitting algorithm. The transfer function model will give valuable information about the performance of the system and thus indicate which parametric model should be applied, e.g. the number of degrees of freedom which should be applied in a parametric model. A curvefitting algorithm can afterwards be applied to the transfer function data, which means that a parametric model is obtained. Transfer function estimates are considered further in chapter 5.3 to 5.5.

The idea with the parametric model with physical parameters is that the physical insight into the system will make it possible to choose a sensible model and take advantage of the a priori knowledge of the system. For instance it may be possible to assume the masses of the model to be known. Furthermore, it should be relatively easy to interpret the parameter estimates. The relation between the model and a structural system is described in chapter 4 and examples of identification methods are in given in chapter 6.

The parametric model with modal parameters is a compromise where the physical insight has been maintained to some extent, but the model has been transformed into modal coordinates to simplify the model as a linear combination of eigenmodes. This leads to a reduction of the model parameters as shown in chapter 4 where the modal formulation is presented. Thus this model type is a trade off between physical insight and a compact mathematical model formulation. Examples of identification algorithms are given in chapter 7.

The idea of the black box model is that the model should be as flexible and compact as possible disregarding the physical insight into the model. The only physical aspect of this kind of model is typically whether the model is stable or not. However, since the purpose is to get physical insight, the black box model is usually related to a modal model. Identification with this kind of model is shown in chapter 8.

The model formulation can again be divided with respect to the independent variable which in this context will be either time or frequency.

3.2 Obtaining Informative Data About the System

The measured data containing the input and the output must be uniquely related to the chosen model which means that information about the model parameters must be contained in the data. This means that there is an upper bound for the complexity of a proper model for a given data set. If the model is made more complex the resulting estimates will become ambiguous. A lower bound also exists since a too simple model will be a too rough approximation to the system all depending on the application of the model.

If for example the response of an offshore structure is given as the superposition of two eigen modes due to wave excitation it may be a too rough approximation to apply a model containing only one degree of freedom while it will be absurd to apply a model containing, say ten degrees of freedom. Thus the model and the given input must be adjusted to each other in such a way that the model is uniquely related to the measured data with a minimum error between the model and the data.

The information in the data will also depend upon the number of independent input/output processes contained in the measured input and the output. The most simple case is the single input and single output case which is usually abbreviated as SISO. The most complicated is the MIMO case signifying multiple input multiple output case. With respect to the title of this thesis the number of input and output processes is related to the number of locations on the offshore structure where the excitation and the reponse have been measured. In this thesis it is almost only the SISO case which is considered corresponding to a wave excitation given as a single random input process and a measured output at some location.

3.3 Estimation of the Model: Parameter Estimation

The estimation of the model is performed by fulfilling some criteria of the fit between the model and the system. This can be done either by fitting a theoretical model to the transfer function or by fitting the simulated response of a model to the measured reponse of the system. The last procedure can be considered as identification by simulation which has been illustrated in chapter 6 and 8.

The parameter estimation is typically performed either by maximum likelihood estimation, MLE or by least squares estimation, LSE. In this thesis the methods are all based on the LSE procedure. MLE is briefly explained at the end of this section.

Parameter estimation can be considered as an optimization problem since it is a question about reducing an error measure of the fit between a model and some data set, that is finding a minimum of the error. The data is obtained by measurement in the time domain and perhaps afterwards followed by a transformation into the frequency domain.

It is assumed that the data can be described by some model, $\mathbf{M}$ and a set of parameters, $\overline{\Theta}$:

$$\mathbf{M} = \mathbf{M}(t|\overline{\Theta}) \tag{3.1}$$

t is here the independent variable belonging to either the time or the frequency domain. It must be noticed that the model concept here includes models of the measured response as well as models of transfer functions, e.g. $\mathbf{M}$ can be a frequency reponse function, an impulse response function or something else. It is assumed that the chosen model given by (3.1) is assumed to be a true model. This means that

by a proper choice of the model parameters the model will be able to describe the data set without any systematic error with respect to the independent variable. Furthermore it is assumed that the model is uniquely determined by its parameters $\overline{\Theta}$. This a fundamental demand which has to be satisfied to obtain a unique model.

The problem is to determine the parameters in the model $\mathbf{M}$ so that the fit to the data $\mathbf{M(t)}$ becomes as good as possible. This is done by formulating an error criterion function :

$$V(\overline{\Theta}) = \frac{1}{N}\sum_{t=1}^{N}\frac{1}{2}\epsilon(t,\overline{\Theta})^2 \tag{3.2}$$

where N is the number of measured data points, the factor, $\frac{1}{2}$ is just a convenient choice related to section 3.5 and $\epsilon(t,\overline{\Theta})$ is the error given by

$$\epsilon(t,\overline{\Theta}) = \mathbf{M}(t|\overline{\Theta}) - \mathbf{M}(t) \tag{3.3}$$

where $\mathbf{M}(t)$ is the given set of measured data. The error $\epsilon(t,\overline{\Theta})$ is also sometimes called the prediction error which refers to the time domain where it will be possible to predict the error at any time when the model has been estimated.

In the present case it is seen that the norm of the error criterion function, (3.2) is the least squares norm. The least squares norm can be argued to be a proper choice, because it can be shown that if $\epsilon(t,\overline{\Theta})$ is normally independently distributed with respect to the independent variable, i.e. time, then this approach is equivalent to the maximum likelihood approach as shown at the end of this section, see also Ljung [1]. This means that parameter estimates, $\overline{\Theta}$ converge asymptotically to their true values, $\overline{\Theta}^{\star}$ as the number of data points go towards infinity:

$$\overline{\Theta} \rightarrow \overline{\Theta}^{\star} \text{ for } N \rightarrow \infty \tag{3.4}$$

see Ljung [1].

If several sets of data are available corresponding to several models with common parameters the least squares problem can be formulated by the prediction error:

$$\epsilon(t,\overline{\Theta}) = \frac{1}{2}\bar{\epsilon}^T\overline{\overline{\Lambda}}\bar{\epsilon} \tag{3.5}$$

where $\bar{\epsilon}$ is a vector containing the elements of the ordinary prediction error, (3.3) found for each data set. Several sets of data will e.g. be the case when the response of a structure is measured at more than one location. This means that several sets of data provide information about the structure, which should consequently be included in the model estimation.

The data sets are equally weighted if $\overline{\overline{\Lambda}}$ is chosen as the identity matrix. Instead of weighting the data sets with respect to each other the data can also be weighted with respect to to the independent variable, t with a weighting function included in (3.3). In both cases this means that the approach becomes a weighted least squares approach, where the measured data are weighted according to the engineer's knowledge about uncertainties of the measurements. Any a priori knowledge about the parameters, $\overline{\Theta}$ and their mutual covariance matrix can also be included in the identification problem by adding an error measure of the deviation between the a priori knowledge and the final parameter estimates. This approach is called a Bayesian identification, see Ljung [1]. The argument for this approach is that the a priori knowledge is introduced, although in practice in a very subjective manner, see e.g. Ibanez [2] and Hart & Yao [3] for practical structural cases.

The proper estimate of $\overline{\Theta}$ is found by minimizing V. V is usually nonlinear with respect to the set of parameters, $\overline{\Theta}$ meaning that some kind of iterative optimization algorithm has to be applied to find the minimum of V. Many different kinds of algorithms are available see Vanderplaats [4] and Gill et al. [5]. The most popular algorithms in this kind of application are the Steepest Descent, the Gauss-Newtons method, the Levenberg-Marquardt method and the Newton method among many others. In the present paper especially the algorithm NLPQL has been applied, see Schittkowski [6]. NLPQL is a sequential quadratic algorithm. This means that it is based on successive solution of a quadratic subproblem and a subsequent one-dimensional line search.

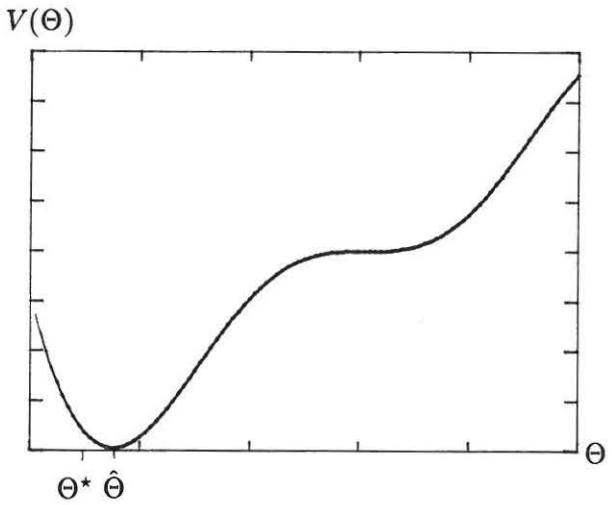

Figure 3.3. Minimum of the error function, V.

As shown for the single parameter case in figure 3.3 a minimum of V is characterized by:

$$\frac{\partial V}{\partial \Theta_i} = 0 \tag{3.6a}$$

$$\frac{\partial^2 V}{\partial \Theta_i \partial \Theta_j} \geq 0 \tag{3.6b}$$

Strictly the last-mentioned condition is insufficient and should state that the matrix containing the second order deriatives of V, given by the left of (3.6b) is positive semi-definite.

In practice some user defined stop criterion determines when the characterization for a minimum is assumed to be satisfied. Alternatively a maximum number of iterations is given.

The estimated $\overline{\Theta}$ will only be a proper estimate if the minimum is a global minimum. This cannot be ensured in general. One has to check the convergence with different start estimates of the parameters to check whether this leads to the same minimum.

A lot of practical problems exist with respect to the estimation of the minimum of an error criteria function. If different start estimates lead to different minima it may be advisable to scale the error criteria function (in optimization language it is called an object function) and/or the parameters included in it. Very small values or very big values of the error criteria function can lead to convergence at a local minimum due to numerical inaccuracies. Similarly, the parameters can be badly scaled such that numerical inaccuracies arise due to large differences in the parameter values or gradient values. In general the error criteria function and the parameters should be scaled to have a magnitude of about one, see Gill et al. [5].

In the optimization algorithm NLPQL it is possible to include constraints to the minimization problem. I.e. simple lower and upper bounds are given on the parameters as input to NLPQL. Further, more constraints, $C(\overline{\Theta})$ can be formulated as an expression in the parameters defined to be greater than or equal to zero.

$$C(\overline{\Theta}) = 0 \tag{3.7a}$$
$$C(\overline{\Theta}) \geq 0 \tag{3.7b}$$

3.3.1 Maximum Likelihood Estimation (MLE)

The parameters $\overline{\Theta}$ can also be estimated by the maximum likelihood estimation, MLE, see Johnson and Leone [7], Ljung [1]. In this case a given likelihood function is maximized with respect to $\overline{\Theta}$:

$$\max\{\mathbf{L}[\overline{\Theta}, \mathbf{M}(t)]\} \tag{3.8}$$

The conventional choice is to use a maximum likelihood function which is related to the maximum probability of the prediction error $\epsilon(t, \overline{\Theta})$ given by the likelihood function:

$$\mathbf{L}[\overline{\Theta}, \mathbf{M}(t)] = \text{Prob}(\epsilon(t_1), \epsilon(t_2), \ldots, \epsilon(t_N) \mid \overline{\Theta},\ \mathbf{M}(t)) \tag{3.9}$$

(3.9) should be interpreted as the probability of obtaining the given prediction error at N time instants given the estimated parameters and the measured data, $\mathbf{M}(t)$. Thus the principle of the MLE is that the most likely prediction error is found by maximizing the $\mathbf{L}[\overline{\Theta}, \mathbf{M}(t)]$ with respect to the unknown parameters, $\overline{\Theta}$. Normally estimates of $\overline{\Theta}$ are found from the maximum of:

$$\log(\mathbf{L}) \tag{3.10}$$

If the measured and the predicted data is given by respectively $\mathbf{M}(t) = \overline{y}(t) = \overline{y}$ and $\mathbf{M}(t|\overline{\Theta}) = \hat{\overline{y}}(t) = \hat{\overline{y}}$, and if $\epsilon(t, \overline{\Theta})$ is assumed to be normally independently distributed with respect to t, $\mathbf{N}(0, \sigma(t))$ then the following likelihood function is obtained:

$$\mathbf{L} = \prod_{i=1}^{N} \frac{1}{\sqrt{2\pi}\sigma_i} \exp -(\frac{(y_i - \hat{y}_i)^2}{2\sigma_i^2}) \tag{3.11}$$

which can be rewritten as :

$$\log(\mathbf{L}) = -\frac{N}{2}\log(2\pi) - \frac{1}{2}\sum_{i=1}^{N}\log(\sigma_i) - \frac{1}{2}\sum_{i=1}^{N}\frac{(y_i - \hat{y}_i)^2}{\sigma_i^2} \tag{3.12}$$

The position of the minimum of this function is seen to be equal to that of the least squares approach, if σ_i is constant with respect to i. It must be noticed that the maximum likelihood estimation requires knowledge about the probability distribution of the prediction error.

3.4 Evaluation of the Results

The model and the estimated parameters should be evaluated in some way to ensure the quality of the estimation. As mentioned it is necessary to check whether a global minimum has been reached in the optimization process. This ensures that the best fit has been found for the given model.

Furthermore, an attempt to evaluate the chosen model should be made. The most simple and perhaps the best is to check the fit by a graph of the data versus the model. This gives a view of the global fit. Beside this check, it is advisable to check the statistics of the prediction error. Ideally the prediction error will behave like white noise with a characteristic autocorrelation function and spectrum, which can both be checked. This is sometimes called a whiteness test. If the parameters have

a physical meaning it will also be natural to try to decide whether the parameters are physically reasonable.

Another indication of low quality of the estimates is large parameter uncertainties. This may mean that the model or data is inaccurate in some way. The model might be too simple or too complex compared with the applied data. This could be checked by repeating the parameter estimation with another model order. The estimation of the covariance matrix will be discussed in the next section.

Finally it should be noticed that the decision whether a satisfactory model has been obtained depends upon the given problem. Some models may be inaccurate with respect to some unimportant parameters while the parameters of importance may be estimated successfully. Thus, the model evaluation should be closely related to the purpose of the model.

3.5 Estimation of the Covariance Matrix

To validate a given model it is important to know the uncertainties of the estimated parameters. In this section the independent variable is time. In the next section the estimation of the covariance matrix is expanded to the frequency domain.

To get an understanding of the derivation of the covariance matrix the starting point here is a set of parameters $\overline{\Theta}$ which is estimated from some time series $y(t)$. The time series, $y(t)$ could e.g. be the measured free decay of a structure from which the eigenfrequency and the damping were to be estimated.

The prediction error is given by:

$$\epsilon(t, \overline{\Theta}) = y(t) - \hat{y}(t|\overline{\Theta}) \tag{3.13}$$

where $\hat{y}(t|\overline{\Theta})$ is the predicted response due to the model. The error criteria function with a least square norm is given by:

$$V(\overline{\Theta}) = \frac{1}{N} \sum_{t=1}^{N} \frac{1}{2} \epsilon^2(t, \overline{\Theta}) \tag{3.14}$$

where N is the number of measured data points in the time series. Now it is assumed that an estimate of the minimum $\hat{\overline{\Theta}}$ has been found for $V(\overline{\Theta})$ i.e. :

$$\overline{V}'(\hat{\overline{\Theta}}) = \overline{0} \tag{3.15}$$

is satisfied. The prime refers to the derivative with respect to $\overline{\Theta}$ which means that $\overline{V}'(\overline{\Theta})$ will be a vector with a dimension corresponding to the dimension of $\overline{\Theta}$. This first derivative is now linearized by a Taylor expansion about the true minimum $\overline{\Theta}^{\star}$, see figure 3.4 :

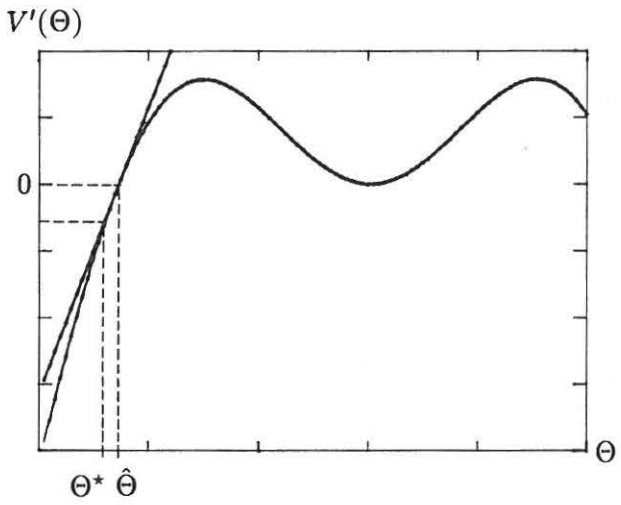

Figure 3.4. Linearization of the first derivative of the error criteria function, V.

$$\overline{V}'(\hat{\overline{\Theta}}) = \overline{0} \simeq \overline{V}'(\overline{\Theta}^\star) + \overline{\overline{V}}''(\overline{\Theta}^\star)(\hat{\overline{\Theta}} - \overline{\Theta}^\star) \tag{3.16}$$

It is assumed that for large values of N:

$$\hat{\overline{\Theta}} \to \overline{\Theta}^\star \text{ for } N \to \infty \tag{3.17}$$

with probability 1 and it follows from (3.16) that :

$$(\hat{\overline{\Theta}} - \overline{\Theta}^\star) = -\overline{\overline{V}}''(\overline{\Theta}^\star)^{-1}\,\overline{V}'(\overline{\Theta}^\star) \tag{3.18}$$

where from (3.14):

$$-\overline{V}'(\overline{\Theta}^\star) = \frac{1}{N}\sum_{t=1}^{N} \overline{\psi}(t, \overline{\Theta}^\star)\,\epsilon(t, \overline{\Theta}^\star) \tag{3.19}$$

where the ith element of the gradient vector, $\overline{\psi}(t, \overline{\Theta}^\star)$ is given by:

$$\begin{aligned} \psi_i(t, \overline{\Theta}^\star) &= -\frac{d}{d\Theta_i}\epsilon(t, \overline{\Theta})|_{\overline{\Theta}=\overline{\Theta}^\star} \\ &= \frac{d}{d\Theta_i}\hat{y}(t|\overline{\Theta})|_{\overline{\Theta}=\overline{\Theta}^\star} \end{aligned} \tag{3.20}$$

By the definition of the minimum (3.15) it follows that:

$$-\overline{V}'(\overline{\Theta}^\star) = \lim_{N\to\infty} -\overline{V}'(\hat{\overline{\Theta}}) = \lim_{N\to\infty} \frac{1}{N}\sum_{t=1}^{N} \overline{\psi}(t,\overline{\Theta}^\star)\,\epsilon(t,\overline{\Theta}^\star) = \overline{0} \tag{3.21}$$

This means that $-\overline{V}'(\overline{\Theta}^\star)$ is a sum of random variables $\{\overline{\psi}(t,\overline{\Theta}^\star)\,\epsilon(t,\overline{\Theta}^\star)\}$ with zero mean. Since the data $y(t)$ are assumed to be the response of a stable system it is assumed that $\{\overline{\psi}(t,\overline{\Theta}^\star)\,\epsilon(t,\overline{\Theta}^\star)\}$ is independent with respect to time. This is not true but holds approximately for distant terms of time, according to Ljung [1]. The independence means that $\overline{V}'(\overline{\Theta}^\star)$ converge to the normal distribution due to the central limit theory,[1].

$$-\sqrt{N}\,\overline{V}'(\overline{\Theta}^\star) \to \mathbf{N}(0,\overline{\overline{Q}}) \tag{3.22}$$

where[2]:

$$\overline{\overline{Q}} = \lim_{N\to\infty} N\,E[\overline{V}'(\overline{\Theta}^\star)\,\overline{V}'(\overline{\Theta}^\star)^T] \tag{3.23}$$

Hence it follows from (3.18) that:

$$\sqrt{N}\,(\hat{\overline{\Theta}} - \overline{\Theta}^\star) \text{ is } \mathbf{N}(0,\overline{\overline{P}}_\Theta) \tag{3.24}$$

with:

$$\overline{\overline{P}}_\Theta = \overline{\overline{V}}''(\overline{\Theta}^\star)^{-T}\,\overline{\overline{Q}}\,\overline{\overline{V}}''(\overline{\Theta}^\star)^{-1} \tag{3.25}$$

and the covariance matrix of $\overline{\Theta}$ is thus given by[3]:

$$\overline{\overline{\mathbf{cov}}}_\Theta = \frac{1}{N}\,\overline{\overline{P}}_\Theta \tag{3.26}$$

In Ljung [1] it is shown that for a least square norm model fit to a stable system it follows that:

$$\overline{\overline{Q}} = \lambda_N\,E[\overline{\psi}(t,\hat{\overline{\Theta}})\,\overline{\psi}(\hat{\overline{\Theta}})^T] \tag{3.27}$$

$$\overline{\overline{V}}'' = E[\overline{\psi}(t,\hat{\overline{\Theta}})\,\overline{\psi}(t,\hat{\overline{\Theta}})^T] \tag{3.28}$$

which leads to :

$$\overline{\overline{P}}_\Theta \simeq \lambda_N[\,E[\overline{\psi}(t,\hat{\overline{\Theta}})\,\overline{\psi}(t,\hat{\overline{\Theta}})^T]\,]^{-1} \tag{3.29}$$

where, λ_N is the variance of $\epsilon(t,\overline{\Theta})$:

$$\lambda_N = \frac{1}{N}\sum_{t=1}^{N} \epsilon^2(t,\hat{\overline{\Theta}}) \tag{3.30}$$

---

1 If a random variable, Y is given by a sum of uniformly distributed random variables with zero mean, X_i, $Y=\frac{1}{N}\sum X_i$ then $E[Y]=0$ and $\sigma_Y^2=\sigma_X^2$.

2 If the relation between two random variables is given by $Y=aX$ it means that $\sigma_Y^2=a^2\sigma_X^2$.

3 If the relation between two random variables is given by $Y=\frac{1}{\sqrt{N}}X$ it leads to $\sigma_Y^2=\frac{1}{N}\sigma_X^2$.

$\underline{\underline{V}}''$ is called the Hermitian matrix. Some important observations can be made about the covariance matrix of the parameter estimates. It is seen from (3.29) that a large variance of the error leads to large uncertainty (large covariance matrix elements) and similarly if the gradient is small with respect to a given parameter then this parameter becomes uncertain. Thus, a model with large gradients (parameter sensitivity) should be chosen to try to keep the variance of the prediction error low. Furthermore an increase in the number of data points will also reduce the variance.

3.5.1 The Simple Case: The Polynomial Model

As a simple case of parameter estimation consider a data set of a set of x-values, $x_1, x_2 \ldots x_N$ representing an input process and a data set of y-values $y_1, y_2, \ldots y_N$ representing the output process of a system. The output process is considered as consisting of the sum of the undistorted output $f(x)$ and the measurement noise $n(x)$:

$$y = f(x) + n(x) \tag{3.31}$$

$n(x)$ is assumed to be some Gaussian white noise process with zero mean, and $f(x)$ is a output of the system assumed to be given by a polynomial of the third order (the true model):

$$f(x) = Ax^3 + Bx^2 + Cx + D \tag{3.32}$$

It is seen that $f(x)$ is linear with respect to the parameters which means that multivariate linear regression can be applied. Normally the model will be non- linear with respect to the parameters. The relation between the x-values and the y-values can be written:

$$\underline{\underline{a}}\,\overline{p} = \overline{y} \tag{3.33}$$

$$\underline{\underline{a}} = \begin{pmatrix} x_1^3 & x_1^2 & x_1 & 1 \\ x_2^3 & x_2^2 & x_2 & 1 \\ \vdots & \vdots & \vdots & \vdots \\ x_N^3 & x_N^2 & x_N & 1 \end{pmatrix} \tag{3.34}$$

$$\overline{p}^T = \begin{pmatrix} A & B & C & D \end{pmatrix} \tag{3.35}$$

$$\overline{y}^T = \begin{pmatrix} y_1 & y_2 & \ldots & y_N \end{pmatrix} \tag{3.36}$$

After premultiplying (3.33) by $\underline{\underline{a}}^T$ an explicit expression for the parameters $\overline{p}$ can be obtained:

$$\overline{p} = (\underline{\underline{a}}^T \underline{\underline{a}})^{-1} (\underline{\underline{a}}^T \overline{y}) \tag{3.37}$$

This approach can be shown to be equal to the LSE-method, see Johnson and Leone [7]. The curve fitting in figure 3.5 was obtained for the given data set which was obtained by simulation of a polynomial of the third order with added Gaussian noise.

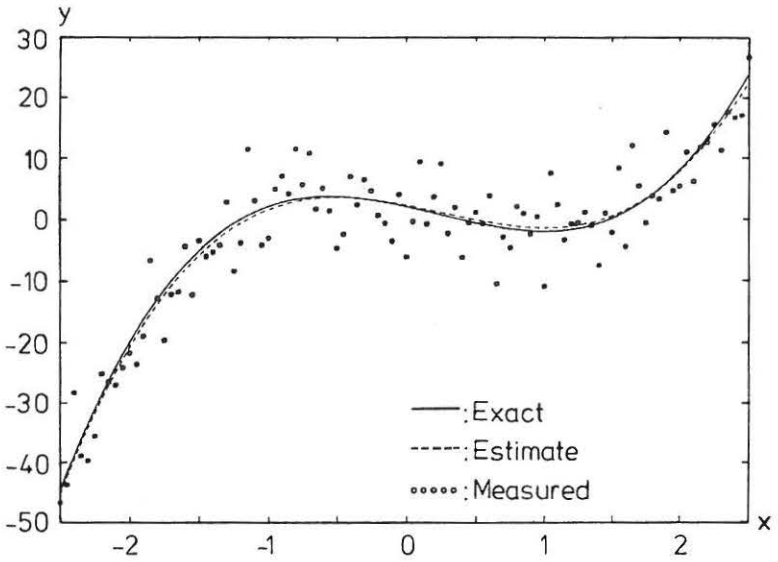

Figure 3.5. LSE Curve fitting of polynomial of third order. The exact model (function) is shown together with the measured values and the estimated function.

The covariance matrix can be obtained by inserting the prediction error, $\epsilon_i = y_i - f(x_i)$ in the expression for the error criteria function, V (3.14) and then evaluating V' and V'' and finally inserting in (3.24), (3.26) and (3.27):

$$\overline{\overline{\mathbf{Cov}}} = \frac{1}{N}\lambda_N (\overline{\overline{aa}}^T)^{-1} \tag{3.38}$$

where:

$$\lambda_N = \frac{1}{N}\sum_{i=1}^{N} \epsilon_i^2 \tag{3.39}$$

and:

$$\epsilon_i = f_i - \begin{pmatrix} x_i^3 & x_i^2 & x_i & 1 \end{pmatrix} \overline{p} \qquad i=1,2...N \tag{3.40}$$

This leads to an estimate of the covariance matrix:

$$\overline{\overline{\mathbf{cov}}} = \begin{pmatrix} 0.0345 & 0.0000 & -0.1319 & -0.0000 \\ 0.0000 & 0.0565 & -0.0000 & -0.1200 \\ -0.1319 & -0.0000 & 0.6004 & 0.0000 \\ -0.0000 & -0.1200 & 0.0000 & 0.4590 \end{pmatrix}$$

The estimated parameters and their coefficient of variations can now be given:

Parameter	Exact Value	Estimated Value	Coefficient of Variation %
A	3.0000	2.8632	6
B	-2.0000	-2.1908	11
C	-5.0000	-4.3109	18
D	2.0000	2.1948	31

The estimated values are seen to lie well within the uncertainty information due to the estimated covariance matrix. This indicates that the assumed model is sensible. It can be noticed that the coefficient of variation is largest for the parameter of the term with the lowest order. This can be explained by the fact that the information about this parameter lies in the range where the noise distortion is relatively large. Thus, all parameters cannot be estimated with the same accuracy.

The figure 3.5 shows that no systematic deviation between the measured values and the estimated function seems to appear. As an extra check the estimated noise, ϵ_i and its correlation function are shown in figure 3.6. From the plot of the noise it is seen that there seems to be no trend in the error. Similarly the correlation function shows that the estimated noise is almost white noise since there is no correlation between noise values far apart with respect to the x-axis. Thus, the estimated model is a proper model.

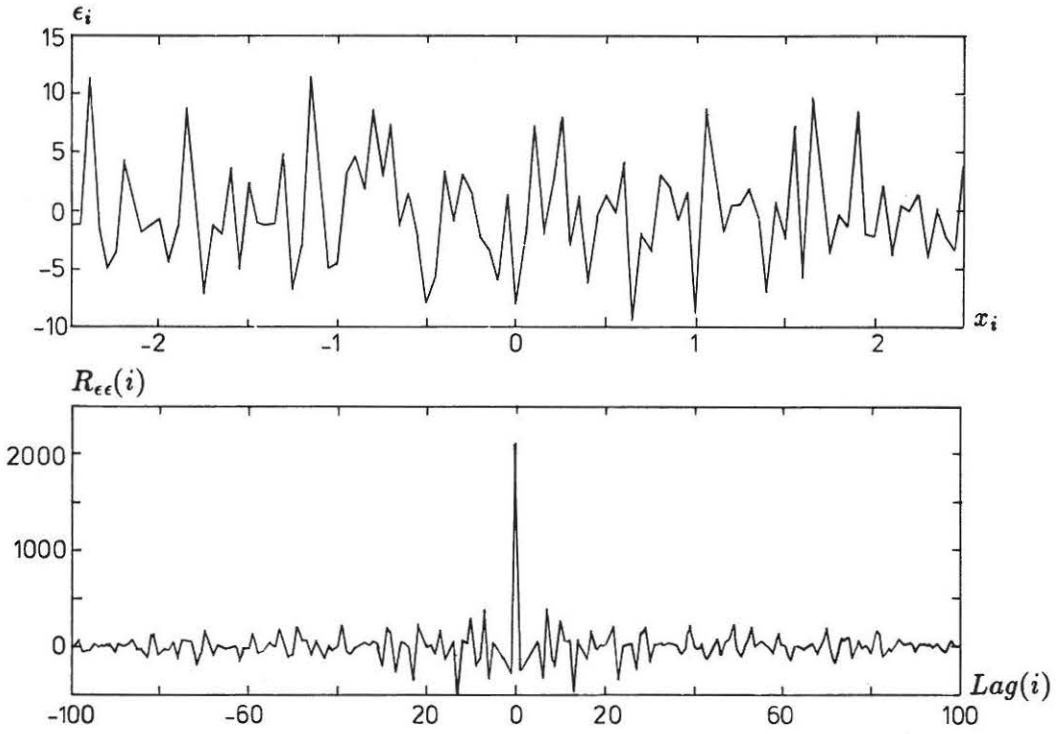

Figure 3.6. Top: The estimated prediction error (noise). Bottom: The estimated correlation function of the prediction error which is seen to be similar to a correlation function of white noise.

3.6 The Frequency Domain

The expression for the covariance matrix can be transformed into the the frequency domain for the least squares norm. This leads to an important expression for the covariance matrix of the parameters which can be applied when the parameter estimation is based upon a measured reponse spectrum. The derivation of a covariance expression in this section will be rather heuristic, a more mathematical presentation is given in Ljung [1].

The present model is a linear model given by an impulse response function $h(\tau)$ with a known input $u(t)$ and a known output $y(t)$ plus some filtered white noise $v(t) = \int_0^t g(t-\tau)e(\tau)d\tau$, see figure 3.7. $g(\tau)$ is the impulse response function of the linear filter and the integration relation is called the convolution integral and applies for linear systems, see also chapter 4. Alternatively, the system and noise filter can in the frequency domain be given by their frequency response functions, $H(\omega)$ and $G(\omega)$. The transformation from the time domain to the frequency domain is described in chapter 5.

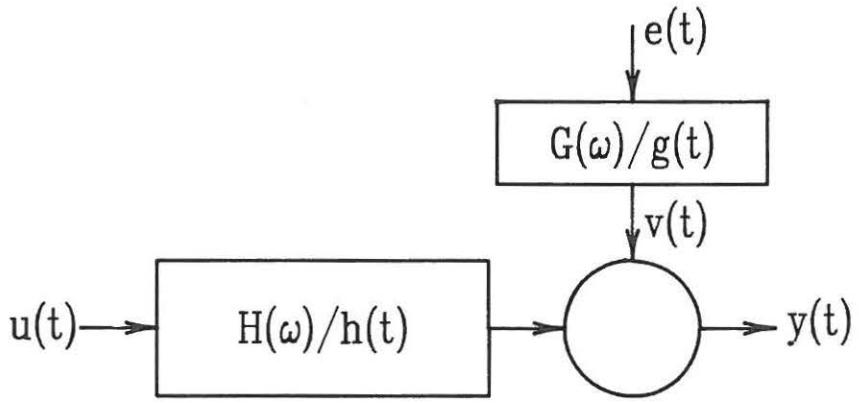

Figure 3.7. Noise model.

The predicted response $\hat{y}(t|\overline{\Theta})$ in the time domain with known excitation and noise disturbance is given by :

$$\hat{y}(t|\overline{\Theta}) = \int_0^t (h(t-\tau|\overline{\Theta})u(\tau) + \underbrace{g(t-\tau)e(\tau)}_{v(t)})d\tau \tag{3.41}$$

$e(t)$ is a white noise process with a variance, λ_0. The error criteria function is in the limit for $N \to \infty$ given by:

$$\underline{V}(\overline{\Theta}) = E[\frac{1}{2}\epsilon^2(t,\overline{\Theta})] \tag{3.42}$$

where the error $\epsilon(t)$ in the time domain is defined by:

$$\epsilon(t,\overline{\Theta}) = \int_0^t g^{-1}(t-\tau_2)\int_0^{\tau_2}\Big([h(\tau_2-\tau_1)-h(\tau_2-\tau_1|\overline{\Theta})]u(\tau_1)+ \underbrace{g(\tau_2-\tau_1)\,e(\tau_1)}_{v(\tau_2)}\Big)d\tau_1 d\tau_2 \tag{3.43}$$

$g^{-1}(t-\tau)$ is here defined by the inverse relation $e(t) = \int_0^t g^{-1}(t-\tau)v(\tau)d\tau$. From this point it is assumed that the true model has been found, $\hat{\overline{\Theta}} = \overline{\Theta}^\star$ which means that the prediction error becomes equal to, $\epsilon(t,\overline{\Theta}) = e(t)$.

In the frequency domain the prediction error given by (3.43) is given by the autospectrum :

$$S_{\epsilon\epsilon}(\omega,\overline{\Theta}) = \frac{|H(\omega)-H(\omega,\overline{\Theta})|^2 S_{uu}(\omega)+|G(\omega)|^2\lambda_0}{|G(\omega)|^2} \tag{3.44}$$

Here, the upper-case letters refer to the Fourier transformed, e.g. $H(\omega)$ is the transfer function of the linear system with the impulse response function $h(\tau)$. The area of the autospectrum equals the variance of, $\epsilon(t,\overline{\Theta})$.

The gradient of the $\epsilon(t,\overline{\Theta})$ is now given by:

$$\overline{\psi}(t,\overline{\Theta}) = \int_0^t g^{-1}(t-\tau_2)\int_0^{\tau_2}\overline{h}'(\tau_2-\tau_1,\overline{\Theta})\,u(\tau_1)d\tau_1 d\tau_2 \tag{3.45}$$

and the variance of the gradient:

$$E[\overline{\psi}(t,\overline{\Theta})\,\overline{\psi}(t,\overline{\Theta})^T] = \frac{1}{\pi}\int_0^\pi |G(\omega)|^{-2}\,\overline{H}'(\omega,\overline{\Theta})\,S_{uu}(\omega)\,\overline{H}'(\omega,\overline{\Theta})^T\,d\omega \tag{3.46}$$

The autospectrum of the filtered white noise is given by:

$$S_{vv}(\omega) = \lambda_0|G(\omega)|^2 \tag{3.47}$$

where λ_0 is the variance of the white noise, $e(t)$. The latter expression can be inserted into (3.46) which means that the covariance matrix due to (3.30) becomes:

$$\overline{\overline{\mathbf{cov}}}_\Theta = \frac{1}{N}\Big[\frac{1}{\pi}\int_0^\pi \frac{1}{S_{vv}(\omega)}\,\overline{H}'(\omega,\hat{\overline{\Theta}})\,S_{uu}(\omega)\,\overline{H}'(\omega,\hat{\overline{\Theta}})^T\,d\omega\Big]^{-1} \tag{3.48}$$

3.6.1 Parameter Estimation From the Transfer Function

It is now assumed that a model is sought for the transfer function and not for the measured reponse. The measured transfer function data is thought to be the result of a spectral analysis. This means that the response spectrum becomes equal to the square of the transfer function if $S_{uu}(\omega) \equiv 1$ is assumed:

$$\begin{aligned} S_{yy}(\omega) &= |H(\omega)|^2 S_{uu}(\omega) \\ &= |H(\omega)|^2 \end{aligned} \tag{3.49}$$

Hence a covariance estimate of the parameters obtained for parameters estimation of measured squared magnitude of the transfer function, $|H(\omega)|^2$ is:

$$\overline{\overline{\mathbf{cov}}}_\Theta = \frac{1}{N}\left[\frac{1}{\pi}\int_0^\pi \frac{1}{S_{vv}(\omega)} \overline{H}'(\omega,\hat{\Theta})\,\overline{H}'(\omega,\hat{\Theta})^T\, d\omega\right]^{-1} \tag{3.50}$$

If, furthermore, the filtered noise is replaced by a pure white noise input the covariance matrix becomes:

$$\overline{\overline{\mathbf{cov}}}_\Theta = \frac{1}{N}\left[\frac{1}{\pi}\int_0^\pi \frac{1}{S_{\epsilon\epsilon}(\omega)} \overline{H}'(\omega,\hat{\Theta})\,\overline{H}'(\omega,\hat{\Theta})^T\, d\omega\right]^{-1} \tag{3.51}$$

This white noise assumption will only be approximately true due to numerical errors in an FFT-analysis. Furthermore the signal/noise ratio will vary throughout the frequency range and thus be filtered white noise. However, an evaluation of a covariance matrix in the prescribed way will give an applicable measure of the uncertainties of the parameters and will also be applicable in a comparison between different fits. Examples of estimation of the parameter uncertainty are given in chapter 7.

3.7 References

[1] Ljung, L. "System Identification - Theory for the User", Prentice-Hall, 1987.

[2] Ibanez,P. "Review of Analytical and Experimental Techniques for Improving Structural Dynamic Models", Welding Research Bulletin, Bull. 249, Welding Research Council, United Engineering Center, New York, June 1979.

[3] Hart.G. and Yao,J.T.P. "System Identification In Structural Dynamics" Journal of The Engineering Mechanics Division, Vol. 103 no. EM6, American Society of Civil Engineers, Dec. 1977.

[4] Vanderplaats,G.N. "Numerical Optimization Techniques For Engineering Design", McGraw-Hill, New York, 1984.

[5] Gill,P.E. , W.Murray and M.H.Wright "Practical Optimization", Academic Press, Inc., 1981.

[6] Schittkowski,K. "NLPQL: A FORTRAN-subroutine Solving Constrained Nonlinear Programming Problems. Annals of operations Research, 1986.

[7] Johnson,N.L. and F.C.Leone, "Statistics and Experimental Design", John Wiley & Sons, 1977.

Alternative references

[8] Goodwin,G.C. and R.L.Payne "Dynamic System Identification - Experiment Design and Data Analysis", Academic Press, 1977.

[9] Eykhoff,P. "System Identification", John Wiley & Sons, 1974.

[10] Sinha,N.K. and B.Kuszta "Modeling and Identification of Dynamic Systems", Van Nostrand Reinhold Company, 1983.

4. STRUCTURAL MODELLING OF OFFSHORE STRUCTURES

The purpose of this chapter is to give a review of structural modelling of offshore structures. The structural model forms the frame within which the structural identification can be performed.

Since the structural model is applied to fit to obtained measurements of real structures the scope is here to provide a model of the given structure for a given load over a period of time. In other words, the purpose is not to create models which can describe the structure for any load at any time. Such models will be absurd, since they will contain characteristics which are not represented in the structural response and consequently not possible to identify. Furthermore, those so-called complete models will also require enormous expenses due to the complexity of the model and the number of parameters which will have to be identified. On the other hand, the model has to contain all the important characteristics, otherwise the parameter estimates become erroneous or limited to some specific excitation range.

4.1 The General Model

As mentioned in chapters 1 and 2, offshore structures must be modelled with respect to some specific marine factors :

- The mass distribution will change continuously due to the industrial process (continuously) going on at the platform.
- The apparent mass of the structure beyond the sea surface will be increased due to added mass of the fluid surrounding the structure. This will depend on the sea state.
- The marine growth which will be created during the first years after installation at location. This will give rise to increased added mass and loading.
- The foundation is assumed to contain important nonlinear stiffness properties and damping mechanisms. The characteristics also seems to be time dependent.
- Energy will dissipate due to several sorts of interaction between the fluid and structure. The damping mechanism will partly be nonlinear and will depend on the sea state.
- Determination of the excitation due to waves will be very uncertain, see Jensen [1]. Furthermore, it will be a non-stationary non-Gaussian load in many sea states.

These marine factors mean that the structural model of an offshore structure should be a nonlinear time dependent model with a response dependent non-stationary non-Gaussian excitation. Assuming that the offshore structure can be described by a discrete model of n degrees of freedom, the response given e.g. by an acceleration can be measured at one or several of the assumed degrees of freedom. The measured acceleration at the jth degree of freedom will be dependent on the time history of the global structure and the excitation at the present time instant:

$$\ddot{x}_j(t) = \mathbf{L_j}(\overline{x}, t) + \mathbf{f}_k(\overline{x}, t) \quad j = 1, 2, \ldots n \quad k = 1, 2, \ldots m \tag{4.1}$$

where $\mathbf{L_j}$ is some nonlinear time-dependent differential operator and $\mathbf{f}_k(\overline{x}, t)$ is an external excitation at m locations depending on time and the reponse of the structure.

Clearly a model like (4.1) would be very complicated and require a fully physical understanding and a mathematical model of all the psysical phenomena mentioned above. Unfortunately, this knowledge does not exist which means that the conventional description is limited to classical linear time invariant models.

The general assumption will be to ignore the nonlinearities and the time dependence of the differential operator in (4.1) assuming a linear differential operator with constant coefficients. Furthermore it is assumed that the excitation of the structure is independent of the response of the structure.

In section 4.2 the link between the discrete model and the continuous structure will be discussed. Afterwards in section 4.3 the discrete model of a lightly damped system is presented. The lightly damped model is the classical model of structures in civil engineering. However in section 4.4 the state space model is presented because the lightly damped model is insufficient in the cases with higher damping or closed spaced eigenfrequencies. Furthermore the state space model is also a classical model within the field of system identification. Since the structure is modelled by a discrete model the effect of a limited number of eigenmodes is discussed in section 4.5.

Since the assumptions mentioned above will generally be a violation of reality, some nonlinear models will be briefly discussed in principle in section 4.6. The discussion of nonlinearities will be further discussed in chapter 9, where the subject will be detection of nonlinear mechanisms.

4.2 Discrete Modelling

The structural model is in general assumed to belong to the special class of linear models which can be described by an n-dimensional linear set of second order differential equations with time invariant constants:

$$\overline{\overline{M}}\ddot{\overline{x}} + \overline{\overline{C}}\dot{\overline{x}} + \overline{\overline{K}}\overline{x} = \overline{f} \tag{4.2}$$

Here it has been assumed that the distributed inertia force of the structure can be discretisized into n degrees of freedom and be given as $\overline{\overline{M}}\ddot{\overline{x}}$. This set of inertia forces is balanced by a set of linear-elastic restoring forces, $\overline{\overline{K}}\overline{x}$, viscous damping forces $\overline{\overline{C}}\dot{\overline{x}}$ and the external loads $\overline{f}$.

It is assumed that the continuous structure of an offshore platform can be equivalent to a structure consisting of beams. It will be the subject of this passage to relate the continuous beam structure to the discrete model given by (4.2). The application of continuous beam and plate models for system identification purposes has e.g. been described in Juang and Sun [2] and will not be further described in this thesis.

4.2.1 Mass Matrix

The mass distribution is assumed to be given as concentrated masses at the chosen degrees of freedom. To predict the response, the mass can be lumped or determined as consistent mass defined by:

$$T = \sum_{i=1}^{nb} \int_0^l \frac{1}{2} m(\kappa^i) \dot{\chi}(\kappa^i)^2 d\kappa^i = \frac{1}{2} \dot{\overline{x}}^T \overline{\overline{M}} \dot{\overline{x}} \tag{4.3}$$

where on the left-hand side of (4.3), $\dot{\chi}(\kappa^i)$ is the velocity and $m(\kappa^i)$ is the mass, both continuous with respect to κ^i with i referring to the ith beam element, while the right-hand side contains the velocity and lumped masses at a finite number of structural locations. nb is the number of beam elements. From (4.3) it can be seen that the mass matrix of the discrete model must be chosen in such a way that the kinetic energy of the discrete model is equal to that of a continuous structure. This means that the consistent mass matrix, $\overline{\overline{M}}$ will generally be a full matrix. The lumped mass procedure is more simple since it just assumes a mass element corresponding to each degree of freedom. This means that the big advantage of the lumped mass procedure is that the mass matrix, $\overline{\overline{M}}$ is bound to be diagonal. This leads to a smaller number of parameters and makes matrix manipulations easier. Furthermore, it is believed that the lumped mass procedure is almost just as accurate as the consistent mass procedure taking other modelling errors into account. Thus considering identification of dynamic properties it is concluded that the lumped mass procedure is the best.

The rotational inertia is assumed to be without any importance since the mass is distributed along the beam axes and the rotational inertia can always be resolved into translation inertia by increasing the number of degrees of translation freedom.

4.2.2 Stiffness Matrix

The stiffness model is based upon the Bernoulli beam theory. Contribution to deformation from shear is assumed negligible:

$$\alpha = \frac{12EI}{GA_s l^2} \ll 1 \tag{4.4}$$

where EI is the bending stiffness, G the shear modulus, A_s the effective shear area and l the length of the beam element.

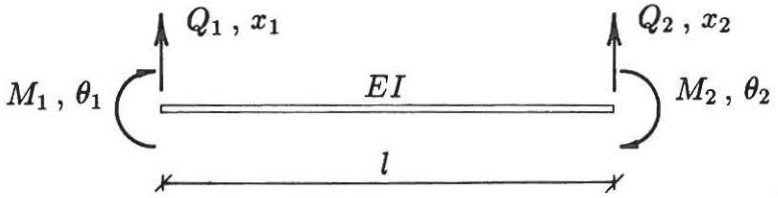

Figure 4.1 Beam model.

Deformations in the direction of the beam axis are disregarded. This means that the stiffness relation of a beam element is reduced to four local degrees of freedom:

$$\begin{pmatrix} Q_1 \\ M_1 \\ Q_2 \\ M_2 \end{pmatrix} = \begin{pmatrix} \frac{12EI}{l^3} & \frac{-6EI}{l^2} & \frac{-12EI}{l^3} & \frac{-6EI}{l^2} \\ \frac{-6EI}{l^2} & \frac{4EI}{l} & \frac{6EI}{l^2} & \frac{2EI}{l} \\ \frac{-12EI}{l^3} & \frac{6EI}{l^2} & \frac{12EI}{l^3} & \frac{6EI}{l^2} \\ \frac{-6EI}{l^2} & \frac{2EI}{l} & \frac{6EI}{l^2} & \frac{4EI}{l} \end{pmatrix} \begin{pmatrix} x_1 \\ \theta_1 \\ x_2 \\ \theta_2 \end{pmatrix} \tag{4.5}$$

The rotational degree of freedom can be ignored in the experimental model if static condensation is assumed to be valid. This is seen for the undamped problem, $\overline{\overline{C}} \equiv \overline{\overline{0}}$ in (4.2), if the degrees of freedom of the structure is divided into translation and rotational degrees of freedom:

$$\begin{pmatrix} \overline{\overline{M}}_T & \overline{\overline{0}} \\ \overline{\overline{0}} & \overline{\overline{M}}_R \end{pmatrix} \begin{pmatrix} \ddot{\overline{x}}_T \\ \ddot{\Theta} \end{pmatrix} + \begin{pmatrix} \overline{\overline{K}}_T & \overline{\overline{K}}_{TR} \\ \overline{\overline{K}}_{TR}^T & \overline{\overline{K}}_R \end{pmatrix} \begin{pmatrix} \overline{x}_T \\ \Theta \end{pmatrix} = \overline{0} \tag{4.6}$$

where the rotational inertia mass is assumed to be equal to zero, $\overline{\overline{M}}_R = \overline{\overline{0}}$ which leads to:

$$\overline{\overline{M}}_T \ddot{\overline{x}}_T + [\overline{\overline{K}}_T - \overline{\overline{K}}_{TR} \overline{\overline{K}}_R^{-1} \overline{\overline{K}}_{RT}] \overline{x}_T = \overline{0} \tag{4.7}$$

4.2.3 Damping Matrix

Above in (4.6) and (4.7) the influence of the viscous damping contribution due to the rotational degrees of freedom has been ignored. This will only be permissible if:

$$\overline{\overline{C}} \simeq \begin{pmatrix} \overline{\overline{C}}_T & \overline{\overline{0}} \\ \overline{\overline{0}} & \overline{\overline{0}} \end{pmatrix} \tag{4.8}$$

If this is not the case the rotational degrees of freedom must be included if they contain a significant damping mechanism. This means that measuring one of the rotational response of the structure should be attempted which is difficult. Normally the static condensed model given by (4.7) is assumed to be valid with the damping included according to (4.8).

The linear damping mechanism has been assumed to be viscous, but it could also have been modelled by structural damping (complex stiffness), $\overline{f}_D = \mathbf{i}\overline{\overline{H}}\overline{x}$ with $\mathbf{i} = \sqrt{-1}$ and $\overline{\overline{H}}$ being the structural damping matrix, see e.g. Ewins [3].

The damping in civil engineering structures are often modelled by viscous damping while aircraft and space structures for a period have also been modelled by structural damping. Langen and Sigbjørnsson [4] generally assume a viscous damping model but admit that structural damping can be applied to describe internal friction in materials such as steel. Cook [5] has found by a study of literature, Angelides [6], Blaney [7], Nowak [8] that the structural damping model is often applied as a model of the internal damping in soil. Nelson and Greif [9] state that the problem with structural damping is the application with non-sinusoidal excitation in which numerical problems arise. This is probably the real reason why viscous damping is more popular than structural damping in civil engineering. This thesis will not go into detail with structural damping. A description of modelling with structural damping is given in Ewins [3].

4.3 The Lightly Damped Model

Civil engineering structures including offshore structures are often considered as lightly damped structures since, as a rule, their largest damping ratio is less than 10%. If a modal model is needed it means that the undamped eigenvalue problem can be solved instead of the damped eigenvalue problem. This procedure is also called the normal mode method since the eigenmodes per definition are real. The undamped eigenvalue problem is given by:

$$(-\omega_i^2\overline{\overline{M}} + \overline{\overline{K}})\overline{\Phi}_i = \overline{0} \tag{4.9}$$

where the eigenvalues as well as the eigenvectors become real, since the mass and

stiffness matrix is assumed to be positive definite. In this case the orthogonality conditions become:

$$\overline{\Phi}_j^T \overline{\overline{M}} \overline{\Phi}_i = 0 \text{ for } i \neq j \tag{4.10}$$

$$\overline{\Phi}_j^T \overline{\overline{K}} \overline{\Phi}_i = 0 \text{ for } i \neq j \tag{4.11}$$

The eigenvectors can be normalized such that:

$$\overline{\overline{\Phi}}^T \overline{\overline{M}} \overline{\overline{\Phi}} = (1) \tag{4.12}$$

$$\overline{\overline{\Phi}}^T \overline{\overline{K}} \overline{\overline{\Phi}} = (\omega_i^2) \tag{4.13}$$

where $\overline{\overline{\Phi}}$ is an n x n matrix with ith column containing the ith eigenvector. The notation (a_i) means a diagonal matrix with the elements, a_i and (1) means the identity matrix.

While the eigenvectors are orthogonal with respect to the mass and stiffness matrix this is not in general the case with the damping matrix:

$$\overline{\overline{\Phi}}^T \overline{\overline{C}} \overline{\overline{\Phi}} \neq (2\omega_i \zeta_i) \tag{4.14}$$

However, if the damping matrix can be written as a linear combination of the mass and stiffness matrix:

$$\overline{\overline{C}} = \alpha \overline{\overline{M}} + \beta \overline{\overline{K}} \tag{4.15}$$

then the damping matrix is diagonalized:

$$(2\omega_i \zeta_i) = \alpha (1) + \beta (\omega_i^2) \tag{4.16}$$

This is called proportional or Rayleigh damping. Caughey [10] has shown that the diagonalization of the damping matrix is also the case for a linear combination of the form:

$$\overline{\overline{C}} = \sum_{k=1}^{R} \alpha_k \overline{\overline{M}} (\overline{\overline{M}}^{-1} \overline{\overline{K}})^k \tag{4.17}$$

The point here is that the attempt to relate the damping matrix to the mass and stiffness matrix is completely without physical rationale and is justified by computational considerations. The assumption means that the response for any

arbitrary excitation can be found by decoupling of the equation of motion (4.2) by replacing $\overline{x}$ by $\overline{\overline{\Phi}}\overline{z}$ and premultiplying by $\overline{\overline{\Phi}}^T$:

$$\ddot{z}_i + 2\omega_i\zeta_i\dot{z}_i + \omega_i^2 z_i = \Phi_{ji}f_j \quad i = 1, 2, \ldots n \tag{4.18}$$

which gives the response:

$$\overline{x} = \sum_{i=1}^{n} \overline{\Phi}_i z_i \tag{4.19}$$

The decoupled system given by (4.18) can be considered as n independent systems of a single degree of freedom corresponding to a mode of vibration. Hence, each mode can be assigned to an impulse response function and a complex frequency response function.

The impulse response function is defined by the reponse for an unit impulse at time zero with initial conditions equal to zero. This can be shown to equivalent to the transient response due to the initial conditions:

$$\dot{z}_i(0) = 1 \quad \text{and} \quad z_i(0) = 0 \tag{4.20}$$

which for an underdamped eigen mode gives the impulse response function:

$$h_i(t) = \frac{1}{\omega_i\sqrt{1-\zeta_i^2}} \exp\left(-\omega_i\zeta_i t\right) \sin\left(\omega_i\sqrt{1-\zeta_i^2}\, t\right) \tag{4.21}$$

Due to linearity the reponse caused by an arbitrary modal excitation can be considered as a superposition of the sum of the reponse due to impulses:

$$z_i(t) = \int_{-\infty}^{t} \Phi_{ji}f_j(t)h_i(t-\tau)d\tau \tag{4.22}$$

which is known as Duhamel's integral or the convolution integral.

The complex frequency response function $H_i(\omega)$ for the i'th eigenmode given by (4.18) is defined as the amplitude of the steady state modal response, z_i due to the modal excitation:

$$\Gamma_i(t) = \Phi_{ji}f_j(t) = \exp\left(\mathbf{i}\omega t\right) \tag{4.23}$$

which gives $H_i(\omega)$:

$$H_i(\omega) = \frac{1}{\omega_i^2 - \omega^2 + 2\omega\omega_i\zeta_i \mathbf{i}} \quad i = 1, 2, \ldots n \tag{4.24}$$

If the modal excitation, $\Gamma_i(t)$ is a stationary random process with zero mean it can be shown, see e.g. Meirovitch [17] that autocovariance function identical with the autocorrelation function of the response is given by:

$$C_{z_i z_i}(\tau) = R_{z_i z_i}(\tau) = \int_{-\infty}^{+\infty} \int_{-\infty}^{+\infty} R_{\Gamma_i \Gamma_i}(\tau - \tau_2 - \tau_1) h_i(\tau_1) h_i(\tau_2) d\tau_1 d\tau_2 \tag{4.25}$$

Due to the Wiener-Khintchine formulas (4.25) can be transformed to give the relation between the autospectra of the modal excitation and of the modal coordinate, z_i:

$$S_{z_i z_i}(\omega) = |H_i(\omega)|^2 S_{\Gamma_i \Gamma_i}(\omega) \tag{4.26}$$

which is an important relation with respect to system identification. The relation between the spectral densities in the original uncoupled coordinates, the generalized coordinates, can be shown, see e.g. Meirovitch [17] to be given by:

$$\overline{\overline{S}}_{xx}(\omega) = \overline{\overline{\Phi}} \left(H_i(\omega) \right) \overline{\overline{\Phi}}^T \overline{\overline{S}}_{ff}(\omega) \overline{\overline{\Phi}} \left(H_i^*(\omega) \right) \overline{\overline{\Phi}}^T \tag{4.27}$$

where $\left(H_i(\omega) \right)$ is a diagonal matrix containing the complex frequency response functions of the n eigen modes.

The transfer function of the ith degree of freedom due to the excitation of the jth degree of freedom is defined by:

$$H_{f_j x_i}(\omega) = \frac{S_{x_i x_i}(\omega)}{S_{f_j f_j}(\omega)} \tag{4.28}$$

$H_{f_j x_i}(\omega)$ will be proportional with the complex frequency response function, $H_i(\omega)$ if only the ith eigen mode is excited. Thus, the two functions representing the structure should not be confused.

4.3.1 Proportional Damping

The application problem when assuming proportional damping, which has been the case in the previous section, has three aspects:

- Computation of the response of a system with a given damping matrix.
- Reconstruction of a damping matrix from estimates of the damping ratios and the eigenfrequencies for a given structure.
- Identification of the damping ratios if a general non-proportional damped structure is assumed.

With respect to system identification the response calculation is a less interesting problem. It can be mentioned that proportional damping can be obtained by:

- ignoring the off-diagonal elements in the generalized damping matrix, $\overline{\overline{\Phi}}^T \overline{\overline{C\Phi}}$.
- least square reduction of the deviation of the damping force in modal coordinates expressed by a diagonalized and a complete damping matrix, see Malhotra and Penzien [11] and Thomson et al. [12].

The reconstruction of a damping matrix can be achieved if a set of damping ratios, eigenfrequencies and eigenmodes has been determined:

$$\overline{\overline{\Phi}}^T \overline{\overline{C\Phi}} = (\, 2\omega_i\zeta_i \,) \tag{4.29a}$$

$$\Downarrow$$

$$\overline{\overline{C}} = \overline{\overline{\Phi}}^{-T} (\, 2\omega_i\zeta_i \,) \overline{\overline{\Phi}}^{-1} \tag{4.29b}$$

($\overline{\overline{\Phi}}^{-T} = (\overline{\overline{\Phi}}^T)^{-1}$). Due to the orthogonality condition (4.12), (4.29b) can be rewritten as :

$$\overline{\overline{C}} = \overline{\overline{M\Phi}} (\, 2\omega_i\zeta_i \,) \overline{\overline{\Phi}}^T \overline{\overline{M}} \tag{4.30}$$

The advantage of the last formulation is that inversion of the eigenmode matrix is avoided and furthermore, a square matrix is not a must. Usually the number of elements in each eigenvector is larger than the number of eigen modes present in the analysis. Another procedure is to estimate the constants in the proportional damping model (4.16) and extract the damping matrix from those with known mass and stiffness matrices.

In principle when a MDOF system has to be identified, all eigenmodes will not be real but to a certain extent complex. Only in the case of $\overline{\overline{C}} = \overline{\overline{0}}$ or proportional damping the eigenmodes will be real. The problem is therefore to determine whether or not proportional damping is an acceptable assumption.

There has been a general discussion in the last twenty years about proportional versus non-proportional damping. There is some disagreement on the application

of proportional damping. However, everybody does agree that heavily damped systems must be modelled by the damped eigenmodes. There is disagreement with respect to lightly damped systems. Some people claim that in general also lightly damped systems must be modelled with non-proportional damping. Others state that this is only necessary in the case of concentrated damping sources such as structural interaction with the foundation in lightly damped systems. However, this discussion is somewhat absurd since each author can construct numerical results giving the proper arguments. The interesting subject must be justification of proportional or non-proportional damping from the measured response of real structures.

Assuming proportional damping for a non-proportionally damped structure means that modal superposition and identified modal parameters may be erroneous since higher modes can contribute to the response of lower modes, see Duncan and Taylor [13]. And vice versa, higher modes can be excited due to an excitation of lower modes. Consequently, it is important to try to evaluate the damping relations before modelling and identification.

Warburton and Soni [14] have tried to quantify when proportional damping will be an acceptable approximation. They have suggested the following expression:

$$\zeta_r < \epsilon \left| \frac{cc_{rr}}{2cc_{rs}} \left(\frac{\omega_s^2}{\omega_r^2} - 1 \right) \right|_{minwrt.s} \tag{4.31}$$

Index r is here the considered mode while index s is a neighbour mode. $cc_{rr} = 2\omega_r\zeta_r$ is the diagonal element and $cc_{rs} = 2\sqrt{\omega_r\omega_s}\zeta_{rs}$ is the off-diagonal element in the generalized damping matrix. ϵ is here a parameter which determines how large errors will be allowed in the model. It is seen that closely spaced eigenfrequencies as well as large off-diagonal elements give a narrow limit for the level of the damping ratio if proportional damping has to be applied as an approximation. Warburton and Soni suggest $\epsilon = 0.05$ which, in a study of simulated response, gave an error of the magnitude about 10% for the maximum response.

With respect to system identification the expression suggested by Warburton and Soni cannot be applied directly since the structure to be identified is unknown. However from a priori knowledge the expression can maybe give an indication of whether the identified quantities could be sensitive to an assumption about proportional damping.

Whether or not proportional damping is a proper assumption can always be checked by applying a general model which allows complex modes. If the identified modes are complex then non-proportional damping has been confirmed.

Another check can be made by estimation of the constants in the proportional damping model by applying (4.16). This is done with a set of eigen frequencies and damping ratios which have been estimated independently of each other for instance from spectral peaks. The constants of (4.16) can be determined by a least square fit and the fit can be evaluated by a covariance matrix for the estimated constants

according to the principles of chapter 3. The proportional damping assumption can now be checked from either the covariance matrix or a plot of the proportionally damped model and the identified set of eigenfrequencies and damping ratios. As an example, see figure 4.2.

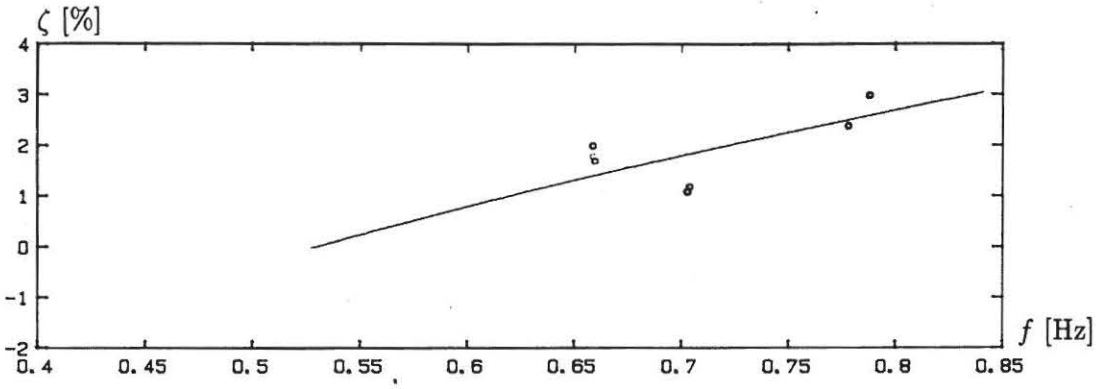

Figure 4.2. Least square approximation of a proportional damping matrix to identified eigenfrequencies and damping ratios. (Analysis of peaks of response spectra of Jacket platform at the Ekofisk Field, Gundy et al [15].

From figure 4.2 it is seen that there is a considerable scattering about the estimated proportional damping model which could indicate non-proportional damping. From (4.16) and figure 4.2 it is seen that the damping ratio is forced to increase with the frequency which is not realistic. As a footnote it can be mentioned that this is another reason why some people prefer a structural rather than a viscous damping model, Ewins [3]. The structural damping model allows the damping ratio to be frequency independent. However, Lang [16] claims that the viscous damping model is becoming increasingly popular since computer progress has led to a replacement of the proportionally damped model with the non-proportional model. The latter will be the subject in the next section.

4.4 The State Space Model

The state space model, see e.g. Meirovitch [17], referring to the reponse vector $\overline{x}$ is replaced by a state vector $\left(\overline{x}^T \dot{\overline{x}}^T\right)$. The formulation is also called the complex mode method since this formulation allows complex eigenvectors due to high damping or closed space eigen frequencies. It is seen that the equation of motion (4.2) can be rewritten as a set of first order differential equations by the state space formulation:

$$\begin{pmatrix} \dot{\overline{x}} \\ \ddot{\overline{x}} \end{pmatrix} = \begin{pmatrix} \overline{\overline{0}} & \overline{\overline{I}} \\ -\overline{\overline{M}}^{-1}\overline{\overline{K}} & -\overline{\overline{M}}^{-1}\overline{\overline{C}} \end{pmatrix} \begin{pmatrix} \overline{x} \\ \dot{\overline{x}} \end{pmatrix} + \begin{pmatrix} \overline{\overline{0}} \\ \overline{\overline{M}}^{-1} \end{pmatrix} \overline{f} \qquad (4.32)$$

or in compressed form:

$$\dot{\overline{y}} = \overline{\overline{A}}\,\overline{y} + \overline{\overline{B}}\,\overline{f} \tag{4.33}$$

where $\overline{\overline{A}}$ is a $2n$ x $2n$ matrix called the system matrix, $\overline{\overline{B}}$ is a $2n$ x n matrix and n is the number of degrees of freedom.

From the homogenous equation:

$$\dot{\overline{y}} = \overline{\overline{A}}\overline{y} \tag{4.34}$$

the complex eigenvalue problem is obtained:

$$p\,\overline{\Psi} = \overline{\overline{A}}\,\overline{\Psi} \tag{4.35}$$

where it has been assumed that $\overline{y}$ is given by: $\overline{y} = \overline{\Psi}\exp pt$ for the nonexcited model: $\overline{f} = \overline{0}$. $2n$ complex eigenvalues will exist since the system matrix $\overline{\overline{A}}$ is not positive definite. For an underdamped system the $2n$ eigenvalues p_i will be given by n conjugated pairs:

$$\begin{aligned} p_i, p_i^* &= -a_i + \mathbf{i}b_i \\ &= -\omega_i\zeta_i \pm \mathbf{i}\sqrt{1-\zeta_i^2}\,\omega_i \quad i = 1,2\ldots n \end{aligned} \tag{4.36}$$

where ω_i and ζ_i is the eigenfrequency and damping ratio of the i'th eigenmode. There will also be $2n$ complex eigenvectors, $\overline{\Psi}_i$ which will also in general consist of conjugated pairs:

$$\begin{aligned} \overline{\overline{\Psi}} &= \begin{pmatrix} \overline{\Phi}_1 & \overline{\Phi}_2 & \ldots & \overline{\Phi}_n & \overline{\Phi}_1^* & \overline{\Phi}_2^* & \ldots & \overline{\Phi}_n^* \\ p_1\overline{\Phi}_1 & p_2\overline{\Phi}_2 & \ldots & p_n\overline{\Phi}_n & p_1^*\overline{\Phi}_1^* & p_2^*\overline{\Phi}_2^* & \ldots & p_n^*\overline{\Phi}_n^* \end{pmatrix} \\ &= \begin{pmatrix} \overline{\Psi}_1 & \overline{\Psi}_2 & \ldots & \overline{\Psi}_n & \overline{\Psi}_1^* & \overline{\Psi}_2^* & \ldots & \overline{\Psi}_n^* \end{pmatrix} \end{aligned} \tag{4.37}$$

where $\overline{\Phi}_i$ is the i'th eigenvector of the damped eigenvalue problem:

$$(p_i^2\overline{\overline{M}} + p_i\overline{\overline{C}} + \overline{\overline{K}})\overline{\Phi}_i = \overline{0} \tag{4.38}$$

In the state space formulation it can be shown, see e.g. Meirovitch [17], that the following orthogonality conditions are fulfilled:

$$w_{ij} = \overline{\Psi}_j^T\overline{\overline{V}}\overline{\Psi}_i = 0 \quad \text{for } i \neq j \tag{4.39}$$

$$e_{ij} = \overline{\Psi}_j^T\overline{\overline{D}}\overline{\Psi}_i = 0 \quad \text{for } i \neq j \tag{4.40}$$

where w_{ij} and e_{ij} are elements in the diagonal matrices, (w_{ii}) and (e_{ii}) and:

$$\overline{\overline{V}} = \begin{pmatrix} \overline{\overline{M}} & \overline{\overline{0}} \\ \overline{\overline{0}} & \overline{\overline{M}} \end{pmatrix} \tag{4.41}$$

$$\overline{\overline{D}} = \begin{pmatrix} \overline{\overline{0}} & \overline{\overline{M}} \\ \overline{\overline{K}} & \overline{\overline{C}} \end{pmatrix} \tag{4.42}$$

These orthogonality properties mean that the equation of motion can be solved for any excitation by decoupling of (4.33) and (4.34) which by pre-multiplication by $\overline{\overline{V}}$ can be rewritten as:

$$\overline{\overline{V}}\dot{\overline{y}} + \overline{\overline{D}}\overline{y} = \overline{0} \tag{4.43a}$$

$$\overline{\overline{V}}\dot{\overline{y}} + \overline{\overline{D}}\overline{y} = \begin{pmatrix} \overline{\overline{0}} \\ \overline{\overline{I}} \end{pmatrix} \overline{f} \tag{4.43b}$$

where $\overline{\overline{V}}$ and $\overline{\overline{D}}$ are related to the system matrix by $\overline{\overline{A}} = -\overline{\overline{V}}^{-1}\overline{\overline{D}}$. If $\overline{y}$ is replaced by $\overline{y} = \overline{\overline{\Psi}}\overline{z}$ and if the (4.43a) and (4.43b) are pre-multiplied by $\overline{\overline{\Psi}}^T$ then the following is obtained:

$$p_i w_{ii} + e_{ii} = 0 \quad i = 1, 2 \ldots 2n \tag{4.44a}$$

$$w_{ii}\dot{z}_i + e_{ii} z_i = g_{ij} f_j \quad i, j = 1, 2 \ldots 2n \tag{4.44b}$$

where g_{ij} is the element of $\overline{\overline{\Psi}}^T \begin{pmatrix} \overline{\overline{0}} \\ \overline{\overline{I}} \end{pmatrix}$. Inserting (4.44a) into (4.44b) gives the final set of $2n$ decoupled equations:

$$\dot{z}_i - p_i z_i = \frac{g_{ij} f_j}{w_{ii}} \quad i = 1, 2 \ldots 2n \tag{4.45}$$

From the decoupled equations z_i will be found as conjugated pairs since the eigenvector will in general be given as complex conjugated pairs, $\overline{\Psi}_i$ and $\overline{\Psi}_i^*$. This means that the response of a given excitation, see e.g. Langen and Sigbjørnsson [4], can be found as:

$$\overline{y} = \sum_{i=1}^{n} \overline{\Psi}_i z_i + \overline{\Psi}_i^* z_i^* \tag{4.46}$$

Instead of calculating the reponse by the complex mode method given by (4.46), the response can be calculated directly by the system matrix as described in Meirovitch [17].

The equations (4.22) and (4.25) to (4.28) do also apply to the state space formulation but with other expressions for the impulse response function and complex frequency response function of the modal coordinate, see e.g. Langen and Sigbjornsson [4]:

$$h_i(t) = \exp\left(p_i(t-\tau)\right) \tag{4.47}$$

$$H_i(\omega) = \frac{1}{w_{ii}(\mathbf{i}\omega - p_i)} \tag{4.48}$$

For the underdamped system there are n conjugated pairs of impulse response functions and frequency response functions due to n conjugated pairs of roots p_i, p_i^*.

4.5 The Effect of a Limited Number of Modes

It has been shown that a discrete model of n degrees of freedom can be decoupled into n modes. The problem in system identification is that no knowledge exists of the number of degrees of freedom which a model of a given structure should contain. However, it is often possible to determine the number of significantly excited modes by an analysis of the spectral peaks in the frequency domain. Those modes are called dynamically excited modes while the modes for which the dynamic amplification is negligible are called statically excited. The statically excited modes will typically be higher modes with only local importance of the modelling of the structure. This means that they will only be of importance for the prediction of local stresses and member forces. A method taking these local effects into account is the mode acceleration method, see Vugts et al. [18] and Anagnostopoulos [19].

By ignoring the terms in modal coordinates containing time derivatives it can be shown that a quasi static approximation of the statically excited modes is given by:

$$\begin{aligned} \ddot{z}_i + 2\zeta_i\omega_i\omega\dot{z}_i + \omega_i^2 z_i &= \frac{\overline{\Phi}_i^T\overline{f}}{\overline{\Phi}_i^T\overline{\overline{M}}\overline{\Phi}_i} \\ &\Downarrow \\ z_i \approx z_i^s &= \frac{1}{\omega_i^2}\frac{\overline{\Phi}_i^T\overline{f}}{\overline{\Phi}_i^T\overline{\overline{M}}\overline{\Phi}_i} \end{aligned} \tag{4.49}$$

Index s here refers to static contribution and the eigenmodes applied are the unweighted mode shapes. The calculated response by modal superposition then becomes:

$$\overline{x} \approx \sum_{i=1}^{nn} \overline{\Phi}_i z_i^d + \sum_{i=nn+1}^{n} \frac{1}{\omega_i^2}\frac{\overline{\Phi}_i\overline{\Phi}_i^T\overline{f}}{\overline{\Phi}_i^T\overline{\overline{M}}\overline{\Phi}_i} \tag{4.50}$$

Index d refers to dynamic contribution up to mode no. nn. The modes, which have been approximated by a static solution, should correspond to eigenfrequencies much larger than the excitation frequencies. In offshore structures this will often be the case since the excitation frequency will be small compared to the magnitude of eigenfrequencies.

The effect of a limited number of modes can also be considered in the frequency domain by approximating the influence of higher modes with a quasi-static contribution. If for instance the model is assumed to be excited by a harmonic force vector the response of the j'th degree of freedom can be shown to be given by:

$$x_j(t) = X_j(\omega)\exp(\mathbf{i}\omega t) = \sum_{i=1}^{N} \frac{\Phi_{ji}\Gamma_i \exp(\mathbf{i}\omega t)}{\omega_i^2 - \omega^2 + 2\omega\omega_i\zeta_i\mathbf{i}} \tag{4.51}$$

If the eigenfrequencies of the higher modes are well above the excitation frequency the amplitude spectrum can be approximated by:

$$X_j(\omega) \approx \sum_{i=1}^{nn} \frac{\Phi_{ji}\Gamma_i}{\omega_i^2 - \omega^2 + 2\omega\omega_i\zeta_i\mathbf{i}} + \sum_{i=nn}^{n} \frac{\Phi_{ji}\Gamma_i}{\omega_i^2} \tag{4.52}$$

for $\omega_i \gg \omega$. nn is the number of modes which is assumed to be dynamically excited. The concept is illustrated in figure 4.3. In Ewins [3] the concept is considered in a graphical way and is further described in Salter [20]. If the excitation vector contains more than one harmonic or is random, then the approximated quasi-static terms of the l'th mode will contain a coupling to the ith mode and thus also be more complicated.

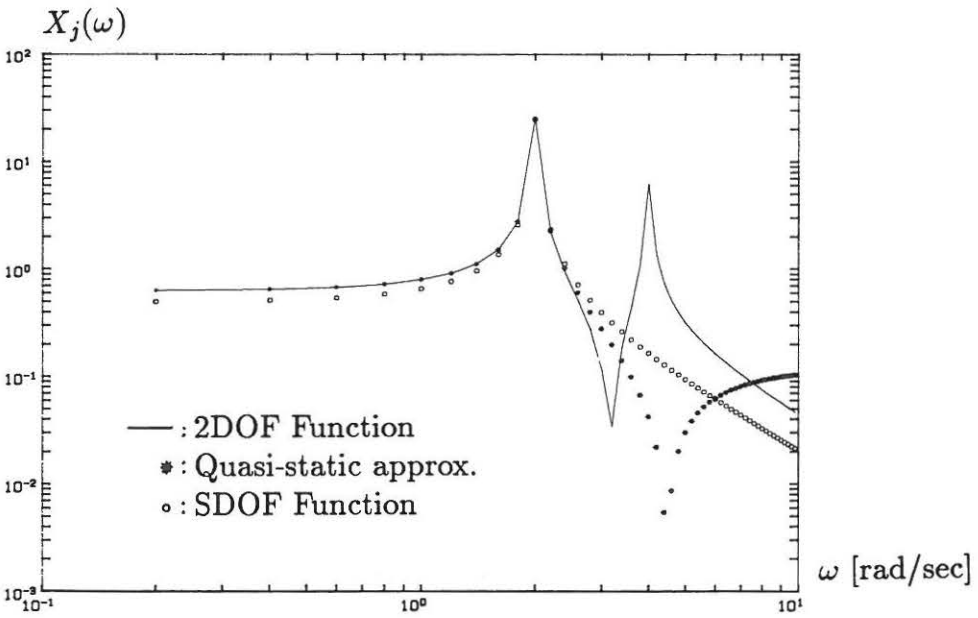

Figure 4.3. Quasi-static approximation of the influence of higher modes.

4.6 Nonlinear Damping and Stiffness Mechanisms

In this thesis as in many others the main assumption is that a linear system is assumed even though everybody knows it is not the case for real structures. However, the linear case forms a unique and well defined class of models, while the class of nonlinear models is very wide. Furthermore, the nonlinear case can often be linearized for the operating range in which the structure is found to act. Since modelling in practice is restricted to linear models the purpose here is to present some of the main principles of nonlinearities.

With respect to the description of damping mechanism of structures, it is based more on computational comfort and empirical knowledge than on physical facts while the linear stiffness assumption can often be justified. From an engineering point of view the aim must be to develop and apply damping models which give a sensible ratio between the description of reality and the costs of this description.

An SDOF system is considered for the general qualitative presentation of nonlinearities. The following sorts of nonlinearities are considered:

1. Coulomb damping.
2. Drag damping (nonlinear viscous damping).
3. Radiation damping.
4. Cubic stiffness.

4.6.1 Coulomb Damping

The damping force is given by:

$$f_D = C^{Cou} \frac{\dot{x}}{|\dot{x}|} F \tag{4.53}$$

where F is the applied friction force. The magnitude of the damping force is seen to be constant, while the damping force in the viscous case is velocity dependent. The equations of motion can only be solved in the case of SDOF systems with or without sinusoidal excitation. Consequently, in general the equation of motion must be solved numerically. In figure 4.4a the simulated free response of a system with two degrees of freedom is shown. The free vibration of a Coulomb damped system is characterized by a linear envelope curve of the decay curve. For an SDOF system the logarithmic decrement can be shown, see e.g. Langen and Sigbjornsson [4] to be given by:

$$\delta = \ln \frac{A_n}{A_{n+1}} = \ln \frac{A_n}{A_n + 4N/k} \tag{4.54}$$

where A_n and A_{n+1} are two subsequent amplitudes of the free vibration and k is the spring constant.

For a sinusoidal excitation a numerical simulation study shows that Coulomb damping causes a transportation of energy into a higher frequency range corresponding to peaks at a multiple of the excitation frequency and possibly also of excited eigenfrequencies, as seen in figure 4.4b.

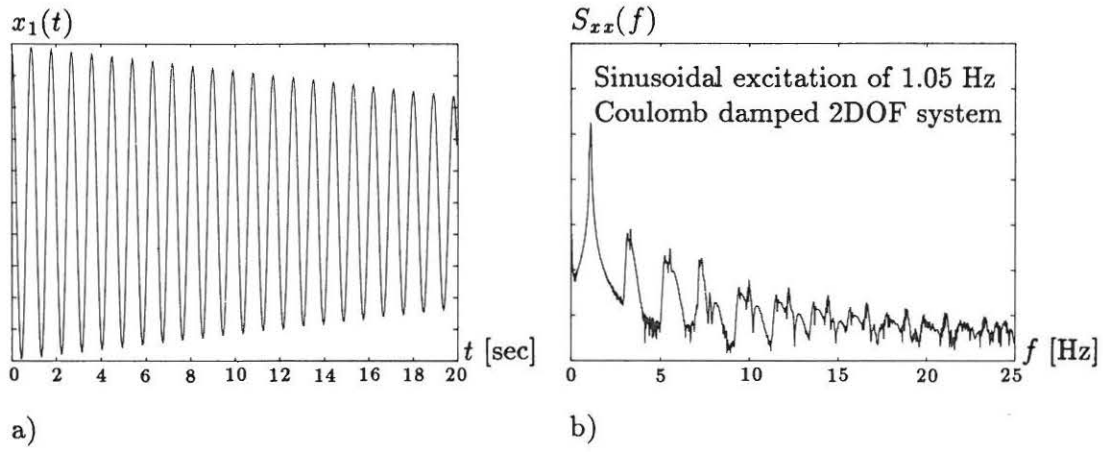

Figure 4.4. a) Free vibration for 2DOF system with Coulomb damping. b) Response spectrum for 2DOF system with sinusoidal excitation. Simulation by PROGSIM [21].

Parts of the damping mechanism in the foundation of structures and in the joints can be adequately described by the Coulomb damping model. This is therefore a very important model even though it creates numerical difficulties.

4.6.2 Drag Damping

The drag damping (/nonlinear viscous damping) model is described by a damping force:

$$f_D = C^{Drag}|\dot{x}|\dot{x} \tag{4.55}$$

The name drag damping arises due to the damping contribution from the drag term in Morison's equation, see Morison et al. [22]. As far as known the equation of motions cannot be solved analytically for drag damped systems. However, numerically the response can be simulated as shown in the figure 4.5 for a free vibration and a sinusoidal excitation. For a harmonic excitation the presence of the nonlinearity due to the drag damping is indicated by peaks at a multiple of the excitation frequency and possibly also the low eigenfrequencies, see figure 4.5b.

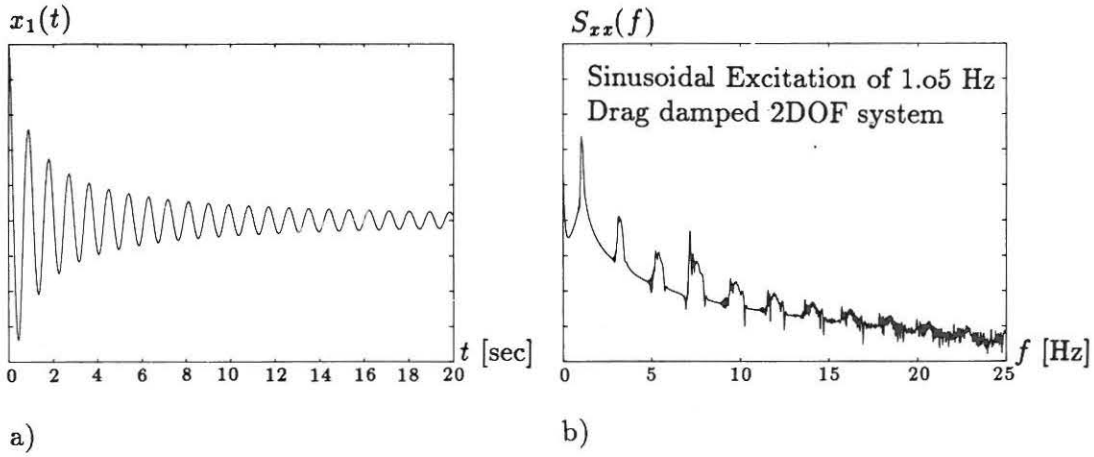

Figure 4.5. a) Simulated free vibration b) Simulated response spectrum for a harmonic excitation. 2DOF system with drag damping. Simulated by PROGSIM [21].

The source of drag damping is due to the fluid structure interaction. Morison's equation for a vertical flexible cylinder with a diameter D in a horizontal current in a fluid with density ρ is given by:

$$q = \frac{1}{2}C_D D\rho(u-\dot{x})|u-\dot{x}| + C_M\frac{\pi}{4}D^2\rho\dot{u} - \rho\frac{\pi}{4}D^2(C_M-1)\ddot{x} \tag{4.56}$$

where C_D and C_M are coefficients depending on the fluid-structure problem given by e.g. a sea state and structural characteristics, such as the diameter D and the relative roughness, see Sarpkaya and Isaacson [23], Jensen [1]. q is the force per unit length of the cylinder.

From the terms in (4.56) including $\dot{x}$ it follows directly that there will be a damping contribution given by:

$$q_D = \frac{1}{2}C_D D\rho\frac{u-\dot{x}}{|u-\dot{x}|}(\dot{x}^2 - 2u\dot{x}) \tag{4.57}$$

If $u \gg \dot{x}$ it is seen that this damping force can be approximated by:

$$q_D = -\frac{1}{2}C_D D\rho\frac{u-\dot{x}}{|u-\dot{x}|}2u\dot{x} \tag{4.58}$$

which means that this part of the hydrodynamic damping will be a viscous term coupled with the severeness of the sea state through the velocity u. However, if $\dot{x} \sim u$ this part of the hydrodynamic damping will contain a drag term as well as a viscous term which will both depend on the sea state through the fluid velocity. If necessary the nonlinear drag terms can be approximated by linear terms due to an equivalent linearization, see e.g. Jensen [1].

4.6.3 Radiation Damping

Radiation damping includes damping due to energy dissipation by waves into surrounding media of the structure. In the case of offshore structures radiation damping will be due to fluid structure and soil structure interaction and it can be shown to be viscous, Petrauskas [24].

It seems that radiation damping due to the soil is less well investigated and the importance of this contribution is rather uncertain. The radiation damping is less important than the internal damping of offshore structures at the Mexican Gulf according to Cook [5].

While radiation damping from the structure into the soil is less known, an expression can be developed for the fluid structure interaction. According to Cook [5], Cook and Vandiver [25] and Vandiver [26], the damping ratio of the ith mode for a vertical cylinder can be shown to be given by:

$$\zeta_i = \frac{cc_{ii}}{2\omega_i m_{ii}} \tag{4.59}$$

where:

$$cc_{ii} = \frac{\pi\rho\omega}{\exp(2kh)+4kh}\Big[\int_{-h}^{0} D(z)p_1(\frac{kd}{2})\phi_i(z)\exp(k(z+h))dz \int_{-h}^{0}\phi(z)\exp(k(z+h))dz\Big] \tag{4.60}$$

ω: Frequency of radiated waves.

d: Water depth.

k: Wave number (2π over the wave length).

z: Vertical coordinate,positive upwards.

$D(z)$: Variable cylinder diameter.

$\phi_i(z)$: The i'th mode shape as a function of z.

$p_1(\frac{kd}{2}) = \frac{\pi}{2}(\frac{kd}{2})^2$ for $\frac{kd}{2} \ll \frac{1}{2}$.

This expression is valid when the radiating waves are considered to be deep water waves for an inviscoid fluid without any interaction with the incoming waves.

Since the expression is evaluated for an inviscoid fluid it will only be valid for sea states where the ratio between the wave length and the cylinder diameter is less than about 5. For increasing wave length corresponding to a more severe sea state the expression will not be valid, and the importance of radiation damping will decrease while the damping due to the drag term in Morison's equation will increase, Jensen [1].

4.6.4 Cubic Stiffness

The cubic stiffness model can be written as a restoring force given by:

$$f_R = k_1 x + k_2 x^3 \tag{4.61}$$

The undamped lightly nonlinear system can be considered with the equation of motion given by:

$$\ddot{x} + \omega_n^2 x + \epsilon x^3 = C \cos(\omega t) \tag{4.62}$$

This is called Duffing's equation. By the perbutation method it can be shown that the response will be given by:

$$x = \sum_{n=1,3,6}^{\infty} A_n \cos(n\omega t) \tag{4.63}$$

where A_n will depend upon ϵ, ω_n and ω. It is seen that the excitation energy will be extended to a higher frequency range. The cubic stiffness model can in the general case only be handled numerically.

Since the structure/soil interaction is generally characterized by nonlinear stiffness the cubic stiffness model will be a better approximation than the linear stiffness model (disregarding the numerical problems).

4.7 References

[1] Jensen, J. L., "An Assessment of Morison's Equation", (in Danish), Institute of Building Engineering and Structural Technology, University of Aalborg, Denmark, 1987.

[2] Juang, J. N. and C. T. Sun, "System Identification of Large Flexible Structures Using Simple Continuum Models", Journal of Astronautical Sciences, Vol. XXX1, no. 1, Jan-Mar., 1983.

[3] Ewins, D. J., "Modal Testing: Theory and Practice", Research Studies Press, England, 1984.

[4] Langen,I., R. Sigbjornsson, "Dynamisk Analyse av Konstruktioner", (In Norwegian), SINTEF, Avdeling for Konstruksjonsteknikk, Tapir, 1979.

[5] Cook, M. F., "Damping Estimation, Response Prediction and Fatigue Calculation of an Operational Single Pile Platform", M.Sc. Thesis at Massachusetts Inst. of Techn., 1978.

[6] Angelides, D. C, and J. M. Roesset, "Nonlinear Dynamic Stiffness of Piles", Research Report R80-13, Dept. of Civil Eng., Massachusetts Institute of Technology, 1980.

[7] Blaney, J. S. and E. Kausel and J. M. Roesset, "Dynamic Stiffness of Piles", 2nd Int. Conf. on Numerical Methods in Geomechanics, Blacksburg VA, 1976.

[8] Nowak,M., "Effect of Soil on Structural Response to Wind and Earthquake", Earthquake Engineering and Structural Dynamics, Vol. 3, 1974.

[9] Nelson, F. C. and Greif R., "Damping Models in Computer Programs", Structural Mechanics Software Series, Vol. 3, ed: N. Perrone and W. Pilkey, University Press of Virginia, 1979(?).

[10] Caughey, T. K., "Classical Modes in Damped Linear Systems", J. Appl. Mech., Vol. 27, 1960.

[11] Malhotra, A. and J. Penzien, "Nondeterministic Aanlysis of Offshore Structures", J. Eng. Mech. Div., Vol. 96, EM6, ASCE, 1970.

[12] Thomson, W. T., T. Calkins, and D. Caravani, "A Numerical Study of Damping", Earthquake Eng. and Struct. Dynamics, Vol. 3, 1974.

[13] Duncan, P. E. and R. E. Taylor, "Short Communication - A Note on the Dynamic Analysis of Nonproportionally Damped System", Earthquake Eng. and Struct. Dynamics, Vol. 7, 1979.

[14] Warburton, C. B. and Soni, S. R., "Errors in Response Calculation for Nonclassically Damped Structures", Earthquake Eng. and Struct. Dynamics, Vol. 5, 1977.

[15] Gundy, W. E., T. D. Schartcon and R. L. Thomas, "Damping Measurements of An Offshore Platform", OTC 3863, Houston, USA, 1980.

[16] Lang, G. Fox, "Demystifying Complex Modes", Sound and Vibration, Jan., 1989.

[17] Meirovitch, L., "Elements of Vibration Analysis", 2nd ed., McGraw-Hill Book Company, 1986.

[18] Vugts, J. H., I. M. Hines, R. Nataraja, and W. Schumm, " Modal Superposition v. Direct Solution Techn. in The Dynamic Analysis of Offshore Structures", BOSS 79, Second Int. Conf. on Behaviour of Offshore Structures, Imperical College, London, UK, 1979.

[19] Anagnostopoulos, S. A., "Wave and Earthquake Response of Offshore Structures: Evaluation of Modal Solutions", J. of the Struct. Div., Proc. of the ASCE, Oct. 82, ST 10, ASCE, 1982.

[20] Salter, J. P., "Steady State Vibration", Kenneth Mason Press, 1969.

[21] PROGSIM, simulation program of nonlinear MDOF systems based on the Runge Kutta Method, developed by A. Rytter, Institute of Building Engineering and Structural Technology, University of Aalborg, 1989.

[22] Morison, J. R., M. P. O'Brien, J. W. Johnson and S. A. Schaaf, "The Forces Excerted By Surface Waves On Piles", Petroleum Transactions, Vol. 189, AIME, 1950.

[23] Sarpkaya, T. and M. Isaacson, "Mechanics of Wave Forces on Offshore Structures", Van Nostrand Reinhold Company, 1981.

[24] Petrauskas, C., "Hydrodynamic Damping and Added Mass for Flexible Offshore Platforms", U.S. Army Coastal Engineering Research Centre, Report CERC-TP-76-18, Oct., 1976.

[25] Cook, M. F. and J. K. Vandiver, "Measured and Predicted Dynamic Response of a Single Pile Platform to Random Wave Excitation", Offshore Technology Conference, Houston, USA, 1982.

[26] Vandiver, J. K., "Prediction of the Damping Controlled Response of Offshore Structures to Random Excitation", Society of Petroleum Engineers Journal, Feb., 1980.

5. EXCITATION, MEASUREMENT AND SIGNAL PROCESSING

The three topics in the title are not directly integrated in system identification but they are nevertheless vital for the results of the system identification. It is necessary to have an understanding of those topics to choose a proper structural model and a proper system identification method. Finally it will often be possible to explain inexplainable results or errors in the system identification process by the performed excitation, measuring or signal processing. Another aspect is that experimental considerations are also important because it is expensive to repeat an instrumentation and perform excitation and measurings. Thus, the three topics will be dealt with here, although only in principle, since they will be large topics in themselves.

The chapter is divided into six parts. In section 5.1 the choice and the importance of proper excitation are discussed. Hence a short review is given about the instrumentation in section 5.2. The signal processing is discussed in section 5.3 after the basic principles of obtaining measurements have been established. Afterwards in section 5.4 the statistics of the obtained data are presented. In section 5.5 the random decrement technique is explained and finally, in section 5.6, some relevant noise models are presented and discussed.

5.1 Choice of Excitation

An excitation is necessary to obtain a structural response. The excitation should ideally be chosen under the following considerations:

- All eigenmodes of interest should be excited and, if possible no other.
- If the structure is thought to be nonlinear the level of excitation should correspond to the operating range of the structure. If possible several levels of excitation should be investigated.
- The excitation should be well defined and possible to measure.

The excitation of all relevant modes is ensured by the frequency content in the excitation signal. The frequency content should be concentrated at such frequencies where the structural response has maximum gradient with respect to the structural parameters to be estimated. This will lead to the most precise estimates as shown

in chapter 3. For an SDOF system this means that the frequency content should be chosen such that :

$$\text{Maximum gradient w.r.t. the eigenfrequency} : \frac{\partial |H_0(f)|}{\partial f_0}$$

$$\text{Maximum gradient w.r.t. the damping} : \frac{\partial |H_0(f)|}{\partial \zeta_0}$$

are obtained. In figure 5.1 the gradients is shown for an SDOF system with either $f_0 = 0.4$ Hz or $\zeta_0 = 0.01$ for different frequencies. Not surprisingly it is seen that maximum information about the eigenfrequency is obtained at resonance where the response also is largest. The damping ratio is seen to be best determined in a range about the eigenfrequency. The range becomes narrower for decreasing damping ratio which makes this range even more important.

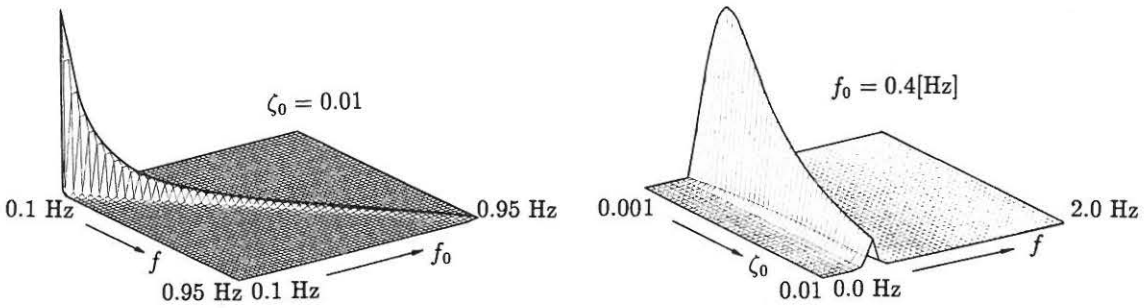

Figure 5.1 Gradient of magnitude of frequency response function with respect to eigenfrequency and damping ratio versus excitation frequencies.

Two fundamental principles of excitation are now discussed with respect to this and the former requirements. The first principle will be ambient excitation due to waves while the second will be external excitation which can be created by commercially available vibrators.

5.1.1 Ambient Excitation: Waves

An excitation such as waves has the obvious advantage that the excitation level will represent an operating range which the structure will experience many times in its lifetime. The wave load will furthermore always be present and cause response. However, the fundamental disadvantage is that the wave load is very difficult to measure, the observation of the excitation is in practice restricted to either mea-

surement of the time series of the surface elevation and the wave direction or the sea state characteristics which are given by a significant wave height H_s and period T_s. The latter is less expensive to obtain but also less informative.

However, during the last thirty years attempts have been made to obtain:

- A wave theory which can describe the waves from the sea state characteristics. The waves can be represented as a time series or as a wave spectrum. The theory for deep water waves consists of a part which deals with harmonic waves, Airy's wave theory and the 5th order Stokes' waves, and a second semi-empirical part which deals with random waves in the frequency domain, most well known as the model spectra: The Pierson-Moskowitz spectra and the Jonswap spectra.
- A wave load model which can establish the link between measured or regenerated waves and a wave load. This is well known as the Morison equation which for a vertical flexible cylinder excited by a horizontal harmonic oscillating wave is given as the force per unit length:

$$q = \underbrace{\frac{1}{2}C_D D\rho(u-\dot{x})|u-\dot{x}|}_{\text{Drag term}} + \underbrace{C_M\frac{\pi}{4}D^2\rho\dot{u} - \overbrace{\rho\frac{\pi}{4}D^2[C_M-1]}^{\text{Added mass}}\ddot{x}}_{\text{Inertia term}} \tag{5.1}$$

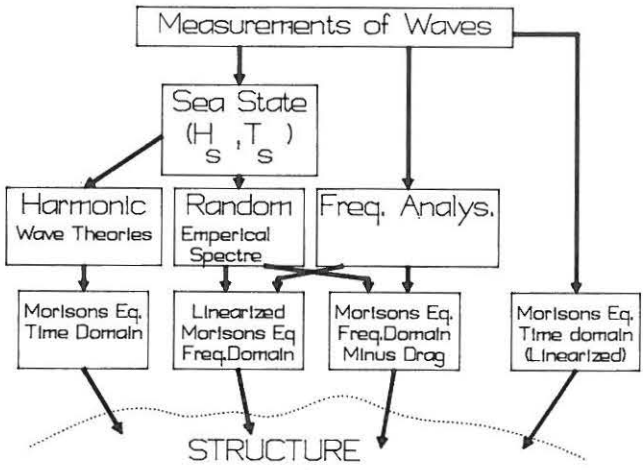

Figure 5.2 Survey of wave load modelling.

C_D and C_M depend, among other factors of the flow problem, on the sea state given by Reynolds' number, $\mathbf{Re} = \frac{UD}{\nu}$ and the Keulegan Carpenter number, $\mathbf{K} = \frac{UT}{D}$ where U and T are a characteristic velocity and period representing the sea state, for further reference see Sarpkaya and Isaacson [1], Jensen [2]. The Morison equation is said to be valid if $\mathbf{K} > 5$, otherwise another theory, such as stream function theory,

has to be applied taking diffraction effects into account.

The Morison equation was originally developed for a vertical cylinder in a harmonic oscillating uniform horizontal flow, see Morison et al. [3]. Since then, during the years, its application has been generalized to include three-dimensional random waves acting on inclined structural members in spite of:

1. The Morison equation cannot fully describe the force signal for a simple harmonic oscillating uniform flow.
2. Knowledge about the coefficients C_D and C_M is difficult to obtain for even simple problems. This means that the prediction of a wave force becomes unreliable.
3. The Morison equation becomes really uncertain in random waves. Even when C_D and C_M are estimated from full-scale measurements a variation coefficient of about 17-35 % is found, Heidemann et al. [4] and Jensen [2].

Another drawback is that the relation between the wave load and the fluid velocity given by the drag term is seen to be nonlinear. The wave load will furthermore interact with the structural response. This means that a uniquely determined transfer function cannot be established between the wave load and the surface elevation and hence neither between the structural response and the wave elevation process.

However, this problem can be ignored if the drag term can be linearized with good approximation. In such cases Morison's equation is replaced by the force per unit length:

$$q = \underbrace{\frac{1}{2}\rho D\sqrt{\frac{8}{\pi}}C_D\sigma_{u-\dot{x}}u}_{\text{Linearized drag term}} + \underbrace{C_M\frac{\pi}{4}D^2\rho\dot{u} - \overbrace{\rho\frac{\pi}{4}D^2[C_M-1]}^{\text{Added mass}}\ddot{x}}_{\text{Inertia term}} \tag{5.2}$$

The linearization is valid when the drag term is of minor importance. The wave load model simplifies substantially if the drag term can be neglected and if deep water waves can be assumed (water depth more than four times larger than wave length). The drag contribution can be neglected if $\mathbf{K} < 10$, Jensen [2]. In such cases the spectrum of the total wave load Q on a vertical cylinder can be shown to be:

$$S_{QQ}(f) = \left(\frac{\pi}{4}\rho g D^2 C_M\right)^2 S_{\eta\eta}(f) \tag{5.3}$$

see e.g. Sarpkaya and Isaacson [1]. In the case of a stationary sea state, the wave spectrum can be given by the spectrum of the Pierson-Moskowitz form, see Sarpkaya and Isaacson [1]:

$$S_{\eta\eta}(f) = Af^{-5}\exp\left(-Bf^{-4}\right) \tag{5.4}$$

where A and B are constant coefficients related to the sea state. When the sea state is only quasi-stationary the spectrum should be modified to the Jonswap form. This will typically be the case in the North Sea when a storm is being built up. In this case the quasi-stationary time interval will be about 3-5 hours, see Burcharth and Larsen [5].

In the above case the wave load process can be considered to be Gaussian distributed since the wave elevation is known to be Gaussian distributed. This is important with respect to signal processing and system identification. In cases where the drag term cannot be neglected the wave load will be non-Gaussian. However, in Krenk and Gluver [6], it is indicated that the response of the linear system due to such an excitation will be approximately Gaussian for lightly damped systems. Thus in general it will be acceptable to assume Gaussian distributed response of offshore structures since they can be considered to be lightly damped.

As shown in figure 5.3 the wave spectrum will have a distinct peak but will generally not be either narrow-banded or broad-banded. The peak frequency will typically be in the range 0.05 (severe sea state) to 0.15 Hz (mild sea state) in the Danish sector of the North Sea. In the case of a non-negligible drag term there will not be affinity between the wave spectrum and the wave load spectrum. Instead there will be secondary peaks as discussed in chapter 4.6. This may lead to excitation of higher structural modes.

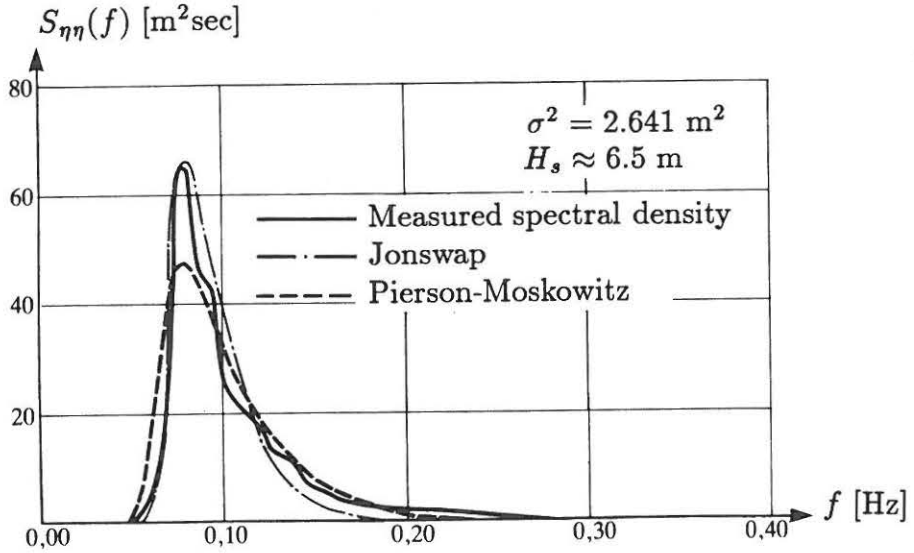

Figure 5.3 Typical wave spectrum during storm in the North Sea, DS449 [7].

With the exception of very simple cases the conclusion is that the wave load has a very complicated form. However in a simple case such as a monopile with ignorable drag loading it seems possible to apply a qualitative model. This means that wave excitation can be transformed to a wave load and applied to a classical system identification process with a known input and output. The coefficient in the wave load spectrum will be more or less unknown but may be estimated together with

the structural parameters.

In the complicated cases with drag loading and complex geometric extension of the structure it seems more adequate to apply the simple white noise approximation, which holds for lightly damped systems. The white noise approximation will be described further in the subsequent chapters.

5.1.2 External Excitation

The external excitations can be divided into three categories:

1. Transient tests.
2. Sinusoidal excitation.
3. Random excitation.

Re 1: Transient tests. The transient tests could be made by some sort of impact or alternatively by a given initial displacement of the structure (snap back testing). A third way to obtain a free decay is to apply a forced excitation and then remove it to obtain the transient decay. The disadvantage of transient tests is that the response will also be due to the simultaneous wave excitation and the influence of this will increase during the transient decay. Another disadvantage is that it will often only be possible to excite the lowest eigenmodes.

Re 2: Sinusoidal excitation. The sinusoidal excitation could be performed with a slow change of the input frequency or as a stepwise change in frequency. The step change test aims at a determination of the dynamic amplification at discrete frequencies while the sine sweep leads to excitation of a wide range of eigenfrequencies.

The exciter for a sine sweep will typically be an eccentric mass vibrator where the excitation force will be given by:

$$f(t) = mr\omega^2 \sin(\omega t) \tag{5.5}$$

where m is the rotating mass and r is the radius of the circle described by the mass rotation. It is seen that the force amplitude will be proportional to the square of the frequency. According to Ibanez [8] the input frequency can be controlled by 0.1% of the desired value. The excitation will be distorted if the structural vibrations become large compared with the orbit of the eccentric mass. A disadvantage of the eccentric mass vibrator is that the force amplitude varies with the frequency. This means the nonlinearities will have systematic effect on an estimate of the transfer function. The eccentric mass vibrators are often limited to frequencies above, say 2 Hz.

One disadvantage of stepwise sinusoidal excitation is that it must be performed very

slowly to eliminate transients from the past excitation frequencies. This means that the test becomes very time-consuming for lightly damped systems. The transient responses from the former harmonics have to be small compared to the steady state response of the present harmonic response. A low eigenfrequency and damping ratio is seen to give a high time interval as shown in figure 5.4. The time interval will be further increased if a resonance peak has been passed in the test. Figure 5.4 is based on an approximated expression developed in appendix 5.1.

Another disadvantage of this method is that it must be used with care since a sinusoidal excitation at resonance could cause significant damage of the structure.

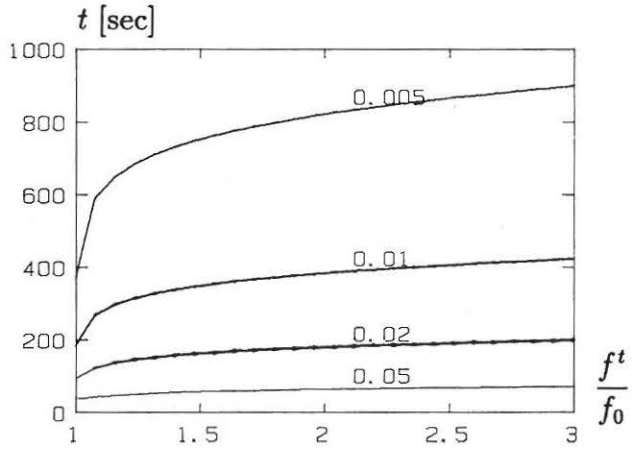

Figure 5.4. Approximate minimum time duration for slow sine sweep for different damping ratios. Condition: Transient response of former frequency input less that 1% of the response of the present frequency input. Excitation frequency $f=f_0$ for $t<0$ and $f=f^t$ for $t\geq 0$.

Re 3: Random excitation. The random excitation could be performed by repeated pulses or by a random signal input to some linear hydraulic vibrator. The disadvantage of hydraulic vibrators are that they are more expensive than the former eccentric mass vibrator. The advantage is that a wide range of eigenfrequencies are excited at one time.

So far single point excitation has been discussed. Instead of the single point excitation several vibrators can be applied at the same time to isolate one single mode. This is called the phase-resonance technique, Kennedy and Pancu [9] and Lewis and Wrisley [10]. If a single mode is excited then it is possible to measure the mode shape directly and apply an SDOF assumption to estimate the eigenfrequency and the damping ratio. It can be shown, see e.g. Kozin and Natke [11] that a single mode is excited if the excitation is given by:

$$\overline{f}(t) = -\omega_i \overline{\overline{C}} \overline{\Phi}_i \sin(\omega_i t) \tag{5.7}$$

This method is popular in the aerospace and car industry, where it is typical that several exciters are applied. The fundamental drawback is that the proper exci-

tation is unknown since the mode shapes and the damping matrix are unknown. The traditional way to cope with this problem is to use the fact that the reponse will be 90° out of phase with the force. Another disadvantage is that the excitation points may have to be placed under the water surface to excite a given mode. Thus, with respect to offshore structures the conclusion is that a single point excitation technique should be applied due to the disadvantages of the phase-resonance technique.

5.1.3 Conclusion

When structural measurements are made most owners of platforms prefer ambient excitation since the platform is assumed to be resistant to such loading, Ting and Sunder [12]. This is a strong argument for concentrating on identification methods based on ambient excitation. Another strong argument for the ambient excitation is that, per definition, it excites the structure in its operating range. Furthermore, all the interaction effect between waves, structure and foundation are included in the measured response. The argument for applying an external excitation is that the ambient excitation cannot be measured or estimated very well. If both sorts of excitation are applied it may perhaps be possible to estimate the importance of the different interaction effects. Consequently, in this thesis both sort of excitation are regarded as a realistic tool to provide time series to a system identification process.

With respect to the external excitation types, the sine sweep excitation seems unappropriate especially for lightly damped structures such as offshore structures. Impulse excitation or random excitation seems more appropiate since they can be performed quickly and at the same time they do only require limited structural modifications as long as the force input is moderate. Both excitation types are typically broad-banded which means that a wide range of modes can be excited. If the signal from the external excitation is measured it will be possible to eliminate the response due the simultaneous wave excitation as will be shown in section 5.6.

5.2 Instrumentation

In chapter 2 a review was given of performed instrumentations and full-scale measurements on offshore platforms during the last twenty years. The typical instrumentation consists of a set of transducers, amplifiers, recording equipment and a control system if external excitation is applied as shown in figure 5.5.

The control system is an on-line system which typically is able to give continuous information about the excitation level, the excited frequency range etc. The control system is necessary to control the excitation level if an external excitation source is applied. The control system will be based on the information obtained from the transducers measuring the response and the force transducers. However, it is also advisable to use a control system in general, since it can reveal whether or not the

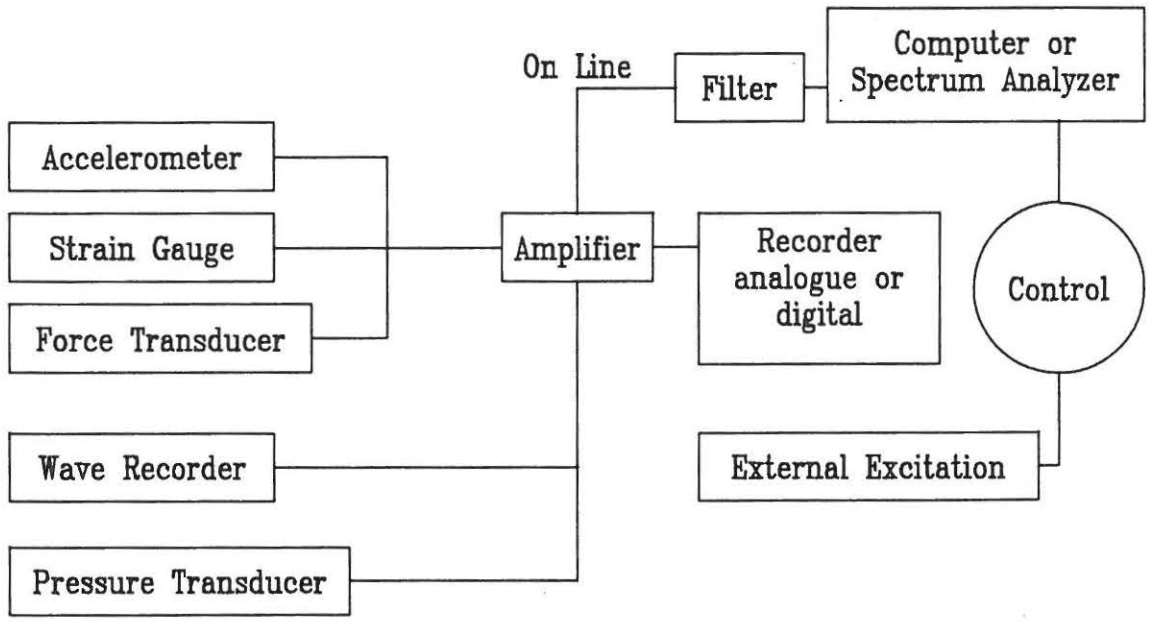

Figure 5.5. Principal instrumentation of offshore structure.

excitation and the response are what they are expected to be.

The transducers should be transducers which are able to measure low frequency signals, say frequencies down to 0.1 Hz. Furthermore, it is necessary that they are not too sensitive towards transverse vibrations which is typically a problem with the accelerometers. Equivalent response information can in principle be obtained from accelerometers as well as strain gauges even though each type of transducer should be placed at such locations where the signal to noise ratio is largest. This will in general not be the same locations. Accelerometers will be more expensive than strain gauges but have a better signal to noise ratio. Accelerometers may be mounted in connection with the test while strain gauges with benefit can be mounted during the construction of the offshore structure. This means that information about the vibrations of the structure can be obtained relatively cheap by mounting strain gauge on the the structure.

The instrumentation has to be increased if the structure has a significant spatial extension. This will be necessary to reveal all the modes of the ambient excitation and the structural response.

The recording of the signals can be done by the analog or digital method. It is advisable to apply both methods since the analog recorder retains the continuous data while the digital recorder loses some information, but on the other hand, it will often be more accurate with respect to the sampling values.

5.3 Signal Processing

After measurement and prior system identification the measured data are signal processed. This will typically be a matter of discretisation of the data with respect to time, filtering the time series and transformation into the frequency domain. The purpose of signal processing is to remove noise from the data and facilitate the interpretation of the measured data.

The general assumption will be that the time series which are processed will be realisations of ergodic random processes with respect to the first and second order statistical properties:

$$E[x(t)] = \mu_x = \lim_{T\to\infty} \frac{1}{T} \int_0^T x(t)dt \tag{5.7}$$

$$E[x(t)x(t+\tau)] = R_{xx}(\tau) = \lim_{T\to\infty} \frac{1}{T-\tau} \int_0^{T-\tau} x(t+\tau)x(t)dt \tag{5.8}$$

The ergodic condition also implies stationarity with respect to the first and second order properties. Thus weak ergodicity implying weak stationarity is assumed. In practice the response due to waves will often only be quasi-stationary with the statistical properties fluctuating within some limits. A stationarity test should therefore be performed.

Bendat and Piersol [13] suggest that a stationarity test may take the following form:

1. The sample record is divided into N equal time intervals where the data in each interval may be considered to independent.
2. A mean square value is computed for each interval aligned in a time sequence.
3. The sequence it tested for systematic trends or variations.

In general the assumption will be that the random processes have a zero mean which also implies that the correlation function becomes identical with the covariance function:

$$\mu_x = E[x(t)] = 0 \tag{5.9}$$

$$R_{xx}(\tau) = C_{xx}(\tau) = E[x(t)x(t+\tau)] \tag{5.10}$$

This means that if $x(t)$ is Gaussian distributed it will be completely statistically described by the autocorrelation function $R_{xx}(\tau)$ since all statistical moments of higher order of a Gaussian process can be decomposed into moments of first and second order, see e.g. Lin [14].

5.3.1 Discretisation in Time

The analysis of the recorded analog time signal is mainly limited to the time during the measuring where the structure is observed to control the quality of the measurements. Afterwards the analysis is mainly performed in the discrete time domain:

$$x(t\Delta) = x_t \tag{5.11}$$

where the analog records have been sampled with time intervals of Δ assuming the signal to be constant within each sampling interval. The sampling interval is primarily determined by Shannon's sampling theorem:

$$\Delta < \frac{1}{2f_{max}} \quad \text{or} \quad f_s > 2f_{max} \tag{5.12}$$

where f_s is the sampling frequency. It is necessary to satisfy (5.12) to ensure a unique interpretation of the frequency content in the signal. If this sampling condition is not satisfactory the sampled data will be aliased which means that the higher frequency content will be interpreted as a content at lower frequencies. $f_c = 2f_{max}$ is called the folding or the Nyquist frequency. Aliasing is handled by lowpass filtering the data prior to sampling to exclude high frequency content. In practice it is advisable to choose the sampling frequency to be at least twice the Nyquist frequency, $f_s = 4f_{max}$.

5.3.2 Frequency Analysis

The cross-spectral density function between two random variables is defined by:

$$S_{xy}(f) = \frac{1}{2\pi} \int_{-\infty}^{+\infty} R_{xy}(\tau) \exp(-\mathbf{i}2\pi f\tau) d\tau \tag{5.13}$$

and the inverse relation :

$$R_{xy}(\tau) = \int_{-\infty}^{+\infty} S_{xy}(f) \exp(\mathbf{i}2\pi f\tau) df \tag{5.14}$$

The two equations are together called the Wiener-Khintchine relations. The autospectral density, $S_{xx}(f)$ is obtained if $x(t) = y(t)$. From (5.14) it is seen that the mean square value is given by:

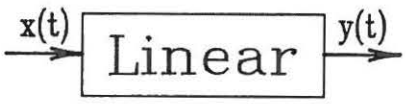

Figure 5.6. Linear stable system.

$$E[x(t)^2] = R_{xx}(0) = \int_{-\infty}^{+\infty} S_{xx}(f)df \tag{5.15}$$

The transfer function of a linear stable system with the response $y(t)$ and the excitation $x(t)$ is defined as:

$$H(f) = H_1(f) = \frac{S_{xy}(f)}{S_{xx}(f)} \tag{5.16a}$$

$$H(f) = H_2(f) = \frac{S_{yy}(f)}{S_{yx}(f)} \tag{5.16b}$$

$H(f)$ will be a complex function if the system is damped. (5.16) means that the magnitude of $H(f)$, the gain function can be found as:

$$|H(f)|^2 = H_1(f)H_2(f)^* = \frac{S_{yy}(f)}{S_{xx}(f)} \tag{5.17}$$

(5.16) and (5.17) indicate that the magnitude of the transfer function can be obtained in three different ways. In Bendat and Piersol [15] it is shown that if the measurements are distorted by noise then (5.17) should not be used to get the best estimates of the transfer function. Instead the estimate of the transfer function H_1 should be used when noise is supposed to dominate the response while H_2 should be used when the excitation is thought to be distorted by noise. If the noise problem is highly frequency dependent the two estimates can be combined into one better estimate.

The two procedures given by (5.16a) and (5.16b) should theoretically give the same transfer function but in practice this is not the case. The coherence function is introduced as a measure of a perfect uniqueness between the excitation and response:

$$\gamma^2(f) = \frac{H_1(f)}{H_2(f)} = \frac{|S_{yx}(f)|^2}{S_{xx}(f)S_{yy}(f)} \tag{5.18}$$

If the uniqueness is perfect then $\gamma^2(f) = 1$ otherwise the coherence will lie between zero and one. The coherence will be less than one in the following cases:

1. Noise in the measurements.
2. Unknown excitation.
3. Nonlinearities in the system giving the response.
4. Numerical errors in the frequency analysis.

Points 1 and 2 will be further discussed in section 5.6 while point 4 will be discussed in this section. Point 3 is briefly discussed in chapter 4 and 9.

The frequency analysis, see Ljung [17], Bendat and Piersol [13],[15] is usually performed by Fast Fourier Transformation technique (FFT), see Newland [16] and Rabiner and Gold [18].

The frequency domain analysis is in practice based on discrete spectra since the measured data have been sampled at discrete time instants. The discrete spectral estimate is obtained from the discrete Fourier transformed of the time series:

$$\begin{aligned} X(f_k) &= \sum_{r=-\infty}^{+\infty} x(r\Delta)\exp\left(-\mathbf{i}2\pi f_k r\Delta\right)\Delta \\ &\approx \sum_{r=0}^{N-1} x_r \exp\left(-\mathbf{i}2\pi f_k r\Delta\right)\Delta \\ x_r &= x(r\Delta) \text{ for } r = 0,1,2,\ldots N-1 \\ x_r &= 0 \text{ for } r < 0 \text{ and } r > N-1 \end{aligned} \tag{5.19}$$

which leads to the spectral estimate:

$$S_{xx}(f_k) = X_k^* X_k \quad k = 0,1,2\ldots N-1, \quad f_k = \frac{k}{T} = \frac{k}{N\Delta} \tag{5.20}$$

where N is the number of sampled points. The approximations in (5.19) are necessary since the signal has only been sampled within a finite time interval, $T = N\Delta$. From (5.20) it is seen that the spectrum is only known at discrete frequencies corresponding to a frequency resolution, $1/T$. The approximation in (5.19) is unfortunate since it can be shown that it leaks energy at a given discrete frequency into a wider frequency range. This phenomenon is called leakage. It is important since it means that spectral peaks in general will be underestimated and thus biased.

The leakage phenomenon can be reduced by smoothing the transition between the known fraction of the time signal and the infinitely long unmeasured part of the random process. The smoothing can be performed by weighting the sampled data by a weight function called a window, w. This is the same as applying a weighting function, W in the frequency domain upon the rough spectral estimate:

$$\tilde{x}_t = \sum_{m=t-N+1}^{t} x_m w_{(t-m)} \tag{5.21a}$$

$$\tilde{S}_{xx}(f_k) = \sum_{v=0}^{N-1} W(f_v - f_k) S_{xx}(f_v) \tag{5.21b}$$

The window function is restricted to be an even function with $\int_{-\infty}^{+\infty} W(f)df = 1$. One main characteristic is given by the effective bandwidth defined by:

$$B_e = \frac{1}{\int_{-\infty}^{+\infty} W^2(f)df} \tag{5.22}$$

Different sorts of windows are shown in figure 5.7. The boxcar window corresponds to the application of (5.19) without modification. The effective bandwidth is parameter dependent and can be adjusted for each type of window. The choice of window type and window parameters is a trade off between variance and bias of the spectral estimate. A broader weighting leads to a reduction of variance while the bias is increased. Ljung [17] suggests that for a given type window one should vary the determining parameter of the window until one is sure that the bias has been minimised. The windows deviate from each other due to the magnitude of the sidelobes. The ideal window would be a window with no sidelobes since this would mean no leakage. In practice the choice of a window will depend upon the frequency resolution, whether the signal is deterministic or random, whether the signal is narrow or broad banded and whether it is possible to adjust a given window type.

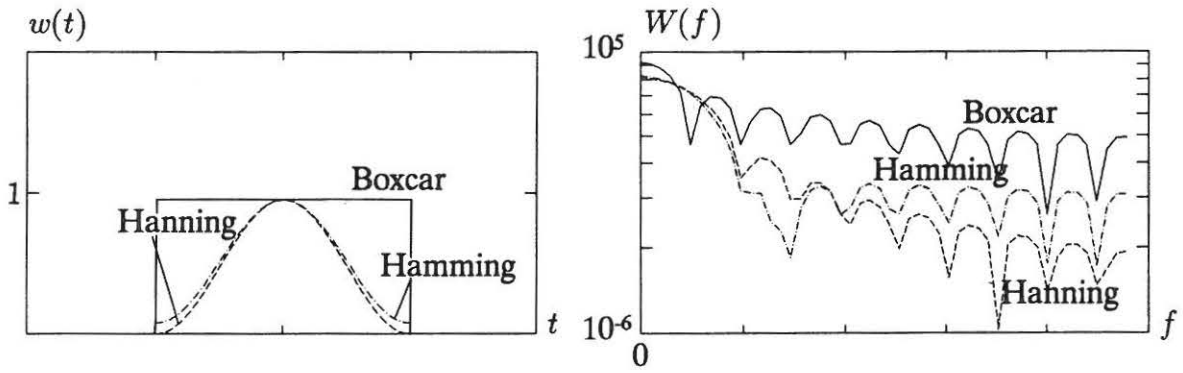

Figure 5.7. Different window types shown in the time and frequency domain.

The frequency resolution was shown to be equal to $df = f_s/N$ which means that the discrete spectrum becomes continuous when N goes against infinity. However this is not a practical way to obtain the true spectrum since the duration of the signals is limited due to non-stationary excitation conditions and the measurement costs.

Instead the zoom algorithm can be applied, see Randall [19]. This is in principle performed by a frequency shift of the Fourier transformed:

$$\begin{aligned} X(f_k) &= \int_{-\infty}^{+\infty} x(t) \exp(\mathbf{i}2\pi f_k t) \exp(-\mathbf{i}2\pi f_{sh} t) dt \\ &= \int_{-\infty}^{+\infty} x(t) \exp(\mathbf{i}2\pi (f_k - f_{sh}) t) dt \end{aligned} \tag{5.23}$$

After the frequency shift the time series is lowpass filtered to obtain a small band about the frequency range of interest. This is followed by a resampling at a lower sampling frequency. The concept is shown in principle in figure 5.8. For instance if the bandwidth after filtering is less than 10% of the original bandwidth ($f_s/2$) then it is possible to resample at a 10 times lower rate, which means that the frequency resolution has been increased 10 times.

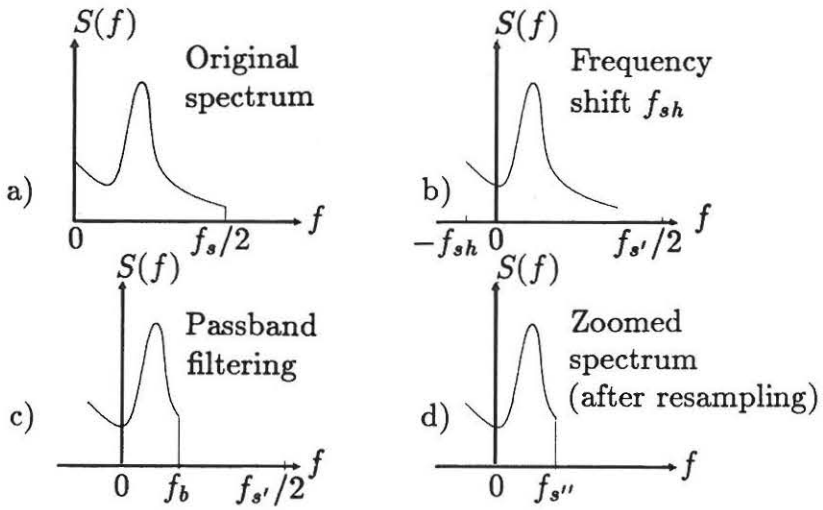

Figure 5.8. Principle of the zoom technique.

5.4 Random and Bias Errors

Since the data records can considered to be realisations of random processes the results due to signal processing will also be sample values of random variables or processes. The errors in the analysis of random analysis can be divided into random errors and bias errors. The former can be eliminated by averaging while the latter will be a systematic error due to the nature of the performed analysis. They are defined as:

$$\begin{aligned} \text{Bias error} \quad & \epsilon_b = (E[\hat{\Theta}] - \Theta^\star) \\ \text{Random error} \quad & \epsilon_r = \sqrt{E[(\hat{\Theta} - E[\hat{\Theta}])^2]} \end{aligned} \tag{5.24}$$

$\Theta^\star$ is here the unknown true value of the random variable while $\hat{\Theta}$ is an estimate. In general it is assumed that randomness can be modelled by the Gaussian distribution since the random error is assumed to be small, say less than 20% in the coefficient of variation.

5.4.1 Autospectral Estimates

If a random process is Gaussian then the autospectral estimate can be considered as a sum of the squares of two independent equal Gaussian distributed variables:

$$S_{xx}(f_k) = X_k^* X_k = (\mathbf{Re}(X_k))^2 + (\mathbf{Im}(X_k))^2 \tag{5.25}$$

This means that the autospectrum can be considered to be χ^2 distributed with 2 degrees of freedom:

$$\frac{\hat{S}_{xx}(f_k)}{S_{xx}(f_k)} \text{ is } \chi^2(2) - \text{distributed} \tag{5.26}$$

with the coefficient of variation:

$$\delta_r = \frac{\sqrt{E[\hat{S}_{xx}(f_k)^2]}}{S_{xx}(f_k)} = \sqrt{\frac{2}{n}}, \qquad n = 2 \tag{5.27}$$

It is seen that the estimate is inconsistent since it does not minimises when the length of the record is extended to infinity, $T \to \infty$. The time length will only affect the frequency resolution. Furthermore, the coefficient of variation will be unacceptably large for $n = 2$. However, the random variation can be reduced by averaging. This can be done either by averaging spectral estimates or by averaging over a frequency range for a given spectral estimate analog to the window principle. If the former procedure is followed :

$$\hat{S}_{xx}(f_k) = \frac{1}{n}(X_{k_1}^* X_{k_1} + X_{k_2}^* X_{k_2} + \cdots + X_{k_n}^* X_{k_n}) \tag{5.28}$$

the degree of freedom is increased to $2n$ for the χ^2 distributed variable . This means that final expression for n averages becomes:

$$\delta_r = \frac{\sqrt{E[\hat{S}_{xx}(f_k)^2]}}{S_{xx}(f_k)} = \frac{1}{\sqrt{B_e T}} \tag{5.29}$$

where T is the total time length and $B_e = \frac{n}{T}$ is the effective bandwidth of each spectral estimate. This means that confidence intervals of the autospectrum can be

estimated. The random error is seen only to be minimised by increasing the number of averages which will be the total time length of the record since the effective bandwidth also has to be minimised to keep the bias errors low. In appendix 5.2 the bias error is shown to be approximately given by:

$$\delta_b = \frac{B_e^2}{24} \frac{S''_{xx}(f_k)}{S_{xx}(f_k)} \tag{5.30}$$

The expression which is due to a second order Taylor expansion, will overestimate the error for sharp peaks, Bendat and Piersol [15]. The total variation coefficient can now be found for the autospectrum:

$$\delta^2 \approx \frac{1}{B_e T} + \frac{B_e^4}{576} \frac{S''_{xx}(f_k)^2}{S_{xx}(f_k)} \tag{5.31}$$

It is seen that the effective bandwidth has to be small to reduce the bias error, while it has to be large to reduce the random error. The error given by the variation coefficient can be minimised with respect to T and B_e (or the number of averages $n = TB_e$) for a given autospectrum:

$$\frac{d\delta^2}{dB_e} = -\frac{1}{TB_e^2} + \frac{4}{576} B_e^3 \frac{S''_{xx}(f_k)}{S_{xx}(f_k)} = 0$$

$$\Downarrow$$

$$B_e = \frac{n}{T} = \left(\frac{576 S_{xx}^2(f_k)}{4T S''_{xx}(f_k)}\right)^{0.2} \tag{5.32}$$

$$\frac{d\delta^2}{dT} = -\frac{4n^4}{T^5 576} \to 0 \text{ for } T \to \infty \tag{5.33}$$

Thus, from this point of view sampling should be performed as long as possible. In practice, however, the measuring time is often limited due to stationarity requirements or purely practical considerations. The total time length will therefore be considered as given in the following.

If an SDOF system excited by white noise is considered the optimal signal processing parameters can be directly related to the half-power band of the system, $B_r = 2f_0\zeta_0$ at resonance as shown in appendix 5.2. The optimum number of averages for different half-power bandwidths has been found for three different sampling times in figure 5.9a. It is seen that a small half-power bandwidth requires a small number of averages because it is more important to reduce the bias error by applying long time series for each spectral estimate. For larger bandwidths the number of averages is allowed to increase because the bias error becomes less vital. In figure 5.9b the coefficient of variation of the spectral peak is shown for optimal choices of the number of averages given a bandwidth and a total sampling time. It is seen that it

is difficult to obtain small errors for small bandwidths. The effect of the sampling time decreases as it is increased.

In figures 5.10a and 5.10b it is seen how the random error and the bias error are related to the effective bandwidth. It is seen that the random error can be eliminated by averaging while the bias error must be eliminated by reducing the effective bandwidth, B_e which means that the necessary length of the measured time series becomes substantially longer, increasing with the number of averages.

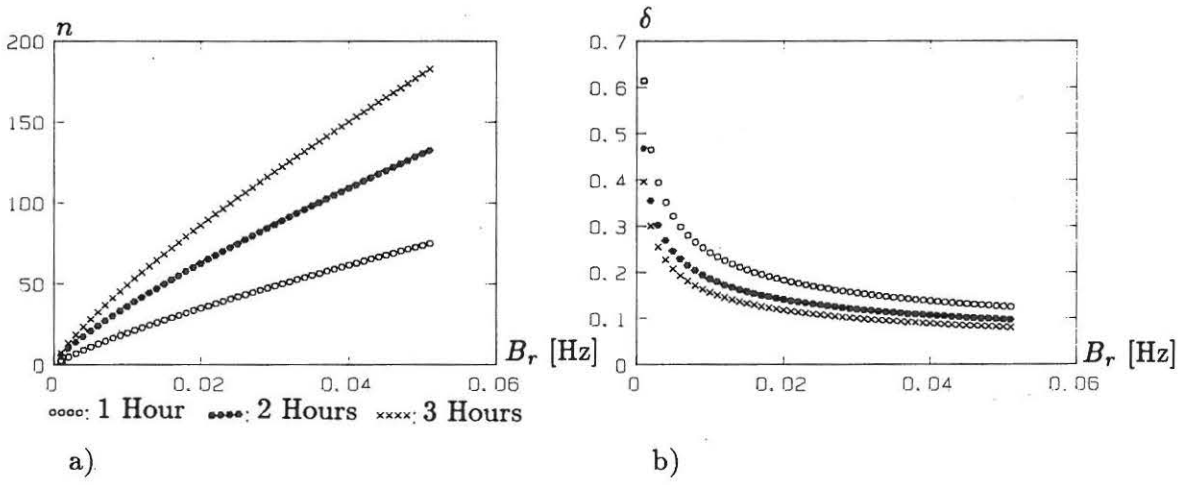

Figure 5.9. a) Optimum number of averages for minimum of the coefficient of variation of the total measuring error. b) The coefficient of variation of the total error for optimum number of averages. The half-power bandwidth is given by $B_r=2f_0\zeta_0$.

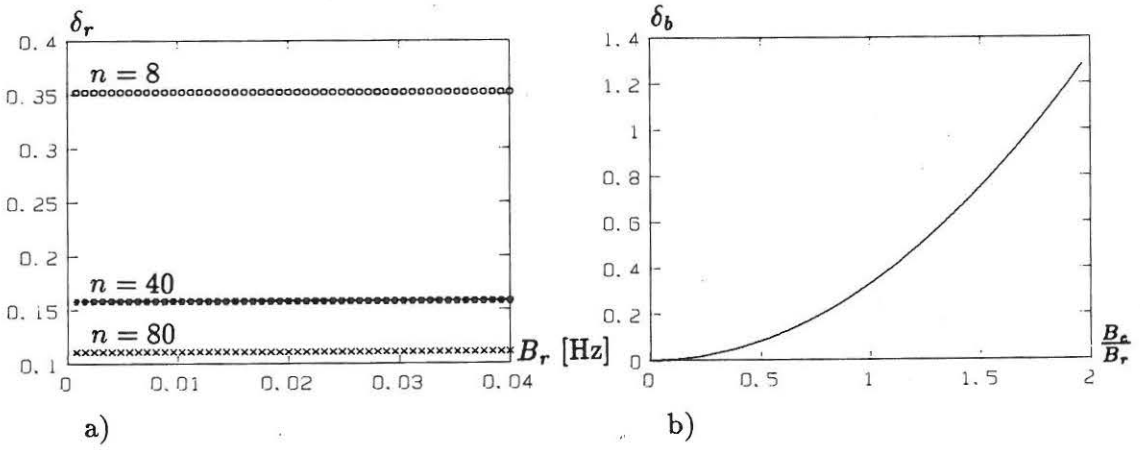

Figure 5.10. a) Random error as a function the half-power bandwidth. b) Bias error as a function of the relative bandwidth, $B=B_e/B_r$.

It should be noted that the relationships shown are not the exact relations but they give an understanding of the influence and the problems of obtaining high quality estimates of the spectral peaks which is so important because the information about

damping and eigenfrequencies are hidden in the peaks. The conclusion is that the records should be long for lightly damped systems, to keep the bias errors low while it is just a question of averaging to reduce the random error independently of the excited system.

Finally, consider a realistic example: Consider a monopile platform with $f_1 = 0.4$ Hz, $\zeta_1 = 0.01$ and a stationary 3 hour excitation. This gives a minimum variance of the spectral peak of 17.4% corresponding to 42 averages and a relative bandwidth $\frac{B_e}{B_r} = 0.49$. The main part of the error is due to the random part but it should be noted that this might be caused by the fact that the error model for the bias error exaggerates this to some extent for lightly damped systems. However, it has been clearly illustrated that an important source to uncertain identification results are due to the randomness of the measurements and the signal processing performed.

5.4.2 Estimates of Covariance Functions

The estimate of the cross-covariance function of $x(t)$ and $y(t)$ is given by:

$$\tilde{C}_{xy}(\tau) = \frac{1}{T}\int_0^T x(t)y(t+\tau)dt, \quad 0 \leq \tau \ll T \tag{5.34}$$

This estimate can be shown to have no bias error, see Bendat and Piersol [13] but the estimate requires that the length of the measured time series is at least T plus the magnitude of the maximum lag τ_{max}.

According to Bendat and Piersol [13] the square of the coefficient of variation of the cross-covariance function can be shown to be:

$$\delta_r^2 = \frac{E[\tilde{C}_{xy}^2(\tau)]}{C_{xy}^2(\tau)} \approx \frac{1}{2B_{white}T}(1 + \frac{C_{xx}(0)C_{yy}(0)}{C_{xy}^2(\tau)}) \tag{5.35}$$

where B_{white} is the total bandwidth of a bandlimited white noise process $x(t)$ and T is the total sampling length. For the autocorrelation function at $\tau = 0$, that is the mean square value , the coefficient of variation will be about $\frac{1}{B_{white}T}$. As τ increases, the coefficient of variation increases rather fast and will tend to be proportional to $\exp(2\zeta_0 2\pi f_0|\tau|)$ for an SDOF system which follows from the autocovariance function derived for bandlimited white noise excitation, see e.g. Lin [14].

5.4.3 Transfer Functions

The transfer function can be written as a product of the gain and phase factor:

$$H(f) = |H(f)| \exp\left(-\mathbf{i}\Phi(f)\right) \tag{5.36}$$

The bias error and the random error of the gain factor can be shown to be given by the following coefficient of variations, Bendat and Piersol [13],[15]:

$$\delta_b = \frac{\sqrt{1-\gamma^2(f)}}{|\gamma(f)|\sqrt{2n}} \tag{5.37}$$

$$\delta_r = \frac{\sqrt{1-\gamma^2(f)}}{\gamma^2(f)\sqrt{2n}} \tag{5.38}$$

And the standard deviation of the phase factor can be shown to be given by Bendat and Piersol [13],[15]:

$$\sigma_b\Phi(f) \approx \frac{\sqrt{1-\gamma^2(f)}}{|\gamma(f)|\sqrt{2n}} \quad \text{(Radians)} \tag{5.39}$$

$$\sigma_r\Phi(f) \approx \frac{\sqrt{1-\gamma^2(f)}}{\gamma^2(f)\sqrt{2n}} \quad \text{(Radians)} \tag{5.40}$$

It is recognised that the error of the phase will be independent of the phase value itself, which means that the relative error will be large for small phase values. This explains why identification based upon phase estimates are used relatively seldom in practice. It is seen that the error in transfer estimate will be zero if the coherence function equals one. Whether the coherence equals one depends highly upon the present noise and the linearity of the system, however, the coherence will also be a random variable itself and will not be equal to 1 per definition. The effect of the present noise will be discussed in the section 5.6.

5.5 Random Decrement Technique

The idea of the random decrement technique is to relate the response of a white noise excited linear system by the impulse response of the same system, see e.g. Vandiver et al. [20]. The technique was developed by Cole [21]. The general feature of the random decrement technique is that it is a tool in signal processing to extract the deterministic properties of a measured time series analog to e.g. FFT-analysis. The random decrement signature can be defined as:

$$D^{X_0}_{x_i x_i}[t_1, t_2] = E[x_i(t_2)|x_i(t_1) = X_0] \tag{5.41a}$$

$$D^{X_0}_{x_j x_i}[t_1, t_2] = E[x_j(t_2)|x_i(t_1) = X_0] \tag{5.41b}$$

$$i, j = 1, 2 \ldots n$$

$D^{X_0}_{x_i x_i}[t_1, t_2]$ is here the random decrement signature for the time series $x_i(t)$ for which a trigger condition, the trigger level X_0, has been given, while $D^{X_0}_{x_j x_i}[t_1, t_2]$ is the random decrement signature of the DOF no j given the trigger condition on $x_i(t)$, see figure 5.11. The time axis of each realization has here been defined such that the trigger condition is fulfilled at the time t_1.

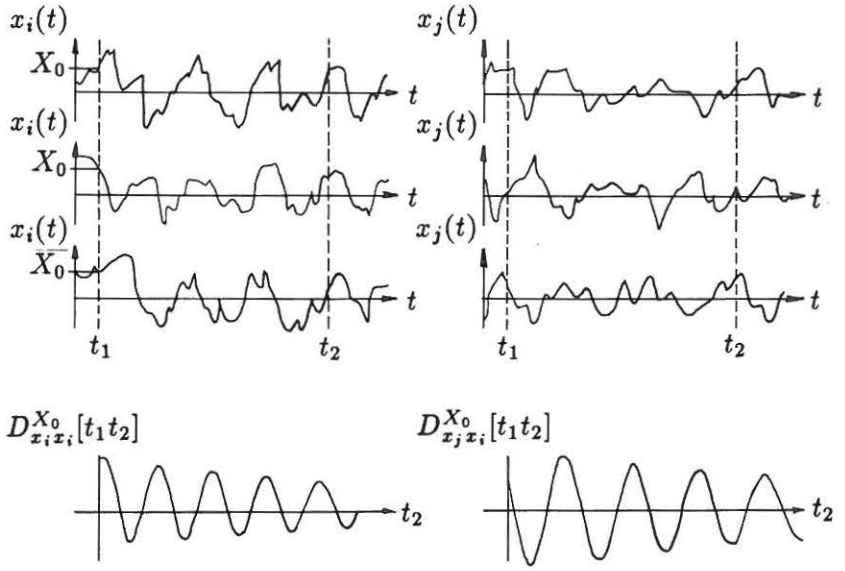

Figure 5.11. Realisations of the random processes, $x_i(t)$ and $x_j(t)$ with a trigger condition, $x_i(t_1)=X_0$ on $x_i(t)$.

In practice, the ensemble averaging is replaced by averaging samples due to an assumption of ergodicity:

$$D^{X_0}_{x_j x_i}[t_1, t_2] = D^{X_0}_{x_j x_i}[\tau] = \frac{1}{N} \sum_{l=1}^{N} x_j(\tau + T_l \mid x_i(T_l) = X_0) \tag{5.42}$$

where $\tau = t_2 - t_1$ and T_l is the time distance from $t = 0$ to the start of the segment no. l and N is the number of segments. The principle is shown in figure 5.12. for $j = i$. When a trigger level has been chosen for a given time series no i, segments of each measured time series are identified and averaged for which the trigger condition of time series no i is fulfilled. This leads to information about autocorrelation and cross-correlation and thus to the deterministic characteristics of the measured time series. In this context the trigger condition has been given as a trigger level, X_0

which is a practical condition to operate with. However, the trigger condition can in principle be chosen quite arbitrarily as conditions on $x_j(t)$, $\dot{x}_j(t)$ and $\ddot{x}_j(t)$.

It can be shown, see Vandiver et al. [20] that the random decrement signature is generally related to the cross-correlation function of the reponse by:

$$\begin{aligned} R_{x_j x_i}(t_1, t_2) &= \int\int x_j(t_1) x_i(t_2) p_{x_j x_i}(x_j, x_i, t_1, t_2) dx_j dx_i \\ &= \int x_j(t_1) p_{x_j}(x_j, t_1) D^{X_0}_{x_j x_i}[t_1, t_2] dx_j \end{aligned} \tag{5.43}$$

where $p_{x_j x_i}(x_j, x_i, t_1, t_2)$ and $p_{x_j}(x_j, t_1)$ is respectively the joint probability density function of $x_j(t)$ and $x_i(t)$ and the marginal probability density function of $x_j(t)$. If the excitation is assumed to be a stationary Gaussian (but not necessarily white) random zero mean process it follows that (5.43) is simplified to:

$$D^{X_0}_{x_j x_i}[\tau] = \frac{R_{x_j x_i}(\tau)}{R_{x_j x_i}(0)} X_0 \tag{5.44}$$

If the system is nonlinear this equation will be an approximation for which the error will depend upon the approximation of the response process to a Gaussian process. It can be noticed that if $D^{X_0}_{x_j x_i}[\tau]$ is Fourier transformed, a spectrum proportional to the cross-spectrum of x_i and x_j is obtained.

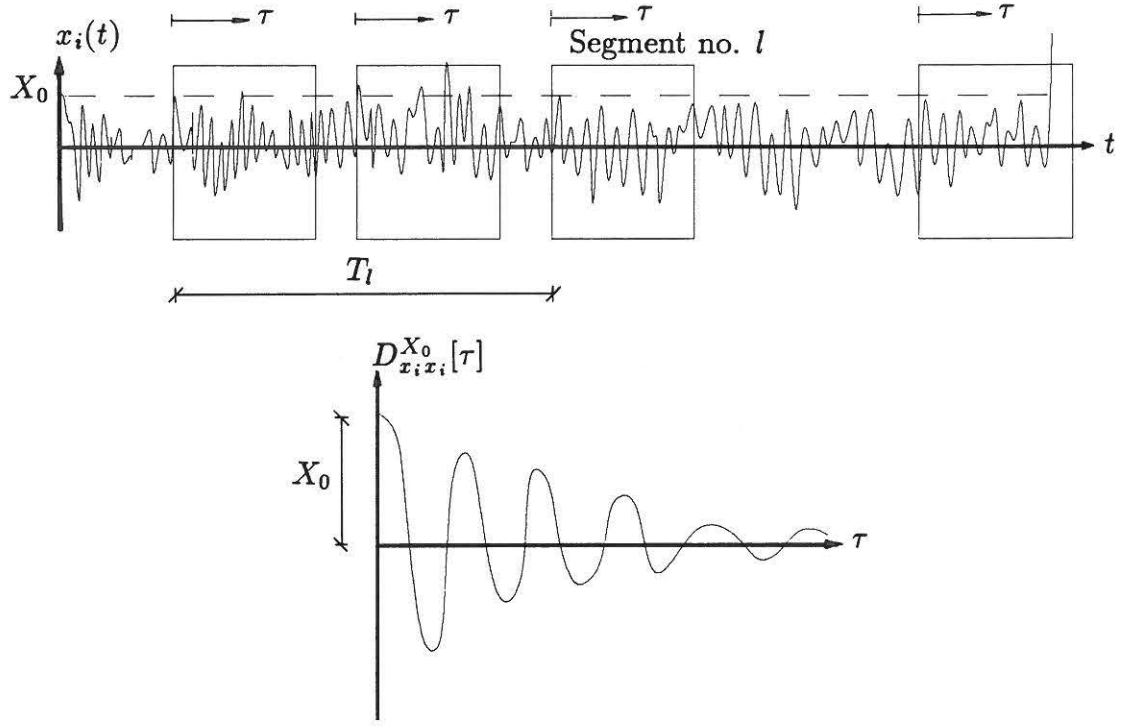

Figure 5.12. The principle of the random decrement signature, $D^{X_0}_{x_i x_i}[\tau]$ obtained by averaging samples.

If stationary Gaussian white noise excitation is assumed and applied on a linear SDOF system then it can be shown that the impulse response function, $h_0(\tau|x_1(0) = X_0)$ will be proportional to the autocorrelation function, $R_{x_1x_1}(\tau)$, see e.g. Meirovitch [22]. This means that the impulse response function will be proportional to the random decrement signature:

$$h_0\big(\tau|x_1(0) = X_0\big) \propto D^{X_0}_{x_1x_1}[\tau] \tag{5.45}$$

For an MDOF system with excitation of only the jth mode, the equivalent relation is obtained:

$$h_j\big(\tau|x_i(0) = X_0\big) \propto D^{X_0}_{x_jx_i}[\tau] \tag{5.46}$$

If several modes are present due to the white noise excitation the arguments will still hold since the correlation function of the response in modal coordinate will still be proportional to the impulse response function of each mode, $R_{z_iz_i}[\tau] \propto h_i(\tau)$. The correlation function matrix in the generalized coordinates will be related to the correlation function vector in modal coordinates by:

$$\overline{\overline{R}}_{xx}[\tau] = \overline{\overline{\Phi}}\overline{R}_{zz}[\tau]\overline{R}^T_{zz}[\tau]\overline{\overline{\Phi}}^T \tag{5.47a}$$

where:

$$\overline{R}^T_{zz}[\tau] = \big(\, R_{z_1z_1}[\tau] \quad R_{z_2z_2}[\tau] \quad \dots \quad R_{z_nz_n}[\tau]\,\big) \tag{5.47b}$$

Due to the proportionality between a given correlation function in modal coordinates and an impulse response function this means that for an MDOF system the correlation function will correspond to a weighted sum of the impulse response functions of each mode present in the response equivalent to a given free decay. Thus, in general:

$$D_{x_jx_i}[\tau] = \sum_{i=1}^{n} a_{ji}h_i(\tau) \tag{5.48}$$

where the weight factors,a_{ji} will depend upon the mode shapes, the imposed condition condition, X_0 and the distribution of the white noise excitation. An interpretation of the MDOF case has also been given in Ibrahim [23].

The expressions will also hold approximately for filtered white noise as input if the system is lightly damped. Thus the random decrement technique can be applied for lightly damped linear systems with a broad-banded excitation to find an impulse response function of the excited modes even though the characteristics of the excitation process also will be present in the signature. An experimental example of a random decrement signature is shown in figure 5.13.

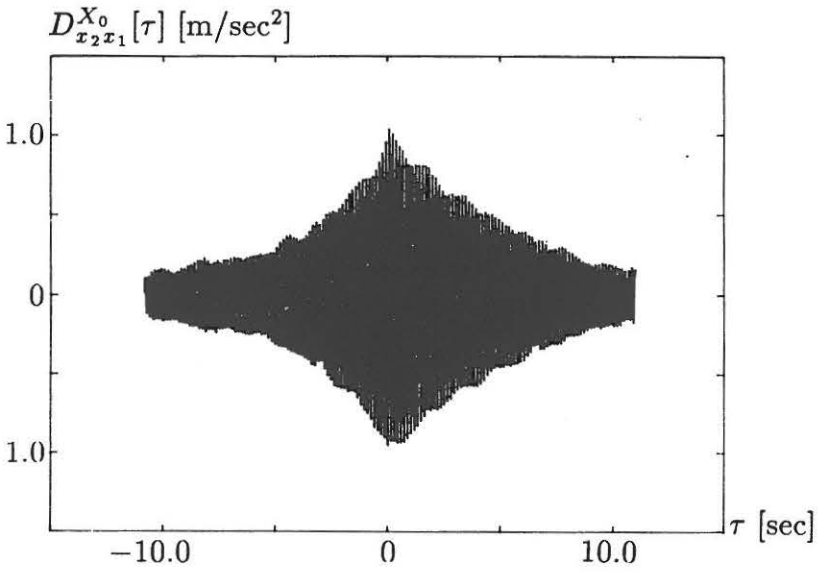

Figure 5.13. Experimental case: Random decrement signature of the response no. 2 with a choosen trigger condition on response no. 1. 100 means have been applied with Δ=0.0213 sec. Total length of signature, 22 sec.

In principle the random decrement technique is able to extract the deterministic characteristics of the stationary response of a randomly excited lightly damped structure provided that the excitation is sufficiently broad-banded and Gaussian distributed. However, there are some practical problems of the random decrement technique with respect to random and bias errors. Several factors can cause errors:

- The number of averages.
- Correlation between the averaged segments.
- The trigger level.
- The way in which the theoretical trigger condition $x_i = X_0$ is realized on the discretised time series.
- The algorithm for choosing one trig point in each segment.

Nasir and Sunder [24] claim that the number of averages should be at least 500 to ensure that the random decrement signature becomes reliable. However, the number of averages depends upon the correlation between the segments. Correlation between segments will increase the variance. While Nasir and Sunder claim that it is better to enlarge the number of averages accepting correlation between segments, Vandiver et al. [20] doubt that it pays off to accept correlation between segments. The presence of correlation between segments is seen from the random decrement signature. If the random decrement signature has faded out to zero at the end of the signature it means that the segments are independent, since the signature is equivalent to the correlation function. Vandiver et al. have obtained good results for 80 averages. It is noticed that the response of lightly damped systems will

require long segments to avoid correlation between segments. Thus, in this sense there is the same problem of obtaining sufficiently long records as in the case of FFT-analysis. However, Vandiver et al. have shown that the random decrement signature obtained by sample averaging will in theory be unbiased which is an important property compared to FFT-analysis.

In practice bias errors on the random dec. signature will exist due to the implementation of the trigger condition into an algorithm and the choice of fulfilment of the trigger condition for each segments. It seems that those problems have not been investigated sufficiently. A sufficiently high trigger level should in any case be specially chosen if additional noise is present in the response. This will prevent false triggering points due to the noise. Nasir and Sunder suggest a trigger level corresponding the rms-value (root mean square) of the response.

Nasir and Sunder [24] have found that the whiteness of the excitation versus the level of the damping of the structure is determing for whether or not the random decrement signature corresponds to a free decay. For white noise the most reliable signature is obtained for an increasing damping level while for non-white excitation the reliability increases with decreasing damping. For non-white excitation the success depends upon the concentration of the energy in the response spectrum at the peak frequency of the excitation versus the resonance peak.

Several other studies have been performed on the random decrement technique. Caldwell [25] has examined the technique with respect to obtaining damping estimates by the method of logarithm decrement (presented in 7.1) and also the effect of obtaining random decrement signatures of filtered response was studied. Ibrahim [23] has applied the technique in connection with a identification method developed by him which gives a complete set of modal estimates (presented in 7.2). Longo [26] has, with limited success, applied the technique together with the identification method of Ibrahim to the response of an offshore platform. The success seems to depend on whether resonance peak frequency or excitation peak frequency dominates the response as observed by Nasir and Sunder. Many others have also applied the method to obtain damping estimates of experimental models, see Yang et al. [27], Yang et al. [28] and Jensen et al. [29]. The application of the random decrement technique in Jensen et al. [29] is based upon a C-programme developed by the supervisor of this Ph.D. study, R. Brincker. The technique has also been applied to damage detection of fatigue cracks. Kummer et al. [30] have used the technique to observe changes in eigenfrequencies due to damages. Yang et al. [31] have observed changes in the random decrement signature with respect to the development of fatigue cracks.

5.6 Noise Models

The effect of the randomness of the measured data has been considered in the previous section. In this section the effect of additional noise sources will be considered with respect to bias of the frequency response estimate and reduction of the coherence function. The three most relevant noise models will be:

1. Noise on the measured response uncorrelated with the real response.
2. Noise on the measured excitation uncorrelated with the real excitation.
3. Noise on the measured excitation correlated with the real excitation.

The first noise source will typically be measuring noise. The second noise source will either be measuring noise upon the excitation or noise due to an unmeasured excitation uncorrelated with the assumed excitation. The third noise source will typical be due to an imperfect modelling/measurement of the excitation. For instance modelling of the wave excitation will always be modelled rather poor. The measuring noise will in general be due to the instrumentation, the recording and numerical errors in the analysis of the data.

Note that in this section the transfer function and the coherence function are marked with indices to avoid ambiguity.

Noise Model No. 1

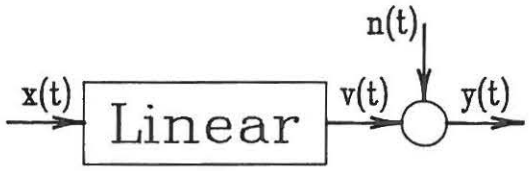

Figure 5.14. Noise model no. 1: Noise in the measured response uncorrelated with the actual response.

Noise model no. 1 is the typical noise model where the measured response, $y(t)$ is assumed to be distorted by the uncorrelated noise, $n(t)$. Since the noise is uncorrelated with the response it must also be uncorrelated with the excitation which has caused the response. Thus: $S_{yn}(f) = S_{xn}(f) = S_{vn}(f) = 0$ which leads to the estimate of the transfer function:

$$\tilde{H}_{xy}(f) = \frac{S_{yx}(f)}{S_{xx}(f)} = \frac{S_{vx}(f)}{S_{xx}(f)} \tag{5.49}$$

which is seen to be unbiased with respect to to the noise. The coherence estimate becomes:

$$\gamma_{xy}^2(f) = \frac{S_{vv}(f)}{S_{vv}(f) + S_{nn}(f)} \tag{5.50}$$

which is seen always to be less than one.

Noise Model No. 2

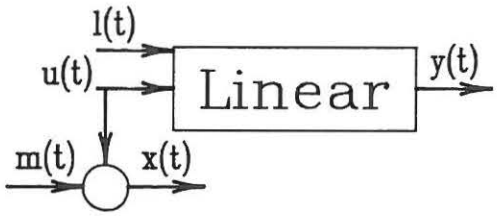

Figure 5.15. Noise model no. 2 ; Noise in the measured excitation uncorrelated with the actual excitation.

Noise model no. 2 is a more general noise model than model no. 1 leading to bias of the transfer function estimates. The system of the noise model is excited by the assumed excitation $u(t)$ and the unknown uncorrelated excitation $l(t)$. The assumed excitation is measured with the measurements being distorted by the noise $m(t)$. Thus the noise model contains in principle two noise sources, $m(t)$ which is noise in the measured excitation and $l(t)$ which passes through the system and thus causes an unexpected response which is considered as noise. Hence the latter noise contribution is in reality covered by the noise model no. 1. Thus in the present noise model this noise source is disregarded, $l(t) \equiv 0$. This means that due to $S_{xm}(f) = S_{um}(f) = S_{ym}(f) = 0$ which leads to the bias of the same magnitude as the transfer function estimate:

$$\tilde{H}_{xy}(f) = \frac{S_{uy}(f)}{S_{uu}(f)} \frac{1}{1 + \frac{\left(S_{mm}(f)\right)}{S_{uu}(f)}} \tag{5.51}$$

and the estimate of the coherence:

$$\gamma_{xy}^2(f) = \frac{S_{uu}(f)}{S_{uu}(f) + S_{mm}(f)} \tag{5.52}$$

which in general becomes less than one.

Noise Model No. 3

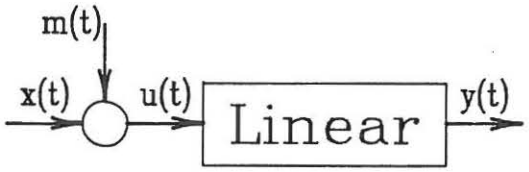

Figure 5.16. Noise model no. 3 : Noise in the measured excitation correlated with the actual excitation.

Noise model no. 3 is an important noise model where noise correlated with the measured excitation is passing through the linear system causing a response contribution. This means for instance that the correlated noise could be due to the model error of the wave loading caused by the application of Morison's equation. Since the input noise $m(t)$ is here correlated with the measured excitation $x(t)$ the measured transfer function becomes:

$$\tilde{H}_{xy}(f) = \frac{S_{uy}(f)}{S_{uu}(f)}(1 + \frac{S_{xm}(f)}{S_{xx}(f)}) \tag{5.53}$$

which will be a biased estimate of the transfer function since the true transfer function will be given by $H_{xy}(f) = \frac{S_{uy}(f)}{S_{uu}(f)}$. The bias will apply to magnitude and phase. The measured coherence function will be given by:

$$\gamma^2_{xy}(f) = \frac{|S_{xy}(f)|^2}{S_{xx}(f)S_{yy}(f)} = \frac{|S_{uy}(f) - S_{my}(f)|^2}{(S_{uu}(f) - S_{mm}(f) - S_{xm}(f) - S_{mx}(f))S_{yy}(f))} \tag{5.54}$$

This expression is not quite easy to interpret.

The noise models presented show that noise may very well affect the measured data, especially at those frequencies where there is little energy in the excitation or the response signal. From noise model 1 it has been seen that measuring noise at the response does not lead to bias of the transfer function estimate. While noise model 2, noise in the measured excitation leads to a bias in the magnitude of the transfer function estimate. Correlated noise on the excitation, noise model 3 has been shown to lead to bias error of the magnitude as well as the phase of the transfer function. The last noise model is thus the most severe and will be of importance if identification of a structural transfer function from measured response and wave excitation is chosen. The noise models causing bias of the transfer function estimates, models no. 2 and no. 3 should be considered when significant models errors are detected in the analysis stage of system identification.

5.7 References

[1] Sarpkaya, T. and M. Isaacson, "Mechanics of Wave Forces on Offshore Structures", Van Nostrand Reinhold Company, 1981.

[2] Jensen, J. L., "Vurdering af Morisons Formel" (in Danish), Institute of Building Technology and Structural Engineering, University of Aalborg, Denmark, 1987.

[3] Morison, J. R., M. P. O'Brien, J. W. Johnson and S. A. Schaaf, "The Forces Excerted by Surface Waves on Piles", Petroleum Transactions, AIME, Vol.189, 1950.

[4] Heideman, J. C., O. A. Olsen and P. P. Johansson, "Local Wave Force Coefficient", Conference On Civil Engineering In The Ocean , 4th Conference, American Society Of Civil Engineering, 1979.

[5] Burcharth, H. F. and T. Larsen, "Noter i Bølgehydraulik" (in Danish), The Laboratory of Hydraulics and Harbour Engineering University of Aalborg, Denmark, 1982.

[6] Krenk, S. and H. Gluver, "An Algorithm for Moments of Reponse from Non-Normal Excitation of Linear Systems", Stochastic Structural Dynamics, editor: S. T. Ariaratnam, G. I. Schueller & I. Elishakoff, Elsevier Applied Sciences, 1988.

[7] "Dansk Ingeniørforening's Code of Practice for the Design and Construction of Pile Supported Offshore Steel Structures" DS 449, Dansk Ingeniørforening,Denmark, 1983.

[8] Ibanez, P., "Review of Analytical and Experimental Techniques for Improving Structural Dynamic Models", Welding Research Council Bulletin no. 246, June 1979, ISSN 0043-2326, United Engineering Center, USA, 1979.

[9] Kennedy, C. D. and C. D. P. Pancu, "Use of Vectors in Vibration Measurements and Analysis", Journal of Aeronautic Science 14, no. 11, Nov. 1947.

[10] Lewis, R. C. and D. L. Wrisley, "A System for Excitation of Pure Natural Modes of Complex Structures", Journal of Aeronautic Science 17, no. 11 , 1950.

[11] Kozin, F. and H. G. Natke, "System Identification Techniques", J. Structural Safety, no. 3, 1986, Elsevier Publishers, 1986.

[12] Ting, S-K. and S. S. Sunder, "Testing and Monitoring of Offshore Structures, A State of the Art Review", In the series "Monitoring of Offshore Structures", report no. 1, Research report R82-48, Massachusetts Inst. of Techn, Dept. of Civil Eng., USA, July 1982.

[13] Bendat, J. S. and A. G. Piersol, "Random Data: Analysis and Measurement Procedures", Wiley & Sons, 1971.

[14] Lin, Y. K., "Probabilistic Theory of Structural Dynamics", McGraw-Hill, 1967.

[15] Bendat, J. S. and A. G. Piersol, "Engineering Applications of Correlation and Spectral Analysis", Wiley & Sons, 1980.

[16] Newland, D. E., "An introduction to Random Vibrations and Spectral Analysis", Longman, England, 1984.

[17] Ljung. L., "System Identification, Theory for the User", Prentice-Hall, USA, 1987.

[18] Rabiner, L. R. and B. Gold, "Theory and Application of Digital Signal Processing", Prentice-Hall, 1975.

[19] Randall, R. B., "Frequency Analysis", Bruel and Kjer, Denmark, 1987.

[20] Vandiver, J. K., A. B. Dunwoody, A. B. Campbell and M. F. Cook, "A Mathematical Basis for the Random Decrement Vibration Signature Analysis Technique", Journal Of Mechanical Design, April 1982, Vol. 104, American Society Of Mechanical Engineers, 1982.

[21] Cole, H. A. Jr., "On-Line Failure Detection and Damping Measurement of Aerospace Structures by Random Decrement Signatures", NASA CR-2205, March 1973.

[22] Meirovitch, L., "Elements of Vibration Analysis", 2nd edition, McGraw-Hill, 1986.

[23] Ibrahim, S. R., "Random Decrement Technique for Modal Identification of Structures", Journal of Spacecraft, Vol. 14, no. 11, Nov. 1977.

[24] Nasir, J. and S. S. Sunder, "An Evaluation Of The Random Decrement Technique Of Vibration Signature Analysis For Monitoring Offshore Platforms", Research Report R82-52, Sep. 1982, Dept. of Civil Engineering, Massachusetts Inst. of Technology, 1982.

[25] Caldwell, D. W., "The Measurement of Damping and the Detection of Damage in Linear and Nonlinear Systems by the Random Decrement Technique", Ph.D. Thesis, University Of Maryland, USA, 1978.

[26] Longo, P., "Vibration Monitoring of Offshore Platforms Using the Ibrahim Time Domain Modal Identification Technique", M.Sc. Thesis, Dept. of Ocean Eng., Massachusetts Inst. of Technology, USA, 1982.

[27] Yang, J. C. S. , M. S. Anggour, N. Dagalakis and F. Miller, "Damping of an Offshore Platform Model by the Random Dec Method", Proc. of the 2nd Speciality Conf. on Dynamic Response of Structures, ed. G. Hart, American Society Of Civil Engineers, Atlanta, USA, 1980.

[28] Yang, J. C. S., C. H. Marks, J. Jiang, D. Chen, A. Elahi and W-H. Tsai, "Determination of Fluid Damping Using Random Excitation", Proc. of the Third Int. Offshore Mechanics and Artic Engineering Symp., Vol. 1, American Society Of Mechanical Engineers, New Orleans, USA, 1984.

[29] Jensen, J. L., R. Brincker and A. Rytter, "Identification of Light Damping in Structures", Presented at the 8th International Modal Analysis Conference, Orlando, USA, Jan-Feb. 1990.

[30] Kummer, E., J. C. S. Yang and N. Dagalakis, "Detection of Fatigue Cracks in Structural Members", Proc. of the 2nd Speciality Conf. on Dynamic Response Of Structures, ed. G. Hart, Atlanta, USA, 1980.

[31] Yang, J. C. S., N. Dagalakis and M. Hirt, "Application of the Random Decrement Technique in the Detection of an Induced Crack on an Offshore Platform Model", In "Computation Methods for Offshore Structures" at the Winter Annual Meeting, American Society Of Mechanical Engineers, Chicago, USA, 1980.

6. IDENTIFICATION OF PHYSICAL PARAMETERS

The most straightforward approach for identification of structural properties is to identify the physical parameters of the structure. The physical parameters, which are also called the structural parameters by some authors, are included in the lumped parameter model which was presented in chapter 4. The advantage of identification of those parameters rather than the modal quantities is that the engineer may have some a priori knowledge about the physical parameters. This could be:

- The mass distribution.
- The stiffness distribution due to a finite element analysis.
- Damping sources.

This a priori knowledge means that it is possible to assume a sensible model with initial assumption of the parameters due to the a priori knowledge. The estimated parameters will deviate more or less from the initial parameters but due to common physical sense it will be possible to determine whether a deviation of an estimated parameter is due to lack of knowledge about a parameter or if it is due to a model error of some sort.

However, as it will be shown, the disadvantage of identification based on physical parameters is the number of parameters and less flexible models. In practice this means that a physical model often becomes a reduced model of a structure and thus to some extent loses its physical meaning.

6.1 The Time Direct Derivative Method (TDDM)

If the state space formulation is considered as given in chapter 4 a very simple formulation of the identification problem can be obtained:

$$\dot{\overline{y}} = \overline{\overline{A}}\,\overline{y} + \overline{\overline{B}}\,\overline{f} \tag{4.33}$$

This equation will hold for any time instant, t_i:

$$\dot{\overline{y}}(t_i) = \overline{\overline{A}}\,\overline{y}(t_i) + \overline{\overline{B}}\,\overline{f}(t_i) \quad i = 1, 2 \ldots N \tag{6.1}$$

where N is the number of observed time instants. (6.1) can be reassembled in the form:

$$\dot{\overline{\overline{Y}}} = \overline{\overline{A}}\,\overline{\overline{Y}} + \overline{\overline{B}}\,\overline{\overline{F}} \tag{6.2}$$

where:

$$\overline{\overline{Y}} = (\,\overline{y}(t_1) \quad \overline{y}(t_2) \quad \overline{y}(t_3) \quad \ldots \quad \overline{y}(t_N)\,) \tag{6.3a}$$

$$\overline{\overline{F}} = (\,\overline{f}(t_1) \quad \overline{f}(t_2) \quad \overline{f}(t_3) \quad \ldots \quad \overline{f}(t_N)\,) \tag{6.3b}$$

If (6.2) is post-multiplied by $\overline{\overline{Y}}^T$ the system matrix $\overline{\overline{A}}$ can be isolated:

$$\overline{\overline{A}} = (\dot{\overline{\overline{Y}}}\,\overline{\overline{Y}}^T - \overline{\overline{B}}\,\overline{\overline{F}}\,\overline{\overline{Y}}^T)(\overline{\overline{Y}}\,\overline{\overline{Y}}^T)^{-1} \tag{6.4}$$

This means that the system matrix $\overline{\overline{A}}$ can be obtained directly without any iterations if $(\overline{Y}\,\overline{Y}^T)$ is positive definite. This is ensured if the number of data points becomes large which means that (6.4) converges to:

$$\begin{aligned} &\lim_{N\to\infty} \frac{1}{N}(\overline{\overline{Y}}\,\overline{\overline{Y}}^T) = E[\overline{y}\,\overline{y}^T] \\ &\qquad\qquad \Downarrow \\ &\qquad\qquad \overline{\overline{A}} = (E[\dot{\overline{y}}\,\overline{y}^T] - \overline{\overline{B}}E[\overline{f}\,\overline{y}^T])(E[\overline{y}\,\overline{y}^T])^{-1} \end{aligned} \tag{6.5}$$

The covariance matrix $E[\overline{y}\,\overline{y}^T]$ will be positive definite and the inverse will thus exist. Thus, the number of sampled data must be large enough to ensure this convergence of (6.4) to (6.5). The speed of the convergence will among other things depend on the choice of the degrees of freedom of the model and the noise level.

The method assumes that the mass distribution and force process are known which is an acceptable assumption. If the system matrix $\overline{\overline{A}}$ is known it is on the other hand possible to estimate the excitation matrix $\overline{\overline{B}}$. By a similar approach the following is obtained:

$$\overline{\overline{B}} = (\; E[\dot{\overline{y}}\overline{f}^T] - \overline{\overline{A}}E[\overline{y}\overline{f}^T]\;)(E[\overline{f}\,\overline{f}^T])^{-1} \tag{6.6}$$

If the excitation matrix $\overline{\overline{B}}$ as well as the system matrix $\overline{\overline{A}}$ is unknown the dimension of the least square problem must be increased to twice the size of the former two problems:

$$\begin{pmatrix} \dot{\overline{\overline{Y}}} \\ \ddot{\overline{\overline{Y}}} \end{pmatrix} = \begin{pmatrix} \overline{\overline{A}} & \overline{\overline{B}} \\ \dot{\overline{\overline{A}}} & \dot{\overline{\overline{B}}} \end{pmatrix} \begin{pmatrix} \overline{\overline{Y}} \\ \dot{\overline{\overline{F}}} \end{pmatrix} \tag{6.7}$$

which can be postmultiplied by:

$$\begin{pmatrix} \overline{\overline{Y}}^T & \dot{\overline{\overline{F}}}^T \end{pmatrix} \tag{6.8}$$

and thus for large N lead to the following expression for $\overline{\overline{A}}$ and $\overline{\overline{B}}$:

$$\begin{pmatrix} \overline{\overline{A}} & \overline{\overline{B}} \\ \dot{\overline{\overline{A}}} & \dot{\overline{\overline{B}}} \end{pmatrix} = \begin{pmatrix} E[\dot{\overline{y}}\,\overline{y}^T] & E[\dot{\overline{y}}\,\overline{f}^T] \\ E[\ddot{\overline{y}}\,\overline{y}^T] & E[\ddot{\overline{y}}\,\overline{f}^T] \end{pmatrix} \begin{pmatrix} E[\overline{y}\,\overline{y}^T] & E[\overline{y}\,\overline{f}^T] \\ E[\dot{\overline{f}}\,\overline{y}^T] & E[\dot{\overline{f}}\,\overline{f}^T] \end{pmatrix}^{-1} \tag{6.9}$$

For the general case there will be $3n^2$ unknown parameters corresponding the number of elements in $\overline{\overline{A}}$ and $\overline{\overline{B}}$. Usually this number is reduced to $n^2 + 2n$ since the mass matrix is assumed to be a diagonal matrix and the stiffness and damping matrix are assumed to be symmetric matrices. However, in spite of the reduction in the number of unknown parameters it is seen that it will be a large number even for a small number of degrees of freedom. Thus, for a large number of degrees of freedom it might be more attractive to apply an estimate of $\overline{\overline{B}}$ and compute $\overline{\overline{A}}$ from (6.4) and then improve the estimate of $\overline{\overline{B}}$ due to (6.9). Finally this approach should be repeated until an acceptable convergence has been obtained. Whether this method works has not been tested.

A very serious argument against the application of the method in practice is that a complete knowledge about the response state vector is assumed:

$$(\,\overline{x} \quad \dot{\overline{x}} \quad \ddot{\overline{x}}\,) \tag{6.10}$$

Usually, only the acceleration is obtained by measuring and thus the displacement and the velocity must be obtained by numerical integration.

$$\dot{\overline{x}}(t) = \dot{\overline{x}}(0) + \int_0^t \ddot{\overline{x}}(\tau)d\tau \tag{6.11a}$$

$$\overline{x}(t) = \overline{x}(0) + \dot{\overline{x}}(0)t + \int_0^t \int_0^{\tau_1} \ddot{\overline{x}}(\tau_2)d\tau_2 d\tau_1 \tag{6.11b}$$

In practice this integration leads to problems:

- Numerical errors due to the finite sampling interval.
- Noisy information about the low frequency content of the signals.

The numerical error of the integration of a single time step can be illustrated for the case of a sinusoidal signal:

$$\text{Velocity}: \quad v(t) = V \sin(2\pi f t) \tag{6.12}$$

which by numerical integration by the trapezoidal rule gives the relative displacement:

$$\hat{u}(t) = \frac{\Delta}{2}(v(t) + v(t - \Delta)) \tag{6.13}$$

where Δ is the sampling interval. The corresponding exact expression is:

$$u(t) = -U \cos(2\pi f t) = -\frac{V}{(2\pi f)} \cos(2\pi f t) \tag{6.14}$$

Due to Kreyzig [1] it can be shown that the maximum error of this integration will be:

$$|\frac{\epsilon}{U}| \ll \frac{2\pi^3}{3}(f\Delta)^3 \tag{6.15}$$

This expression is shown in figure 6.1. It is seen that it is necessary to keep a small sampling interval compared to the frequency of the sinusoidal signal. The numerical error depends on the second derivative of the measured quantity, see Kreyzig [1].

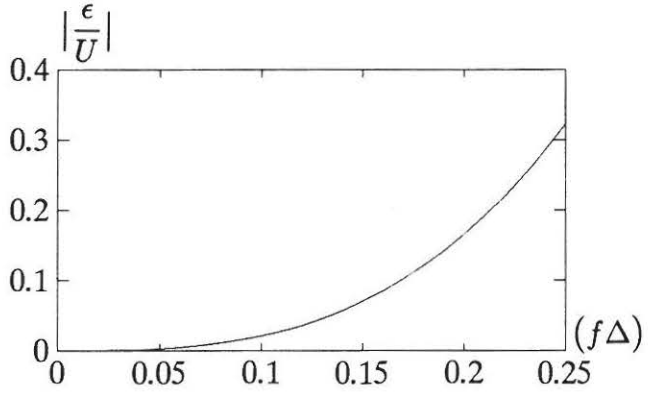

Figure 6.1. Maximum error due to numerical integration of a sinusoidal signal as a function of sampling interval multiplied by the period time.

The recording of acceleration signals means that the frequency content at the lower frequencies will be uncertain because the accelerations will be small at those frequencies and thus vulnerable with respect to noise. This means that the signal

integration may not lead to an accurate integrated signal at the low frequencies. In practice the signal integration is often performed by analog filtering built into the accelerometers, see e.g. Schmidt [2] and [3]. Information about the signal distortion due to this technique has not been obtained.

The serious consequences of potential noise in the response state vector have been shown by Fritzen [4]. He points out that the TDDM is indeed very sensitive to noise because a bias error is unavoidable. If the applied response is given by $\overline{y}(t) = \overline{y}_0(t) + \overline{n}(t)$, where $\overline{y}_0(t)$ is the true response and $\overline{n}(t)$ is uncorrelated noise, then the estimate of the system matrix $\overline{\overline{A}}$ is obtained as:

$$\begin{aligned}\overline{\overline{A}} = &\left(E[\overline{y}_0(t)\dot{\overline{y}}_0^T(t)] + E[\overline{n}(t)\dot{\overline{n}}^T(t)] - \overline{\overline{B}}E[\overline{f}(t)\dot{\overline{y}}_0^T(t)]\right) \\ &\left(E[\dot{\overline{y}}_0(t)\dot{\overline{y}}_0^T(t)] + E[\dot{\overline{n}}(t)\dot{\overline{n}}^T(t)]\right)^{-1}\end{aligned} \tag{6.16}$$

This estimate of $\overline{\overline{A}}$ is seen to be a biased estimate of the true matrix with a bias error depending upon the noise level.

Hart et Yao [5] has illustrated the influence of the mentioned problems by a simulation study of the model:

$$m\ddot{x} + k_1 x + k_2 x^3 + c_1\dot{x} + c_2\dot{x}^3 = f \tag{6.17}$$

where m was a known mass and f was a measured time series of the 1934 El-Centro earthquake and noise was added to the simulated measured response. Three cases were considered: Case A, the complete state vector was known, case B, the acceleration and the displacement were known and finally, case C the realistic case where only the acceleration was known. The parameters, k_1, k_2, c_1 and c_2 were estimated by the explained method with the modification that $\overline{y}(t_i)$ in the state space formulation, (6.1) also contained terms of x^3 and $\dot{x}^3$. The results are shown in table 6.1. The table illustrates that the realistic case where only the acceleration was observed, leads to a deviation of 33 % for the estimate of k_2 while the other more pleasant cases lead to acceptable estimates. The fact that the system is nonlinear is unimportant in this discussion since the error criterion function is linear to all the parameters.

Parameter	True values	Case A $\{\ddot{\bar{x}},\dot{\bar{x}},\bar{x}\}$	Case B $\{\ddot{\bar{x}},\bar{x}\}$	Case C $\{\ddot{\bar{x}}\}$
k_1	25.0000	24.9897	25.0577	24.8168
k_2	2.5000	2.4157	2.5616	3.2679
c_1	1.0000	0.9957	1.0012	1.0094
c_2	0.1000	0.0998	0.0991	0.0981

Table 6.1. Estimated parameters of (6.17) with a noise added to the observed response of a time length, T=10 sec., Hart and Yao [5].

6.2 Identification by Response Simulation (IRS)

The time direct derivative method (TDDM) aimed at an identification algorithm which gave a simple and compact formulation of the problem by considering the state space formulation. Instead of this approach a more straightforward approach can be applied for the purpose of obtaining estimates of the physical parameters. The response can be simulated by a numerical model and adjusted until the simulated response corresponds to the measured response as shown in figure 6.2.

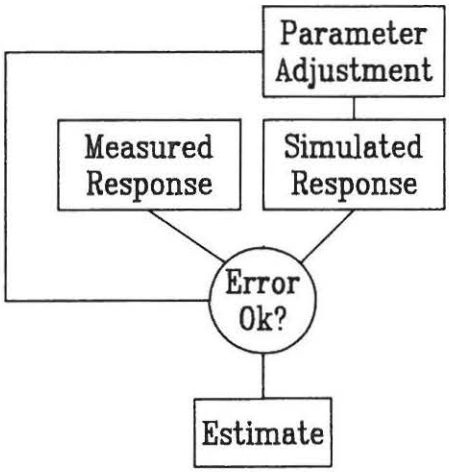

Figure 6.2. Principle of identification by response simulation.

The error between the measured response and the simulated response of a free decay

is minimized with respect to the unknown parameters:

$$V(\overline{\Theta}) = \frac{1}{N}\sum_{i=1}^{N} \overline{\epsilon}^T(t_i|\overline{\Theta})\overline{\epsilon}(t_i|\overline{\Theta}) \tag{6.18}$$

where:

$$\overline{\epsilon}(t_i|\overline{\Theta}) = \overline{x}(t_i) - \hat{\overline{x}}(t_i|\overline{\Theta}) \tag{6.19}$$

and $\hat{\overline{x}}(t_i|\overline{\Theta})$ is the predicted response due to $\overline{\Theta}$ which is a vector containing the unknown parameters. The minimum of the error function, $V(\overline{\Theta})$ with respect to the unknown parameters, $\overline{\Theta}$ can be found by an iterative optimization, in the present paper by the algorithm NLPQL, Schittkowski [6].

In principle the IRS can be applied to any type of measured response, but it is assumed that the best results are obtained with measured time series with a minimum of noise such as a measured free decay. The number of iterations will increase if the time series is distorted by noise. Thus, in this context, the measured time series has in any case been a free decay. This can either be obtained directly from a free decay or from an application of the random decrement technique. The latter has been presented in chapter 5. Another reason for the choice of a simulation of the free decay is that it also requires extra computer time to simulate a response due to a forced excitation.

The response simulation of $\hat{\overline{x}}(t_i|\overline{\Theta})$ has been performed by the Runge Kutta method of a general lumped mass system. A Runge Kutta algorithm was formulated in a FORTRAN routine, PROGSIM developed by my colleague Anders Rytter. This has been built into an optimization program, OPT which includes computation of the error criteria function $V(\overline{\Theta})$, numerical calculation of gradients and call of the optimization routine, NLPQL, see Schittkowski [6]. The program is able to simulate a model containing nonlinear damping mechanisms such as Coulomb and nonlinear viscous damping (drag damping) mechanisms given by :

$$m_j\ddot{x}_j + c_{ij}\dot{x}_j + c_{ij}^{Cou}\frac{\dot{x}_j}{|\dot{x}_j|} + c_{ij}^{nlv}|\dot{x}_j|\dot{x}_j + k_{ij}x_j = 0 \quad \text{for } i,j = 1,2,\ldots n \tag{6.20}$$

The algorithm applies a set of initial conditions which may be known or included as unknown parameters. Thus the parameter vector $\overline{\Theta}$ will in the general case be given as:

$$\begin{aligned} \overline{\Theta}^T &= (m_j, c_{ij}, c_{ij}^{Cou}, c_{ij}^{nlv}, k_{ij}, x_i(0), \dot{x}_i(0)) \\ i,j &= 1,2\ldots n \end{aligned} \tag{6.21}$$

The method has been tested by a series of simulated examples with nonlinear viscous damping and Coulomb damping present at the same time.

The features of the IRS method have been investigated by application of the method of simulated as well as experimental data for a system of two degrees of freedom.

6.2.1 Simulated Case

The measured response has been simulated for different models by the same algorithm as applied in the IRS method, PROGSIM. Noise has been added to obtain realistic simulated measured free decays.

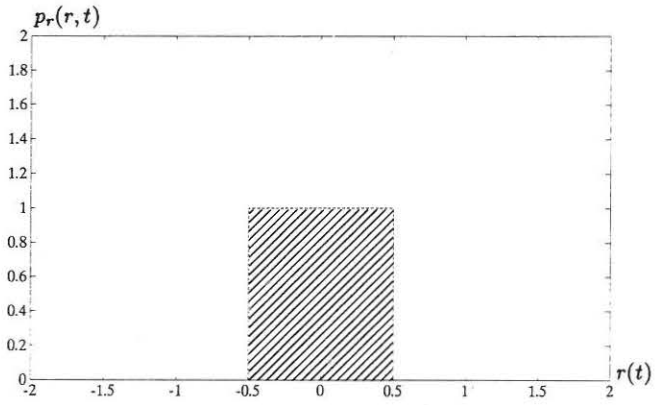

Figure 6.3 Probability density function of unit noise, $r(t)$.

The noise process was due to the random function in Vax FORTRAN [7]. The density function of the unit noise, $r(t)$ is shown in figure 6.3. The noise process, $n(t)$ was given as:

$$n(t) = A\, r(t) \tag{6.22}$$

where A was a chosen amplification factor. The noise to signal ratio was defined as:

$$(n/s)_i = \sqrt{\frac{\int_0^T n(t)^2 dt}{\int_0^T x_i(t)^2 dt}} \tag{6.23}$$

for the record measured for the ith degree of freedom. It is seen that the noise ratio will depend upon the chosen amplification factor A and the length of the applied time series T, because the time series will be due to a free decay. The equivalent

noise-to-signal ratio for all the applied records in the identification session was defined as:

$$n/s = \sqrt{\sum_{i=1}^{R} (n/s)_i^2} \tag{6.24}$$

where R is the number of applied records which will usually correspond to the number of degrees of freedom, n of the model.

Several simulation studies have been performed but only the results from a single model case will be presented in this context. The model was a 2DOF system with nonlinear viscous and Coulomb damping included. The model was given by (6.20) with the parameters inserted:

$$\begin{pmatrix} 25.56 & 0 \\ 0 & 35.65 \end{pmatrix} \begin{pmatrix} \ddot{x}_1 \\ \ddot{x}_2 \end{pmatrix} + \begin{pmatrix} 1.5 & -0.8 \\ -0.8 & 2.0 \end{pmatrix} \begin{pmatrix} \dot{x}_1 \\ \dot{x}_2 \end{pmatrix} + \begin{pmatrix} 0.2 & 0 \\ 0 & 0.2 \end{pmatrix} \begin{pmatrix} \frac{\dot{x}_1}{|\dot{x}_1|} \\ \frac{\dot{x}_2}{|\dot{x}_2|} \end{pmatrix} +$$
$$\begin{pmatrix} 1.0 & 0 \\ 0 & 1.0 \end{pmatrix} \begin{pmatrix} |\dot{x}_1|\dot{x}_1 \\ |\dot{x}_2|\dot{x}_2 \end{pmatrix} + \begin{pmatrix} 9783 & -22468 \\ -22468 & 60851 \end{pmatrix} \begin{pmatrix} x_1 \\ x_2 \end{pmatrix} = \begin{pmatrix} 0 \\ 0 \end{pmatrix}$$

with the initial conditions:

$$\begin{pmatrix} x_1(0) \\ x_2(0) \end{pmatrix} = \begin{pmatrix} 0.20 \\ 0.15 \end{pmatrix} \quad \begin{pmatrix} \dot{x}_1(0) \\ \dot{x}_2(0) \end{pmatrix} = \begin{pmatrix} 0 \\ 0 \end{pmatrix}$$

Identification of this model was simulated for two different lengths of the time series with three different noise levels, $A = 0.0$, 0.02 and 0.04:

- T=40 sec. with $n/s = 0.0$, 0.16 and 0.32 sampled at 50 Hz.
- T=60 sec. with $n/s = 0.0$, 0.21 and 0.42 sampled at 50 Hz.

Two examples of the simulated and estimated response are shown in figures 6.4 and 6.5 also showing the influence of the noise level.

In table 6.2, the exact parameter values and the estimated parameters are shown for the two lengths of the time series. The estimates of the linear mechanisms are quite satisfactory. However, it is seen that that the estimates depend upon the length of the applied time series. An increase of the time length reduces the deviation from the exact values significantly. It is seen that the estimates of the nonlinear damping parameters are improved and, especially, better estimates are obtained for the Coulomb damping.

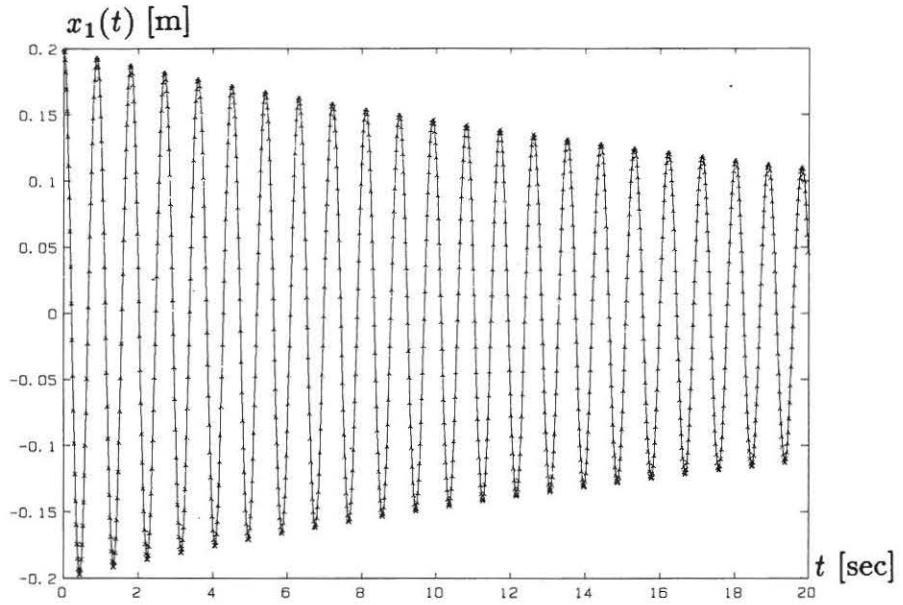

Figure 6.4 Simulated measured response of x_1 with n/s=0 (points) and the estimated response (line).

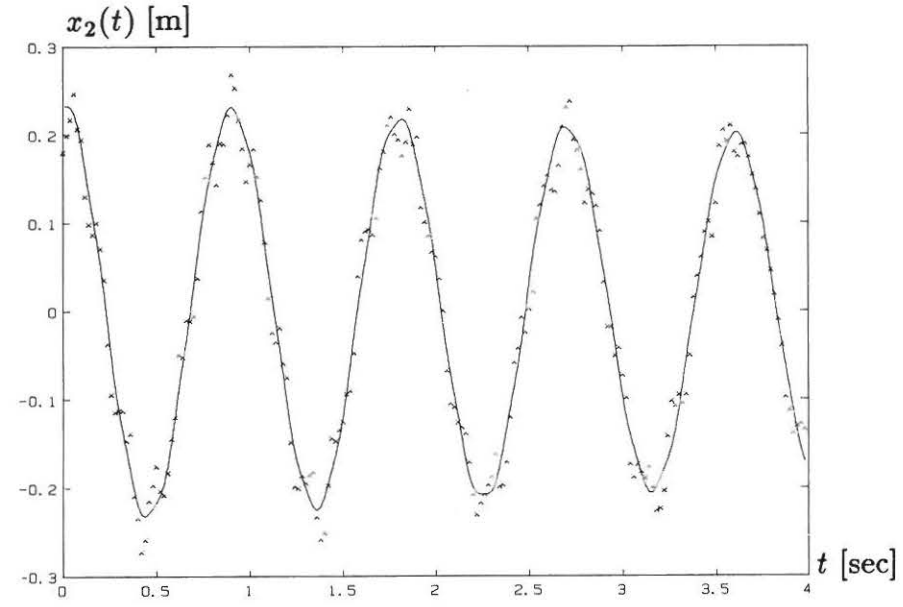

Figure 6.5 Simulated measured response of x_2 with n/s=0.32 (points) and the estimated response (line).

	m_1 Kg	m_2 Kg	$x_1(0)$ m	$x_2(0)$ m	$\dot{x}_1(0)$ m/sec	$\dot{x}_2(0)$ m/sec
Exact	25.56	35.65	0.200	0.150	0	0
T=40 sec.						
n/s=0.0	25.99	35.43	0.199	0.150	0.003	0.001
T=60 sec.						
n/s=0.0	25.51	35.70	0.192	0.177	0.006	-0.010

	k_{11} N/m	k_{12} N/m	k_{22} N/m	c_{11} Kg/sec	c_{12} Kg/sec	c_{22} Kg/sec
Exact	9783	-22468	60851	1.500	-0.800	2.000
T=40 sec.						
n/s=0.0	9836	-22471	60631	1.458	-0.829	1.972
T=60 sec.						
n/s=0.0	9787	-22470	60821	1.503	-0.795	1.998

	c_{11}^{Cou} N	c_{12}^{Cou} N	c_{22}^{Cou} N	c_{11}^{nlv} Kg/m	c_{12}^{nlv} Kg/m	c_{22}^{nlv} Kg/m
Exact	0.200	0	0.200	1.000	0	1.000
T=40 sec.						
n/s=0.0	0.066	-0.072	0.122	0.829	-0.067	0.541
T=60 sec.						
n/s=0.0	0.196	-0.007	0.183	1.079	0.027	0.944

Table 6.2. The estimated parameters compared with exact values for time series of length T=40 sec. and T=60 sec.

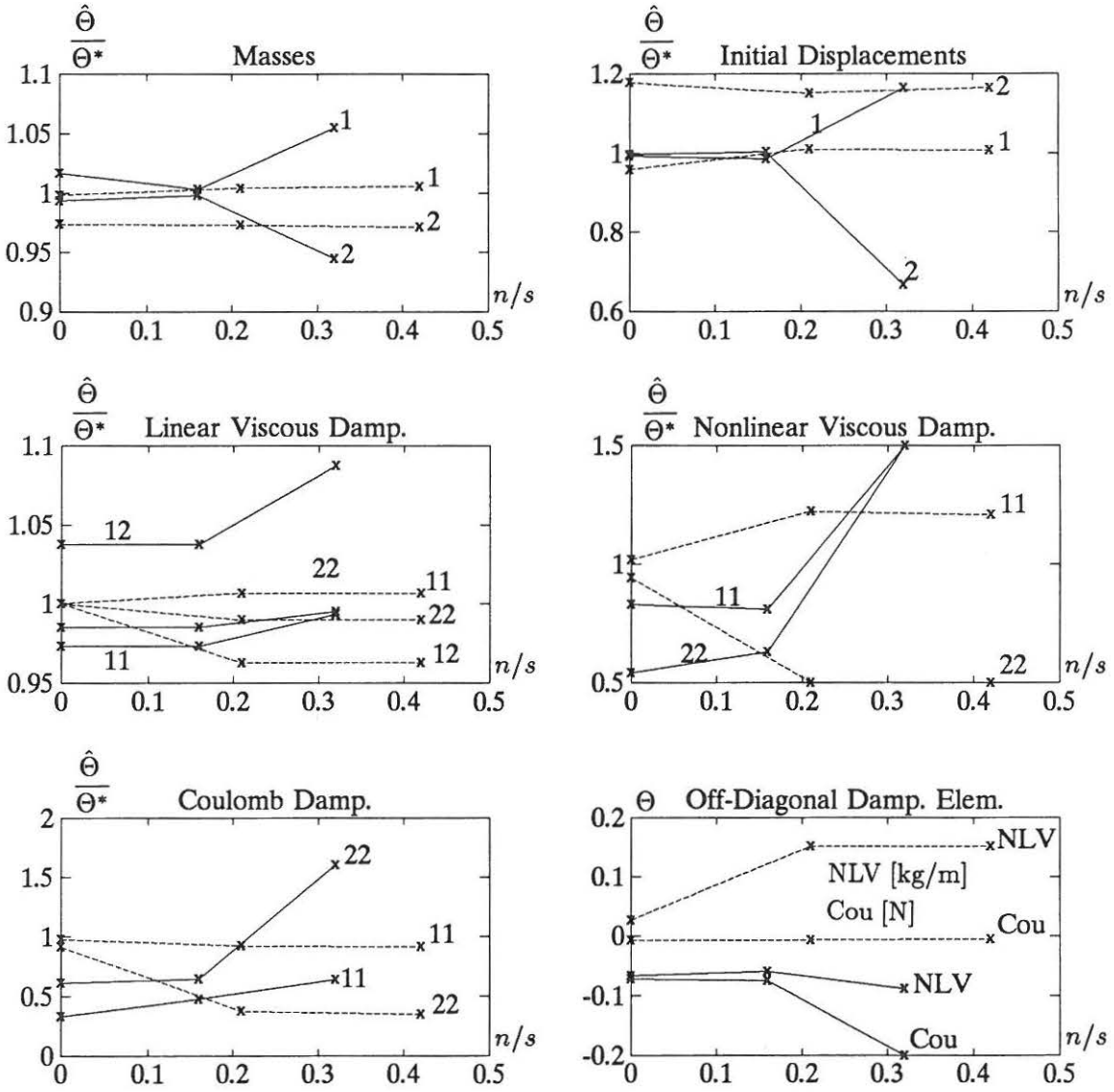

Figure 6.6 Parameter estimates for different noise level and length of time series (estimate $\hat{\Theta}$ over true value Θ^*). The fully drawn line: T=40 sec. and the dotted line: T=60 sec.

In figure 6.6 it is shown how the parameter estimates depend upon the noise-signal ratio for the two different time lengths. In general it is seen that the application of a longer time series has improved the estimates with respect to the noise level even though the noise-signal ratio has been increased. The time length of 60 sec. should be compared with the fact that for a time length of 70 sec. the oscillations disappear due to the Coulomb damping. Thus, in any case the presence of the Coulomb damping limits the length of the applied time series. The figure also shows that estimation of especially the Coulomb damping seems to be difficult, while the nonlinear viscous damping estimates perform better even though they are quite sensitive to noise.

	f_1 Hz	f_2 Hz	ζ_1	ζ_2
Exact	1.1102	7.1902	0.00276	0.000845
n/s=0.0	1.1102	7.1902	0.00259	0.00086
n/s=0.16	1.1102	7.1904	0.00258	0.000843
n/s=0.32	1.1104	7.3262	0.00252	0.000861

Table 6.3. Estimated modal parameters for simulated nonlinear damped system without any equivalent contribution from the estimated nonlinear mechanisms, T=40 sec..

	f_1 Hz	f_2 Hz	ζ_1	ζ_2
Exact	1.1102	7.1902	0.00276	0.000845
n/s=0.0	1.1102	7.1864	0.00277	0.000844
n/s=0.21	1.1102	7.1863	0.00283	0.000832
n/s=0.42	1.1102	7.1865	0.00282	0.000832

Table 6.4. Estimated modal parameters for simulated nonlinear damped system without any equivalent contribution from the estimated nonlinear mechanisms, T=60 sec.

The modal parameters corresponding to the estimated physical parameters are shown in table 6.4. The modal parameters have been estimated from the parameters included in $\overline{\overline{M}}$,$\overline{\overline{K}}$ and $\overline{\overline{C}}$ corresponding to a conventional linear model. It is seen that the increase of the time length from 40 to 60 sec. also in general leads to more accurate modal estimates, which was to be expected. However, it is seen that the

second eigenfrequency is better determined by the short time series. This might be related to the influence of the Coulomb damping. The modal estimates are seen to be relatively insensitive with respect to the noise level compared with the estimates of the physical parameters. The modal parameters may thus be a more robust representation of the structural model.

6.2.2 The Experimental Case

The IRS method has also been applied to the experimental data obtained for the monopile structure shown in figure 6.7 which was presented in chapter 1, see also Jensen [8].

Forced excitation as well as a free vibration were considered. The applied excitation was filtered white noise which meant that only two eigenmodes were excited, primarily the second. In the case of the performed free vibrations the most active eigenmode was the first. Thus, the two kinds of response contained different weighting of the eigenmodes and consequently also of the reliability of the modal estimates.

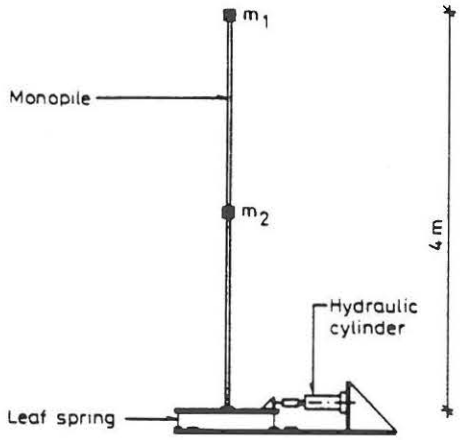

Figure 6.7. Monopile structure.

The two experimental cases which were considered were the monopile structure with two different damping configurations:

- The naturally damped monopile which was assumed to be proper modelled by a linear viscous damping model.
- The extra damped monopile due to a mounted nonlinear viscous damper on the concentrated mass in the middle of the monopile m_2.

The first configuration is called linear viscous damping while the second is called nonlinear viscous (nlv) damping. The mathematical model of the mounted damper was confirmed by a calibration which showed that the damping force could be

described by $f_D^{nlv} = (73.8\dot{x} + 0.4)\dot{x}$ [N] where $\dot{x}$ is given in [m/s].

The response was measured at two locations. The response of the mass at the top was labelled response no. 1 while the reponse of the mass at the middle of the monopile structure was labelled reponse no. 2. The response was acceleration measured by accelerometers.

In the case of linear viscous damping the identification by response simulation (IRS) of a measured free decay was performed using a linear damping model. The following parameters were estimated:

Free Decay:

$$\begin{pmatrix} 29.8 & 0 \\ 0 & 34.5 \end{pmatrix} \begin{pmatrix} \ddot{x}_1 \\ \ddot{x}_2 \end{pmatrix} + \begin{pmatrix} 1.38 & -1.49 \\ -1.49 & 1.75 \end{pmatrix} \begin{pmatrix} \dot{x}_1 \\ \dot{x}_2 \end{pmatrix} + \begin{pmatrix} 9819.8 & -22406.3 \\ -22406.3 & 61665.6 \end{pmatrix} \begin{pmatrix} x_1 \\ x_2 \end{pmatrix} = \begin{pmatrix} 0 \\ 0 \end{pmatrix}$$

The parameters agree fairly well with the physical a priori knowledge. The stiffness matrix was theoretically found from the given model data, see Jensen [8]:

$$\overline{\overline{K}} = \begin{pmatrix} 8955.0 & -22387.5 \\ -22387.5 & 71640.0 \end{pmatrix} \quad [N/m]$$

and the mass matrix was theoretically found as the sum of the concentrated masses and the respective elements in the consistent mass matrix (two beam elements), see Thomson [10]:

$$\overline{\overline{M}} = \begin{pmatrix} 24.60 + 4.53 & 1.57 \\ 1.57 & 24.56 + 9.06 \end{pmatrix} = \begin{pmatrix} 29.1 & 1.57 \\ 1.57 & 33.6 \end{pmatrix} \quad [Kg]$$

A good agreement is shown with respect to the mass matrix. The disagreement of the estimated and the calculated stiffness matrix might be explained by the contribution from the rotational degrees of freedom which was not measured, see chapter 4.1.

In figure 6.8 an example of a fit of the free decay response is shown. A fairly good agreement is seen. The deviation probably reflects the difficulties of identifying the second eigenmode which was only weakly excited in the free decay response.

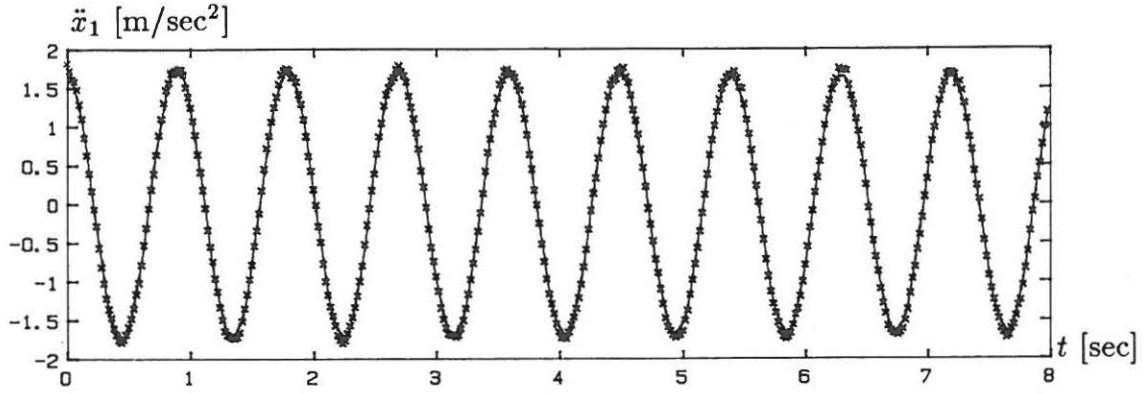

Figure 6.8. Identification by response simulation (IRS). Fit of the response no. 1 for linear viscous damped case. Measured response (points), estimated response (line). The figure shows a segment of a 120 sec. time series sampled with Δ=0.02 sec.

In the case of nonlinear viscous damping two procedures were followed. Firstly the IRS method was applied to a measured free decay with a model including the expected nonlinear damping mechanism: A nonlinear viscous damping source at mass 2. Secondly a random decrement signature was obtained for the response due to the random excitation. The principles behind the random decrement signature have been given in chapter 5, in this context the signature can be considered as a measured free decay of the structure. The linear assumptions included in the random dec. signature lead to models which are least square approximations of a linear model to a nonlinear system. The two model estimates were found to be:

Free Decay:

$$\begin{pmatrix} 30.6 & 0 \\ 0 & 31.9 \end{pmatrix} \begin{pmatrix} \ddot{x}_1 \\ \ddot{x}_2 \end{pmatrix} + \begin{pmatrix} 1.86 & -3.67 \\ -3.67 & 12.38 \end{pmatrix} \begin{pmatrix} \dot{x}_1 \\ \dot{x}_2 \end{pmatrix} + \begin{pmatrix} 0 & 0 \\ 0 & 49.3 \end{pmatrix} \begin{pmatrix} |\dot{x}_1|\dot{x}_1 \\ |\dot{x}_2|\dot{x}_2 \end{pmatrix} + \begin{pmatrix} 9812.1 & -22182.7 \\ -22182.7 & 60508.8 \end{pmatrix} \begin{pmatrix} x_1 \\ x_2 \end{pmatrix} = \begin{pmatrix} 0 \\ 0 \end{pmatrix}$$

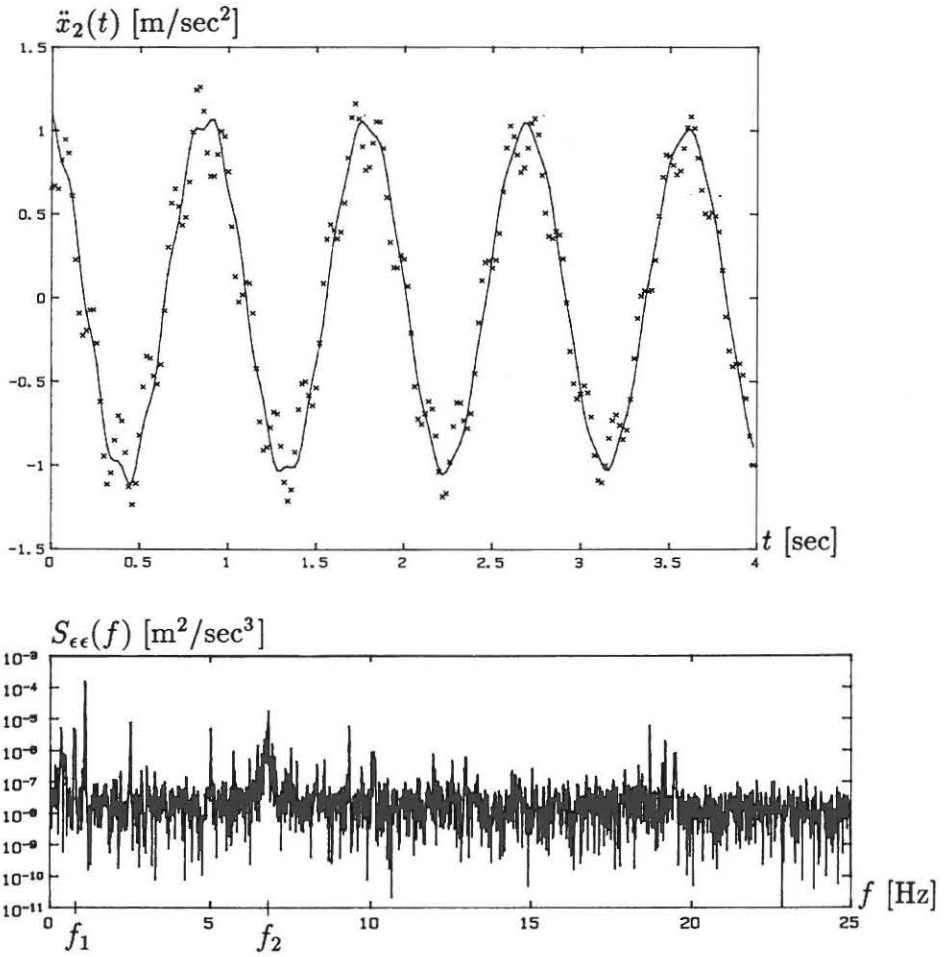

Figure 6.9. Top: IRS applied to the measured free decay, Δ=0.02 sec. and time length 120 sec. Measured response (points), estimated response (line). Bottom: Autospectrum of the error between measured and simulated response.

Random Decrement:

$$\begin{pmatrix} 20.5 & 0 \\ 0 & 44.1 \end{pmatrix} \begin{pmatrix} \ddot{x}_1 \\ \ddot{x}_2 \end{pmatrix} + \begin{pmatrix} 0.38 & -0.05 \\ -0.05 & 19.03 \end{pmatrix} \begin{pmatrix} \dot{x}_1 \\ \dot{x}_2 \end{pmatrix}$$
$$+ \begin{pmatrix} 9400.0 & -23750.4 \\ -23750.4 & 60000.0 \end{pmatrix} \begin{pmatrix} x_1 \\ x_2 \end{pmatrix} = \begin{pmatrix} 0 \\ 0 \end{pmatrix}$$

The corresponding fit between the simulated and the measured free decay response is shown in figure 6.9. The autospectrum of the error is also shown in figure 6.9. It is seen that the noise spectrum is quite flat indicating that the noise is close to be white noise although it is seen that there seems to be noise peaks at the locations of the two eigenfrequencies at 1.11 Hz and 7.20 Hz. Thus even though the model is able to describe the measured response quite well there seems to be some model error.

It is seen that the IRS method applied to the free decay data gave in fact a fairly good estimate of the mounted damper characteristics. The damper calibration gave $c_{22}^{nlv} = 73.8$ [kg/m] while the estimate was $c_{22}^{nlv} = 49.3$ [kg/m]. It should be noticed that the calibration was performed with at velocity in one direction while the mounted damper was excited backwards and forwards. Thus, this result shows that it is possible to identify a concentrated damping source.

From the estimated parameters of the two models it is seen that there are large deviations between the estimated parameters of the two models. The estimated lumped masses deviate as much as 50% while the stiffness elements deviate about 5%. For a further comparison the estimates of the two models were transformed into modal parameters. For the nonlinear model due to the IRS method the equivalent damping ratios were determined by a least square approach. The equivalent modal estimates are shown in table 6.5 and in the brackets are shown the ratio obtained by the logarithmic decrement, see chapter 7. It is seen that the equivalent damping ratios correspond well to the damping ratios obtained by the logarithmic decrement. For the nonlinear damped case it is seen that the eigenfrequencies obtained from the free decay and the random decrement signature do not agree at all. This can be explained by the fact the first eigenmode was only weakly represented in the random decrement signature while the second was only weakly represented in the measured free decay. The mounted damper is seen to have increased the damping ratios considerably and has also caused a change in the eigenfrequencies due to the added mass of the damper.

	Linear damped free decay	Nonlinear damped free decay	Nonlinear damped random dec.
f_1 Hz	1.1104	1.1022	0.0464/0.0271 *)
ζ_1	0.0009	0.0029	1.0/-1.0 *)
	(0.0007)	(0.0033)	
f_2 Hz	7.2417	7.4094	6.8782
ζ_2	0.0010	0.0058	0.0039
			(0.0041)

Table 6.5. Estimated modal parameters for linear and nonlinear viscous damping. For the nonlinear case equivalent modal ratios have been obtained by a least square approach. The numbers in the brackets are estimated damping ratio obtained from the logarithmic decrement. *) Two overdamped eigenmodes were estimated instead of the underdamped first eigenmode.

6.2.3 Experiences

The application of the IRS method has been illustrated by simulated and experimental examples. The method has proven to be able to identify the physical parameters and is furthermore able to quantify nonlinearities. The latter feature is perhaps the most important one of the method. The method has not yet been fully tested with respect to the number of degrees of freedom, the noise level, the length of the time series, the sampling frequency, different model assumptions etc. Thus, if the method is supposed to have a general application in practice those aspects should be investigated.

With respect to the length of the time series two aspects should be noticed:

- The noise signal ratio will increase as the signal decays. Thus, there is a conflict between the need for data and the minimization of the influence of noise.
- The influence of the different damping mechanisms will depend on the vibration level. The significance of the nonlinear viscous damping in the free decay response will decrease faster than the linear viscous damping while the significance of the Coulomb damping will increase as the vibration level decreases.

The optimum length of the time series can for instance be found as the length of the time series which gives the minimum sum of the variance of the parameters, see also chapter 14 in Ljung [11].

Comments on the problem with the model assumption should also be given. The fundamental problem seems to be whether or not a model is over or underdetermined with respect to the number of parameters. For instance simulation studies have shown that a proportionally damped system described by a non-proportional damped model makes it difficult to obtain convergence, because the model contains too many parameters. The obtained parameter estimates may be quite accurate anyway. If the model contains too few parameters the model estimate will be a rough approximation. The proper model can be found by comparing the error of the fit for different models. As long as the model is underdetermined, a further refinement will give a decrease in the error while, when the model becomes overdetermined, the error will decrease insignificantly, or it may start to increase.

Attentions should also be given to the fact that the quality of the estimates and the number of iterations in IRS highly depend on whether or not all eigenmodes are sufficiently excited. To ensure good estimates all eigenmodes must be excited and the response of all degrees of freedom must be applied to the analysis.

The computer time is probably the largest limitation of the IRS method. A session of the cases presented in this chapter may last between 6 and 13 hours on a Microvax or 30 minutes and 90 minutes on a Vax 8700. This limits the number of degrees of freedom of the model since the number of parameters has significant influence on the computation time. The reason is that the response has to be simulated twice the number of parameters to find a search direction in the iterative least square approach (numerical gradients) and furthermore, response simulations must

be performed until convergence along the search direction has been reached, and then a new search direction is found and a new search is started. For a linear system the number of parameters will be $(n^2 + 2n)$ plus the number of initial conditions $(2n)$. Thus, the method is extremely sensitive with respect to computer time used to simulate the response. This will also depend upon the length of the time series to be simulated and the time step in the Runge Kutta routine. The latter is determined by the highest frequency component of the structure, i.e. the highest eigenfrequency. Thus, the computer time will depend upon three factors:

- The number of parameters.
- The length of the time series.
- The highest frequency component of the structure.

To improve the method one should concentrate on optimization of the simulation algorithm and a more effective computation of the search direction. Perhaps the numerical gradient calculation could be replaced by analytical expressions.

Due to the considerable computer time used the parameter uncertainties have not been evaluated according to the principles presented in chapter 3. The calculation of the covariance matrix of the parameters requires a very large number of numerical gradient calculations. Thus, the method must be optimized before the evaluation of the parameter uncertainties can be made.

Another problem is that the final parameter estimates seem to depend weakly upon the initial estimates. In principle the only way to handle this problem is to repeat the estimation with different initial estimates until a minimum of the error criteria function has been obtained. In practice, the search should be started by applying a relatively large time step in the response simulation to get a rough estimate of the best initial estimate which leads to the global minimum. Afterwards the time step can be decreased to get a final estimate.

The identification by response simulation of a structural model has also been investigated by Juang and Sun [12]. To keep the number of parameters small they applied a response surface technique which related a simple continuum model to a finite element model. The proposed method led to identification of structural parameters such as bending stiffness and shear modulus.

6.3 Conclusion

In this chapter two methods have been presented which are able to identify the physical parameters of vibrating structures. Both methods are formulated in the time domain. No methods in the frequency domain have been discovered but some references are given in Hart and Yao [5], which is a review of identification methods in the seventies. In the frequency domain the general approach seems to be identification of modal parameters. However, if the modal parameters have been identified, information about physical parameters can be obtained.

It is seen that if the n eigenfrequencies the n damping ratios and the n mode shapes have been estimated for a structure assumed to be proportionally damped the physical parameters will be obtainable from:

$$\begin{aligned}
\overline{\overline{\Phi}}^T \overline{\overline{M\Phi}} &= (\, m_{ii} \,) \\
\overline{\overline{\Phi}}^T \overline{\overline{K\Phi}} &= (\, (2\pi f_i)^2 \,) \\
\overline{\overline{\Phi}}^T \overline{\overline{C\Phi}} &= (\, (4\pi \zeta_i f_i) \,)
\end{aligned} \tag{6.25}$$

However, it is seen that $(n^2 + 2n)$ physical parameters will be unknown and only $(n^2 + n)$ modal parameters known. Thus, either n extra parameters should be known or else the mode shapes should be replaced with the weighted mode shapes.

Link [13] has dealt with the problem of determining the physical parameters from modal parameter estimates. He notices that the stiffness matrix will typically be more uncertain than the mass matrix because it will be dominated by higher modes and thus be sensitive to small error in those modal estimates. Link also discusses the choice of the number of degrees of freedom in the lumped parameter model versus the number of measured response points. A further discussion with respect to the estimates of the damping matrix is given in chapter 4.

Udwadia [14] has investigated the uniqueness of the estimates of the physical parameters with respect to the excitation and the number of measured response points. For a simple structural model of a tall building with band limited damping and stiffness matrices with known mass distribution it is shown that the estimates of the stiffness and the damping can be uniquely determined from the measured response and excitation at the topmost mass level. Juang and Sun [12] also deal with the problem of uniqueness of the estimated parameters.

Instead of the direct relations between the modal and the physical parameters Leonard and Khouri [15] have applied a finite element procedure to obtain physical knowledge from given modal estimates. A similar approach has been made by Vandeurzen et al. [16] to obtain integrity information for a simulated offshore structure. Sunder and Sanni [17] have applied a more refined response surface technique to obtain information of the foundation stiffness from simulated as well as measured response of an offshore platform. The response surface technique is applied to relate a finite element model to a simple structural model compatible with the performed response measurements. A practical example of a combined estimation of stiffness elements and modal parameters of a tall building are given in Bèliveau and Favillier [18]. Another practical application is given by Natke and Schulze [19] who from identified eigenfrequencies have identified the deck mass of an offshore platform. In general all investigators claim to have success.

With respect to the presented methods formulated in the time domain some comments must be made.

In theory the time direct derivative method (TDDM) is a very quick way of obtaining information about the physical parameters because the parameters are obtained directly without any iterations. In practice, however, the method seems to be quite unrealistic outside the laboratory since there are two significant disadvantages. First of all the measured response must contain the complete state vector to obtain good parameter estimates. If the complete state vector is obtained by numerical integration errors are likely to distort the results. Secondly the response has to be measured at all degrees of freedom which are included in the model. This means that in practice very simple models have to be accepted.

The last disadvantage is also present for the identification by response simulation (IRS) in two aspects. Firstly the response has to be measured at all the assumed degrees of freedom. Secondly, the computation time increases quickly with the number of parameters. The major advantage of this method is that it is able to include nonlinear mechanisms in the model.

6.4 References

[1] Kreyszig, E., "Advanced Engineering Mathematics", 6th edition, John Wiley & Sons Inc., 1988.

[2] Schmidt, T. R., "Offshore Platform Displacement with an Inertial Reference System", Offshore Technology Conference, OTC 2554, Houston, USA, 1976.

[3] "Piezoelectric Accelerometers and Vibration Preamplifiers", Bruel & Kjer, Theory and Application Handbook, Denmark, 1978.

[4] Fritzen, C-P. "Identification of Mass, Damping and Stiffness Matrices of Mechanical Systems", Journal of Vibration, Acoustics, Stress and Reliability in Design, Vol. 108, Jan. 1986.

[5] Hart, G. C. and J. T. P.Yao, "System Identification in Structural Dynamics", ASCE J. Engineering Mechanics. EMC, Dec 1977.

[6] Schittkowski, K., "NLPQL: A FORTRAN Subroutine Solving Constrained Non-linear Programming Problems", Annals of Operation Research, 1986.

[7] "Programming in VAX FORTRAN", Software version V4.0, Digital Equipment Corporation, 1984.

[8] Jensen, J. L., "Dynamic Analysis of a Monopile Model", Series of Fracture and Dynamics Papers, no 4. Institute of Building Technology and Structural Engineering University of Aalborg, Denmark, 1988.

[9] Jensen, J. L., "Identification of Light Damping in Structures", The Eighth International Modal Analysis Conference, Orlando, USA, Jan. 1990.

[10] Thomson, W. T., "Theory of Vibration with Applications", George Allen & Unwin, 1981.

[11] Ljung, L., "System Identification, Theory for the User", Prentice-Hall, 1987.

[12] Juang, J. N. and C. T. Sun, "System Identification of Large Flexible Structures Using Simple

Continuum Models", Journal of Astronautical Sciences, Vol. XXX1, no. 1 Jan-Mar., 1983.

[13] Link, M., "Theory of a Method For Identifying Incomplete System Matrices From Vibration Test Data", Z. Flugwiss. Weltraumforsch. 9, Heft 2., 1985.

[14] Udwadia, F. E., "Some Uniqueness Results Related to Soil and Building Structural Identification", Journal of Applied Mathematics, Vol. 45, no. 4, Society for Industrial and Applied Science, Aug. 1985.

[15] Leonard, J. W. and B. R. Khouri, "System Identification Using a Standard Finite Element Program", Engineering Structure, Vol. 7, July, Butterworth & Co. Ltd., 1985.

[16] Vandeurzen, U., J. Leuridan and Y. Doucet, "Structure Monitoring Using a Diagnosis Technique Based On Combined Use of FEA and Test", Temadag - Modal Analyse og Dynamiske Elementberegninger, Jydsk Teknologisk, Denmark, Feb. 1987.

[17] Sunder, S. S. and R. A. Sanni, "Foundation Stiffness Identification For Offshore Platforms", Applied Ocean Research , Vol. 6, no. 3, CML Publications, 1984.

[18] Béliveau, J-G. and M. Favillier, "Parameter Estimation From Full-Scale Cyclic Testing", Proc. of the 2nd Speciality Conf. on Dynamic Response of Structures, (ed. G. Hart), American Society of Civil Engineers, Atlanta, USA, 1980.

[19] Natke, H. G. and H. Schulze, "Parameter Adjustment of a Model of an Offshore Platform From Estimated Eigenfrequencies Data", Journal of Sound and Vibration, Vol. 77 ,no. 2, Academic Press Inc., 1981.

Alternative References

[20] Sun, C. T., B. J. Kim and J. L. Bogdanoff, "On the Derivation of Equivalent Simple Models for Beam- and Plate-like Structures in Dynamic Analysis", paper no. 81-624, 22th Conference on Structures, Structural Dynamics and Materials, American Institute of Aeronautics and Astronautics, Palm Springs, 1981.

[21] Hollowell, W. T., W. D. Pilkey and E. M. Sieveka, "System Identification of Dynamic Structures", Finite Elements in Analysis and Design, 4, pp. 65-77, Elsevier Science Publishers B.V., 1988

[22] Berman, A., "System Identification of Structural Dynamic Models - Theoretical and Practical Bounds", paper no. 84-929, 25th Conference on Structures, Structural Dynamics and Materials, American Institute of Aeronautics and Astronautics, Palm Springs, 1984.

[23] Juang, J. N., and E. C. Wong, "System Identification of Large Space Structures", the 18th Aerospace Sciences Meeting, American Institute of Aeronautics and Astronautics, Pasadena California, January 1980.

[24] Norris, M. A. and L. Meirovitch, "On the Problem of Modelling for Parameter Identification in Distributed Structures", International Journal for Numerical Methods in Engineering, Vol. 28, pp. 2451-2463, John Wiley & Sons, 1989.

[25] Ibanez, P., "Methods for the Identification of Dynamic Parameters of Mathematical Structural Models from Experimental Data", Journal of Nuclear Engineering and Design, Vol. 27, pp. 209-219, North-Holland Publishing Company, 1974.

[26] Masri, S. F. and S. D. Werner, "An Evaluation of a Class of Practical Optimization Techniques for Structural Dynamics Applications", Earthquake Engineering and Structural Dynamics, Vol. 13, pp. 635-649, John Wiley & Sons, 1985.

[27] Hoff, C., "The Use of Reduced Finite Element Models in System Identification", Earthquake Engineering and Structural Dynamics, Vol. 18, pp. 875-887, John Wiley & Sons, 1989.

7. IDENTIFICATION OF MODAL PARAMETERS

Identification of modal parameters is the most frequently applied way of identification of the properties of vibrating structures. This is probably due to the fact that the modal formulation is a compact formulation which describes the structure with a minimum of parameters and at the same time the parameters have a physical meaning which makes them easy to interpret.

The modal parameters can be identified in the time domain as well as in the frequency domain. Examples of both formulations will be presented in this chapter. The formulation in the time domain is based on measured free decays while the formulation in the frequency domain is more flexible. However, a measured response due to white noise can for a linear system be transformed to a free decay signature by the mean of the random decrement technique which was described in chapter 5.

7.1 The Method of the Logarithmic Decrement

A free vibration gives direct information about the eigenfrequency and the damping ratio of a mode if only this mode is excited corresponding to an approximation of the vibrating system to a single degree of freedom. The logarithmic decrement for this mode can be given by:

$$\delta(n) = \ln(\frac{A_n}{A_1}) \tag{7.1}$$

where the logarithmic decrement, $\delta(n)$ is a function of the amplitude of the cycle number n, A_n given an amplitude for the oscillation number 1, A_1. From the relations developed in chapter 4 as well in any standard textbook on the subject, the following is obtained:

$$\begin{aligned} \delta(n) &= \zeta_0(2\pi f_0)(n-1)\frac{2\pi}{(2\pi f_0)\sqrt{1-{\zeta_0}^2}} \\ &\approx 2\pi\zeta_0 n - 2\pi\zeta_0 \end{aligned} \tag{7.2}$$

If $\delta(n)$ is plotted as a function of n a straight line is obtained with the slope $2\pi\zeta_0$ and the intersection $-2\pi\zeta_0$ with the ordinate axis. The approximation in (7.2) holds if ζ_0 is small, say $\zeta_0 \leq 0.05$.

Since $\delta(n)$ and n are known from the measured record the problem of estimating the damping ratio is a linear regression problem which can be easily solved either geometrically or by calcultaion. According to standard textbooks on statistics, see e.g. Johnson and Leone [1], the variance of the slope and thus also of the damping ratio can be found from:

$$\sigma^2 = \frac{\sum_{n=1}^{N} \left(\ln(\frac{A_n}{A_1}) - (2\pi\zeta_0 n - 2\pi\zeta_0)\right)^2}{N-2} \frac{1}{\sum_{n=1}^{N} n^2 - \left(\sum_{n=1}^{N} n\right)^2 / N} \tag{7.3}$$

where N is the number of applied points. The slope is assumed to be normally distributed. It can be noticed that the estimated mean value of the damping ratio and the eigenfrequency is independent. The eigenfrequency is usually estimated from the zero crossing period of the signal.

An example of the application of the logarithmic decrement is shown in figure 7.1. The points are seen to lie closely on a straight line which is indicated by a correlation coefficient of 0.9989. The corresponding damping ratio was found very accurately to be:

$$\zeta_0 = 0.108 \pm 0.002[\%] \quad (95\% \text{ confidence})$$

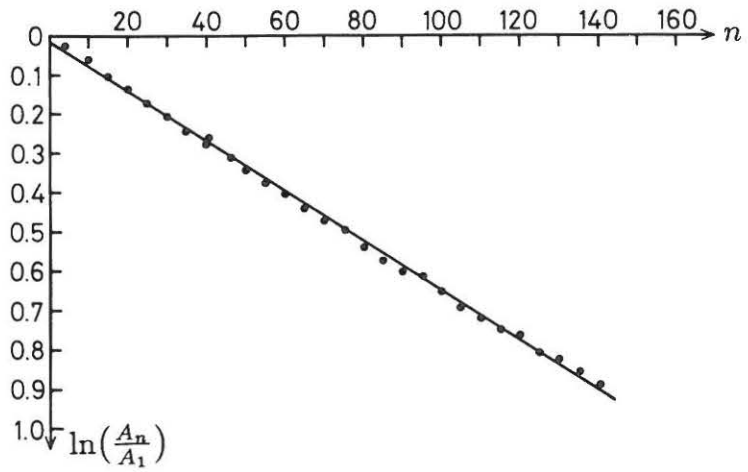

Figure 7.1. The logarithmic decrement for the experimental case. The monopile structure vibrating in first mode, Jensen [2].

A problem with the method is to ensure that only one mode is excited and furthermore, it can be difficult to excite higher modes. Another problem with respect to offshore structures is that it is not common practice to let an offshore structure perform a free vibration since it requires an impulse excitation or a snapback testing which is expensive and often considered to be too risky by the platform owners. In spite of those objections such procedures have been widely applied on other types

of civil engineering structures during the sixties and seventies, see Langen and Sigbjornsson [3], in which a review of damping estimates is given. A free vibration can also be obtained by removing a steady state force due to some external excitation.

An alternative to this kind of excitation method is the application of the random decrement technique which was presented in chapter 5. Nasir and Sunder [4] have investigated the application of the random decrement technique upon the response due to ambient excitation of a jacket platform, a simulation study has also been performed. The simulation studies showed that the eigenfrequencies can be estimated quite accurately from the zero crossing period while the reliability of the damping ratio depends upon the frequency content in the excitation signal and the level of damping. In general the results depend upon whether the resonance peak or the peak due to the wave excitation dominate the response spectrum. The application of the approach in practice gave reliable eigenfrequency estimates and fairly good damping estimates even though the latter showed a scatter corresponding to a coefficient of variation of about 60 %.

7.2 The Ibrahim Time Domain Method (ITD)

This method has been given a lot of attention in the seventies and the first part of the eighties because it has shown to be an effective method for obtaining information about all the modal parameters at one time, see Ibrahim [5] to [9]. The method was developed by S.R.Ibrahim. The requirement of the method is that the measured data represent a free decay and this is also the main limitation of the method.

The solution of the complex eigenvalue problem:

$$\overline{\overline{M}}\ddot{\overline{x}} + \overline{\overline{C}}\dot{\overline{x}} + \overline{\overline{K}}\overline{x} = \overline{0} \tag{7.4}$$

can be assumed to be of the form $\overline{x} = \overline{\Phi} e^{pt}$ with $2n$ complex eigenvalues, $p_i = a_i + \mathbf{i}b_i$ and $2n$ complex eigenvectors, $\overline{\Phi}_i = \overline{c}_i + \mathbf{i}\overline{d}_i$. The eigenvalues and the eigenvectors are found as conjugated pairs for underdamped systems, each pair corresponding to a single degree of freedom. The measured response at discrete times can be given by:

$$\ddot{\overline{x}}(t_i) = \ddot{\overline{x}}_i = \sum_{j=1}^{2n} p_j^2 \overline{\Phi}_j e^{p_j t_i} \tag{7.5}$$

The response can for $2n$ times be given as:

$$(\ddot{\bar{x}}_1 \quad \ddot{\bar{x}}_2 \quad \dots \quad \ddot{\bar{x}}_{2n}) = (\bar{\Phi}_1 \quad \bar{\Phi}_2 \quad \dots \quad \bar{\Phi}_{2n}) \begin{pmatrix} p_1^2 e^{p_1 t_1} & p_1^2 e^{p_1 t_2} & \dots & p_1^2 e^{p_1 t_{2n}} \\ \vdots & \vdots & \vdots & \vdots \\ p_{2n}^2 e^{p_{2n} t_1} & p_{2n}^2 e^{p_{2n} t_2} & \dots & p_{2n}^2 e^{p_{2n} t_{2n}} \end{pmatrix} \tag{7.6}$$

which can be rewritten as:

$$\ddot{\bar{\bar{X}}}(0) = \bar{\bar{Q}}(0)\bar{\bar{A}} \tag{7.7a}$$

where:

$$\bar{\bar{Q}}(0) = (\bar{\Phi}_1 \quad \bar{\Phi}_2 \quad \dots \quad \bar{\Phi}_{2n}) \tag{7.7b}$$

and:

$$\bar{\bar{A}} = \begin{pmatrix} p_1^2 e^{p_1 t_1} & p_1^2 e^{p_1 t_2} & \dots & p_1^2 e^{p_1 t_{2n}} \\ \vdots & \vdots & \vdots & \vdots \\ p_{2n}^2 e^{p_{2n} t_1} & p_{2n}^2 e^{p_{2n} t_2} & \dots & p_{2n}^2 e^{p_{2n} t_{2n}} \end{pmatrix} \tag{7.7c}$$

A time interval later, Δ, the expression still holds and can be written as:

$$\ddot{\bar{\bar{X}}}(\Delta) = (\ddot{\bar{x}}_{1+\Delta} \quad \ddot{\bar{x}}_{2+\Delta} \quad \dots \quad \ddot{\bar{x}}_{2n+\Delta}) = \bar{\bar{Q}}(\Delta)\bar{\bar{A}} \tag{7.8a}$$

$\bar{\bar{Q}}(\Delta)$ is equal to $\bar{\bar{Q}}(0)$ multiplied by the factor $p_j^2 e^{p_j \Delta t}$ on the jth column vector $\bar{\Phi}_j$. Another time interval later, Δ the expression is given by:

$$\ddot{\bar{\bar{X}}}(2\Delta) = (\ddot{\bar{x}}_{1+2\Delta} \quad \ddot{\bar{x}}_{2+2\Delta} \quad \dots \quad \ddot{\bar{x}}_{2n+2\Delta}) = \bar{\bar{Q}}(2\Delta)\bar{\bar{A}} \tag{7.8b}$$

where the $\bar{\bar{Q}}(2\Delta)$ equals $\bar{\bar{Q}}(0)$ multiplied by the factor $p_j^2 e^{p_j 2\Delta t}$.

From the equations, (7.7a), (7.8a) and (7.8b) the following two equivalent relations are obtained:

$$\begin{pmatrix} \ddot{\bar{\bar{X}}}(0) \\ \ddot{\bar{\bar{X}}}(\Delta) \end{pmatrix} = \begin{pmatrix} \bar{\bar{Q}}(0) \\ \bar{\bar{Q}}(\Delta) \end{pmatrix} \bar{\bar{A}} \qquad \begin{pmatrix} \ddot{\bar{\bar{X}}}(\Delta) \\ \ddot{\bar{\bar{X}}}(2\Delta) \end{pmatrix} = \begin{pmatrix} \bar{\bar{Q}}(\Delta) \\ \bar{\bar{Q}}(2\Delta) \end{pmatrix} \bar{\bar{A}} \tag{7.9a}$$

Those can be rewritten as:

$$\bar{\bar{\Upsilon}}(0) = \bar{\bar{\Psi}}(0)\bar{\bar{A}} \qquad \bar{\bar{\Upsilon}}(\Delta) = \bar{\bar{\Psi}}(\Delta)\bar{\bar{A}} \tag{7.9b}$$

After some matrix manipulation it can be shown to lead to one single expression, Ibrahim [5]:

$$\overline{\overline{\Psi}}(\Delta) = \overline{\overline{\Upsilon}}(\Delta)\overline{\overline{\Upsilon}}^{-1}(0)\overline{\overline{\Psi}}(0) \tag{7.10}$$

which can be rewritten as the classical eigenvalue problem:

$$\overline{\overline{\Upsilon}}(\Delta)\,\overline{\overline{\Upsilon}}^{-1}(0)\,\overline{\psi}_j = p_j^2 e^{p_j \Delta t}\,\overline{\psi}_j \tag{7.11}$$

where $\overline{\psi}_j$ is the jth column vector of $\overline{\overline{\Psi}}(0)$ corresponding to a the complex eigenvector including the eigenvector $\overline{\Phi}$ of the original eigenvalue problem and with $p_j^2 e^{p_j \Delta t}$ as the eigenvalue. Remembering $p_j = a_j + \mathbf{i}b_j$, a_j and b_j can be determined from the computed eigen values, $p_j^2 e^{p_j \Delta t}$ and the known sampling interval, Δ. Finally, since $p_j = -\zeta_j 2\pi f_j \pm 2\pi f_j \sqrt{1-\zeta_j^2}$, the eigenfrequency, f_j and damping ratio, ζ_j can be estimated from:

$$f_j = \frac{1}{2\pi}\sqrt{a_j^2 + b_j^2} \tag{7.12a}$$

$$\zeta_j = \frac{a_j}{\sqrt{a_j^2 + b_j^2}} \tag{7.12b}$$

The sampling interval, Δ will enter into the calculation and Parseval's sampling theorem must not be violated: $\Delta \leq \frac{1}{2f_{max}}$. This demand can be modified by an approach equivalent to the zoom approach in an FFT-analysis presented in chapter 5, see Ibrahim [6].

The method assumes that the number of degrees of freedom in the model is equal to the number of excited modes in the measured response. As an estimation of the proper model order, Ibrahim [6] suggests that the number of excited modes present in the response is determined by the rank of $\overline{\overline{\Upsilon}}(0)$. In practice this is done by considering the relative decrease in the $\det[\overline{\overline{\Upsilon}}(0)]$, expanding the dimension of $\overline{\overline{\Upsilon}}(0)$ until the determinant is defined to be equal to zero. (Noise in the measurement will prevent the determinant from becoming exactly equal to zero). If the determinant never gets small enough the cause is that the number of excited modes is too large compared with the number of measuring points equivalent to the dimension of $\overline{\overline{\Upsilon}}(0)$. Thus, the number of measuring locations must be increased or, alternatively, $\overline{\overline{\Upsilon}}()$ can be blown up by applying more time shifts in the derivation of the eigen value problem, i.e. taking $\overline{\overline{X}}(m\Delta)$ into the analysis for $m \geq 3$. In principle the latter approach means that it is possible just to measure at two locations to identify a large number of modes. The estimation of the model order by considering the determinant leads in practice to too large model orders compared with the number of excited modes. This means that the noise will be incorporated in the estimated

model which also often in practice has shown to lead to better modal estimates. Ibrahim has developed concepts which gives a distinction between structural modes and noise modes, Ibrahim [7].

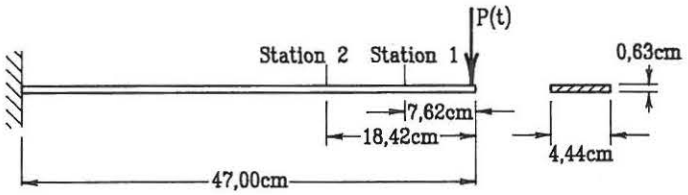

Figure 7.2 Randomly excited cantilever beam in Ibrahim [6], [10].

The method has been widely tested. In table 7.1 the results of an application to a cantilever beam which was randomly excited with a point load are given, see figure 7.2. The ITD method was applied together with the random decrement technique. The theoretical values are also shown in table 7.1 for an undamped beam and the results of a modified method of the time derivative method (TDDM) explained in chapter 6.1, see Ibrahim [10]. The eigenfrequencies and the mode shapes are seen to be very accurate estimates while some deviation exists for the damping ratios. It can be noticed that even though only two measuring points were applied the method succeeded in estimating three modes very accurately.

Method		Mode 1	Mode 2	Mode 3
Theory	f_j	23.82	149.06	417.61
Undamped	Φ_{1j}	1.0000	1.0000	1.0000
Beam	Φ_{2j}	0.6066	-2.4363	2.6064
	f_j	22.86	145.63	404.85
ITD	ζ_j	0.0018	0.00055	0.00141
	Φ_{1j}	1.0000	1.0000	1.0000
	Φ_{2j}	0.5862-i0.0084	- 2.1354+i0.1809	2.3725+i0.0924
Modified	f_j	22.87	145.58	404.41
TDDM	ζ_j	0.00162	0.00055	0.00129
see [10]	Φ_{1j}	1.0000	1.0000	1.0000
	Φ_{2j}	0.5873-i0.0081	- 2.1364+i0.1853	2.3711+i 0.0920

Table 7.1. Estimated parameters of cantilever beam. The mode shapes refer to points 1 and 2 in the figure. T=0.33 sec. and Δ=0.0004 sec. The eigenfrequencies are given in Hz., Ibrahim [6]

The method has also been applied to the measured and simulated response of an offshore monopile by Longo [11]. The random decrement technique, see chapter

5, was applied for transforming the measured ambient response into free decay signatures. For a single degree of freedom assumption the damping ratio was found to have a mean value, $\zeta_0 = 0.0095$ from estimates in the interval $0.0089 - 0.0107$. The eigenfrequency was found to be 0.3226 Hz. Both estimates corresponded to estimates obtained by other methods. Thus the method may be applicable together with the random decrement technique applied to the measured response of offshore structures.

7.3 The Bandwidth Method

A classic and simple method is damping estimation from the half power bandwidth which is a method formulated in the frequency domain. Since it is in principle a curvefit of two points of a resonance peak it can be applied to frequency response function data as well as data for a response spectrum if a white noise approximation is acceptable. The method assumes that the damping is small which means that the peak frequency is approximately equal to the eigenfrequency.

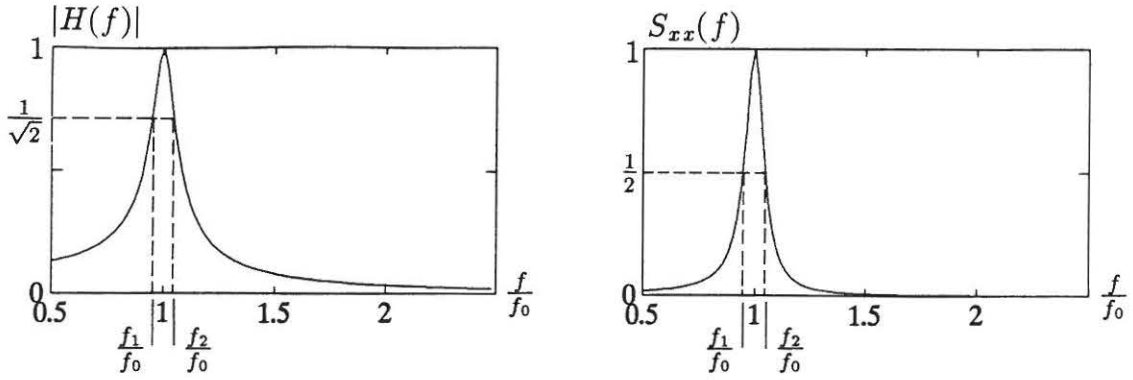

Figure 7.3. The halfpower bandwidth for a frequency response function and a response spectrum of an SDOF system.

The method requires that the estimated frequency response function is approximated to a single degree of freedom system. This means that the magnitude is given by:

$$|H(f)| = \frac{1}{\sqrt{\left(f_0^2 - f^2\right)^2 + \left(2\zeta_0 f_0 f\right)^2}} \frac{1}{(2\pi)^2} \frac{1}{m} \tag{7.13}$$

where m is the mass of the SDOF system which cancels out in the estimation of the damping ratio. The peak value of the eigenfrequency is seen be $\frac{1}{m}\frac{1}{(2\pi)^2}\frac{1}{2\zeta_0 f_0^2}$. If the frequency points for which $|H(f)|$ is equal to $1/\alpha$ of the peak value are determined, a relation to the damping ratio ζ_0 can be found. This gives the following relation,

see Hansen [12]:

$$\zeta_0 = \frac{f_2 - f_1}{2\sqrt{\alpha^2 - 1} f_0} \tag{7.14}$$

Normally α is chosen to be $\sqrt{2}$. If it is the autospectrum of the response and not the frequency response function which is known, a similar expression is obtained due to the relation $S_{xx}(f) = |H(f)|^2 S_{pp}(f)$:

$$\zeta_0 = \frac{f_2 - f_1}{2\sqrt{\alpha - 1} f_0} \tag{7.15}$$

For $\alpha = 2$ in (7.15), the distance, $B_r = f_2 - f_1 = 2f_0\zeta_0$ is called the half-power bandwidth, see figure 7.3. The frequency points f_1 and f_2 will be equal to $\alpha = \sqrt{2}$ and $\alpha = 2$ in (7.14) and (7.15), respectively. The method is highly unreliable because only two points are used to obtain the estimate. An expression for the coefficient of variation has been evaluated in appendix 7.1 for the application of the method to a response spectrum:

$$\delta_{\zeta_0} = \sqrt{\frac{1}{n} + \frac{10B_e}{36B_r}} \tag{7.16}$$

where $B_r = 2f_0\zeta_0$ is the half-power bandwidth, B_e is the effective bandwidth and n is the number of averages in an FFT-analysis. The two latter quantities are related by $B_e = \frac{n}{T}$ where T is the total length of the time series.

The estimate of the uncertainty of the damping given by (7.16) has been compared with the errors of different estimates obtained for the FFT-analysis of a simulated white noise response of an SDOF system, see figure 7.4.

The fully drawn lines are the estimated 95%-confidence interval of the damping ratio as a function of applied means for different B_r to B_e ratios while the points are estimates from the damping ratio obtained by the bandwidth method. It is seen from figure 7.4 that most of the observed errors lie within their respective estimated 95%-confidence limits. This indicates that the expression for the uncertainty works quite well. The figure also shows the error of the estimates obtained for $B_r/B_e = 1.0$ which gives significantly large errors due to the bias contribution. It can be noticed that the improvement in the bias error is relative small when B_r/B_e is increased from 5 to 20. This is in agreement with the fact that a relative bandwidth of 5 is recommended, Bendat and Piersol [13]. However, in the author's opinion a stronger criterion should be chosen if a reliable estimate is needed. It is also seen that the number of means must be very large to reduce the uncertainty significantly. Thus, even though the bandwidth method is very easy to apply it can not be recommended as a method for obtaining final damping estimates. The method has been applied in several cases, see the review in chapter 2.

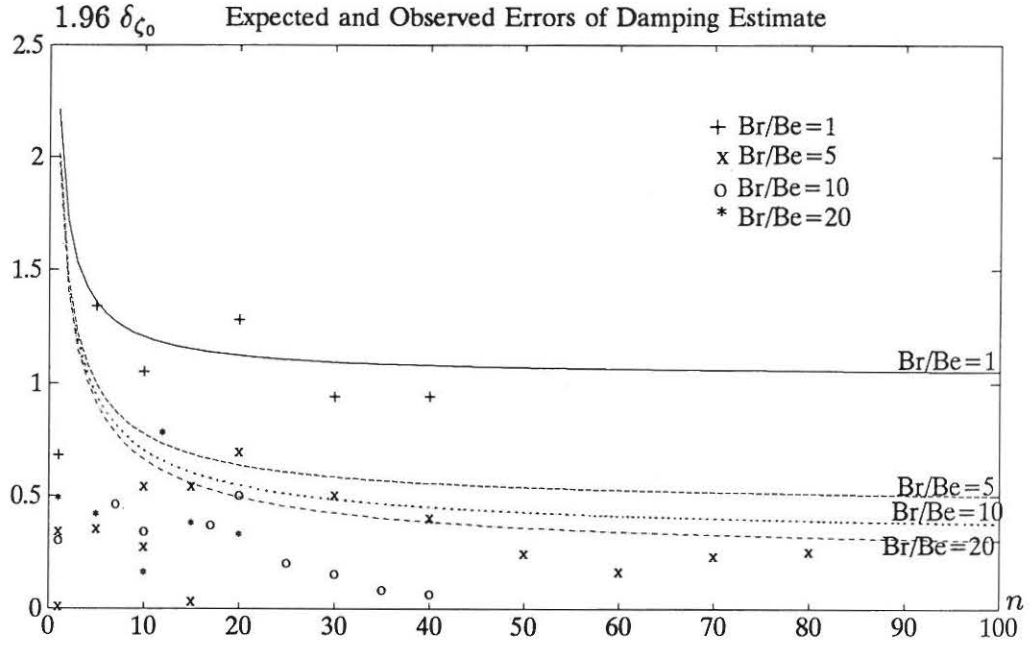

Figure 7.4. One-sided 95%-confidence interval and errors of damping estimate obtained by halfpower bandwidth of the response spectrum of a white noise excited single-degree-of-freedom system, f_0=1.0 Hz and ζ_0=0.01.

7.4 The Method of Spectral Moments

Instead of applying two points for obtaining a damping estimate another approach can be made. The idea is that the spectral ordinate estimate of autospectra are more uncertain than spectral moment estimates, see Bendat and Piersol [13]. The method of spectral moments is based on the information of the damping which is contained in the zeroth, the first and second moment of the response spectrum of a white noise excited single-degree-of-freedom system.

If the one-sided response spectrum for a structure described by a single-degree-of-freedom system is considered:

$$S_{xx}(f) = \frac{S_0}{(f_0^2 - f^2)^2 + (2\zeta_0 f_0 f)^2} \tag{7.17}$$

then the three parameters f_0, ζ_0 and S_0 can be found from the three lowest spectral moments:

$$\lambda_i = \int_{f_1}^{f_2} f^i S_{xx}(f) df \quad i = 0, 1, 2 \tag{7.18}$$

where f_1 and f_2 are the chosen lower and upper frequency limits. The unknown parameters can be estimated from the three spectral moments obtained from the measured spectral quantities and from a theoretical expression. If the structure is

excited by white noise, a set of compact equations can be derived, see Vanmarcke and Iascone [14] and Vanmarcke [15], who developed the original identification algorithm. In Pulgrano et al. [16] it has been shown that the spectral moments can be expressed by:

$$\lambda_i = \frac{S_0 I_i}{4\zeta_0 f_0^{(3-i)}} \quad i = 0,1,2 \tag{7.19}$$

with:

$$I_0 = (D_1 + D_2)|_{r_1}^{r_2} \qquad 0 \leq I_0 < \pi \tag{7.20a}$$

$$I_1 = \frac{2}{d}(D_3)|_{r_1}^{r_2} \qquad 0 \leq I_1 < \pi \tag{7.20b}$$

$$I_2 = (D_1 - D_2)|_{r_1}^{r_2} \qquad 0 \leq I_2 < \pi \tag{7.20c}$$

where:

$$D_1 = \arctan\left(\frac{2\zeta_0 r}{1-r^2}\right) \qquad 0 \leq D_1 < \pi \tag{7.20d}$$

$$D_2 = \frac{\zeta_0}{d}\ln\left(\frac{1+rd+r^2}{1-rd+r^2}\right) \qquad -\infty < D_2 < +\infty \tag{7.20e}$$

$$D_3 = \arctan\left(\frac{\zeta_0 d}{1-2\zeta_0^2-r^2}\right) \qquad 0 \leq D_3 < \pi \tag{7.20f}$$

where the notation $g(x)|_{r_1}^{r_2} = g(r_2) - g(r_1)$ has been applied and $d = 2\sqrt{1-\zeta_0^2}$. It is seen that I_i only depends on the damping ratio and the normalised integration interval, $r = f/f_0$.

According to Vanmarcke [15] the response spectrum can be described by the zero upcrossing frequency, ω_z and the spectral bandwidth parameter ,κ :

$$\omega_z = \sqrt{\frac{\lambda_2}{\lambda_0}} = 2\pi f_0 \sqrt{\frac{I_2}{I_0}} \tag{7.21}$$

$$\kappa^2 = 1 - \frac{\lambda_1^2}{\lambda_0\lambda_2} = 1 - \frac{I_1^2}{I_0 I_2} \tag{7.22}$$

ω_z and κ are seen only to be functions of ζ_0 and the integration interval. This means that if the integration interval is given, then the damping ratio, ζ_0 can be found from the zero value of the error function:

$$V(\zeta_0) = \frac{I_1^2}{I_0 I_2} - \frac{\lambda_1^2}{\lambda_0\lambda_2} = 0 \tag{7.23}$$

where the first term on the right-hand side is theoretically given by (7.20) and where the second term can be numerically estimated from the spectrum of the measured response. Furthermore, the eigenfrequency, f_0 and the constant, S_0 in (7.17) can be found from:

$$f_0 = \frac{\omega_z}{2\pi}\sqrt{\frac{I_0}{I_2}} \tag{7.24}$$

and

$$S_0 = \frac{\lambda_0 4\zeta_0(2\pi f_0)^3}{I_0} = \frac{\lambda_1 4\zeta_0(2\pi f_0)^2}{I_1} = \frac{\lambda_2 4\zeta_0(2\pi f_0)}{I_2} \tag{7.25}$$

The search for the zero point of (7.23) will be iterative with V as a monotonic decreasing function with respect to ζ_0, see figure 7.5. The integration limits r_1 and r_2 is initially estimated to be:

$$\hat{r}_1 = \frac{f_1}{f_{peak}} \qquad \hat{r}_2 = \frac{f_2}{f_{peak}} \tag{7.26}$$

and afterwards adjusted during the iteration by the current estimate of the eigenfrequency, f_0 replacing f_{peak}. This correction has importance if the damping is relatively large.

The zero point of $V(\zeta_0)$ can be found by a simple optimization routine such as the Newton-Raphson method or a more general routine.

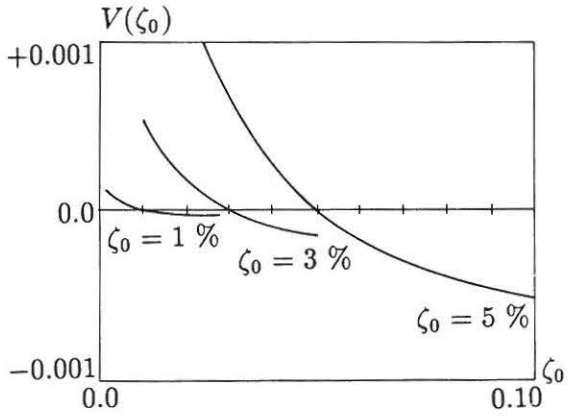

Figure 7.5. The error function as a function of the damping ratio.

The method has been tested in different ways. The method and its principle was developed by Vanmarcke [14] and a more extended version of the method was presented and investigated by Sunder et al. [17], Grewatz [18]. The latter two authors investigated the effect of non-white excitation and additive noise by simulation of spectra. It was found that the integration intervals, r_1 and r_2 should

not be too wide for the estimation of light damping. It was suggested that the half-power points were applied. It was also found that while estimates obtained by the bandwidth method tend to overestimate the damping, the estimates of the present method could not be claimed to be either inflated or deflated. The method has been applied in practice in several relations, see e.g. Vanmarcke and Iascone [15] and Sigbjornsson [19]. To the knowledge of the author the method has not been systematically investigated for spectra obtained by FFT-analysis.

The method has also been implemented and tested in relation to this thesis and some experiences have been made. It was found that the number of frequency points around the spectral peak had a significant influence upon the damping estimate. It was also found that the spectral moments were best obtained by numerical integration by Simpson's rule. Several integration methods of higher order were tried but gave no significant improvement. The main error of the estimates of very lightly damped systems, $\zeta_0 \leq 0.01$ seems to be due to this numerical integration provided that no error of the spectral points is present.

It was attempted to use the integration limits r_1 and r_2 as variables but this did not work out. Nor was it a good idea to apply a direct determination of the theoretical moments by numerical integration even though one could hope that the integration errors in this way would cancel out. The method is clearly a better method than the spectral bandwidth method.

As mentioned in the start of the section the spectral estimates are more uncertain than the spectral moments. This means that if FFT analysis is applied the reduction of bias errors should be weighted more than the reduction of random errors compared with for example the bandwidth method.

The uncertainty of the damping estimate can be found approximately. From the approximate expression valid for an SDOF system excited by white noise and with $r_1 = 0$ and $r_2 = \infty$:

$$\kappa^2 = \frac{4\zeta_0}{\pi} = [1 - \frac{\lambda_1^2}{\lambda_0 \lambda_2}] \tag{7.27}$$

one obtains:

$$\zeta_0 = \frac{\pi}{4}[1 - \frac{\lambda_1^2}{\lambda_0 \lambda_2}] \tag{7.28}$$

This means that the expression for the variance becomes:

$$\sigma_{\zeta_0}^2 = (\frac{\pi}{4})^2 \mathrm{VAR}[\frac{\lambda_1^2}{\lambda_0 \lambda_2}] \tag{7.29}$$

where:

$$\begin{aligned}\mathrm{VAR}[\frac{\lambda_1^2}{\lambda_0 \lambda_2}] = &(\frac{\lambda_1^2}{\lambda_0^2 \lambda_2})^2 \sigma_{\lambda_0}^2 + (\frac{2\lambda_1}{\lambda_0 \lambda_2})^2 \sigma_{\lambda_1}^2 + (\frac{\lambda_1}{\lambda_0 \lambda_2^2})^2 \sigma_{\lambda_2}^2 + 2(\frac{\lambda_1^2}{\lambda_0^2 \lambda_2})(\frac{2\lambda_1}{\lambda_0 \lambda_2})\sigma_{\lambda_0 \lambda_1}^2 \\ &+ 2(\frac{\lambda_1^2}{\lambda_0^2 \lambda_2})(\frac{\lambda_1}{\lambda_0 \lambda_2^2})\sigma_{\lambda_0 \lambda_2}^2 + 2(\frac{2\lambda_1}{\lambda_0 \lambda_2})(\frac{\lambda_1}{\lambda_0 \lambda_2^2})\sigma_{\lambda_1 \lambda_2}^2\end{aligned} \tag{7.30}$$

The three last terms in (7.30) contain the cross-variances between the three spectral moments. The covariance of the spectral moments can be computed from a straightforward calculation introducing the variance of the spectral density in the expression of the variance of the spectral moments. The approach becomes equivalent to the approach for the bandwidth method given in appendix 7.1.

7.5 The Circle Fit Method

If the excitation as well as the response can be measured then the structural information should be extracted from the measured transfer function data. The circle fit method can be applied to the case where such a controlled external excitation has been applied to a structure. It is assumed that a forced excitation has been applied at one point and the response has been measured at another point. Then the structural information can be extracted applying both the gain and the phase information in the identification. This is accomplished if the real and the imaginary part of the transfer function are evaluated from the data:

$$H_{ki}(f) = \mathbf{Re}[\frac{S_{p_k\dot{x}_i}(f)}{S_{p_kp_k}(f)}] + \mathbf{i}\,\mathbf{Im}[\frac{S_{p_k\dot{x}_i}(f)}{S_{p_kp_k}(f)}] \tag{7.31}$$

where i is the index of the degree of freedom at which the response has been measured and index k is the degree of freedom, where the force p_k has been applied. It can be shown that if the measured response is a velocity process and if an SDOF system is assumed then a circle fit can be obtained as shown in figure 7.6 by plotting the real and the imaginary part of transfer function against each other for the given frequency range. The transfer function of velocity response versus force excitation is called a mobility transfer function. The circle plot is also called a Nyquist plot or a Kennedy-Pancu plot, Kennedy and Pancu [20].

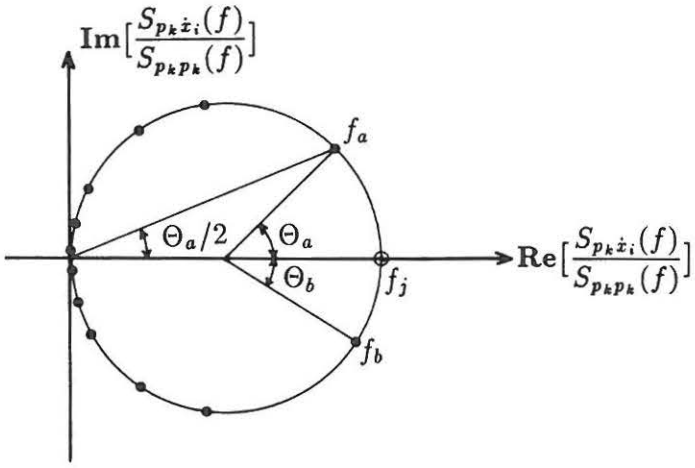

Figure 7.6. Circle plot of mobility function of viscous damped system.

It is assumed that in the frequency domain the transfer function in the neighbourhood of the jth mode can be described by an SDOF system. Then according to Ewins [21] the real and the imaginary part of the mobility transfer function will be given by:

$$\mathbf{Re}[\frac{S_{p_k\dot{x}_i}(f)}{S_{p_kp_k}(f)}] = \frac{2K_{ki}^j(2\pi f_j)\zeta_j(2\pi f)^2}{((2\pi f_j)^2-(2\pi f)^2)^2+4(2\pi f_j)^2\zeta_j{}^2(2\pi f)^2} \tag{7.32a}$$

$$\mathbf{Im}[\frac{S_{p_k\dot{x}_i}(f)}{S_{p_kp_k}(f)}] = \frac{K_{ki}^j(2\pi f)((2\pi f_j)^2-(2\pi f)^2)}{((2\pi f_j)^2-(2\pi f)^2)^2+4(2\pi f_j)^2\zeta_j{}^2(2\pi f)^2} \tag{7.32b}$$

which will be approximately valid in some frequency region around the jth eigenfrequency, $f_j-\Delta f \leq f_j \leq f_j+\Delta f$ corresponding to an approximation of the vibration system to an SDOF system.

The real and imaginary part of the mobility transfer function given by (7.32) can be plotted against each other for discrete frequencies and will appear as points lying on a circle as shown in figure 7.6.

K_{ki}^j is a constant containing information of the mode shapes. Remembering the assumption of an excitation at only a single point, k , the modal constant K_{ki}^j will be given as:

$$K_{ki}^j = \Phi_{ij}\Phi_{kj} \tag{7.33}$$

with Φ_{ij} being the ith element of the jth weighted mode shape. This information may be extracted if a set of circle fits of different eigenmodes has been estimated as shown in Ewins [21]. The radius of the circle can be shown to be:

$$R_{ki}^j = \frac{K_{ki}^j}{4(2\pi)f_j\zeta_j} \tag{7.34}$$

and the centre of the circle by:

$$\overline{C}_{ki}^j = (\frac{K_{ki}^j}{4(2\pi)f_j\zeta_j}, 0) = (R_{ki}^j, 0) \tag{7.35}$$

The angular spacing between discrete points in the circle plot will vary if the frequency resolution is constant. The angular spacing will contain information of the eigenfrequency and the damping ratio of mode no. j. Considering two points corresponding to f_a and f_b in figure 7.6, it follows, see e.g. Ewins [21], that:

$$\tan(\Theta_b/2) = (1 - (\frac{f_b}{f_j})^2)/(2\zeta_j \frac{f_b}{f_j}) \tag{7.36a}$$

$$\tan(\Theta_a/2) = ((\frac{f_a}{f_j})^2 - 1)/(2\zeta_j \frac{f_a}{f_j}) \tag{7.36b}$$

The eigenfrequency and the damping ratio can thus be estimated from a pair of points in the circle plot. Assuming constant frequency resolution the eigenfrequency, f_j will be located between the discrete points where the angular spacing is largest and can be found from linear interpolation. The damping ratio can be estimated directly from (7.36) when the eigenfrequency has been estimated:

$$\zeta_j = \frac{((2\pi f_a)^2 - (2\pi f_b)^2)}{2(2\pi f_j)((2\pi f_a)\tan(\Theta_a/2) + (2\pi f_b)\tan(\Theta_b/2))} \tag{7.37}$$

where $\Theta_a, \Theta_b, f_a, f_b, f_j$ are given by figure 7.6. From each pair of data points, an estimate of the damping ratio can be computed. If the damping ratio obtained from this method is assumed to be normally distributed, a confidence interval can be determined for the different damping estimates obtainable from each pair of frequencies located around the eigenfrequency.

The circle fit algorithm has been implemented in a C-program on a personal computer and works quite well. The circle is estimated by non-linear least square estimation which converges very quickly (3 to 5 iterations). The single-degree-of-freedom assumption has been applied but it is possible to modify the method to several degrees of freedom. This can be done as an iterative procedure where the influence of the neighbouring modes is "subtracted" from the mode of interest. This iteration process gives a quick convergence with respect to the damping ratio (maximum 4 adjustments). The program has been tested for simulated data and works well. It has also been tested for experimental data but the data obtained by FFT were so biased that the circle fit method failed just as other methods, see Jensen [2].

The disadvantage of the method is that the exact relation between the response and excitation must be known. On the other hand, if it is known this method uses all the available information in the obtained measurements since both the amplification and the phase information are applied. This means that the method in such cases gives the best possible modal estimates. Another disadvantage is that the circle fit method, as it has been presented, requires that the response has been measured as velocities. Usually it is only the acceleration which has been measured and integration is in general not advisable. However, the principle of the method taking the phase information into account can be extended to the cases where the response has been measured as accelerations even though a less elegant algorithm is to be expected.

To the author's knowledge the method has not been used on offshore structures or civil engineering structures but in any case if the exact relation between the response and the excitation is known both the gain and the phase information should be applied to obtain more reliable estimates. It should be noticed that the phase information should be given by the real and the imaginary part of the transfer function since the phase evaluated as a phase angle leads to larger uncertainty, see chapter 5.

The circle fit method is in general applied to a single point excitation but can be applied to multiple point excitation. However, this complicates the algorithm, especially if the forces are not completely correlated.

7.6 Global Curve Fit in the Frequency Domain

The identification concept in the frequency domain is typically formulated as some sort of curvefitting approach. This can be a local curve fit of the resonance peak such as the bandwidth method or it can be a global curve fit taking a wide frequency region into account containing several resonance peaks.

The local curve fit leads to information about the eigenfrequency and the damping ratio of a given eigenmode. The fit is based on the single-degree-of-freedom assumption where each resonance peak in the response spectrum or in the transfer function is considered as the resonance peak in an SDOF system. The review in chapter 2 showed that this approach is widely applied in practice but there may be several reasons to consider a global curvefit in some cases.

- If some modes are closely spaced it may be impossible to apply a local curvefit on each resonance peak.
- If prior estimates of e.g. eigenfrequencies have been obtained from local fits, a global fit may give additional information about mode shapes, mass distribution etc.
- A global curve fit will provide estimate which are proper correlated with respect to each other. Ignoring the correlation between certain parameters by a separate parameter estimation gives errors in the estimates.
- If a weighting function is included in the global fit of the data a smooth relation will exist between a local and a global fit corresponding to the judgement of which frequency region should be considered most reliable.

Due to the above reasons a global curvefitting algorithm has been considered for measured data represented by a transfer function. A global fit can also be performed for a measured response spectrum due to the relation:

$$S_{xx}(f) = |H(f)|^2 S_{pp}(f) \tag{7.38}$$

where the shape of the force spectrum can be parameterized and included as unknown in the estimation procedure, or the force spectrum can be considered to

approximate white noise within some given frequency region. A few cases of identification by including parameters of the force spectrum as unknown parameters have been studied by A. Rytter and the author. It seems to be a possible approach in some cases although in other cases problems with an ambiguous estimation of the unknown parameters may arise.

A global fit including the phase information has not been considered even though it is possible. It has been considered that often no phase information will be available since the excitation due to waves will only be indirectly known from the wave elevation, see chapter 5. On the other hand, if phase information is available it will often be possible to separate different modes by choice of the force input. Thus, in those cases a method such as the circle fit method with an SDOF assumption will be applicable taking the phase information between the excitation and the response into account.

Thus, in the present section a global curvefit of a set of measured transfer functions is considered. It is formulated as an optimization problem of an error criterion function given by:

$$V(\overline{\Theta}) = \frac{1}{N}\sum_{i=1}^{N}\frac{1}{2}\overline{\epsilon}^T(f_i|\overline{\Theta})\,\overline{\epsilon}(f_i|\overline{\Theta}) = \frac{1}{2N}\sum_{i=1}^{N}\sum_{j=1}^{m}\epsilon_j^2(f_i|\overline{\Theta}) \tag{7.39}$$

where $\overline{\epsilon}(f_i|\overline{\Theta})$ is an $m\ x\ 1$ vector where each element is the error of a measured transfer function no. j for a given frequency:

$$\epsilon_j(f_i|\overline{\Theta}) = H_j(f_i) - H_j(f_i|\overline{\Theta}) \quad j = 1,2\ldots m \tag{7.40}$$

where $\overline{\Theta}$ is a vector containing the unknown parameters to be estimated by finding the minimum of $V(\overline{\Theta})$. The unknown parameters could for instance be the eigenfrequencies, the damping ratios and the mode shapes. N is the number of data points and is assumed to be the same for all the transfer function data, $H_j(f_i)$, $j = 1,2,\ldots m$.

According to the principle in chapter 3 the given error criterion function $V(\overline{\Theta})$ corresponds to a least square formulation. The minimum can be found by an optimization algorithm such as the NLPQL algorithm which has been widely used in this thesis, Schittkowski [22]. Also as shown in chapter 3 it is possible to find the covariance matrix of the estimated parameters when a least square approach is applied. However, this requires that the assumed model is also the true model. E.g. the model must not contain too many parameters since no convergence in those cases can be achieved. The model must either not be too simple since this will lead to a rough model approximation. However, in the latter case it will be possible to obtain convergence in general. Finally, the true model may belong to another class of models which means that the estimated model will only be a least square approximation to the true model.

Even though the least square norm is an approach consistent with the maximum likelihood estimation as shown in chapter 3 there is really no objective reasons for not choosing another norm e.g. to formulate the error as a sum of errors raised to the fourth power or another higher norm, p. In Xinsen and Vandiver [23] the norm p is considered as an optimization variable of values $2, 4, \ldots, 10$ in the estimation algorithm called the least pth optimization technique. The optimized norm will depend upon the estimated errors and will influence the iterative search for a minimum of the error criterion function. The method has been successfully applied in practice for an offshore structure in Xinsen and Vandiver [23]. Ljung [30] has discussed the choice of an optimal norm intensively in mathematical terms.

7.6.1 Simulated Case

A curvefit algorithm OPT has been implemented into a FORTRAN program based upon the NLPQL optimization algorithm. The program is able to find a set of modal parameters from a curvefit of measured transfer functions. The estimates are given as a set of mean values and standard deviations according to the principles of chapter 3. The complete covariance matrix of the parameters is also available. The numerically estimated standard deviation has been checked for numerical errors. The estimated standard estimation has been found to be numerically stable for relative numerical steps of order 10^{-8} to 10^{-3} in the gradient calculations. Furthermore, the magnitude of the estimated standard deviations were in general found to be sensible.

Another important result of the estimation algorithm is the error of the fit. It is important because a comparison of the errors of runs using different initial estimates makes it possible to justify that the best fit has been obtained. The error can furthermore be applied for comparing the fit of different models and thus justifying a given model.

The curvefit algorithm has been applied to simulated noise distorted data of the transfer functions of the acceleration response towards the base displacement of a two degrees of freedom structure with a base excitation as shown in the figure 7.7 quite analogous to the experimental case presented in chapter 1.

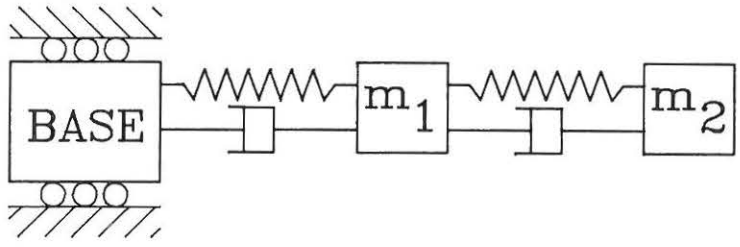

Figure 7.7. 2DOF system with f_1=1.1054 Hz , f_2=7.1921 Hz, $\overline{\Phi}_1^T$=(1.0 0.3805), $\overline{\Phi}_2^T$=(1.0 −1.8864) with different damping ratios in the range 0.001 to 0.13. The lumped masses were m_1=25.56 kg. and m_2=35.65 kg.

The model for the transfer function between the displacement response and the base displacement excitation of the two-degrees-of-freedom, proportionally damped system was formulated as shown in Jensen [2]:

$$H_j(f) = \sum_{i=1}^{2} \frac{-(2\pi f)^2 K_{ji}}{((2\pi f)^2 - (2\pi f_i)^2) + 2\mathbf{i}(2\pi f_i)(2\pi f)\zeta_i} \quad j = 1,2 \tag{7.41}$$

The transfer function could without problems have been replaced by the acceleration response versus the base acceleration or another transfer relation. The constant K_{ji} was given by:

$$K_{11} = \tilde{\Phi}_{11}^2 m_1 + \tilde{\Phi}_{11}\tilde{\Phi}_{21} m_2 = \frac{1}{1+\alpha^2\mu} + \frac{\alpha}{\mu+\alpha^2} \tag{7.42a}$$

$$K_{12} = \tilde{\Phi}_{12}^2 m_1 + \tilde{\Phi}_{22}\tilde{\Phi}_{21} m_2 = \frac{1}{1+\beta^2\mu} + \frac{\beta}{\mu+\beta^2} \tag{7.42b}$$

$$K_{21} = \tilde{\Phi}_{21}\tilde{\Phi}_{11} m_1 + \tilde{\Phi}_{21}^2 m_2 = \frac{\alpha}{1+\alpha^2\mu} + \frac{\alpha^2}{\mu+\alpha^2} \tag{7.42c}$$

$$K_{22} = \tilde{\Phi}_{12}\tilde{\Phi}_{22} m_1 + \tilde{\Phi}_{22}^2 m_2 = \frac{\beta}{1+\beta^2\mu} + \frac{\beta^2}{\mu+\beta^2} \tag{7.42d}$$

$\tilde{\Phi}_{ij}$ is the ith element of the weighted jth mode shape $\tilde{\overline{\Phi}}_j$ and $\mu = \frac{m_2}{m_1}$ is the mass distribution given by the ratio between the two lumped masses, and α and β are related to the unweighted mode shapes by:

$$\overline{\Phi}_1^T = (1 \quad \alpha) \tag{7.43a}$$

$$\overline{\Phi}_2^T = (1 \quad \beta) \tag{7.43b}$$

As a constraint to the curvefitting the mode shapes were forced to be orthogonal which can be shown to be equal to:

$$1 + \alpha\beta\mu = 0 \tag{7.44}$$

The presented model contains seven unknown parameters. It was found that for a 2DOF system, this was the number of parameters which could be identified uniquely from the two measured transfer functions of the two degrees of freedom. The seven parameters corresponded to 6 modal parameters plus the mass distribution ratio, μ. The 6 modal parameters consisted of two eigenfrequencies, two damping ratios and two unweighted mode shape coordinates. If also a transfer function between the response of the two degrees of freedom had been included it would

probably also have been possible to estimate the absolute values of the lumped masses corresponding to eight unknown parameters.

The seven parameters of the two transfer functions were estimated for a simultaneous curvefitting of the two estimated transfer functions of the two degrees of freedom. The algorithm was able to estimate all the parameters within a deviation less than 0.1 % with a standard deviation of the same magnitude (maximum). This applied to a lightly damped system with $\zeta_1 = 0.00127$ and a resolution of 0.001 Hz. Those results were very acceptable. As a further test of the algorithm the following subjects were investigated:

- The effect of frequency resolution (number of points).
- The effect of the damping level.
- The effect of closely spaced eigenmodes.

The simulation study was made realistic by adding noise to the simulated measured transfer function data. The noise-to-signal ratio was defined as:

$$n/s = \sqrt{\frac{\sum_{i=1}^{N} 1 - \left(\frac{|H(f_i)|}{|H(f_i|\overline{\Theta})|}\right)^2}{\sum_{i=1}^{N} \left(\frac{|H(f_i)|}{|H(f_i|\overline{\Theta})|}\right)^2}} \tag{7.45}$$

where the simulated measured transfer function was given by:

$$|H(f_i)| = |H(f_i|\overline{\Theta})| \frac{1}{1 + n(f_i)} \quad n(f_i) \in [0, n_{max}] \tag{7.46}$$

corresponding to a noise model no. 2 with noise on the measured input, see chapter 5, figure 5.15. The noise contribution, $n(f_i)$ at the frequency f_i was computed from a random generator function in FORTRAN with a rectangular probability density function. This particular noise model will lead to bias of the measured transfer function and is therefore quite serious. In figure 7.8 an example of a curvefit with simulated noise corrupted data is shown. Considering the scatter it should be remembered that scales are logarithmic. Besides illustrating the noise-to-signal level, figure 7.8 also shows that the method succeds in obtaining a fit of the measured transfer function.

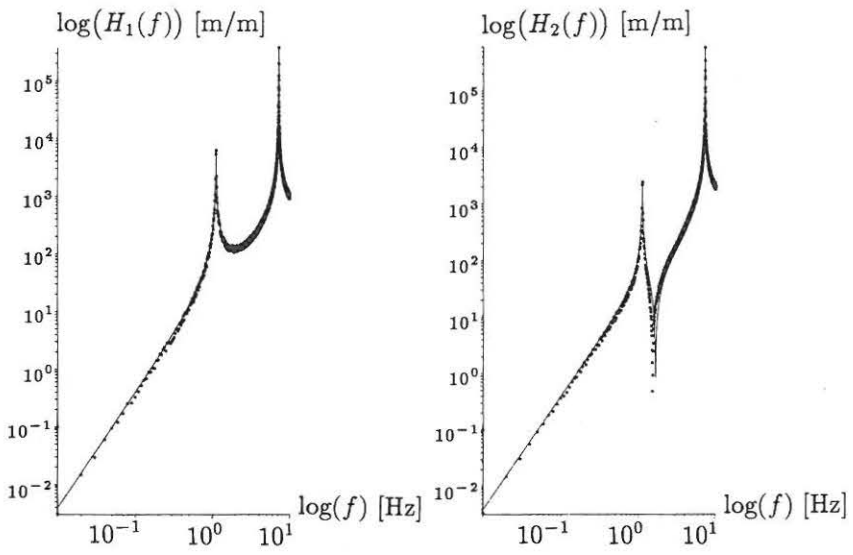

Figure 7.8. Curvefit of simulated transfer function with n/s=0.32.

7.6.2 The Effect of the Number of Data Points

The effect of the frequency resolution, that is the number of data points in the frequency domain, has been investigated. Since the data has been simulated directly in the frequency domain there is no bias error present due to a performed signal processing such as an FFT-analysis.

It is generally known that especially the estimation of the damping ratio is sensitive to the resolution since all the information of the damping is given by the points located at the resonance peaks. This was confirmed by the estimation based on different resolutions as shown in figure 7.9. Here the deviation and the coefficient of variation of the first damping ratio are shown. The resolution is seen to have a tremendous effect upon the deviation as well as the coefficient of variation when noise is present. Thus it is not only due to the bias error in the FFT analysis that it is necessary to ensure a high resolution. It is equally important when biasing noise is suspected to be present. With respect to the other modal quantities it was found for $n/s = 0.32$ that the mode shapes only deviated from 4 to 8% while the eigenfrequencies were estimated very accurately within 0.1%. The deviation of the mass ratio corresponded to the mode shape estimates.

It can be noticed that the curves in figure 7.9 and the following similar figures are not smooth but fluctuate. This is explained by the fact that the curves consist of estimates of random variables. Smooth curves (in mean) would have been expected if many realizations of measured data had been investigated.

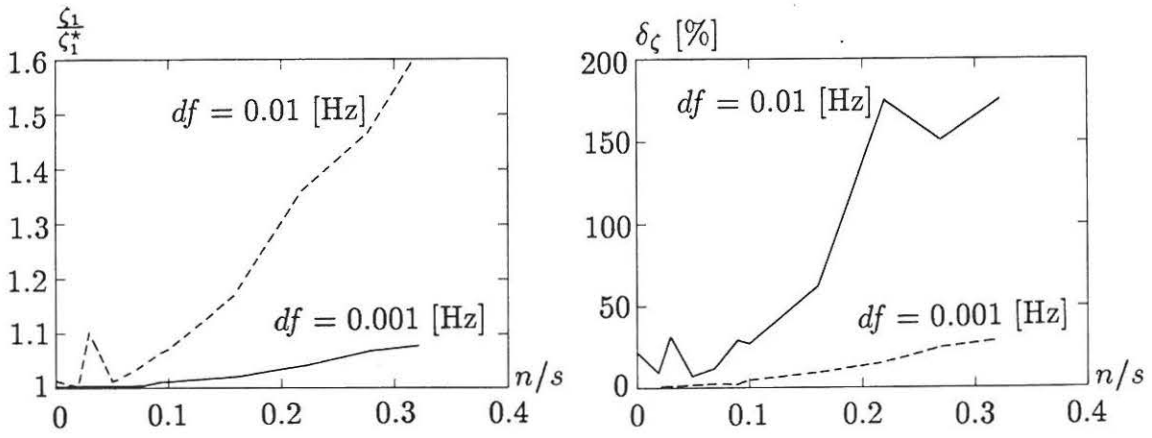

Figure 7.9. Deviation and variation coefficient of the first damping ratio for different resolution, df with variation in the noise level, ζ_1^*=0.00127 (true value).

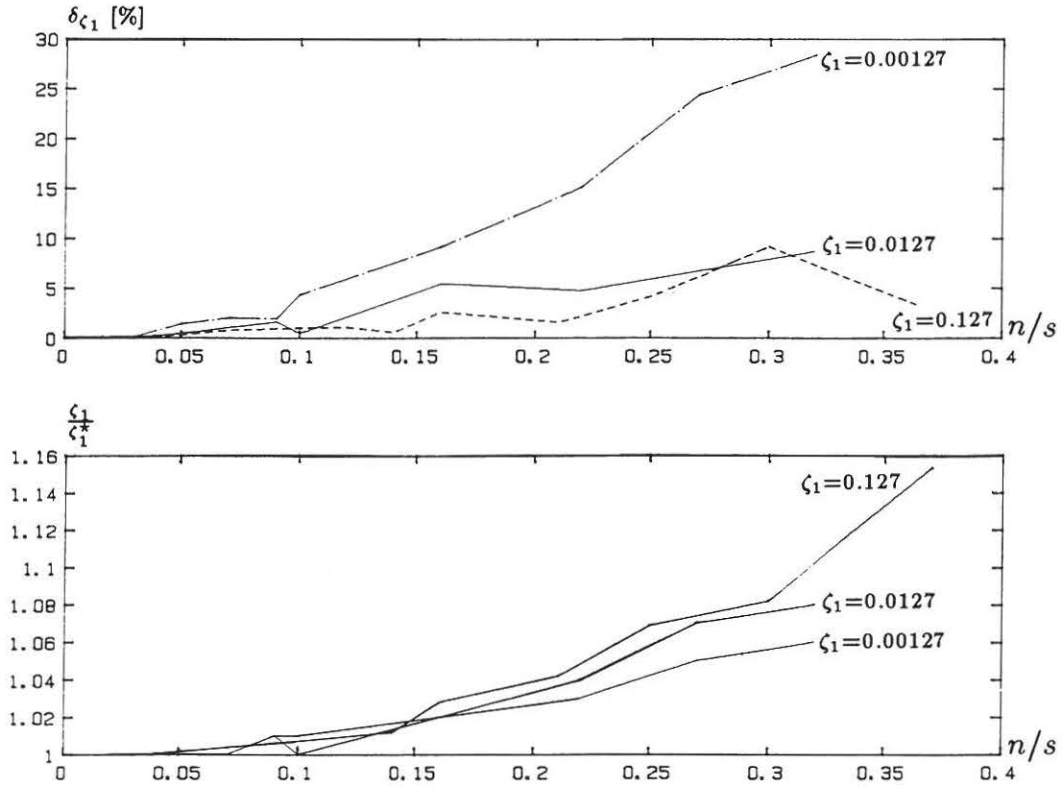

Figure 7.10. Deviation and coefficient of variation of the damping ratio for different damping level given by the numbers at the curves (ζ_1^*: true value).

7.6.3 The Effect of the Damping Level

The influence of the damping level upon the parameter estimates has also been investigated. It is obvious that it is easier to identify the eigenfrequency of a lightly damped system since the eigenfrequency in that case becomes equal to the peak frequency. Thus this influence should also be investigated applying a general curvefit.

To get a unified measure of the damping level a relative bandwidth has been defined as the half-power bandwidth of the resonance peak over the frequency resolution:

$$B = \frac{2\pi f_i \zeta_i}{df} \tag{7.47}$$

where f_i and ζ_i are the ith eigenfrequency and damping ratio, respectively. The effect of the damping level has been investigated for given values of B corresponding to keeping the number of measured data points constant within the half-power bandwidth.

The effect of different damping levels has been investigated with a constant relative bandwidth of $B_1 = 2.8$ and $B_2 = 9.3$ for the 1st and 2nd eigenmodes, respectively with three levels of damping $\zeta_1 = \zeta_2 = 0.127$, 0.0127 and 0.00127 for the system in figure 7.7.

From figure 7.10 it is seen that the coefficient of deviation of the first damping ratio is only moderate sensitive to the damping level for different noise level while the coefficient of variation is significantly sensitive to the damping level. It seems that a small damping level causes a slight overestimation of the damping estimate. Figure 7.10 also shows that a larger damping level gives an estimate which is less sensitive to the noise level even though the relative bandwidth is the same. Thus it is in fact more difficult to estimate the damping in lightly damped systems.

The eigenfrequencies showed a coefficient of variation less than 1% and were estimated very accurately indeed although it seemed that the estimates became slightly more uncertain for larger damping ratios which is also a generally accepted experience. The behaviour of the estimated mode shapes and the mass ratio is shown in figure 7.11. It is seen that while the deviations of the estimates seem to be independent of the damping level the coefficient of variation seems to increase with increasing damping which is probably the same effect as for the eigenfrequency estimates. Larger damping leads to a more uncertain interpretation of the resonance peak and thus also the eigenfrequencies, the mode shapes and the mass ratio.

7.6.4 The Effect of Closely Spaced Eigenmodes

The effect of eigenmode proximity has been investigated for the system in figure 7.7 with the first eigenfrequency $f_1 = 1.1054$ Hz and the second eigenfrequency $f_2 = 1.1554$ Hz with different damping ratios $\zeta_1 = \zeta_2 = 0.005$, 0.01 and 0.05. This has been made for different noise levels.

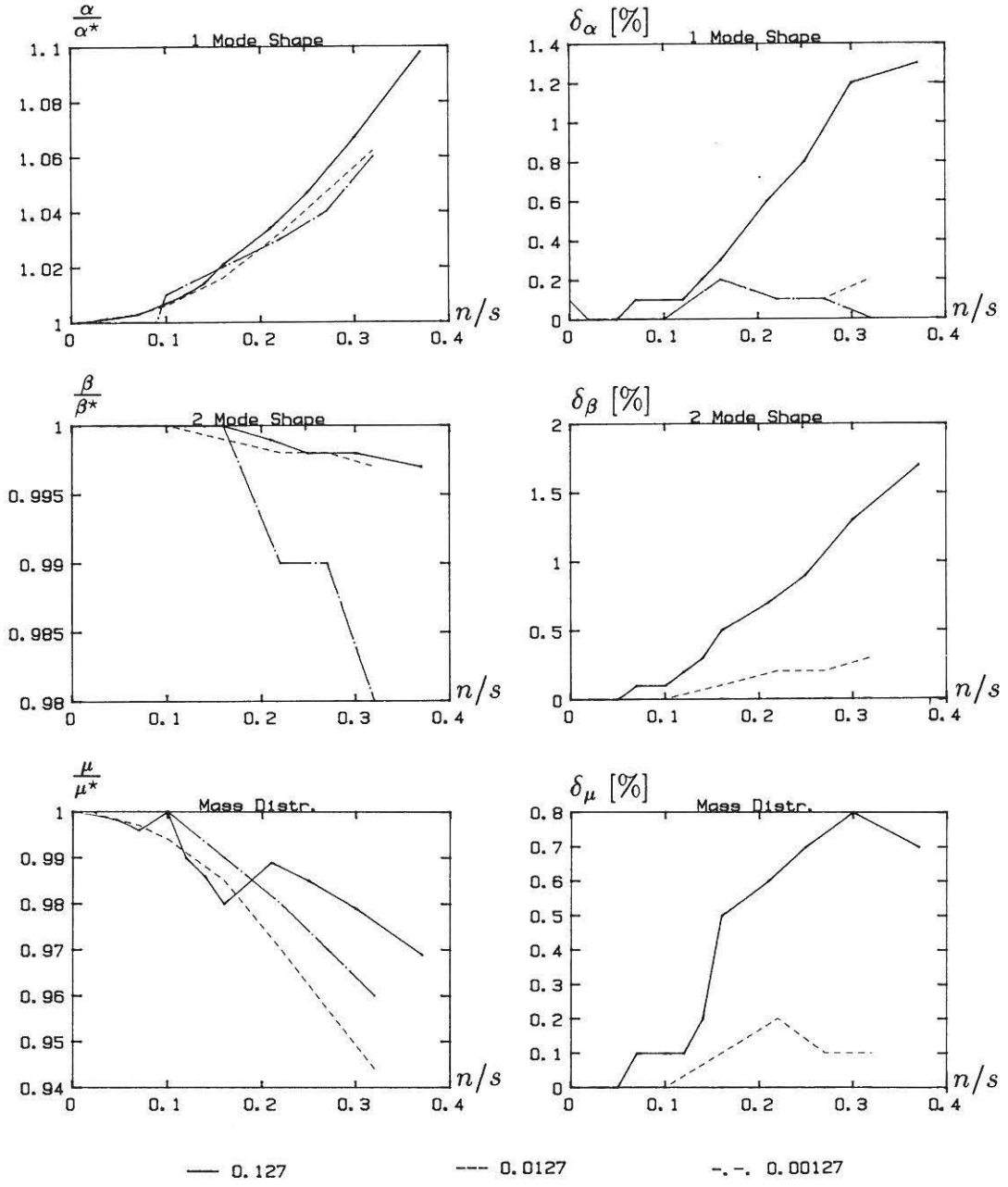

Figure 7.11. Deviation and coefficient of variation of the mode shapes and the mass ratio for different damping level (true values $\alpha^\star$, $\beta^\star$, $\mu^\star$).

As a measure of the proximity of the eigenmodes the following measure has been introduced:

$$B = \frac{2f_1\zeta_1}{df}\frac{2(f_2 - f_1)\zeta_2}{df} \tag{7.48}$$

The dimensionless measure ensures that for a given system a unified measure for the relative frequency resolution is obtained. The transfer function $H_2(f)$ is shown for $B = 0.009$, 0.22 and 0.88 in figure 7.12. It is seen that an increasing B for a given damping level reveals the correct picture of the two resonance peaks. Note that the theoretical separation of the resonance peaks will only be a fact if the damping level is not too large compared with the density of the eigenfrequencies.

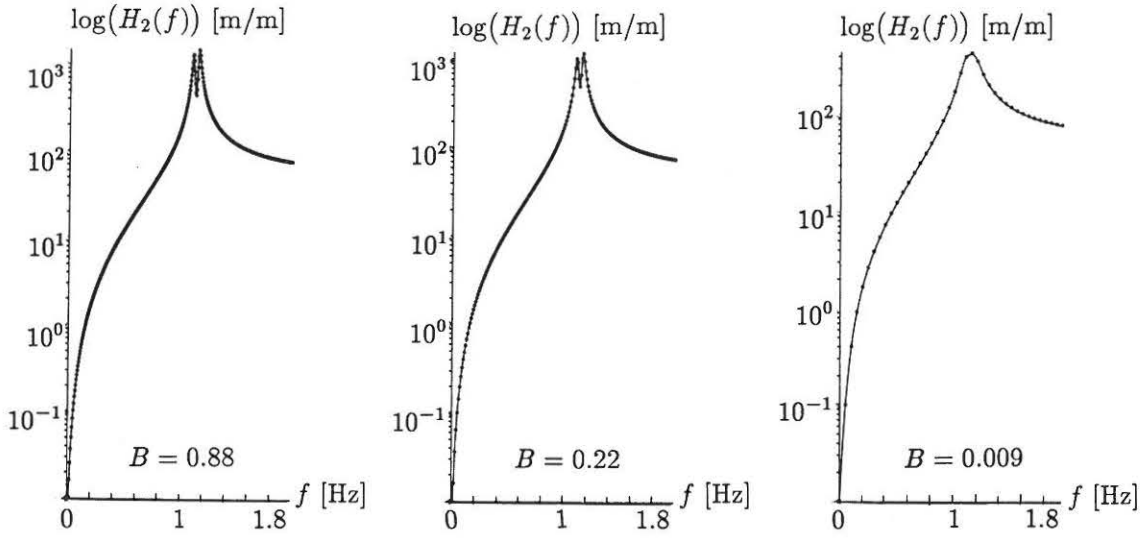

Figure 7.12. Examples of closely spaced eigenmodes for different frequency resolutions of the transfer function $H_2(f)$. B=0.009, 0.22 and 0.88 for the damping ratio ζ=0.01.

The estimates were investigated for the case where no noise was present. It is seen from figure 7.13 that the damping ratios cannot be estimated uniquely for the largest damping ratio independent of B. The deviation and the coefficients of variation are fluctuating with respect to the B with no trend. For the lower damping ratio the estimates are seen to converge in some sense with respect to a large B. The conclusion is that the transfer function data do not contain enough information to separate closely spaced eigenmodes when they are closely spaced with relatively large damping. In those cases it would have helped significantly if the phase information of the transfer function had been applied, e.g. by a circle fit.

The level of variation and deviation were highest for the estimates of the eigenmodes and the mass distribution as shown in figure 7.14. This may be explained by the fact that the error function is most sensitive to these parameters in the frequency range between the two resonance peaks where an antiresonance is hidden. Since the number of points in this range were relatively few, this effect could be expected. With respect to the estimates of the eigenfrequencies the largest deviation was found to be about 0.1% for the highest level of damping with the poorest resolution. Generally the magnitude of the estimated standard deviations corresponded to the deviations.

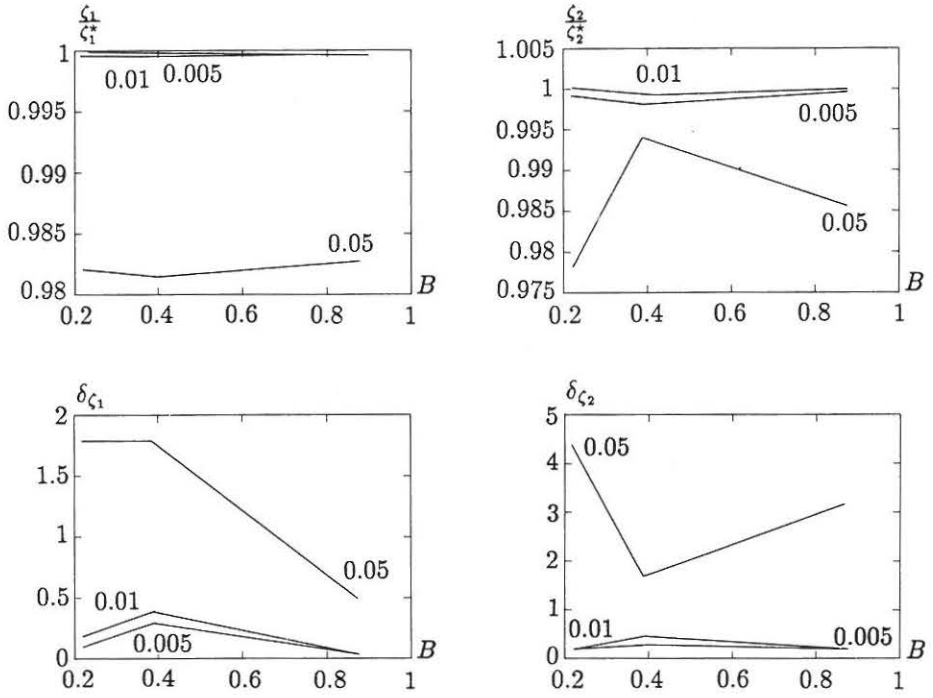

Figure 7.13 Deviation and coefficient of variation for first and second damping ratio with respect to B for different damping levels (true values: ζ_1^*, ζ_2^*).

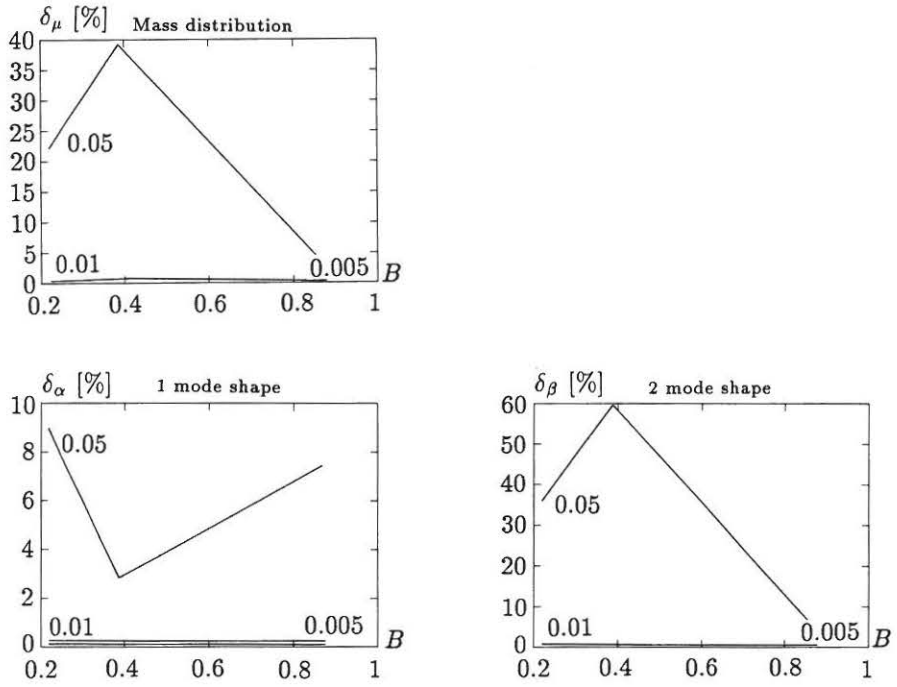

Figure 7.14. The coefficient of variation of the mode shapes and the mass distribution with respect to B for different damping levels.

7.6.5 Conclusion on the Simulation Study

The performed simulation study has revealed some of the features and problems of a global curvefit of a transfer function (or a response spectrum). The algorithm gives perfect estimates when neither noise nor closely spaced modes exist provided that the resolution has been chosen sufficiently high. However, when noise is present the damping ratios become distorted with the distortion depending upon the ratio between the damping level (the width of the peaks) and the frequency resolution applied.

A small damping level will in general cause damping estimates which are more sensitive to noise than estimates obtained for more damped systems. The effect upon the eigenfrequencies and the other parameter estimates is reverse but less significant which means that the most reliable estimates of eigenfrequencies and mode shapes are obtained for lightly damped systems.

In the case of closely spaced eigenmodes the level of damping is of vital importance with respect to the reliability of the estimates. As long as the damping is small enough to keep the existence of two peaks visible it is mainly a matter of choosing a sufficiently small frequency resolution but for increasing damping level the peaks grow together and the effect of the resolution decreases. In those cases the estimates cannot be estimated uniquely unless the phase information is also applied in the curvefitting.

Beyond the above limitations the simulation study has shown how reliable the different parameters can be estimated. The eigenfrequencies can be estimated very accurately within much less that 1% while the damping ratios may be distorted up to $50 - 100\%$ and the mode shapes and mass ratios lie within 10%. Those uncertainties correspond very well to those found in a wide range of references, see e.g. the review in chapter 2.

7.7 Interpretation of Response Spectra

In the case where the transfer function cannot be evaluated a global fit or at least some general interpretation of the response spectra is needed. This subject has not been investigated in detail in this thesis but some aspects and existing knowhow should be outlined.

In Bendat and Piersol [13] a very simple procedure of interpretation of the measured response is suggested. The eigenfrequencies can be identified by considering the phase spectra between the response at different locations. Assuming the mode shapes to be real, an eigenfrequency will be characterized by a response being in phase (0°) or out of phase (180°). Thus, the phase spectra of the reponse at different points will reveal the eigenfrequencies. The estimated coherence functions should confirm the phase spectra with high coherence at the eigenfrequencies. And at a given eigenfrequency the relative mode shape of the ith eigenmode will be

obtainable from the autospectrum:

$$\Phi_{ji} = \sqrt{S_{x_j x_j}(f_i)} \tag{7.49}$$

Index j refers to the measuring location. To identify a mode shape the number of measuring locations should at least have the same order as the mode to be estimated $j = i$. This means in practice that only modes of lower order can be identified.

A more sophisticated procedure of obtaining information of the mode shapes and the eigenfrequencies from measured response spectra was proposed by Burke et al. [24], [25]. The purpose of the procedure was to apply the hole analyzed frequency range to obtain information about the mode shapes and furthermore be able to separate closely spaced eigenmodes.

The measured response cross-spectrum of the response at two points can be written as:

$$S_{x_i x_j}(f) = \sum_{k=1}^{n} \sum_{l=1}^{n} S_{z_k z_l}(f) \Phi_{ik} \Phi_{jl} \qquad i,j = 1,2 \ldots m \tag{7.50}$$

where the modal cross-spectrum is given by:

$$S_{z_k z_l}(f) = H_k^*(f) H_l(f) \sum_{u=1}^{n} \sum_{v=1}^{n} S_{f_u f_v}(f) \Phi_{uk} \Phi_{vl} \tag{7.51}$$

where n is the number of degrees of freedom and m is the number of measured response locations. The shape vectors proportional to the mode shapes are now introduced for the kth eigenmode as a function of frequency:

$$r_{i(k)}(f) = \sqrt{S_{z_k z_k}(f)}\ \Phi_{ik} \tag{7.52}$$

It is defined as being permanently proportional to the mode shapes where the proportional factor is frequency dependent and hence where also the magnitude of the shape vector is frequency dependent. If this expression is introduced into (7.50) the following expression is obtained:

$$S_{x_i x_j}(f) = \sum_{k=1}^{n} \sum_{l=1}^{n} \gamma_{kl}(f) r_{i(k)}(f) r_{j(l)}(f) \tag{7.53}$$

where $\gamma_{kl}(f)$ is the complex coherence function:

$$\gamma_{kl}(f) = \frac{S_{z_k z_l}(f)}{\sqrt{S_{z_k z_k}(f) S_{z_l z_l}(f)}} \tag{7.54}$$

This complex coherence will be equal to one in magnitude for $k = l$ where k and l refer to two measuring points. From (7.53) it is possible to estimate a number of shape vectors and coherence values from the measured response spectra for $i, j = 1, 2 \ldots m$ for the spectral density at each frequency in the frequency region considered. In (7.53) n is replaced by rn since only a smaller number of modes are assumed to give a contribution to the vibration at a given frequency:

$$S_{x_i x_j}(f) = \sum_{k=1}^{rn} \sum_{l=1}^{rn} \gamma_{kl}(f) r_{i(k)}(f) r_{j(l)}(f) + e_{ij}(f) \tag{7.55}$$

where $e_{ij}(f)$ is the error due to the truncated number of modes and noise in the response spectrum, e.g. noise due to the wave excitation. The unknown shape vectors and the complex coherencies can now for each frequency be estimated by minimizing the error by a least square approach applying a general optimization program.

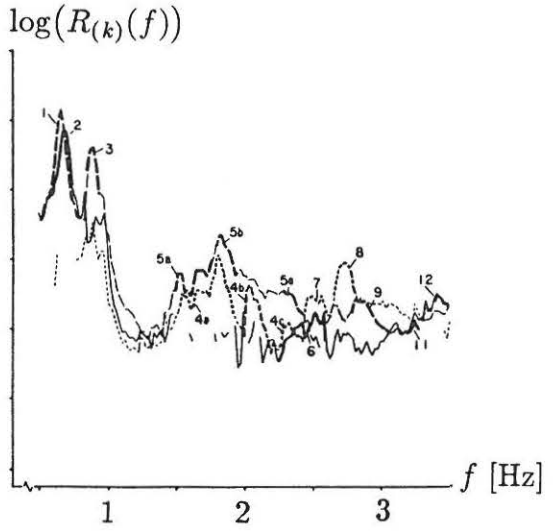

Figure 7.15. The logarithm of the length of the estimated shape vectors $R_{(k)}(f)$ for different modes (k) versus frequency, obtained from measurement of a jacket platform, Burke [25].

The length of each estimated shape vector, $R_{(k)}(f) = \sum_{i=1}^{m} r_{i(k)}^2(f)$ will be proportional to the autospectrum of the modal response of the given mode. This means that the eigenfrequency of each mode can be estimated by plotting the length of the response shape vector over a certain frequency region. This feature of the shape vector method makes it possible in principle to estimate the eigenfrequencies and the mode shapes. An example of a plot of the length of the estimated shape vectors obtained from response measurements of a jacket platform is shown in figure 7.15. In practice however the method has been reported to show some difficulties in separating closely spaced eigenfrequencies, Burke et al. [25].

7.8 Conclusion

The chapter has shown that a wide range of identification methods is available making it possible to identify modal parameters from measured time series. Many other methods exist especially if the response as well as the excitation is considered to be known, see e.g. Allemang [26], Chen [27] and Blakely et al. [28]. A hole group of methods based upon a formulation of the model in the Laplace domain have not been considered even though they are also applied in practice, see e.g. Natke and Schulze [29].

In this chapter the presented methods can be said to belong to of the following three groups:

- Methods based upon the assumption that an eigenmode can be separated and approximated with a single-degree-of-freedom system.
- Methods based upon a global fit taking several eigenmodes in a given frequency region into account.
- The Ibrahim time domain method which provides a complete modal model of a system.

Some of the methods could be based solely upon the measured response while others were based upon a measured response as well as the excitation, e.g. given by an external excitation. Quite obviously the most reliable information can be expected when the latter methods are applied. However, in practice there may be a problem if the ambient excitation is present at the same frequencies as the external excitation, which will influence the coherence function, see section 5.6 and thus make increased averaging necessary, see Bendat and Piersol [13].

The methods based upon the measured response will typically be applicable if the eigenmodes are well separated and the structure is lightly damped. In such cases methods such as the method of spectral moments, the random decrement technique followed by the method of the logarithmic decrement as well as the interpretation approach given in chapter 7.7 can be applied. A method such as the bandwidth method can only be recommended as a quick way of obtaining information of the magnitude of the damping.

When the eigenmodes are closely spaced such as for jacket structures the problems increase. In cases where the peak in the spectrum of the wave excitation is well defined a successful approach may be to perform a global fit to the response spectrum by a curvefitting algorithm with a parameterized force spectrum. Alternatively approximate white noise can be assumed over a close region covering several resonance peaks. This approximation makes it possible to estimate the parameters in the transfer functions directly corresponding to the approach in chapter 7.6. In the time domain the Ibrahim time domain method can be applied to a random decrement signature.

7.9 References

[1] Johnson, N. L. and F. C. Leone, "Statistics and Experimental Design", John Wiley & Sons, 1977.

[2] Jensen, J. L., "Dynamic Analysis of a Monopile Model", Paper no. 4 in the series Fracture and Dynamics, Institute of Building Technology and Structural Engineering, University of Aalborg, Denmark, 1988.

[3] Langen, I. and R. Sigbjornsson, "Dynamisk Analyse av Konstruktioner", (In Norwegian), SINTEF, Avdeling for Konstruktionsteknik, Tapir Norway, 1979.

[4] Nasir, J. and S. S. Sunder, "An Evaluation of the Random Decrement Technique of Vibration Signature Analysis for Monitoring Offshore PLatforms", Research Report R82-52, Department of Civil Engineering, Massachusetts Institute of Technology, USA, Sept. 1982.

[5] Ibrahim, S. R. and E. C. Mikulcik, "A Time Domain Modal Vibration Test Technique", The Shock and Vibration Bulletin, Bull. 43, Part 4, June 1973.

[6] Ibrahim, S. R. and E. C. Milkulcik, "A Method for the Direct Identification of Vibration Parameters from the Free Response", The Shock and Vibration Bulletin, Bull. 47, Sept 1977.

[7] Ibrahim, S. R., "Modal Confidence Factor in Vibration Testing", Journal of Spacecraft, Vol. 15, no. 5, Sept-Oct 1978.

[8] Pappa, R.S. and S. R. Ibrahim, "A Parametric Study of the Ibrahim Time Domain Modal Identification Algorithm", The Shock and Vibration Bulletin no. 51, part 3, March 1981.

[9] Yang, Y., "A Time Domain Identification Technique: The Oversized Eigenmatrix (OEM) Method", Journal of Vibration, Acoustics, Stress and Reliability in Design, Vol 107, Jan 1985.

[10] Ibrahim, S. R. and E. C. Mikulcik, "The Experimental Determination of Vibration Parameters from Time Responses", The Shock and Vibration Bulletin, Bull. 46, 1976.

[11] Longo, P., "Vibration Monitoring of Offshore Platforms using the Ibrahim Time Domain Modal Identification Technique", M.Sc. Thesis, Massachusetts Institute of Technology, USA, May 1982.

[12] Hansen, L. Pilegaard, "Jernbetons Dynamiske Opførsel - Del 1", (In Danish), Institute of Building Technology and Structural Engineering, University of Aalborg, Denmark, 1979.

[13] Bendat, J. S. and A. G. Piersol, "Engineering Applications of Correlation and Spectral Analysis", John Wiley & Sons Inc., 1980.

[14] Vanmarcke, E. H., "Method of Spectral Moments to Estimate Structural Damping", Stochastic Problems in Dynamics, ed. B.L. Clarkson, Pitmann, UK, 1977.

[15] Vanmarcke, E. H. and Iascone, R. N., "Estimation of Dynamic Characteristics of Deep Water Ocean Tower Structures", Report no. MITSG72-12, Massachusetts Institute of Technology, USA, 1972.

[16] Pulgrano, L. J. and M. Ablowitz, "The Response of Mechanical Systems to Bands of Random Excitation", The Shock and Vibration Bulletin, Vol. 39, part 3, Jan. 1969.

[17] Sunder, S. S., S. E. Grewatz and S. K. Ting, "Modal Identification using Spectral Moments", Structural Safety 3, Elsevier Science Publishers, 1985.

[18] Grewatz, S. E., "Vibration Monitoring in the Spectral Domain using the Method of Moments", M.Sc. Thesis, Dep. of Civil Engineering, Massachusetts Institute of Technology, USA, 1982.

[19] Sigbjornsson, R., "STARTIMES: A Computer Program for Statistical Analysis of Random Time Series with Special Reference to Structural Dynamics", SINTEF, Division of Structural Engineering, Report no. STF71 A82011, Trondheim, Norway, 1982.

[20] Kennedy, C. D. and C. D. P.Pancu, "Use of Vectors in Vibration Measurements and Analysis", J. Aeronautical Sciences, Vol. 14, no. 11, 1947.

[21] Ewins, D. J., "Modal Testing: Theory and Practice", Research Studies Press, UK, 1985

[22] Schittkowski, K., "NLPQL: A FORTRAN Subroutine Solving Constrained Nonlinear Programming Problems", Annals of Operation Research, 1986.

[23] Xinsen, L. and J. K. Vandiver, "Damping and Natural Frequency Estimation using the Least Pth Optimization Technique", Offshore Technology Conference, OTC 4283, Houston, USA, 1982.

[24] Burke, B. G. ,C. Sundarajan and F. M. Safaie, "Characterization of Ambient Vibration Data by Response Shape Vectors", Offshore Tecnology Conference, OTC 3862, Houston, USA, 1980.

[25] Burke, B. G. and N. R. Sosdian, "Analysis of Ambient Vibration by Multiple Shape Vectors", Offshore Technology Conference, OTC 4284, Houston, USA, 1982.

[26] Allemang, R. J., "Investigation of some Multiple Input/Output Frequency Response Function Experimental Modal Analysis Techniques", Ph.D. Thesis, University of Cincinnati, USA, 1980.

[27] Chen, J.-C., "Evaluation of Modal Testing Methods", AIAA paper 84-1071, American Institute of Aeronaustics and Astronautics, 1984.

[28] Blakely, K. , P. Ibanez, B. Cooper and J. Stoessel, "System Identification: Review and Examples", Proc. of the 2nd Speciality Conference on Dynamic Response of Structures, ed. G. Hart, ASME, Atlanta , USA, 1980.

[29] Natke, H. G. and H. Schulze, "Parameter Adjustment of a Model of an Offshore Platform from Estimated Eigenfrequencies Data", Journal of Sound and Vibration, Vol. 77, Academic Press Inc. Limited, 1981.

[30] Ljung, L., "System Identification - Theory for the User", Prentice-Hall, 1987.

Alternative References

[31] Rades, M., "Frequency Domain Experimental Modal Analysis Techniques", The Shock and Vibration Digest, Vol. 17, no. 6, 1985.

[32] Norris, M. A. and L. Silverberg, "Modal Identification of Self-Adjoint Distributed- Parameter Systems", Earthquake Engineering and Structural Dynamics, Vol. 18, pp. 633-642, John Wiley & Sons, 1989.

8. IDENTIFICATION BY TIME SERIES MODELS

Many of the presented identification methods in the previous chapter have been based on spectral estimates obtained by FFT-analysis even though chapter 5 clearly showed that such spectral estimates can be very unreliable, especially for analysis of the response of lightly damped structures with only short-term series available due to nonstationary excitation. During the last 15 years alternatives to the conventional FFT-analysis have been sought. In this chapter two powerful alternatives are presented, the ARMA model and the AR model. The latter is also called the maximum entropy method (MEM).

Both methods are based on parametric models which are fitted to the measured time series of the response. They are formulated in the discrete time domain but can alternatively be transformed into the frequency domain as parametric response spectra comparable with those obtained by FFT-analysis. It could have been argued that the methods should have been presented in chapter 5 as a tool in signal processing. However, since the methods to be presented are parametric with a direct relation to modal parameters, the methods are in this context considered as methods integrating signal processing and system identification. This means that several advantages are obtained compared with the conventional approach:

1. The eigenfrequencies and the damping ratios can be estimated directly from the parameters in the time series model if the proper relations are known.
2. If the uncertainties of the parameters in the time series model are given by a covariance matrix then the confidence intervals can be computed for the eigenfrequencies and damping ratios.
3. The numerical inaccuracies of the FFT analysis due to insufficient frequency resolution and leakage (windowing) are avoided by the application of time series models. However, to avoid aliasing the sampling frequency still has to exceed the Nyquist frequency.

However, some problems also exist. Bias and random errors still exist to some extent, but more important larger computer capacity and speed are required by the methods. Furthermore, a subjective element exists because a model order has to be chosen. However the subjective element exists also in methods based on FFT-analysis where the width of the window is chosen by the analyst or perhaps more often by the company, which has produced the spectrum analyzer. The advantages and disadvantages of identification by time series models will be discussed in this chapter together with the general application.

8.1 Identification by ARMA-Models

An ARMA model is a parametric model of a discrete time series of a realization of some measured random process. Any stationary time series can be considered as the output of some time invariant black box model with stationary Gaussian distributed white noise as input $\epsilon(t)$, see figure 8.1. Hence the black box model transforms the white noise $\epsilon(t)$ into some specific random noise time series $x(t)$.

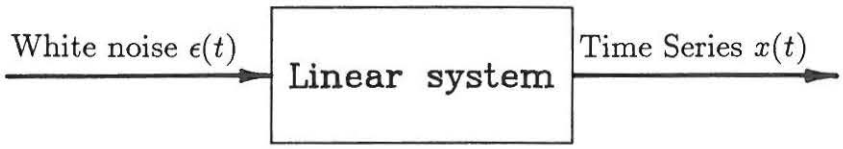

Figure 8.1. Black box model.

The black box is assumed to be a linear time invariant system which means that the measured time series is assumed to be Gaussian distributed. Throughout the chapter $x(t)$ is assumed to have a zero mean.The time series is assumed to be obtained with constant sampling of a continuous signal, $x_t \equiv x(t\Delta), \quad t = 1, 2, 3 \ldots N$. The ARMA model of the time series is defined by:

$$x_t = \underbrace{\sum_{i=1}^{n} \Phi_i x_{t-i}}_{AR\ part} + \epsilon_t - \underbrace{\sum_{i=1}^{m} \Theta_i \epsilon_{t-i}}_{MA\ part} \tag{8.1}$$

This is called an ARMA(n, m) model. The parameters in the ARMA model are real numbers. It is seen that x_t is expressed as a linear combination of the x_t-values and ϵ_t-values of the past plus of course a contribution from the white noise at the time t, ϵ_t. The sum of the x_t-values of the past refers to the autoregressive part of the ARMA model (the AR part) and the sum of the ϵ_t-values of the past refers to the moving average part of the ARMA model (the MA part). Hence the Φs are the AR parameters and the Θs are the MA parameters.

An ARMA$(2n, 2n-1)$ model should be chosen for the response of a linear system of n degrees of freedom excited by white noise:

$$x_t = \sum_{i=1}^{2n} \Phi_i x_{t-i} + \epsilon_t - \sum_{i=1}^{2n-1} \Theta_i \epsilon_{t-i} \tag{8.1a}$$

This choice of a model order $(2n, 2n-1)$ will be a proper choice since it can be shown that the covariance function of the response will be identical with the covariance function due to the ARMA model, see e.g. Natke and Kozin [1]. This

means that the ARMA model will have exactly the same statistical properties as the measured time series since it was assumed to be Gaussian distributed due to the Gaussian distributed excitation. Hence in principle an unbiased estimate of the true autocorrelation function and thus autospectrum can be obtained.

The linear system will be characterized by the roots λ_i of the characteristic polynomial of the AR parameters:

$$\lambda^{2n} + \Phi_1 \lambda^{2n-1} + \cdots + \Phi_{2n-1}\lambda + \Phi_{2n} = 0 \tag{8.2}$$

where the roots will be directly related to the eigenvalues of system matrix $\overline{\overline{A}}$ of the vibrating system formulated in the state space, Natke and Kozin [1]. The system matrix, $\overline{\overline{A}}$ was introduced in chapter 4, see (4.33). While the AR parameters contain information about the vibrating system, the MA parameters, the Θs will contain information of the force distribution of the white noise excitation and the influence of different eigenmodes.

8.1.1 The Autocovariance and the Autospectrum

The covariance equivalence condition ensures that the statistical moments up to the second order of the time series are reproduced in the ARMA model in the most accurate way. In fact it means that the autocovariance function of the ARMA model will be equal to the autocovariance function of the response of the white noise excited identified structure of n degrees of freedom.

The autocovariance function of the ARMA$(2n, 2n-1)$ model is given by:

$$\gamma_k = \sum_{i=1}^{2n} d_i \lambda_i^k \tag{8.3}$$

where λ_i is the ith root of (8.2) and d_i is given by:

$$d_i = \sigma_\epsilon^2 \sum_{j=1}^{2n} \frac{g_i g_j}{1 - \lambda_i \lambda_j} \quad i = 1, 2, 3 \ldots, 2n \tag{8.4}$$

g_i is given by:

$$g_i = \frac{\lambda_i^{2n-1} - \Theta_1 \lambda_i^{2n-2} \cdots - \Theta_{2n-2}\lambda_i^1 - \Theta_{2n-1}}{(\lambda_i - \lambda_1)(\lambda_i - \lambda_2)\cdots(\lambda_i - \lambda_{i+1})\cdots(\lambda_i - \lambda_{2n})} \tag{8.5}$$
$$i = 1, 2, 3 \ldots 2n$$

The autospectrum of the ARMA$(2n, 2n-1)$ model can be shown to be given by:

$$S_{xx}(f) = 2\Delta\sigma_\epsilon^2 \frac{\left|e^{(2n-1)if2\pi\Delta} - \Theta_1 e^{(2n-2)if2\pi\Delta} - \ldots - \Theta_{2n-1}\right|^2}{\left|e^{nif2\pi\Delta} - \Phi_1 e^{(2n-1)if2\pi\Delta} - \ldots - \Phi_{2n}\right|^2} \qquad (8.6)$$

$$0 \leq f \leq \frac{1}{2\Delta}$$

see e.g. Jensen [9]. Thus a complete description of the time series in the time domain as well as in the frequency domain can be derived once an ARMA model has been estimated.

8.1.2 Estimation Strategy

The parameters of the ARMA model have to be estimated from the time series x_t only. This is done by minimising the criteria function which in the present chapter is identical with the computed variance of the assumed white noise input, ϵ_t:

$$\sigma_\epsilon^2(\Phi_i, \Theta_j, x_t) = \frac{1}{N}\sum_{t=1}^{N} \epsilon_t^2 \qquad (8.7)$$

N is the number of sampled points of $x(t)$. (8.7) is also sometimes called the residual sum of squares or the loss function. The minimization can be done by a recursive or batch algorithm. According to Lefkowitz [2], the most efficient methods of each type are the RPEM method (Recursive Prediction Error Method), see Ljung [3], and the Box and Jenkins Maximum Likelihood algorithm, see Box and Jenkins [4]. In this chapter both algorithms have been used for obtaining ARMA models in the experimental case. Shinozuka et al. [17] have investigated several other estimation methods.

The subject of the least square problem is to minimize a function which is nonlinear with respect to the ARMA parameters. The nonlinear nature of the problem is seen from the rewriting of (8.1a):

$$\epsilon_t = x_t - \sum_{i=1}^{2n} \Phi_i x_{t-i} - \sum_{i=1}^{2n-1} \Theta_i \epsilon_{t-i} \qquad (8.8)$$

where ϵ_t becomes a non-linear function of the ARMA parameters if ϵ_{t-i} is eliminated from the expression by the equation itself. The non-linear least square problem can e.g. be solved by Marquardt's algorithm, which is related to the Steepest Descent method and the Newton method, see Marquardt [5]. The result of the least square solution includes a set of estimates of the ARMA parameters, the covariance matrix of the parameters and the time series of the assumed white noise, ϵ_t, $t = 1, 2, \ldots N$.

(8.8) is limited to the case where $t \geq n + 1$ because x_{-1}, x_{-2} etc. is unknown. Therefore, the initial values:

$$\epsilon_t = 0, \quad t = 0, 1, 2, 3 \ldots, 2n \tag{8.9}$$

are applied. Some initial estimates of the ARMA parameters are also necessary because ϵ_t has to be computed in (8.7) and (8.8). Different methods are available, see Box and Jenkins [4] and Pandit and Wu [6], but it might be sufficient to choose estimates equal to zero.

When the ARMA model has been estimated it must be checked that the assumed model order of the ARMA model, $(2n, 2n-1)$ also was a proper choice. First of all the estimated time series, ϵ_t must be identified as the assumed white noise. This can be done by checking the autospectrum of the time series or the autocorrelation function which have a unique signature if the time series can be assumed to be white noise. If the estimated time series is not likely to be white noise it can indicate either that the model order is still too small or that the model assumption has been violated. The latter case can be due to non-white excitation or nonlinearities in the excited system. However, also in the latter case the model order should be increased if a best model fit to the measured time series is wanted. The model order should be increased until the ARMA model takes all the deterministic characteristics of the measured time series into account.

Another point of view is to consider the loss function σ_ϵ^2 as function of the model order. As long as an increase in the model order of the ARMA model leads to a significant decrease in the loss function it means that the ARMA model is able to give a deterministic description of a large portion of the measured time series, x_t. When the significant decrease is replaced by an insignificant decrease in the loss function it indicates that the proper model order has been exceeded. The insignificant decrease will in general continue as the model order increases since it can be shown that any time series can be fitted to an ARMA model provided that the model order has been chosen sufficiently high, Wold [7]. However, it is characteristic that when the model order exceeds the proper choice, the parameters in the ARMA model become highly uncertain corresponding to the fact that the properties of the assumed white noise grow into the ARMA model. This is known as overfitting and leads to distorted models, Ljung [3], Box and Jenkins [4]. Instead of considering the decrease in the loss function Akaike [8] has proposed that the model should be determined from the minimum of:

$$(AIC) = \mathbf{min}[\sigma_\epsilon^2 + \frac{4n-1}{N}] \tag{8.10}$$

which is called Akaikes Information Criterion, (AIC). N is the number of sampled points of $x(t)$. This criterion can be justified from probability theory, see e.g. Ljung [3] but it also makes sense from a intuitive point of view. An increase in the model order is seen to lead to an increase due to the ratio of number of parameters to be estimated and the number of sampled data points. Thus, the proper model order is limited by the amount of avaiable data which should in principle prevent

overfitting. In this thesis the development in the decrease of the loss function has been considered but it has been noticed that the application of the (AIC) would in general have led to the same choices of model orders. Several other model order criteria have been developed during the years, see Ljung [3].

8.1.3 Estimation of the Modal Parameters

After deriving the principles of the ARMA model the last step is to determine the relationship between the parameters in the ARMA model and the dynamic parameters of the vibrating system. The dynamic parameters are here given by the eigenfrequencies and the damping ratios. It follows from a derivation of the ARMA model that the parameters of the ARMA model are related to the equations of motion for the damped system, Natke and Kozin [1]. Thus no restrictions exist with respect to the viscous damping matrix.

The dynamic parameters are found from the $2n$ eigen values of the system matrix, $\overline{\overline{A}}$ in the state space formulation, given by the diagonal matrix $(\, p_i \,)$. The $2n$ diagonal elements will be related to the modal parameters through the relations:

$$p_{(i)12} = -2\pi f_i \zeta_i \pm 2\pi f_i \sqrt{{\zeta_i}^2 - 1} \qquad \zeta_i \geq 1.0 \tag{8.11a}$$

$$p_{(i)12} = -2\pi f_i \zeta_i \pm \mathbf{i} 2\pi f_i \sqrt{1 - {\zeta_i}^2} \qquad \zeta_i < 1.0 \tag{8.11b}$$

If the system is underdamped the eigenvalues are seen to be found as complex conjugated pairs.

Since the discrete time domain is considered, the eigenvalues of $\overline{\overline{A}}$ will be related to the eigenvalues of $\exp\left(\overline{\overline{A}}\Delta\right)$ defined by:

$$\exp\left(\overline{\overline{A}}\Delta\right) \equiv \overline{\overline{1}} + (\overline{\overline{A}}\Delta) + \frac{1}{2!}(\overline{\overline{A}}\Delta)^2 + \frac{1}{3!}(\overline{\overline{A}}\Delta)^3 + \cdots \tag{8.12}$$

and it can be shown that the $2n$ eigen values of $\exp(\overline{\overline{A}}\Delta)$, given by the diagonal matrix $(\, \lambda_i \,)$ can be found as the roots of the characteristic polynomial related to the ARMA model:

$$\lambda^{2n} + \Phi_1 \lambda^{2n-1} + \cdots + \Phi_{2n-1}\lambda + + \Phi_{2n} = 0 \tag{8.2}$$

Furthermore, it can be shown, see e.g. Jensen [9], that the roots of (8.2) are identical with the values in the diagonal matrix $(\, \exp(p_i \Delta) \,)$:

$$(\, \lambda_i \,) = (\, \exp(p_i \Delta) \,) \tag{8.13}$$

This means that eigenvalues of $\overline{\overline{A}}$ can be determined from the roots of (8.2) obtained from the estimated ARMA model and the sampling interval Δ:

$$p_{(i)12} = \ln(\lambda_{(i)12})/\Delta \tag{8.14}$$

Finally, due to (8.11), the values of the corresponding eigenfrequencies and damping ratios can be found. Hence, the relationship between the AR parameters and the eigenfrequencies and damping ratios has been established

Since the coefficients of the characteristic equation (8.2) are real it follows that the roots of (8.2) will occur as complex roots in conjugated pairs if the modes are underdamped. Otherwise, the roots will be real values.

The n pairs of roots will correspond to the roots of n polynomials of the second order derived from the polynomial of order $2n$ given by (8.2). Consequently, if only underdamped modes are considered each polynomial of the second order will represent an eigenmode given by an eigenfrequency and a damping ratio which can be found from the two roots of the polynomium. It can be noted that the even AR order $2n$ means that all the eigenmodes of the vibrating system are allowed to be underdamped, see e.g. Jensen [9]. These model considerations mean that generally the AR order should be chosen to be even.

A multivariate version of identification by ARMA models has also been developed which makes it possible also to estimate a unified set of the modal parameters including the eigenmodes, see e.g. Pi and Mickleborough [12] or Pandit [11]. However, this requires measurings at several points.

8.1.4 Statistic Distribution

If the AR parameters are assumed to be jointly Gaussian distributed and if knowledge of the covariance matrix exists then confidence intervals of the dynamic parameters can be estimated. This is a very important feature of using ARMA models although some problems exist in evaluating the confidence intervals.

First of all it is not possible to establish an explicit density function of the dynamic parameters because they are determined implicitly from the AR parameters due to the polynomial relationship. This means that the distribution of dynamic parameters must be found by simulation of events in the sample space of the AR-parameters or by some linearization of the relation between the modal parameters and the AR parameters. The latter approach has been performed by Gersch [13] and Gersch et al. [14].

In the present thesis a simulation program has been developed and the required number of simulated events has been found from the convergence of the statistical estimates. Acceptable convergence for the estimates of mean values and standard deviations were found for about 10 sample points for each AR parameter in the model while convergence of the correlation coefficient between the eigenfrequency

and the damping ratio of a given mode required at least 100-200 points.

It is to be noticed that the eigenfrequencies and the damping ratio cannot be expected to be normally or logarithmically normally distributed due to the non-linear relation to the AR parameters. Thus any approximation to a given distribution function has to be checked by e.g. a χ_i^2 test.

By the linearization approach Gersch [13] has performed a simulation study to investigate how the variance of the eigenfrequency and the damping ratio behaves with respect to the amount of data, N, the sampling interval Δ, the level of damping and number of degrees of freedom, n. An SDOF and a 2DOF system with damping ratios between 0.01 and 0.05 and $f_1 = 1.01$ Hz and in the case of the 2DOF system $f_2 = 2.76$ Hz were considered. The coefficient of variation of f_1 and ζ_1 was found to be as large as 0.01 and 0.3 respectively, for $N = 1000$. Generally it was concluded that:

- δ_f and δ_ζ are inversely proportional to $\sqrt{N}$.
- δ_f and δ_ζ are inversely proportional to Δ.
- δ_f increases while δ_ζ decreases with increasing damping level.
- δ_f and δ_ζ for a fixed Δ for any particular mode in the system, are quite insensitive to the number of modes present.
- δ_f and δ_ζ are quite insensitive to additive noise.
- δ_f and δ_ζ are independent whether the response is given as displacement, velocity or acceleration.

Those experiences show that problems of obtaining good estimates of the modal parameters are qualitatively the same as for FFT-analysis combined with some curvefitting algorithm. To obtain good estimates it is necessary to sample many times in long-term intervals and the requirements increase if the damping is small. Thus the application of ARMA models is not a question of avoiding those problems but rather a question of minimizing the problems.

8.1.5 The Experimental Case

The lightly damped system with two degrees of freedom corresponding to the experimental case was investigated with respect to identification by ARMA models, see figure 8.2.

Two procedures of ARMA modelling were performed. The purpose of the first procedure was to fit an ARMA model to the measured time series containing two excited eigenmodes. The second procedure contained a bandpass filtering of the time series which meant that in principle only one of the eigenmodes was present when the ARMA models were estimated. The second procedure resulted in ARMA models corresponding to each eigenmode.

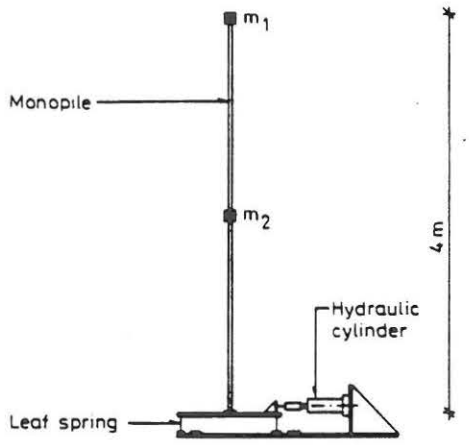

Figure 8.2. Experimental case: Monopile model.

The first procedure was performed applying the NAG library [15]. The time series were the measured displacements (double integration of accelerations) of the two masses of the monopile. For mass no. 1 at the top and mass no. 2 at the middle the sampling rates were 40 Hz and 60 Hz, respectively. The cut-off frequency was about 12 Hz and the sampling time was 120 seconds.

The satisfactory model order was determined from the reduction in the model error, σ_ϵ^2. When the model error had obtained a minimum, the model order was considered as being satisfactory. Furthermore, convergence of the eigenfrequencies and the damping ratios was considered as a measure of the applicability of the model. Finally, the agreement between the results of the two measured time series also gave some indication of the appropriate model order.

As an example, figure 8.3 shows the convergence of the eigenfrequencies and damping ratios compared with the development of the model error as a function of the model order. The expected order of the model was an ARMA(4,3) model but both figures show that a considerably higher order is necessary before some kind of convergence has been obtained. In fact it seems as if an ARMA(14,13) model is satisfactory corresponding to a system with 7 degrees of freedom. Any higher order of the models is seen to give no reduction in the model error and the parameters have also converged somewhat. Hence the ARMA(14,13) is chosen as the correct model.

A plausible explanation of this high model order is the shape of the force spectrum given by $S_{FF}(f) = (2\pi f)^4 S_0$. Due to the violated white noise assumption the first eigenmode has not been very strongly represented in the time series. In fact the ratio between the force spectral density at the two eigenfrequencies was a factor of approx. 1835. This explains why it has been impossible to identify the first mode in the ARMA models of lower order, see figure 8.3. The mode has simply been hidden in noise.

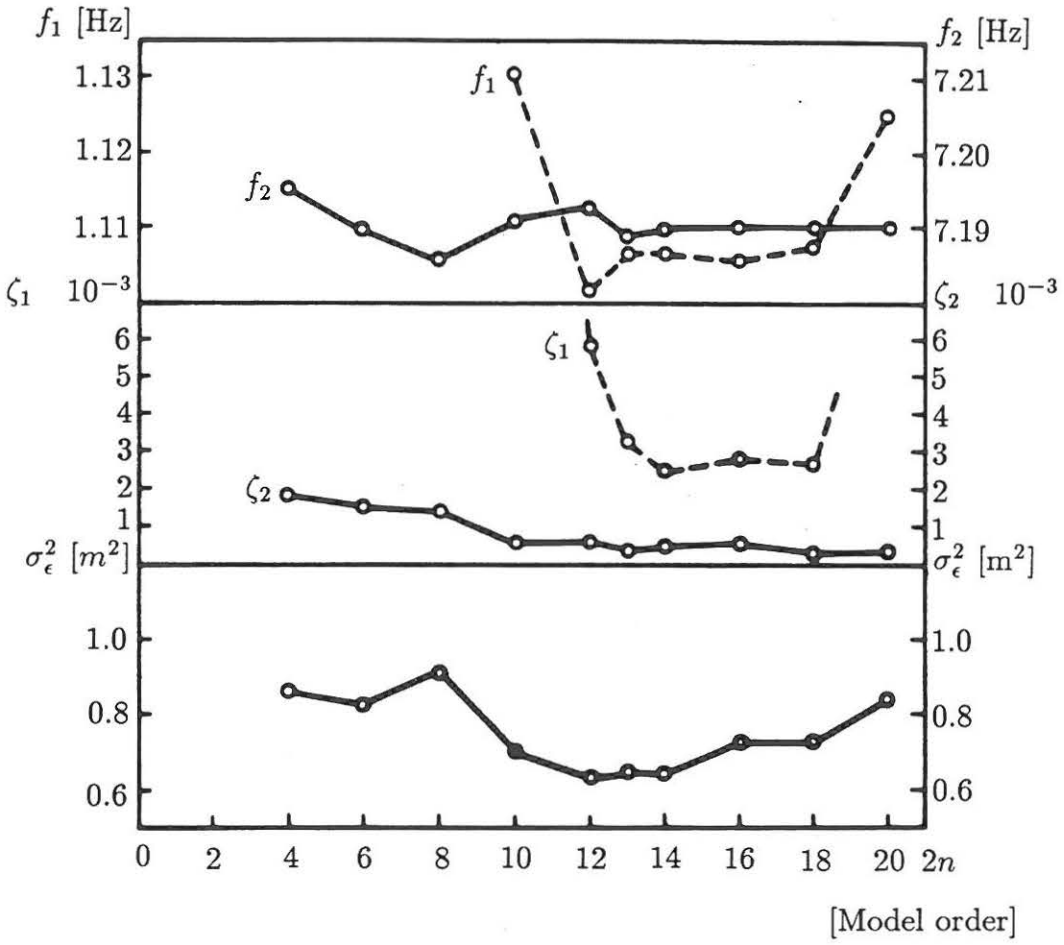

Figure 8.3. The convergence of the eigenfrequencies, damping ratios and σ_ϵ^2 as functions of the model order. Factor on σ_ϵ^2 : 10^{-3}. Time series: The displacement response of mass no 2.

The convergence of the eigenfrequencies and the damping ratios can be compared in figure 8.3. It is seen that the eigenfrequencies converge much more quickly than the damping ratios (notice the scales in the figure). This shows the basic fact that the estimation of the damping ratio of a lightly damped system is more uncertain than the estimation of the eigenfrequencies.

The estimated eigenfrequencies and damping ratios are shown in table 8.1. From the table it is seen that the estimated eigenfrequencies of the two models agree very well. On the other hand, it is seen that the agreement between the damping ratios based on the response of the two different masses does not seem to be satisfactory. However, since the statistical uncertainty is not known this might be a false conclusion. The statistical uncertainty has not been computed because the NAG-routine failed to give information about the covariance matrix of the ARMA parameters. The different sampling rates may also have had influence on the results.

	f_1 Hz	ζ_1	f_2 Hz	ζ_2
ARMA(14,13) for the displacement of mass 1.	1.1054	0.00127	7.1921	0.00065
ARMA(14,13) for the displacement of mass 2.	1.1070	0.00256	7.1900	0.00045

Table 8.1 Computed eigenfrequencies and damping ratios from the estimated ARMA parameters.

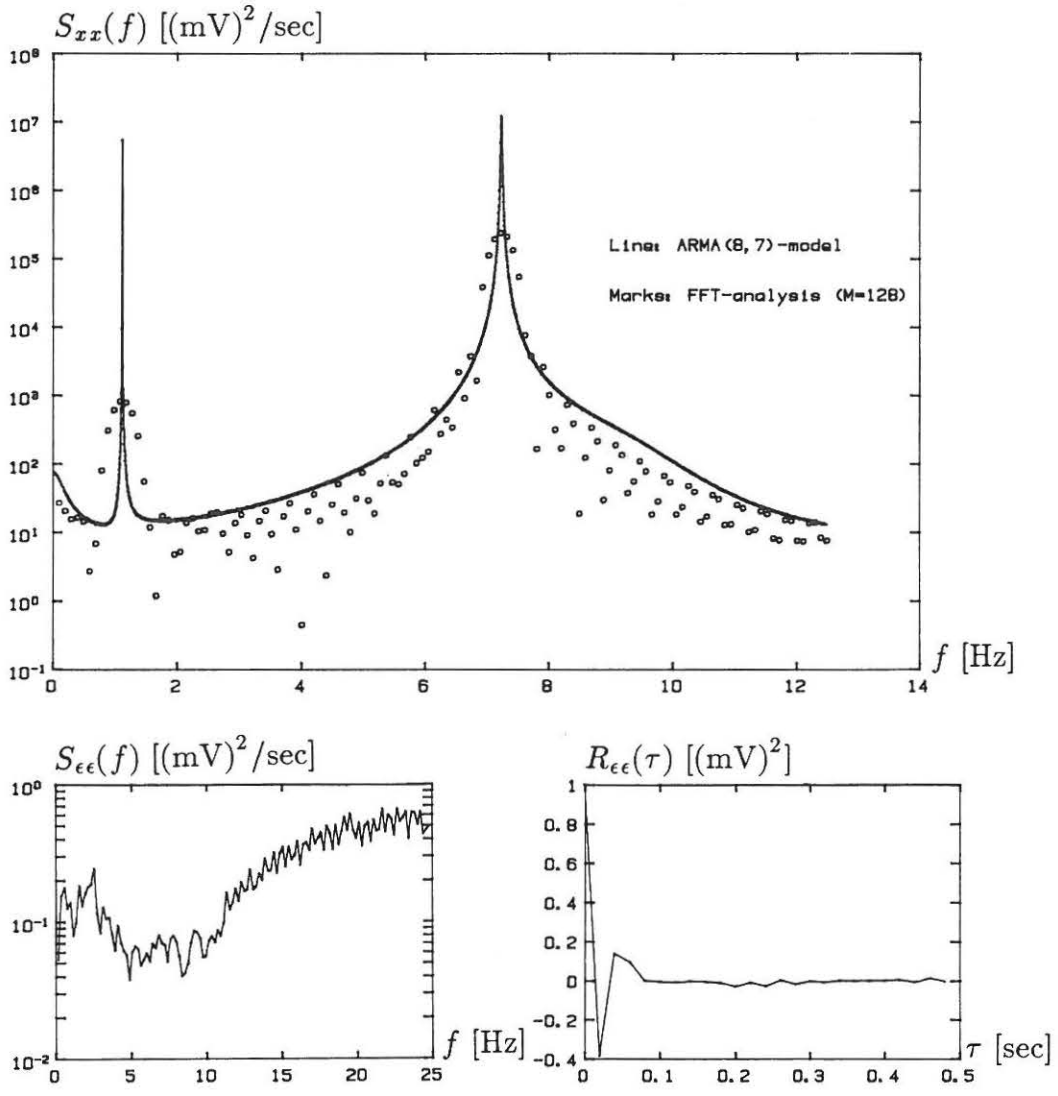

Figure 8.4. Top: The autospectrum of an ARMA(8,7) model compared with the spectrum estimated by FFT with B_e=0.04 Hz and time series length of 120 sec (acceleration). Left, respectively right bottom: The spectrum and the autocorrelation function of the estimated time series of the residual of the ARMA(8,7). Calibration factors on all ordinate axises.

To illustrate the ARMA approach in the frequency domain the results of an ARMA-(8,7) model have been transformed into the frequency domain and compared with a corresponding FFT-analysis as shown in figure 8.4. Even though that an ARMA model of this order just has been shown not to be a proper model it is seen that it is superior to the response spectra estimated by the FFT-technique, MATLAB [16]. The FFT-analysis has been performed with a resolution $B_e = 0.04$ Hz which is insufficient to reveal the true spectral peaks. The spectrum of the estimate residual is also shown together with the corresponding autocorrelation function. The non-white spectrum confirms that the ARMA(8, 7) is not the correct model. It is noticed that it is much easier from the autospectrum than from the autocorrelation function to determine whether or not it is white noise (the autocorrelation function for a white noise process is a delta function).

The second procedure of the ARMA modelling was to filter the time series before an ARMA model was estimated. This procedure ensured that only one mode was present in the time series. The purpose was to obtain a stronger representation of the first eigenmode and to reduce the proper order of the ARMA models.

The filtering was performed with a Yulewalker filter of order 10, available in the software package MATLAB [16]. The sampling frequency of the time series was 50 Hz and the cut-off frequency about 12 Hz. The sampling time was 120 seconds. The expected model was an ARMA(2,1) model because only one mode was supposed to be present in the signals. However, it was found that an ARMA(4,3) model might also be appropriate while all the models of higher order did not provide reasonable results or any substantial reduction in the model error σ_ϵ^2, see figure 8.5. Thus these models of higher order were considered as overfitted models.

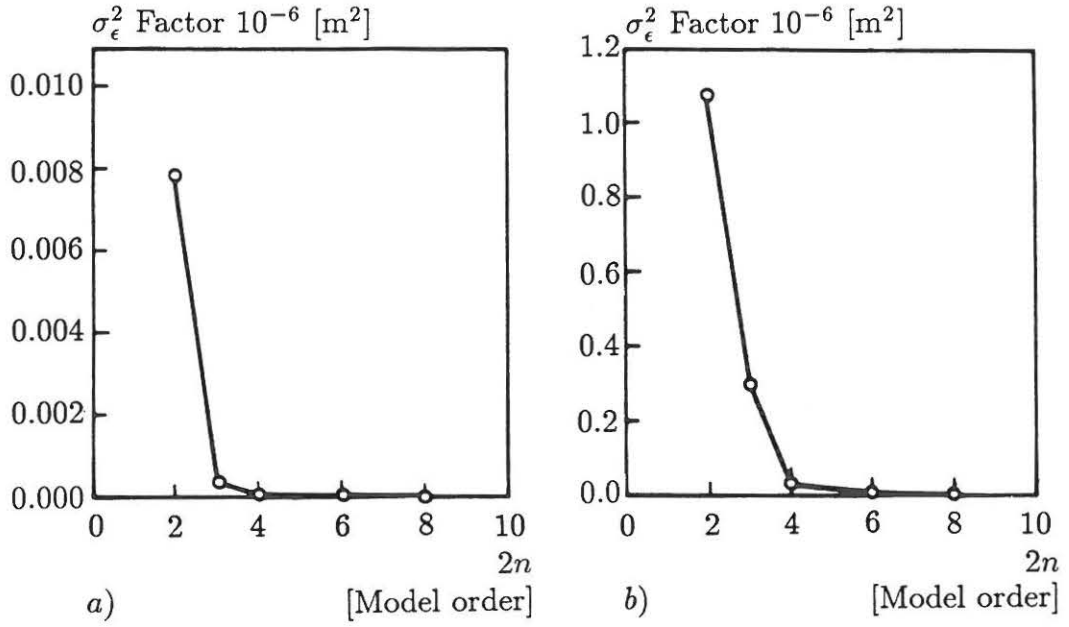

Figure 8.5. The model error expressed by σ_ϵ^2). a) First eigenmode. b) Second eigenmode. Time series: Displacement response of mass no 2.

In fact the development of σ_ϵ^2 as a function of the order of the model order showed that when the time series was filtered to obtain only the second mode the reduction of σ_ϵ^2 obtained by going from an ARMA(2,1) to an ARMA(4,3) model was about a factor 35. When the first eigenmode was considered this ratio was about 3000 to 4500 in magnitude. This indicates that the correct model of the time series of the first eigenmode is an ARMA(4,3) model while the second eigenmode may be modelled by an ARMA(2,1) model.

The explanation of the different models is the applied force spectrum which primarily led to an excitation of the second eigenmode while the first eigenmode was only weakly excited and consequently uncertain to any interpretation. Furthermore, the applied filter was not able to completely eliminate the influence of the second mode in the time series where only the first mode was intended to be present.

The mean values and the standard deviations of the eigenfrequencies and the damping ratios have been computed by simulation of the sample space of the ARMA parameters, see table 8.2. The ARMA parameters were assumed to be normally distributed with some limitations. The limitations appeared because negative values of the eigenfrequencies and the damping ratios were not allowed. The eigenfrequencies were assumed to be normally distributed and the damping ratios were assumed to follow a logarithmic normal distribution. This was justified by a χ^2-test. The statistical analysis showed that the eigenfrequency and damping ratio of a given mode were uncorrelated. An example of the simulated joint probability density function of the eigenfrequency and the damping ratio is shown in figure 8.6.

Time series	ARMA Model	f_i Hz		ζ_i	
Mode 1					
Displ.	(2,1)	1.1116	±0.0019	0.00109	±0.00065
Mass 1	(4,3)	1.1069	±0.0001	0.00189	±0.00101
Mode 1					
Displ.	(2,1)	1.1129	±0.0020	0.00294	±0.00154
Mass 2	(4,3)	1.0964	±0.0001	0.00118	±0.00083
Mode 2					
Displ.	(2,1)	7.1935	±0.0008	0.00005	±0.00003
Mass 1	(4,3)	7.1906	±0.0000	0.00066	±0.00000
Mode 2					
Displ.	(2,1)	7.1938	±0.0008	0.00007	±0.00004
Mass 2	(4,3)	7.1813	±0.0301	0.00274	±0.00115

Table 8.2. Computed eigenfrequencies and damping ratios from the estimated ARMA parameters with standard deviations.

It is seen that the ARMA models of the two analysed time series can now be compared by the sample values of the mean values and standard deviations of the eigenfrequencies and damping ratios given in table 8.2.

If the ARMA(4,3) model is chosen as the proper model of the time series containing the first eigenmode a deviation between the estimated mean values of the parameters is found depending on whether the response was measured at mass 1 or 2. The deviation between the eigenfrequencies is about 1% while the deviation between the damping ratios is about 60%. However, the latter is covered by the standard deviation corresponding to a coefficient of variation of about 50-70% of the damping ratio. The deviation between the eigenfrequencies cannot be directly explained by the uncertainty of the parameter. A possible explanation may be insufficient convergence criteria of the estimations of the ARMA models. The bandpass filtering may also have had some influence.

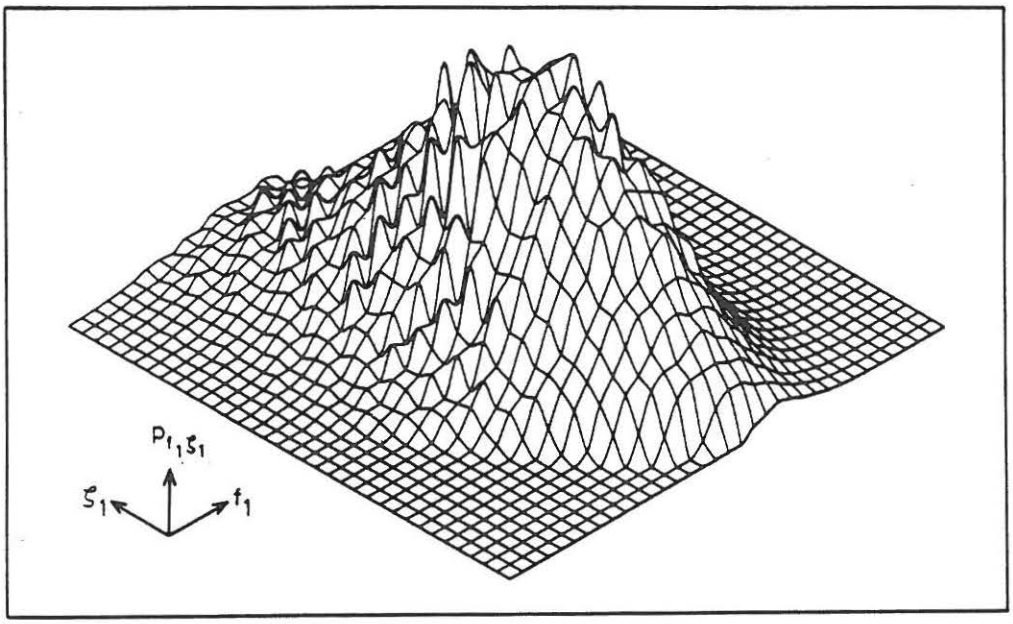

Figure 8.6. Simulated joint probability density function of the eigenfrequency and the damping ratio obtained by an ARMA(2,1) model.

It is seen that if the ARMA(2,1) model is chosen as the correct model of the time series containing the second eigenmode, the estimated values of the eigenfrequency and damping ratio are almost independent of whether the time series has been chosen as the response of mass 1 or 2. This means that the second eigenfrequency and damping ratio has been uniquely determined for this model. With respect to the ARMA(4,3) model of the two time series it is seen from table 4.3 that neither the eigenfrequencies nor the damping ratios agree. Nevertheless, for the time series of the displacement of mass 1 a comparison shows that the results of the ARMA(4,3)

model agree very well for the second mode. Consequently, the ARMA(4,3) model cannot be rejected. The disagreement of the results of the two ARMA(4,3) models might be due to insufficient convergence.

Having discussed the proper models of the two procedures it is now possible to compare the results and discuss the advantages and disadvantages of the two procedures.

A comparison of the estimates of the eigenfrequencies shows that they deviate about 1% with a coefficient of variation of less than 0.02% of the ARMA(2,1) or ARMA(4,3) models. This is quite acceptable since the deviations are likely to be covered by the uncertainties of the ARMA(14,13) models which the applied ARMA algorithm was not able to compute.

From the second procedure it was found that the damping ratios of the first mode had a coefficient of variation of about 50%. The deviations between the damping ratios of the two procedures were about 54% or up to 116% depending on the choice of reference value. Due to the high uncertainty this deviation does not indicate any significant error between the two procedures, especially because the deviations are ambiguous. However, with respect to the second mode this is not the case. A comparison of the two procedures shows that the first procedure gave estimates of the second damping ratio which exceeded the estimates of the ARMA(2,1) model of the second procedure by a factor 10. On the other hand, if the ARMA(4,3) model was chosen as the proper model of the second procedure the damping estimates deviate less than 2% for the results of the time series of the displacement of mass 1 while the estimates from the time series of the displacement of mass 2 disagree completely. Hence some confusion exists with respect to the proper model order and the determination of the second damping ratio. The explanation might be an insufficient convergence criterion. This should have been studied further if any final conclusion were to be made.

The damping estimate of the first eigenmode has also been compared with the results of a free decay. Here the damping ratio was found as $\zeta_1 = 0.00108 \pm 0.00002$ which lies within the uncertainty of the estimates of the ARMA models provided by the second procedure.

The comparison of the two procedures has shown that both procedures can be applied since the parameter estimates computed by the two proceduress agree quite well with the exception of the second damping ratio. However, the second procedure seems to be the most favourable because of the considerably smaller order of the most appropriate model. The small model order means that the estimation requires considerably less computer time and it means that the ARMA estimation algorithm almost always succeeds in computing the uncertainty of the ARMA parameters. Finally, due to the low model order it is a practicable task to compute the statistics of the eigenfrequencies and the damping ratios by simulation of the sample space of the AR parameters.

8.1.6 Conclusion

The presentation of identification by ARMA models has shown that it is a possible way for estimating modal parameters. Even in the case of non-white random excitation the experimental case has illustrated that sensible results can be obtained. The feature of estimation of the uncertainty of modal parameters makes the method extra attractive. The knowledge of parameter uncertainty makes it possible to validate the estimates as illustrated in the experimental case but it is just as important that it makes continuous improvement of the measurement and identification procedure possible.

However, the research of Gersh [13] has shown that essentially the same problems with respect to the length of the time series and the sampling rate as in FFT-analysis exist. Thus, the question is just whether the performance with ARMA models is qualitatively better. Even though there is no final reply to this question the experience with identification by ARMA models has shown that there seems to be less bias and less uncertainty in the parameter estimates.

With respect to choice of model order methods which are based on the subjective judgement of the engineer must and can be used. The subjective judgement in finding a model and thus a set of modal estimates is not unique for the application of ARMA models. It should be pointed out that the same subjective element exists e.g. in FFT-analysis where the engineer chooses a window and thus makes a decision on the weighting of bias versus random errors as discussed in chapter 5.

The application of ARMA models has shown that probably the most favourable procedure to estimate the eigenfrequencies and the damping ratios is to ensure that only one mode is present in the time series. This has been done with success when one of two modes was weakly excited. However, if two eigenmodes are coupled closely this cannot be expected to be possible and a model containing more than one degree of freedom must be used.

The applications of ARMA models in practice have also shown the usefulness of the method. Safak [18] has applied the method for identification of the eigenfrequencies and damping ratios of the four lowest modes of a nine storey building. An ARMA(24, 23) model was applied. Shinozuka et al. [17] have estimated structural matrices and the aerodynamic coefficients on a suspension bridge applying different sorts of ARMA algorithms. Olagnon and Prevosto [19] have estimated the eigenfrequencies and the damping ratios of two offshore structures with success, a jacket structure and a monopile were considered. The method has also been applied for controlling the dynamic behaviour of large space structures, see Sundarajan,N. and R.C.Montgomery [20]

8.2 Maximum Entropy Method (AR Models)

As shown in the previous section the estimation of ARMA models is a nonlinear problem which makes the method time consuming and computer expensive. The nonlinear character of the estimation problem is due to the MA part of the ARMA model. Consequently a large effort during the last 15 years has been made to apply purely autoregressive models as parametric time series models, AR models. With respect to obtaining an alternative spectral estimation method, this method is usually called maximum entropy method (MEM) which will also be the name in this context.

The AR model, ARMA(n,0) is given by:

$$x_t = \sum_{i=1}^{n} \Phi_i x_{t-i} + \epsilon_t \tag{8.15}$$

Wolds [7] has shown that any ARMA model can be represented by an AR model provided that the model order is chosen sufficient high. Thus the AR model can be just as proper a model of a measured time series as the ARMA model. The application of the AR model to spectral estimation was started by Burg [21],[22], introducing the maximum entropy concept in spectral estimation. The frequency formulation of AR models is analogous to the transformation of ARMA models into the frequency domain. The autospectrum of the AR model of a measured time series is given by:

$$\begin{aligned} S(f) &= \frac{2\Delta\sigma_\epsilon^2}{\left|e^{nif2\pi\Delta} - \Phi_1 e^{(n-1)if2\pi\Delta} - \ldots - \Phi_n\right|^2} \\ 0 &\leq f \leq \frac{1}{2\Delta} \end{aligned} \tag{8.16}$$

see e.g. Jensen [9]. The AR parameters can be estimated directly by linear regression obtaining a least square fit between the measured time series and the AR model. This is the method which has been widely recommended, see Kay and Marple [23], in some modified forms. Alternatively, the parameters can be obtained from the Yule-Walker equations, which was the original approach proposed by Burg [21] and others. The Yule-Walker equations relate the AR parameters to the obtainable autocorrelation function of the measured time series:

$$\begin{pmatrix} R_{xx}(0) & R_{xx}(1) & \ldots & R_{xx}(n-1) \\ R_{xx}(1) & R_{xx}(0) & \ldots & R_{xx}(n-2) \\ \vdots & \vdots & \vdots & \vdots \\ R_{xx}(n-1) & R_{xx}(n-2) & \ldots & R_{xx}(0) \end{pmatrix} \begin{pmatrix} \Phi_1 \\ \Phi_2 \\ \vdots \\ \Phi_n \end{pmatrix} = \begin{pmatrix} R_{xx}(1) \\ R_{xx}(2) \\ \vdots \\ R_{xx}(n) \end{pmatrix} \tag{8.17}$$

A recursive algorithm called the Levinson/Durbin algorithm makes it possible to

obtained quick estimates of the AR parameters by continuously increasing the model order.

The AR model for a random process given by a measured time series happens to be related to the principle of maximum entropy, see Burg [22]. The fundamental principle is that only a finite segment of a realization of the random process is known. Thus the rationale for the choice of the maximum entropy estimate is that it imposes fewest constraints on the unknown time series by maximizing the randomness of the unknown part of the random process, which leads to a minimum of bias. Ables [24] has given a popular introduction to the principle. Thus, while the FFT-analysis forces the unknown part of the random process and thus also the autocorrelation function to be zero, see figure 8.7, the MEM estimate lets the unknown values be as uncertain as possible since no knowledge about the random process exists. The maximum entropy spectral estimate given by an AR model is restricted to Gaussian distributed random processes. In Ljung [3] it is shown that in fact the maximum entropy estimate equals a maximum likelihood estimation which means that the spectral estimate in theory will be unbiased and converge as the number of observed data goes towards infinity.

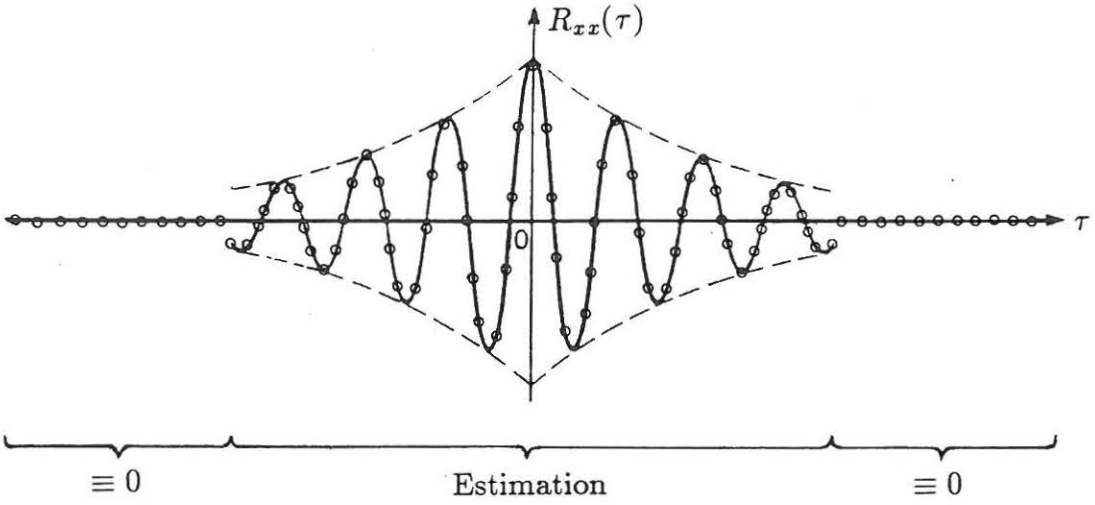

Figure 8.7. The auto-correlation function in practice which FFT-analysis is based on.

Just as in the case of ARMA models the problem of the method is the choice of the model order. The variance of the residuals will decrease as the model order increases and when the right model order has been obtained the residual time series should be equal to white noise. Thus this could be applied as a check. However, a more effective criterion may be the Akaike information criterion defined earlier for ARMA models with $(4n-1)$ instead of (n) see (8.10):

$$(AIC) = \min\left((\sigma_\epsilon^2) + \frac{n}{N}\right) \tag{8.18}$$

N is the number of sampled points of $x(t)$. If the model order of the AR model becomes too high the spectral estimate degenerates and spurious peaks arise and

distort the spectrum. This is particular a problem with AR models based on short-term series containing harmonics and noise. In those case Kay and Marple [23] recommend the application of ARMA models.

When a proper order has been found the eigenfrequencies and the damping ratios can be estimated from the AR model represented in the frequency domain by the spectrum given by (8.16). A curvefit of the spectral peak can be applied or the eigenfrequencies and the damping ratio can be evaluated directly from the parametric expression (8.16), e.g. by determining the peak frequency and the half-power point of the spectrum of the model, see Vandiver and Campbell [25]. The direct evaluation of estimates of eigenfrequencies and damping ratios has the advantage that the covariance matrices of those estimates can be determined from the estimated covariance matrix of the AR model by linearization of the relation, Campbell [26]. By an extensive simulation study it was shown in the latter references that the damping estimates will be made with a bias error up to a magnitude of about 5%. This error will decrease with increasing damping. The coefficient of variation was found to be about 10-15%.

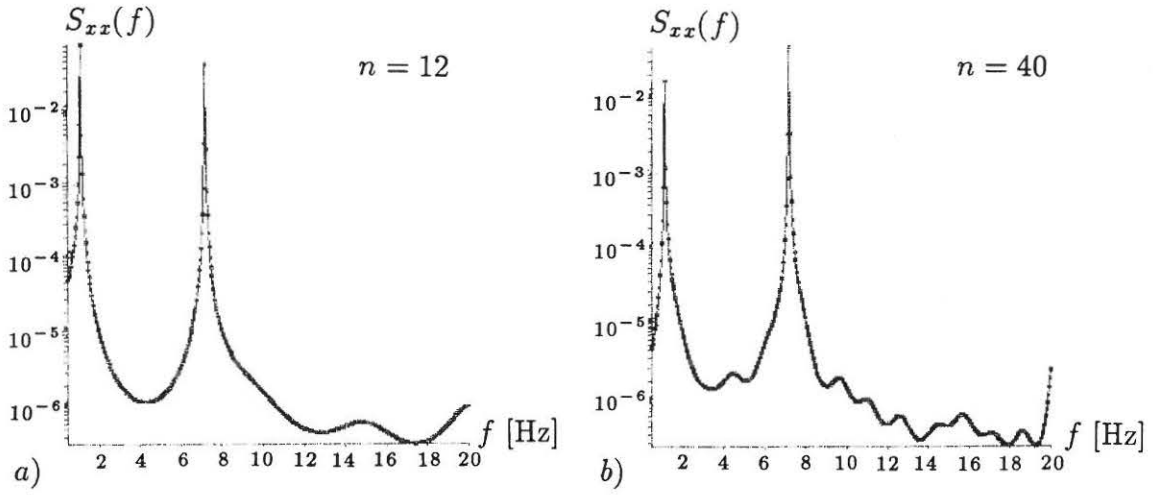

Figure 8.8. Experimental case: MEM estimate of autospectrum. a) n=12, b) n=40. T=120 sec.,Δ=0.02 sec. for acceleration response.

An example of a MEM spectrum is shown in figure 8.8 for an analysis of data obtained in the experimental case. The MEM spectrum was estimated by a FORTRAN program but only limited experiences have been obtained. The program was based upon an algorithm proposed by Anderson [27] essentially the same as the original algorithm developed by Burg [21]. However, several algorithms for estimating AR models have been proposed during the years and it seems that the bias and random errors of the spectrum to some extent depends on the algorithm applied. Marple and Kay [23] recommend the approach called the least square rather than the Burg algorithm since the latter has larger bias at the peaks plus some other disadvantages, the cost is a slight increase in computer time.

A multivariate MEM version also exists which makes it possible to estimate cross-

spectra and thus obtaining transfer functions, phase functions and coherence functions in complete analogy with the conventional FFT-analysis, see e.g. Campbell [26] which has applied the technique to measured data from an offshore structure and compared the results with a FFT-analysis. The MEM analysis was found to be superior.

As illustrated by the review given in chapter 2 the MEM analysis has been applied in practice by many engineers for the purpose of obtaining reliable damping estimates of offshore structures and the results are in general concluded to be better than the results of simultaneous FFT analysis. In fact it seems that the MEM analysis has been implemented in several commercial software and hardware packages, e.g. MATLAB [16] and SAPS [28].

8.3 Conclusion

The principle of identification by time series models has been explained and illustrated in the experimental case. Spectrum analysis by MEM has been shown to be a special case of applying ARMA models for the identification of the modal parameters.

Identification by ARMA or MEM has trough own experience and a review of existing literature shown to give better estimates of especially the damping ratios, because the bias error is kept small. However, the cost is larger computer storage and increased computation time. Analysis of a typical session with an ARMA model of order (8,7) may last 20 cpu minutes for one time series of 6000 points and for MEM about 3 minutes for an order of 40. The corresponding computer time of two-channel FFT-analysis will typical take less than one minute and require smaller storage, however it is strongly emphasized that MEM spectral estimates are obtained almost equally fast which explains the increasing popularity. No experience has been gained with respect to the application of the multivariate versions of identification by ARMA models and MEM but it is suspected that the computer time may increase substantially.

One limitation of identification by ARMA models or MEM is that white noise excitation is assumed. This means that the methods should only be applied in case of lightly damped systems with a broad-banded excitation. The prize of non-white excitation will be an increase model order for the proper time series model. Pi and Mickleborough [12] have shown how identification by ARMA models can be generalized for non-white excitation simply by accepting this higher model order, and the ARMA relation to a free vibration is also established. In fact, Leuridan et al. [29] have shown that the identification by ARMA models can be directly related to the Ibrahim time domain method presented in chapter 7. Another way to cope with non-white excitation is to apply more generalized time series models, see e.g. Ljung [3].

Another limitation which is quite general for the most identification methods is

that it is assumed that the system to be identified can be modelled by a linear model. Identification of nonlinear structures by time series models has been an interesting subject during the eighties, see e.g. Yun and Shinozuka [30], Hoshiya [31]. However the practical application of the methods seems to be limited at the current stage. Thus, in practice the linear assumption will be assumed to be valid and the obtained modal estimates correspond to an equivalent linearized model of the real structure.

8.4 References

[1] Kozin, F & H. G. Natke, "System Identification Techniques", Structural Safety 3, 1986 pp. 269-316 Elsevier Science Publ.,Amsterdam, 1986.

[2] Lefkowitz, R., "Evaluation of Various Methods of Estimating the Parameters of ARMA Processes", Polytechnic Institute of New York, USA, 1986.

[3] Ljung, L., "System Identification - Theory for the User", Prentice-Hall, USA, 1987.

[4] Box, G. E. P. & G. M. Jenkins, "Time Series Analysis - Forecasting and Control", Holden-Day, USA, 1969.

[5] Marquardt, D. W., "An Algorithm for Least-Square Estimates of Nonlinear Parameters", Journal of Society of Industrial Applied Mathematics, Vol. 11, no. 2, USA, June 1963.

[6] Pandit, S. M. & S-M Wu., "Time Series and System Analysis with Applications", John Wiley & Sons Ltd, USA, 1983.

[7] Wold, H. O., "A Study in the Analysis of Stationary Time Series", Almquist and Wicksell, Uppsala, 2nd ed., 1954.

[8] Akaike, H., "A New Look at the Statistical Model Identification", IEEE Transactions on Automatic Control, Vol. AC-19, no. 9, Dec. 1979.

[9] Jensen, J. L., "System Identification 1: ARMA Models", Paper no. 10 in Fracture & Dynamics, Institute of Building Technology And Structural Engineering, University Of Aalborg, Denmark, 1989.

[10] Pandit, S. M., "Analysis of Vibration Records by Data Dependent Systems", Shock and Vibration Bulletin, no. 47, part 4, 1977.

[11] Pandit, S. M. and N. P. Mehta, "Data Dependent Systems Approach to Modal Analysis via State Space", Journal of Dynamic System, Measurement and Control, Vol. 107, no. 2, Jun., American Society Of Mechanical Engineers, 1985.

[12] Pi, Y. L. and N. C. Mickleborough, "Modal Identification of Vibrating Structures using ARMA Model", Journal of Engineering Mechanics, Vol.115, no.10, Oct., American Society Of Civil Engineers, 1989.

[13] Gersh, W., "On the Achievable Accuracy of Structural System Parameter Estimates", Journal

of Sound and Vibration, Vol. 34, no. 1, 1974.

[14] Gersh, W., N. N. Nielsen and H. Akaike, "Maximum Likelihood Estimation of Structural Parameters from Random Vibration Data", Journal of Sound and Vibration, Vol. 31, no. 3, 1973.

[15] NAG library, version 1987, NAG Central Office Mayfield House, 256 Banbury Road, Oxford OX2 7DE, UK, 1987.

[16] MATLAB, Package of MATLAB and System Identification Toolbox., The Math Works,Inc., 20 North Main St.,Suite 250, Sherborn, MA 01770, USA, 1989.

[17] Shinozuka, M., C. Yun & H. Imai, "Identification of Linear Structural Dynamic Systems", Journal of Engineering Mechanics Division, Proceedings of ASCE, Vol. 108, USA, Dec 1982.

[18] Safak, E., "Stochastic System Identification in Structural Dynamics", Conf. on Probabilistic Methods in Civil Engineering, P. D. Spanos, ed., ASCE, New York, 1988.

[19] Olagnon, M. and M. Prevosto, "The Variations of Damping Ratios with Sea State Conditions for Offshore Structures under Natural Excitations", Offshore Technology Conference, OTC4654, Houston, USA, 1984.

[20] Sundararajan, N. and R. C. Montgomery, "Experiments using Lattice Filters to Identify the Dynamics of a Flexible Beam", Journal of Dynamic Systems, Measurements and Control, Sept., Vol. 107, American Society of Mechanical Engineers, 1985.

[21] Burg, J. P., "Maximum Spectral Analysis", Presented at the 37th Annual Int. Meeting , Society of Expor. Gephys., Oklahoma, USA, 1967.

[22] Burg, J. P., "Maximum Entropy Spectral Analysis", Ph.D. Thesis, Standford University, USA, 1975.

[23] Kay, S. M. and S. L. Marple, Jr., "Spectrum Analysis - A Modern Perspective", Proc. of the IEEE, Vol. 69, no. 11, Nov. 1981.

[24] Ables, J. G., "Maximum Entropy Spectral Analysis", Proc. Symp. on the Collection and Analysis of Astrophysical Data, Nov. 13-15, 1972.

[25] Vandiver, J. K. and R. B. Campbell, "The Determination of Modal Damping Ratios from Maximum Entropy Spectral Estimates", Presented at Winter Annual Meeting of the Dynamic System & Control Division of the American Society of Mechanical Engineers, Chicago, USA, Nov. 1980.

[26] Campbell, R. B., "The Estimation of Natural Frequencies and Damping Ratios of Offshore Structures", Ph.D. Thesis, Massachusetts Institute of Technology, USA, 1980.

[27] Anderson, N., "On the Calculation of Fitted Coefficients for Maximum Entropy Spectral Analysis", Geophysics, Vol. 39, pp. 69-72, 1974.

[28] SAPS, AV Technology, AVTECH House, Birdall Lane, Cheak Heath, Stockport, Cheshire SK3 oxu, UK, 1988.

[29] Leuridan, J. M., D. L. Brown and R. J. Allemang, "Time Domain Parameter Identification Methods for Linear Modal Analysis: A Unifying Approach", Journal of Vibration,Acoustics,Stress,

and Reliability in Design, Vol.108, no.1, American Society of Mechanical Engineers, Jan. 1986.

[30] Yun, C-H. and M. Shinozuka, "Identification of Nonlinear Structural Dynamic Systems", Journal of Structural Mechanics, 8 (2), 1980.

[31] Hoshiya, M., "Application of the Extended Kalman Filter-WGI Method in Dynamic System Identification", Stochastic Structural Dynamics: Progress in Theory and Application, S. T. Ariaratnam, G. I. Schueller and I. Elishakoff, ed. , Elsevier Applied Science, 1988.

Alternative References

[32] Hoen, C., "MARCO - A Program System for Estimation of Structural System Modal Parameters from Vibration Measurements. Theory Manual", Report STF71 F87057, SINTEF, Trondheim, Norway, 1987.

[33] Safak, E., "Adaptive Modeling, Identification, and Control of Dynamic Structural Systems. I: Theory", J. Engineering Mechanics, Vol. 115, no. 11, ASCE, November 1989.

[34] Safak, E., "Adaptive Modeling, Identification, and Control of Dynamic Structural Systems. II: Applications", J. Engineering Mechanics, Vol. 115, no.11, ASCE, November 1989.

[35] Mickleborough, N. C. and Y. L. Pi, "Modal Parameter Identification Using Z-Transforms", International Journal for Numerical Methods in Engineering, Vol. 28, pp. 2307-2321, John Wiley & Sons, 1989.

[36] Prevosto, M., B. Barnouin and C. Hoen, "Frequency versus Time Domain Identification of Complex Structural Modal Shapes", Proceedings of the 1983 IFIP Symposium, 1983.

[37] Romberg, T. M., A. G. Cassar and R. W. Harris, "A Comparison of Traditional Fourier and Maximum Entropy Spectral Methods for Vibration Analysis", J. Vibration, Acoustics, Stress, and Reliability in Design, Vol. 106, January, American Society of Mechanical Engineers, 1984.

[38] Davies, P. and J. K. Hammond, "A Comparison of Fourier and Parametric Methods for Structural System Identification" J. Vibration, Acoustics, Stress, and Reliability in Design, Vol. 106, January, American Society of Mechanical Engineers, 1984.

9. DISCUSSION AND CONCLUSIONS

A presentation and discussion of different methods for system identification has been given in chapter 6 to 8. In this chapter it is intended to summarize the practical aspects of the methods and system identification of offshore platforms.

In figure 9.1 a diagram of the methods which have been considered is shown. They have been divided into groups with respect to the kind of measured data on which each method is based. It is considered that the most frequently used methods are based upon ambient excitation which is no doubt is due to the fact that it is a less expensive way of obtaining structural information. A perhaps more important fact is that this kind of excitation has been included in the design basis whereas external excitation due to an external force or impulse will in principle constitute an extra risk of structural damage. On the other hand it is also quite logical that more structural information is gained when the phase information about the excitation versus the response is applied in the analysis, e.g. by the circle fit method. It has also been shown that very reliable information can be obtained from records containing free decay data.

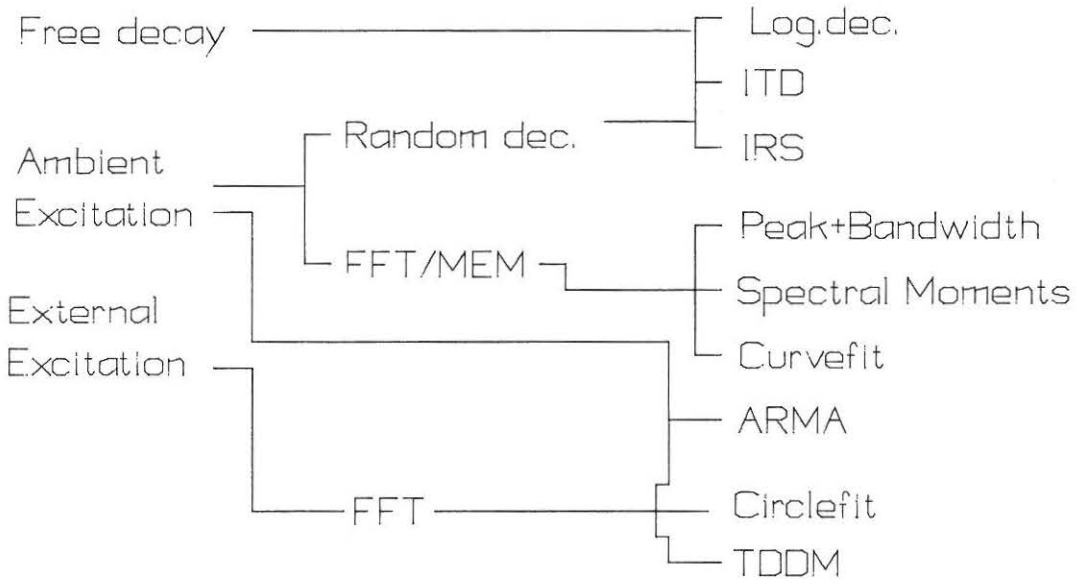

Figure 9.1. Diagram of methods for system identification.

When applying such methods which are not based on ambient excitation but also a known external excitation, the noise from ambient excitation must be considered. However, if this noise can be considered as uncorrelated with the response due to the external excitation no problem will exist if cross-spectral information is applied as discussed in chapter 5.

The methods which have been considered have all to some extent been based on approximated structural models, typically using one or several of the assumptions:

- The SDOF assumption: The measured response has been analysed by approximating the structure to a single-degree-of-freedom system.
- The white noise assumption: The ambient force process has been considered to be white noise.
- The linear model assumption: The structure has been considered to behave linearly with no time dependence or interaction between the excitation and the response.

9.1 The SDOF Assumption

With respect to the single degree of freedom assumption, two aspects exist. First of all, if the damping is large then the half-power bandwidth will be large. This means that if the half-power bandwidth is large, due to large damping, compared with the closeness of the eigenfrequencies then the assumption of proportional damping will not hold in general as discussed in chapter 4. Secondly, in the case where the assumption of proportional damping can be applied, the frequency region, where only a single eigenmode dominates will be limited or may even not exists. The latter means that it may be necessary to assume a model containing two or more degrees of freedom as proposed in chapter 7 by the general curvefitting method. However, essential for this approach will be that it will not be applicable when the modes become too close. In those cases it is necessary to include the phase information if information of two closely spaced modes has to be obtained.

Alternatively, it may be sensible to apply the approach of identification by ARMA models in the case of close spaced eigenfrequencies. Identification by ARMA models does not contain any assumption of proportional damping or the level of the damping. However, the effectivity of the method with regard to this problem remains to be investigated. Similarly the Ibrahim time domain method (ITD) may be applied combined with the random decrement method in the case of ambient excitation. But also the effectivity of this approach remains to be investigated.

9.2 Violation of the White Noise Assumption

The effect of non-white excitation has been investigated. The realistic case will be that the peak of the wave excitation spectrum will lie below the first eigenmode

of the structure. This means that the average slope of the force spectrum can be expected to be negative and approximated with a straight line in the resonance region of the first eigenmode:

$$S_{pp}(f) = S_0(1 + a(1 - \frac{f}{f_1})) \tag{9.1}$$

A situation where the peak of the excitation spectrum coincides with the resonance region will never arise in practice, because the design concept will never allow this to happen. The case of a positive slope of the excitation spectrum will be possible if there is a significant peak beyond the resonance frequency. However, this will give rise to a significant dynamic amplification which the survey of literature has indicated is only seldom seen in practice.

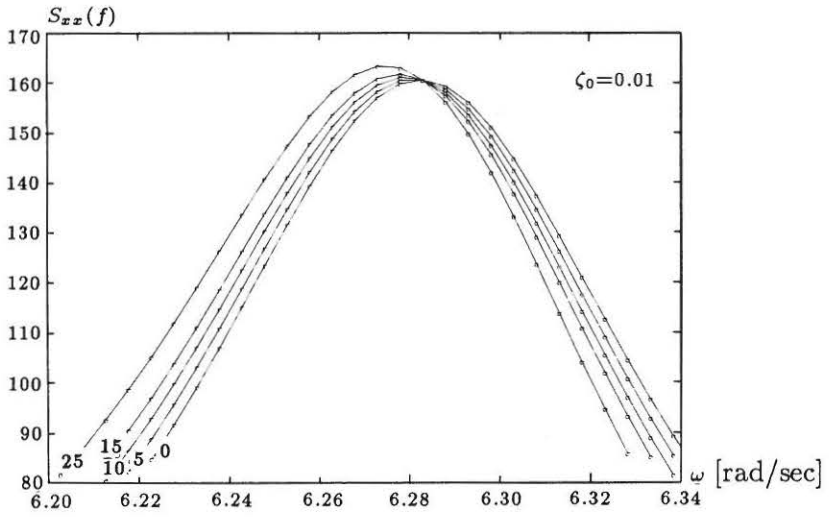

Figure 9.2. Distorted resonance peaks of response spectrum due to non-white excitation. The numbers correspond to the slope factor a.

The effect of the violated assumption has been investigated by a simulation study of an SDOF system with $f_0 = 1$ Hz with two different damping values, $\zeta_0 = 0.01$ and 0.05 with the slope a from $0 - 30$, where a is defined as in (9.1). An example of the response spectrum is shown in figure 9.2 for the different slopes. It is seen that an increasing slope of the excitation spectrum leads to a distortion of the resonance peak corresponding to an increasing skewness of the peak. A curvefit of the part of the resonance peak lying between the half-power points of the response spectrum has then been applied for identification of the eigenfrequency and the damping ratio. The curvefit algorithm which has been applied is called the peak shape method, see Jensen [1]. If the resonance peak is undistorted a straight line with a slope, ζ_0^2 is supposed to be identified. As shown in figure 9.3 the skewness of the resonance peak splits the straight line into two curves with an increasing effect as the slope of the excitation spectrum grows larger. In figure 9.4 the estimate damping ratio is shown as a function of the slope of the force spectrum. As expected it is seen that

the sensitivity with respect to the non-whiteness is significantly less for $\zeta_0 = 0.01$ than for $\zeta_0 = 0.05$ and it is seen that the effect increases with increasing non-white excitation. In any case the effect is a bias error leading to an inflated damping ratio. The magnitude of the error may become significantly large. The effect upon the eigenfrequency was found to be significantly less leading to an insignificant underestimation for the given damping ratios.

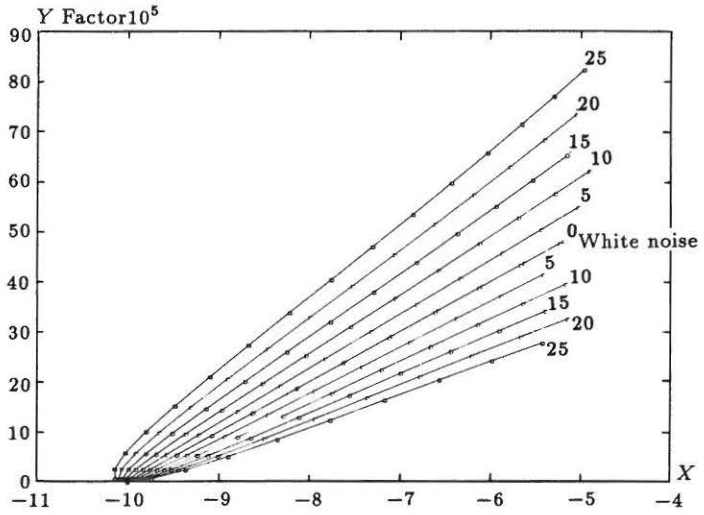

Figure 9.3. Curvefit of resonance peak data for non-white excitation. The numbers correspond to the slope factor a.

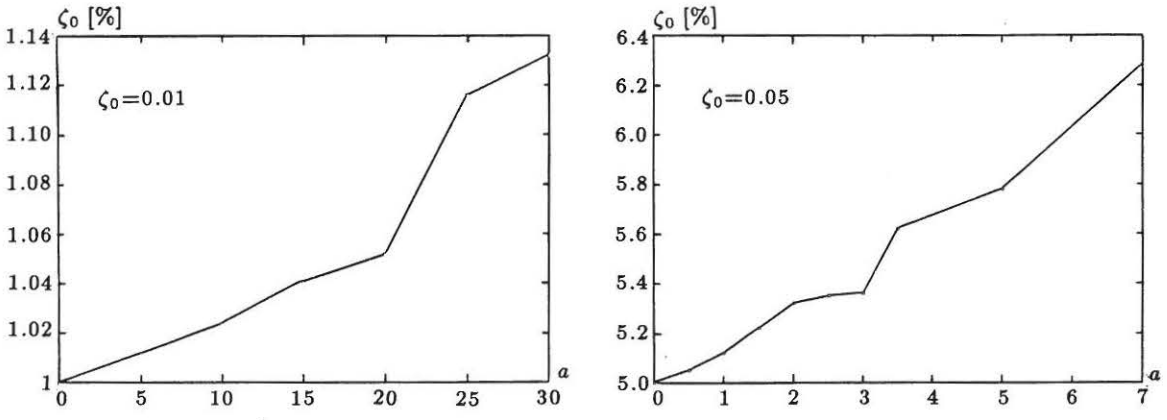

Figure 9.4. Estimated damping ratio as a function of the slope factor a.

Campbell [2] has investigated the effect of a violated white noise assumption for the bandwidth method while Sunder et al. [3] has investigated the method of spectral moments. The latter found that the method of spectral moments always gave

an underestimation of the damping ratio of the same magnitude as the overestimation given above. The eigenfrequency was slightly underestimated. In general the bandwidth method gave overestimated estimates. Thus it seems that effect to some extent depends upon the applied identification method, but in any case the estimate of the damping ratio can be biased to some degree due to non-white noise.

It can be concluded that for lightly damped structures the bias will decrease with the magnitude of the damping due to a violation of the white noise assumption. The bias is believed to be small in practice. However, more important is the fact that the alternatives to the white noise assumption do not seem to be very attractive. The analysis of non-white excitation will require more computations, and in the case of wave excitation higher accuracy will not be ensured since the models of wave forces are quite uncertain as mentioned in chapter 5.

9.3 How to Cope with Nonlinearities

The general assumption of the methods presented in chapters 6 to 8 was that the structure was assumed to behave linearly, only the IRS-method (identification by response simulation) allowed the possibility of nonlinear mechanisms. Thus, in practice, the effect of nonlinearities upon estimates obtained for linear models should be assessed and the detection of nonlinearities should also be considered.

An essential aspect of nonlinearities which should be remembered, is that the detection of nonlinearities is an important part of system identification. Besides being vital for the evaluation of the resulting parameter estimates of linear models it is also important for e.g. fatigue life calculations with regard to structural knowledge, see e.g. Brouwers [4].

The problem of the detection was mentioned in chapter 4 in the description of structural models. It was recognized that it was not possible to detect even simple kinds of nonlinearities such as Coulomb or drag damping from signatures in the time or frequency domain when the excitation had a random character. In the cases of free vibration the IRS-method could be applied and in the cases of sinusoidal excitation the presence of nonlinearities could be detected by second order peaks at a multiple of the excitation frequency and/or the resonance peak. In the case of a sinusoidal excitation it would in general not be possible to recognize the different sorts of nonlinear mechanisms.

In the situation with ambient random excitation the detection of the presence of nonlinearities can be performed if the statistics of the response is considered, provided that the force process is assumed to be Gaussian distributed. Brouwers [4] has shown that nonlinearities due to mechanisms such as Coulomb or drag damping, affects the response statistics of a Gaussian excited SDOF system significantly. While the Gaussian excitation of a linear structure will also lead to a Gaussian distributed response, the presence of nonlinearities leads to a probability distribution which deviates especially at extreme response events. The method has been applied

in practice to offshore structures to indicate the influence of those mechanisms, see Langen et al. [5], Spidsøe and Leite [6] and Spidsøe and Langen [7]. The method has also been applied in practice in the experimental case where the influence of drag as well as Coulomb dampers were tested experimentally with one of two modes dominating the response. In figure 9.5 the results of the experimental case together with the theoretical signatures given by Brouwers are shown. The abscissa is here due to the theoretical cumulative probability according to a Gaussian distribution given the estimated standard deviation while the ordinate is obtained from the estimated cumulative probability found from the histogram of the measured time series. Both axes have been normalized with respect to the estimated standard deviation. Thus a straight line would indicate that the measured time series was Gaussian distributed which also would be an indication of a linear structure assuming the excitation to be Gaussian distributed.

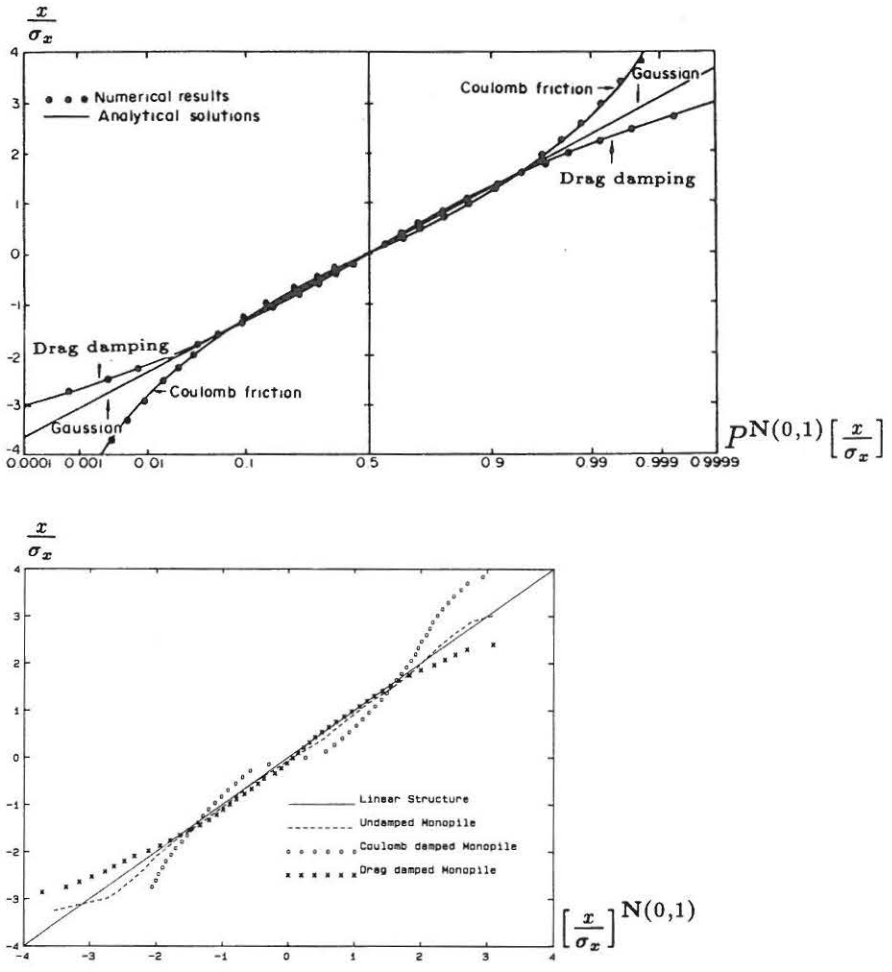

Figure 9.5. Top: The theoretical signatures of a linear SDOF system, Brouwers [4]. Bottom: The estimated signature in the experimental case.

Figure 9.5 clearly illustrates the useful perspective of the principle. The signatures obtained for the nonlinear dampers in the experimental case are clearly characteristic signatures of Coulomb and drag damping. It can be noticed that the undamped structure which was thought to behave linearly shows a weak nonlinear signature.

However, this may very well be due to non-Gaussian distribution of the excitation. The latter observation reveals the weak point of the approach since in practice especially drag dominated wave forces will be non-Gaussian distributed. However, the application of the approach in practice has shown that the principle works.

Nonlinear effects due to nonlinear stiffness can be evaluated if the eigenfrequency estimates are correlated with the response intensity as illustrated in Spidsøe and Langen [7],[5].

The presence of nonlinearities or coupling between the structure and the excitation can in general be evaluated by correlating the structural estimates with the sea state over a longer period of time, see Olagnon and Prevosto [8] who applied this principle to correlate the damping ratio with the sea state, see figure 9.6, which is an example of the correlation.

Besides the correlation of the estimates with the environment it is also necessary to be aware of structural changes such as a change in the deck mass or any modification in the structure. However, such structural changes will usually be isolated events which will not be a problem in the interpretation of the results if they have been detected prior to the analysis. An example of this aspect was given in chapter 2.

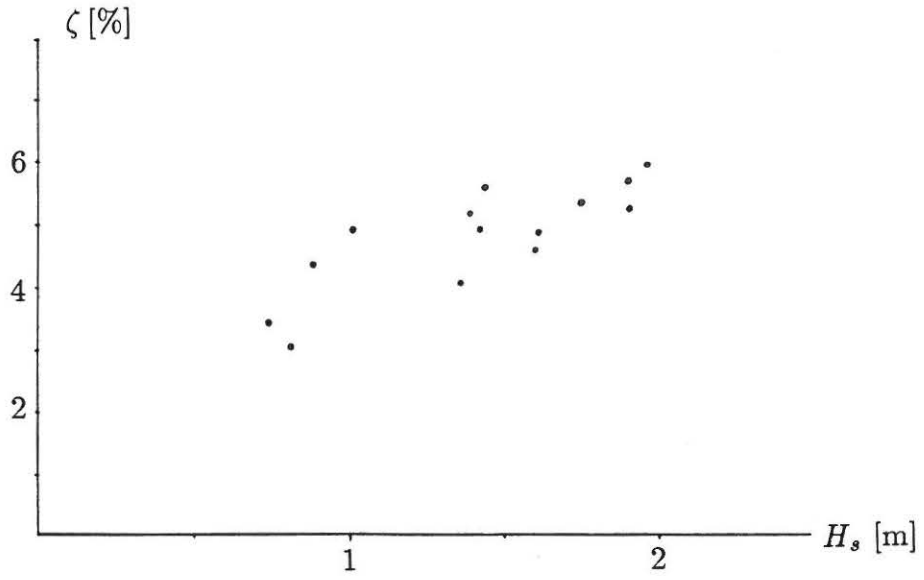

Figure 9.6. Variation of the damping ratio with H_s for the three first modes of a jacket platform, Olagnon and Prevosto [8].

When a nonlinear mechanism has been detected in the structure it should be integrated in the interpretation of the results. Either should a system identification method taking nonlinearities into account be applied or else should the effect upon a linear model assumption be evaluated. In the latter case, which will be the most frequent, the system identification based on a linear model assumption can be considered as an equivalent linearization, see e.g. Lin [9]. For the SDOF case the

nonlinear structure can be given by:

$$\ddot{x}(t) + g(x(t), \dot{x}(t)) = f(t) \tag{9.2}$$

which can be approximated by the linear model:

$$\ddot{x}(t) + c_{eq}\dot{x}(t) + k_{eq}x(t) = f(t) \tag{9.3}$$

by a least square minimization of the error:

$$\epsilon(t|c_{eq}, k_{eq}) = g(x(t), \dot{x}(t)) - c_{eq}\dot{x}(t) - k_{eq}x(t) \tag{9.4}$$

Thus, due to nonlinearities, this error can in the system identification approach be considered as an additional noise source. Consequently, it leads to an increase in the variance of the model error which causes a larger variance of the estimated parameters according to the principle given in chapter 3. Furthermore, this noise source will definitely in general not be Gaussian distributed, which means that unbiased convergence of the estimates is not guaranteed according to the principles of chapter 3. Thus, structural nonlinearities will be an important source to errors in the parameter estimates. Although it will not be possible to avoid the problem, the knowledge of its existence will make it possible to take the proper precautions in the interpretation of the results.

Simulation studies of the effect of nonlinearities upon parameter estimates obtained by typical methods for system identification have not been performed in any paper included in the literature survey performed in relation to this thesis. Thus, this may be an important topic in future research within the field, especially it is assumed that an investigation should be performed of the effect of the coupling between the water particle velocity and the structural response due to the drag term in the Morison equation which was briefly discussed in chapter 4.

9.4 Strategy in Practice

The strategy of system identification in practice will typically not include just one method of identification but a wide range of methods applying different assumptions. The choice of identification method in practice will depend on several aspects:

- Cost-benefit considerations.
- Measuring setup.
- The speed, simplicity and reliability.
- A proper range of methods.

9.4.1 Cost-Benefit Considerations

The choice of method for system identification interacts with the choice of measuring program of the structure. The different system identification methods set some basic requirements with respect to the type, the quality and the amount of measurings to be performed if the results of the system identification are supposed to be useful. On the other hand, the costs of the system identification have to be kept low. Thus, it is essentially a cost-benefit problem with the income due to the extra structural information versus the costs of measuring and analysis. This thesis has only considered the problem of ensuring the highest quality of the system identification while the problem of establishing the cost-benefit problem has not been considered. It is thought that it is a very difficult problem to set a prize on the obtainable structural information and compare it with the prize of obtaining it. A solution of the problem will probably tend to be more of academic interest than of practical value.

The purpose of performing a system identification session on an offshore structure will either be to improve structural knowledge or it can be permanently to monitor the integrity of the given structure.

In the first case the income is expected to be new structural knowledge which can give a less conservative design in general or which can give a reestimated strength or lifetime for the given structure, e.g. it might be concluded that the deckmass of a structure can be increased without alternating the design basis. Here it is assumed that the applied codes in the design per definition is conservative which means that the results of a system identification will always give a less conservative basis of structural design.

In the second case, the integrity monitoring case, the income lies in a reduction in the costs applied to inspection of the structure currently being performed due to authority requirements. The applicability and the reduced costs of vibration monitoring have been a popular subject during the late seventies and the eighties.

As an example of a concrete cost-benefit problem, consider e.g. the problem of choosing a method. If for instance a system identification method such as the circlefit method is applied, the phase information would lead to better estimates but it would require an external force excitation. Thus it is necessary to know how much is gained by taking this phase information into account instead of thus applying a white noise assumption. However, in the author's opinion, the decision in practice about what to do will depend highly on the given amount of money available for this sort of activities and the coincidence due to the interests of different persons and institutions.

On the other hand even though the cost-benefit consideration in principle has to be made, some minimum requirements also exist with respect to the quality of the methods which makes it easy to reject a method. For instance the damping information obtained by the half-power method will in general give an upper limit for the true damping ratio. However, since this will be an unconservative estimate,

the estimates will be more or less worthless providing no applicable information about the structure.

9.4.2 Measuring Setup

The most important cost source in the described cost-benefit problem is probably the instrumentation of the structure. One sensor is expected to cost about 10.000 DKK (1990) while the cost for filters and computer capacity for control and sampling may be about 1.000.000 DKK. Thus the cost due to the number of sensors will be relatively small compared with the rest of the costs. However, it should be noticed that the number of sensors will influence the amount of recorded data and thus also the subsequent cost of the analysis.

The relatively small costs of an extra sensor mean that the number of sensors is mainly determined by the the information needed. In principle, one sensor is sufficient for identification of the eigenfrequencies and the damping ratios of the excited eigenmodes. However, if the mode shapes are of interest the number of sensors must be increased to something like twice the number of mode shapes to be estimated. This will also increase the reliability of the other modal estimates and structural knowledge in general.

The location of the sensors must be such that maximum information is obtained about the mode of interest. A priori finite element analysis is a proper tool for determining the optimal location of the sensors, see e.g. Kientzy [10].

Besides a number of sensors on the structure it will also be important to have sensors observing the sea state, at least the significant wave height, a main direction and a significant wave period.

9.4.3 Speed, Simplicity and Reliability

The methods which were presented in chapter 6 to 8 differed with respect to:

- The simplicity of the application and the subsequent interpretation of the results.
- The reliability of the results due to model assumptions and the performance of the method.
- The speed of the methods.

The simplicity requirement is important if the methods are going to be widely used not only by the persons who have developed and implemented the methods. The amount of subjective judgement in a method also reduces its general applicability. If a method e.g. includes a number of parameters which have to be properly chosen for good estimates, it will require that the know-how is precisely documented. It should also be possible to present the results of the method in a simple and comparable

manner so that clarity is kept on any important aspect.

The reliability of the results must be ensured. First of all this is guaranteed if the methods have been tested and documented so that their limitations have been revealed. Secondly a wide range of methods should always be applied as cross checking of the results.

The speed of the method is quite obviously important if it is an on-line application. However, also in the case of off-line application the speed is important when the analysis must be repeated perhaps many times to obtain satisfactory results. Thus, it does matter whether an analysis takes three hours or two minutes, especially if the result of the analysis may be unaccurate the first 20 times.

Table 9.1 is attempted to give a rough survey of the considered methods with respect to the three properties. The quality has been divided into three levels , +++ the best, ++ medium and + basic quality. This review is rather subjective and should be nothing but a rough indication of the properties of the methods which should be considered with criticism.

In the column labelled "pre-processing" different alternatives have been given. "Direct" means that no pre-processing other than sampling and filtering is performed. In general it is assumed that the spectral analysis by MEM gives better damping estimates than FFT and consequently it should be used together with FFT as supplement. While MEM and FFT transform the data into a frequency formulation the random decrement (ran. dec.) technique works in the time domain extracting the characteristics of the random process. Even though the random decrement technique has been widely applied the features of the processing method have not been completely documented.

In the column indicating the simplicity of the application, +++ means that the method requires a minimum of documentation and guiding while a single + shows that the method requires a great deal of know-how which in practice only is obtainable through long experience. Thus the most user-friendly methods are typically the bandwidth method, the logarithmic decrement technique, the method of spectral moments and the circle fit method.

The reliability of the estimates which has been shown in the next column is correlated with the simplicity of the method meaning that a simple method gives less reliable estimates, however the one important exception is the logarithmic decrement technique applied to free decay data, which has shown to be quite superiour with regard to all properties. Unfortunately free decay records are only seldom available.

It is also seen, as expected, that the computation speed follows the simplicity of the method. The computation time of the fastest method may be less than 1 cpu minute on a Vax8700 while the slowest method might take more than 1 cpu hour. However, a detailed study of the speed of the different approaches has not been performed.

In general the most reliable parameter estimate methods tend to be obtained from the most complicated methods requiring some amount of computer time, which means that they are less applicable as on-line tools during measurings.

With respect to the model assumptions it is seen that only the identification by response simulation method (IRS) applied directly to the sampled data is able to take nonlinearities into account. The importance of the white noise assumption and the SDOF assumption is seen by the fact that almost all methods are based on either one or the other. Only the IRS-method gives direct estimates of the lumped physical parameters as described in chapter 6 while all the other methods end up with a set of modal parameters.

Method	Pre-processing	Simplicity of Method	Reliability of Estimates	Computation Speed	Model Assumptions
Bandwidth+ peak frequency	FFT	+++	+	+++	White noise,SDOF linearity
Bandwidth+ peak frequency	MEM	+++	++	++	White noise,SDOF linearity
Spectral moments	FFT	++	++	+++	White noise,SDOF linearity
Spectral moments	MEM	++	+++	++	White noise,SDOF linearity
General curvefit	FFT	+	+++	++	Linearity
Circle Fit	FFT	++	+++	+++	Known excitation SDOF,linearity
Log.dec.	Direct	+++	+++	+++	Meas.free decay, SDOF linearities
Log.dec.	Ran.dec.	+	++(+)	++(+)	white noise, SDOF linearity
ITD	Direct	+	+++	++	Meas.free decay linearity
ITD	Ran.dec.	+	++(+)	++	White noise linearity
IRS	Direct	+	+++	+	Meas.free decay nonlinearities
IRS	Ran.dec.	+	++	+	White noise linearity
ARMA	Direct	+	+++	++	White noise linearity
TDDM	Direct	++	+	+++	White noise linearities

Table 9.1. Comparison of the properties of different methods for system identification.

9.4.4 A Proper Range of Methods

The strategy of system identification in practice is thought to contain three analysis stages:

1 stage: Rough on-line analysis to get approximate information about the structure, which can be applied to adjust the setup during the full-scale measuring and also afterwards give a basis to the the more refined analysis in stage 2.

2 stage: Conventional analysis where the model building based on a priori knowledge is applied for obtaining reliable model estimates. At this stage the general assumption will be linearity.

3 stage: Advanced analysis where the model assumptions applied in stage 2 are assessed e.g. to detect nonlinearities or trends in the measurements and the obtained results.

At stage 1 the methods should be simple and the results easy to interpret and applicable to on-line analysis meaning that the computer speed must be high and the required amount of data small. Thus, stage 1 will typical contain a simple analysis of the peaks in the estimated spectra leading to estimates of the eigenfrequencies and the damping ratios. The half-power bandwidth should be rejected as an estimation method, but the minimum requirements for reliable estimates of this method should be applied as the general minimum requirements of the identification method used, which for instance could be the method of spectral moments.

At stage 2 the methods should be as reliable as possible with the given model assumptions. Furthermore, the statistics of the parameter estimates must also be included. The results must be fairly easy to interpret. The computer speed and the storage capacity is less important, although the methods should be so flexible that transition between stage 1 and stage 2 becomes somewhat smooth with regard to the level of the analysis.

Stage 2 should be initiated by a peak analysis of stationary records leading to identification of peaks due to eigenmodes, dominating excitation frequencies and noise sources. If records from several sensors have been applied, the shape vector method will be applicable to a detailed peak analysis leading to estimates of eigenfrequencies and mode shapes. Otherwise, if only few sensors have been applied the peak analysis must be based on an observation of the peaks due to records obtained for different sea states. For the more advanced analysis ARMA models, MEM analysis and the random decrement technique could be used for a more precise estimation of the eigenfrequencies and the damping ratios. The random decrement technique will in this case be applied to either the logarithmic decrement method, the Ibrahim time domain method (ITD) or the identification by response simulation method (IRS).

At stage 3 the goal is to evaluate the results of stage 2 rather than to obtain directly interpretable results. Thus, stage 3 must be the quality control of the general results of the system identification by applying less restrictive model assumptions

and seeking for trends and correlations in the results.

In stage 3 it is suggested that a qualitative check of nonlinearities is performed for records obtained for different sea states. Subsequently this should be followed by a detection of any possible correlation between the sea state and the identification results which means that the parameter estimates and their uncertainty should be correlated with the sea state. If records of free decays are available the identification by response simulation method (IRS) may be applied for the quantitative identification of nonlinearities of a simple structural model. Otherwise the conclusion with respect to nonlinearities must be limited to qualitative terms.

9.5 Conclusion

This thesis has attempted to provide a basis of system identification of offshore structures. The principles which have been established are generally applicable to all structures in civil engineering. The most important subjects and methods have been discussed even though many topics could have been discussed in further detail. However, the literature on the general subject of system identification is so extensive that the author felt that a more detailed treatment of some topics unavoidably have had the effect that some perhaps more important subjects were ignored (yet this may still be the case). The thesis has concentrated on system identification methods based on the response records due to ambient excitation even though there is a large number of methods which are based on input-output relations.

In chapter 2 it was shown that the damping of offshore structures cannot be predicted in general but must identified for the given structure. Similarly it was shown that also the a priori knowledge about the eigenfrequency is quite uncertain even when detailed finite element analysis has been performed. Thus, system identification is necessary if reliable structural information is important. However, while the eigenfrequency can be identified quite precisely within, say $1-2\%$ the damping ratio seems to be significantly more uncertain with an uncertainty of the magnitude $10-50\%$ depending on the quality of the identification. For a white noise driven SDOF system Kozin [11] has shown for a given identification method that, as a law of nature, it seems that the uncertainty of the damping will be something like $\frac{1}{\zeta_0}$ larger than the uncertainty of the eigenfrequency. Thus, the conclusion with regard to the damping is that every effort must be applied to keep the uncertainty of the damping ratio as low as possible by providing data with sufficient structural information and by choosing the best identification methods.

Apart from ensuring the highest possible quality of the system identification by proper measurements and analysis it is thought that an important improvement of system identification will in practice be due to statistical analysis of the parameter estimates and the sea state. Furthermore, the integration of finite element analysis in the system identification may also lead to increased information of the structure and especially the structure-foundation interaction. However, this subject has

unfortunately been beyond the scope of this thesis.

Since the thesis must be seen as a basis for system identification of offshore structures it is clear that a lot of subjects deserve to be further studied if they are supposed to become practical applicable. E.g. the method presented in chapter 8, the identification by ARMA models, is still quite an undescribed topic with respect to the practical application. Many aspects with respect to model assumptions, uncertainty of estimates still remain to be considered.

A subject, which still lacks practically applicable methods, is the identification of nonlinear structures. The assessment of nonlinearities is at the present stage limited to either simple problems or on empirical approaches with respect to the detection of the nonlinearities. Both concepts have been illustrated in this thesis in chapter 6 and the present chapter. The basic problem seems to be that just as the class of linear models is a specific class of models with limited validation, a given class of nonlinear models will also belong to a specific class of models which will also only be a rough approximation to the performance of a real structure. At the current stage the state-of-the-art must be concluded to be limited to qualitative nonlinear models of offshore platforms which incorporates the different sources of nonlinearities as mentioned in chapter 4.

The more sophisticated identification methods which were dealt with in chapter 8 such as the application of ARMA models and MEM-analysis have in this thesis only be considered for the case of univariate analysis. However, multivariate versions exist meaning that the structural model is estimated by a simultaneous fit to the response measured synchronously at several locations on the structure. Even though the multivariate case is suspected to have a significant increase in the computation time as a disadvantage it should be considered as a possible way of extracting maximum information of the structure from the response measured at several locations.

This thesis has included a survey and research on applicable methods for system identification and some software has been developed. However, to some extent documentation of the methods in detailed way and introduction of userfriendly implementations of the methods still remain. Even though this is partly accomplished by commercial packages such as MATLAB [12], there is a strong need for more specialized identification programs with respect to identification of offshore platforms.

9.6 References

[1] Jensen, J. L., "Dynamic Analysis of a Monopile Model", Paper no. 10 in Fracture & Dynamics, Institute of Building Technology and Structural Engineering, University of Aalborg, Denmark, 1989.

[2] Campbell, R. B., "The Estimation of Natural Frequencies and Damping Ratios of Offshore Structures", Ph.D. Thesis, Dept. of Ocean Engineering, Massachusetts Institute of Technology, USA, 1979.

[3] Grewatz, S. E. and S. S. Sunder, "Vibration Monitoring in the Spectral Domain using the Method of Moments", Research Report R82-47, Dept. of Civil Engineering, Massachusetts Institute of Technology, USA, 1982.

[4] Brouwers, J. J. H., "Response near Resonance of Non-Linearly Damped Systems Subject to Random Excitation with Application to Marine Risers", Ocean Engineering, vol. 9, no. 3, Pergamon Press Ltd., 1982.

[5] Langen, I., N. Spidsøe, R. L. Bruce and J. W. Heavner, "Measured Dynamic Behaviour of North Sea Jacket Platforms", Offshore Technology Conference, OTC 4655, Houston, USA, 1984.

[6] Spidsøe, N. and B. A. Leite, "Statistical Properties of Measured Wave-Induced Section Forces in a Gravity Platform Shaft", Offshore Technology Conference, OTC 5415, Houston, USA, 1986.

[7] Spidsøe, N. and I. Langen, "Damping of Fixed Offshore Platforms", Behaviour of Offshore Structures, BOSS85, Elsevier Science Publishers B.V., 1985.

[8] Olagnon, M. and M. Prevosto, "The Variation of Damping Ratios with Sea Conditions for Offshore Structures under Natural Excitation", Offshore Technology Conference, OTC 4654, Houston, USA, 1984.

[9] Lin, Y. K., "Probabilistic Theory of Structural Dynamics", McGraw-Hill Book Company, 1967.

[10] Kientzy, D., M. Richardson and K. Blakely, "Using Finite Element Data to Set Up Modal Tests", J. Sound and Vibration, June 1989.

[11] Kozin, F., "Estimation of Parameters for Systems Driven by White Noise Excitation", Proc. of the IUTAM Symp., Frankfurt/Oder (GDR), in "Random Vibrations and Reliability", ed. K.Hennig, Akademie Verlag, Berlin, 1982.

[12] MATLAB, version 3.5, 1989, The MATH WORKS Inc., 21 Eliot Street, South Natick, MA 01760, USA.

10. RESUMÉ (IN DANISH)

Formålet med denne afhandling er at undersøge metoder til systemidentifikation af offshore platforme med henblik på at få et grundlag for bestemmelse af de dynamiske egenskaber. De dynamiske egenskaber er i hovedsagen givet ved et sæt af egenfrekvenser, dæmpningsforhold og egensvingningsformer.

Offshore platformes dynamiske egenskaber er interessante, idet anvendelsen af offshore platforme på stadig større vanddybder, samt udvikling af slankere design koncepter, fører til stadig mere svingningsfølsomme konstruktioner. Dette betyder, at behovet for viden om de dynamiske egenskaber vokser. Den viden tilvejebringes bedst ved systemidentifikation, idet teoretiske og numeriske studier er forbundet med store usikkerheder, ikke mindst med hensyn til bestemmelse af dæmpningen af offshore platforme.

I Kapitel 2 er givet en oversigt over udførte fuldskalamålinger i 70'erne og 80'erne og de dertil hørende bestemte dynamiske egenskaber. Oversigten viser, at kun de laveste egensvingsningsformer exciteres af bølgebelastningen. Normalt måler man kun på platformen udsat for bølgebelastning, idet det er forholdsvis dyrt at påsætte en ydre belastning i form af vibratorer eller lignende.

I kapitel 3 er gennemgået de fundamentale principper for systemidentifikation. De helt generelle aspekter, der eksisterer, når en model med nogle givne parametre skal tilpasses til et sæt af målte data, betragtes. Specielt opstilles principperne for bestemmelse af kovarians-matricen for de givne parametre. Denne giver en vigtig information om usikkerheden ved den valgte model og de estimerede parametre.

Kapitel 4 omhandler de matematiske modeller, der passende kan anvendes for offshore platforme. Kun diskrete modeller betragtes, idet der gøres rede for sammenhængen mellem den kontinuerte konstruktion og den diskrete model. Både en let dæmpet model og den mere generelle tilstandsvektor model (state space model) er medtaget. Betydningen af den typiske antagelse om proportional dæmpning diskuteres også. Selvom den generelle antagelse er, at lineære modeller er tilstrækkelig gode som modeller af offshore platforme, præsenteres afslutningsvis nogle vigtige former for ikke-lineære mekanismer.

I første del af kapitel 5 diskuteres, hvorvidt man bør påsætte en ydre belastning, når man skal måle platformens bevægelser, eller om man blot skal måle bevægelserne fremkaldt af bølger. Problemet er, at bølgebelastningen kun er indirekte kendt og derfor usikkert bestemt. Forudsætninger og problemerne med at behandle de målte

data diskuteres i den sidste halvdel af kapitlet. Især behandles usikkerheder og fejlkilder i tilknytning til FFT analyse. En relativ ny teknik kaldet random decrement teknikken præsenteres også. Endelig præsenteres nogle relevante støjmodeller.

I kapitel 6,7 og 8 præsenteres og diskuteres en bred vifte af metoder til system identifikation. Grundlaget herfor er dels simuleret målte data, dels de målte data opnået ved et forsøg, som er nærmere beskrevet i kapitel 1. Endvidere henvises der løbende til litteraturen.

I kapitel 6 betragtes metoder, som giver direkte information om parametre, der har en fysisk betydning såsom masser, stivhedskoefficienter etc. Først betragtes en klassisk metode baseret på tilstandsvektor formuleringen, der er elegant men ikke særlig anvendelig i praksis. Dernæst betragtes en metode baseret på simulering af responsen for et svingende ikke-lineært system. Denne er kun egnet til systemer med et lille antal frihedsgrader.

Kapitel 7 omhandler metoder, der er beskrevet ved et sæt af modal parametre. Dette er den klassiske fremgangsmåde ved systemidentifikation af svingende systemer. De omtalte metoderne strækker sig fra den simple båndbredde metode til mere generelle kurvetilpasnings metoder. Fælles for de fleste af metoderne er, at de er baseret på, at belastningenprocessen antages at kunne beskrives som hvid støj.

Kapitel 8 omhandler identifikation med tidsserie modeller, hvilket vil sige ARMA-modeller og AR-modeller. Sidstnævnte kaldes også maksimum entropy metoden. Dette er metoder baseret på en direkte tilpasning af en model til en målt tidsserie, hvilket giver indirekte information om modalparametrene.

I kapitel 9 gives en generel diskussion og konklusion. Antagelsen om, at bølgebelastningen kan modelleres med hvid støj, diskuteres. Endvidere behandles problemet med at beskrive ikke-lineære systemer med lineære modeller. Endelig sammenlignes de i kapitel 6, 7 og 8 beskrevne metoder, og en praktisk strategi for systemidentifikation af offshore platforme skitseres.

APPENDICES

Appendix 5.1: Time Consumption During Sine Sweep

The time consumption of a slow sine sweep is investiagted for an SDOF system. Until the time t=0 a harmonic excitation with the frequency f^0 has been applied to the system and has resulted in a stationary response. At t=0 the excitation frequency is shifted to f^t and the subject is now to estimate how large t should be to make the response stationary again.

At time t=0 the response is given by:

$$x(0) = X(f^0)\sin(2\pi f^0 0 + \Phi^0)$$

where:

$$X(f^0) = \frac{F/k}{\sqrt{\left(1-\left(\frac{f^0}{f_1}\right)^2\right)^2 + \left(2\zeta_1\frac{f^0}{f_1}\right)^2}}$$

After removing the harmonic excitation at the frequency f^0 the system will exhibit a transient response contribution at time t:

$$\begin{aligned}\delta x(t) &= X(f^0)e^{-2\pi f_1\zeta_1 t}\left[\frac{\zeta_1}{\sqrt{1-\zeta_1^2}}\sin(\sqrt{1-\zeta_1^2}2\pi f_1 t)+\cos(\sqrt{1-\zeta_1^2}2\pi f_1 t)\right]\\ &\approx X(f^0)e^{-2\pi f_1\zeta_1 t}\cos(\sqrt{1-\zeta_1^2}2\pi f_1 t)\end{aligned}$$

The removed harmonic excitation at the time t=0 with the frequency f^0 has been replaced by a new harmonic excitation with the frequency, f^t. Thus, a stationary contribution will be added to the response:

$$\Delta x(t) = X(f^t)\sin(2\pi f^t t + \Phi^t)$$

The time for obtaining a stationary response may now be estimated from:

$$\frac{\delta x(t)}{\Delta x(t)} < \alpha$$

where α is some criterion for retaining stationary reponse. By inserting the expressions for the declining amplitude $\delta x(t)$ and the stationary amplitude $\Delta x(t)$ the following condition is obtained:

$$t \gg \frac{1}{\zeta_1 4\pi f_1}\ln\left[\frac{(1-(\frac{f^t}{f_1})^2)^2+(2\zeta_1\frac{f^t}{f_1})^2)\alpha}{(1-(\frac{f^0}{f_1})^2)^2+(2\zeta_1\frac{f^0}{f_1})^2}\right]$$

The expression is in practice an approximation, since the excitation frequency will not be applied at discrete frequencies but will be varied continuously through the given frequency range.

Appendix 5.2: Bias of Resonance Peak

According to "Random Data: Analysis and Measurement Procedures" by J. S. Bendat and A. G. Piersol, Wiley Interscience, 1971, the estimate of the spectral density, $S(f)$ can be given as:

$$E[S(f)]=\frac{1}{B}\int_{f-B/2}^{f+B/2} S(f)df$$

If $S(f)$ is approximated by a second order Taylor expansion:

$$S(f)=S(f_0)=(f-f_0)S'(f_0)+\frac{(f-f_0)^2}{2}S''(f_0)$$

Then it follows:

$$\int_{f_0-B/2}^{f_0+B/2}(f-f_0)df = 0$$
$$\int_{f_0-B/2}^{f_0+B/2}\frac{(f-f_0)^2}{2}df = \frac{B^3}{24}$$

and finally:

$$E[S(f_0)] = S(f_0)+\frac{B^2}{24}S''(f_0)$$

Thus the spectral estimates will be bias and the bias will depend upon the bandwidth, B. In the following B is named the effective bandwidth B_e meaning that the bandwidth given by the distance between the frequency points may be smaller due to the windows applied.

The total mean square error of the spectral density can be found from the sum of the variances due to random and bias errors and thus also to the coefficient of variation:

$$\sigma^2 = \frac{S(f)^2}{B_e T}+\frac{B_e^4 S''(f)^2}{576}$$
$$\delta^2 = \frac{1}{B_e T}+\frac{B_e^4}{576}\left(\frac{S''(f)}{S(f)}\right)^2$$

A minimum of the error can be found with respect to B_e by setting the deriative equal to zero:

$$\frac{\partial \delta^2}{\partial B_e}=\frac{-1}{B_e T}+\frac{4B_e^3}{576}\left(\frac{S''(f)}{S(f)}\right)^2=0$$

This gives:

$$B_e=\left(\frac{576S(f)^2}{4TS''(f)^2}\right)^{1/5}$$

which is a minimum since the second deriative is positive.

For a white noise excited SDOF sytem the response spectrum will be given by:

$$S(f) = |H(f)|^2 S_0$$
$$|H(f)|^2 = \frac{1}{(f_0^2 - f^2)^2 + (2 f f_0 \zeta_0)^2}$$

This expression and the second deriative of this expression can now be found and inserted to give the error of the spectral estimates as a function of the structural parameters of a white noise excited SDOF system. At resonance, where the bias error will be largest, a very simple expression can be found:

$$S(f_0) = \frac{S_0}{4 f_0^4 \zeta_0^2}$$

$$S''(f_0) = -\frac{S_0(1+3\zeta_0^2)}{2 f_0^6 \zeta_0^4} \approx -\frac{S_0}{2 f_0^6 \zeta_0^4}$$

which means that the coefficient of variation of the bias error becomes:

$$\delta_b^2 = \frac{B_e^4}{576} \frac{4}{f_0^4 \zeta_0^4}$$
$$= \frac{B_e^4}{B_r^4} \frac{1}{9}$$
$$\delta_b = \frac{B_e^2}{B_r^2} \frac{1}{3}$$

where the half-power bandwidth, $B_r = 2 f_0 \zeta_0$ has been introduced.

The expression is only an approximation due to the Taylor expansion in the start which means that $B_e^2 S''(f) < S(f)$ should be satisfied to ensure a certain accuracy. This means that the estimate of the bias error is only reliable when it is not too large.

Appendix 7.1: Uncertainty of the Bandwidth Method

A white noise excited single-degree-of-freedom system is assumed:

$$S_{xx}(f) = |H(f)|^2 S_0$$

and the damping ratio is estimated by:

$$\zeta_0 = \frac{f_2 - f_1}{2 f_0} = \frac{1}{2}\beta_2 - \frac{1}{2}\beta_1$$

$$S_{xx}(f_2) = S_{xx}(f_1) = \frac{1}{2} S_{xx}(f_0)$$

If the half-power points β_1 and β_2 are assumed to be uncorrelated then the variance of the damping ratio is given by:

$$\sigma_{\zeta_0}=\tfrac{1}{4}\sigma_{\beta_1}^2+\tfrac{1}{4}\sigma_{\beta_2}^2$$

$$d\beta_1=\frac{\partial\beta_1}{\partial S_r(f)}dS_r(f) \quad d\beta_2=\frac{\partial\beta_2}{\partial S_r(f)}dS_r(f)$$

where $S_r(f)=\frac{S_{xx}(f)}{S_{xx}(f_0)}$ which means that $S_r(f_1)=S_r(f_2)=\frac{1}{2}$ and $S_r(f_0)=1$. The partial deriative is approximated to:

$$\frac{\partial\beta_1}{\partial S_r(f)}\Big|_{f=f_1}=2\zeta_0 \quad \frac{\partial\beta_2}{\partial S_r(f)}\Big|_{f=f_2}=2\zeta_0$$

This means that the variance of β_1 and β_2 can be found as:

$$\sigma_{\beta_1}^2=\left(\frac{\partial\beta_1}{\partial S_r(f)}\right)^2\sigma_{S_r}^2\Big|_{f=f_1}=4\zeta_0^2\sigma_{S_r}^2$$

$$\sigma_{\beta_2}^2=\left(\frac{\partial\beta_2}{\partial S_r(f)}\right)^2\sigma_{S_r}^2\Big|_{f=f_2}=4\zeta_0^2\sigma_{S_r}^2$$

The variance of $S_r(f)$ can be found from the linearization:

$$dS_r(f)=\frac{1}{S(f_0}dS(f)|_{f=f_i}-\frac{S(f)}{S(f_0)^2}dS(f)|_{f=f_0}$$

which leads to:

$$\sigma_{s_r}^2=\left(\frac{1}{S(f_0}\right)^2\sigma_{S(f)}^2|_{f=f_i}+\left(\frac{S(f)}{S(f_0)^2}\right)^2\sigma_{S(f)}^2|_{f=f_0}$$

Here it has been assumed that the spectral estimate of a half-power point is uncorrelated with the spectral estimate of the peak.

In appendix 5.1 the coefficient of variation of spectral estimates was found to be:

$$\delta^2=\frac{\sigma_{S(f)}^2}{(S(f))^2}=\frac{1}{B_eT}+\frac{B_e^4}{576}\left(\frac{S''(f)}{S(f)}\right)^2$$

Notice that this expression is a good expression when the bias error is not too large: $B_e^2S''(f)<S(f)$, see "Random Data: Analysis and Measurement Procedures" by J. S. Bendat and A. G. Piersol, Wiley Interscience, 1971. An expression for the second deriative of $Sxx(f)$ was found in appendix 5.1. If $f_1\approx f_0$ and $f_2\approx f_0$ then this leads to the following expression:

$$S''_{xx}(f)=-\frac{(1+5\zeta_0^2)}{2f_0^6\zeta_0^4}\approx-\frac{1}{2f_0^6\zeta_0^4}$$

and since $S_{xx}(f_1)=S_{xx}(f_2)=\frac{1}{2}S_{xx}(f_0)=\frac{1}{8f_0^4\zeta_0^2}$ and $S_{xx}(f_0)=\frac{1}{4f_0^4\zeta_0^2}$ the coefficent of variation of the spectral estimate at the half-power point is obtained as:

$$\delta=\left[\frac{1}{n}+\frac{1}{576\,T_e}\left(\frac{4}{f_0^2\zeta_0^2}\right)^2\right]$$

and the resonance peak:

$$\delta=\left[\frac{1}{n}+\frac{1}{576\,T_e}\left(\frac{2}{f_0^2\zeta_0^2}\right)^2\right]$$

where n is the number of averages, $T_e=\frac{1}{B_e}$ is the effective length of the time series and $T=nT_e$ is the total length of the time series. The expression of the variance of $S_r(f)$ can now be rewritten as:

$$\sigma^2_{S_r}=\tfrac{1}{4}\sigma^2_{S_{xx}(f)}+\tfrac{1}{4}\sigma^2_{S_{xx}(f_0)}$$

due to $S_{xx}(f_1)=S_{xx}(f_2)=\frac{1}{2}S_{xx}(f_0)$. This leads with the application of the expression of δ as:

$$\sigma^2_{S_r}=[\tfrac{1}{2n}+\tfrac{5}{576T_e^4 f_0^4 \zeta_0^4}]$$

which can be inserted into the expression of the variance of β_1 and β_2:

$$\sigma^2_{\beta_1}=\sigma^2_{\beta_2}=4\zeta_0^2[\tfrac{1}{2n}+\tfrac{5}{576T_e^4 f_0^4 \zeta_0^4}]$$

This leads to the final expression for the variance of the damping ratio estimated by the bandwidth method:

$$\sigma^2_{\zeta_0}=2\zeta_0^2[\tfrac{1}{2n}+\tfrac{5}{576T_e^4 f_0^4 \zeta_0^4}]$$

which gives the coefficient of variation:

$$\delta_{\zeta_0}=\sqrt{\tfrac{1}{n}+\tfrac{10}{576T_e^4 f_0^4 \zeta_0^4}}=\sqrt{\tfrac{1}{n}+\tfrac{10B_e}{36B_r}}$$

The expression of the uncertainty of the damping estimate gives a rough uncertainty estimate which will be an upper limit of the uncertainty. It can be used as guideline in optimizing measurings programmes and as explanation of part of the scatter in the estimates after the measuring and the analysis.

LIST OF SYMBOLS

This list contains the most frequently used symbols, typically applied to several sections of the thesis. Symbols not included in the list (or alternative application of symbols) are explained when used.

a_j	Real part of complex eigenvalue p_j.
A	Amplitude.
$\overline{\overline{A}}$	System matrix.
b_j	Imaginary part of complex eigenvalue p_j.
B_e	Effective bandwidth in Hz.
B_r	Half-power bandwidth in Hz.
$\overline{\overline{B}}$	Load matrix .
c	Damping constant of an SDOF system.
C_D	Drag constant.
C_M	Inertia constant.
$C_{xy}(\tau)$	Cross-covariance function of $x(t)$ and $y(t)$.
$\overline{\overline{C}}$	Damping matrix.
$\overline{\overline{\mathbf{cov}}}_\Theta$	Covariance matrix of $\overline{\Theta}$.
d	Water depth.
D	Cylinder diameter.
$D_{x_j x_i}^{X_0}[\tau]$	Random decrement signature.
f	Frequency in Hz.
f_i	Eigen frequency no. i in Hz., (f_0 for an SDOF system).
f_{max}	Maximum frequency in Hz.
f_s	Sampling frequency in Hz.

f_D	Damping force.
f_R	Restoring force.
$\overline{f}(t)$	Excitation vector at the time t.
$h_i(t)$	Impulse response function no. i ($h_0(t)$ for an SDOF system).
H_s	Significant wave height.
$H_i(f)$	Complex frequency response function no. i ($H_0(f)$ for an SDOF system).
$H_{xy}(f)$	Transfer function of a system with excitation $x(t)$ and response $y(t)$. (also $H(f)$).
g	Gravity.
$\overline{\overline{I}} = (1)$	Identity matrix.
k	Stiffness constant of SDOF system.
$\overline{\overline{K}}$	Stiffness matrix.
l	Length.
m	Mass of an SDOF system.
m_i	Lumped mass no. i.
m_{ii}	Modal mass /generalized mass.
$\overline{\overline{M}}$	Mass matrix.
n	Number of degrees of freedom.
n	Number of averages.
$n(t)$	Noise signal.
N	Number of sampled points/ points in data set.
p_i	Complex eigenvalue.
$p_{xy}(x, y, t_1, t_2)$	Joint probability density function of two random processes.
$P_{xy}(x, y, t_1, t_2)$	Joint probility distribution function of two random processes.
$\overline{p}(t)$	Alternative symbol for excitation process.
q	Wave force per unit length.
q_D	Damping force per unit length due to the drag term in Morison's equation.
$R_{xy}(\tau)$	Cross-correlation function of $x(t)$ and $y(t)$.
S_0	Spectral constant in white noise spectrum.

$S_{xy}(f)$	Cross-spectral density function of $x(t)$ and $y(t)$.
$S_{\overline{x}\overline{x}}(f)$	Spectral density matrix of the response vector $\overline{x}$.
t	Time.
t_i	Discrete time instant.
T	Record length (sec).
$V(\overline{\Theta})$	Error function.
$x(t)$	Random process (excitation or response).
$x_b(t)$	Base displacement.
x_t	x(t) to the discrete time t.
$\overline{x}(t)$	Response vector at the time t.
$X(\omega)$	Amplitude of harmonic time process $x(t)$.
X_k	Discrete forrier transformed of $x(t)$.
X_0	Trigger level.
$y(t)$	Random process.
$\overline{y}(t)$	State vector of the response.
$\overline{z} = \overline{z}(t)$	Response vector in the decoupled vector space.

Greek Symbols

$\gamma(f)$	Coherence function.
$\overline{\Gamma} = \overline{\Gamma}(t)$	Modal/generalized load vector.
δ	Logarithmic decrement, alternatively $\delta(n)$.
δ	Coefficient of variation.
Δ	Sampling interval (sec).
$\epsilon(t\|\overline{\Theta})$	Prediction error.
ϵ_b	Bias error.
ϵ_r	Random error.
$\overline{\epsilon}$	Vector of prediction errors.
ζ_i	Damping ratio no. i (ζ_0 for an SDOF system).
$\eta(t)$	Wave elevation process.
Θ_i	MA-parameter in ARMA model.

$\overline{\Theta}$	Parameter vector.
λ_N	Variance of the prediction error.
μ_x	Mean value of $x(t)$.
ρ	Fluid density.
σ	Standard deviation.
τ	Time variable.
$\Phi(f)$	Phase function.
Φ_i	AR-parameter in ARMA model.
$\overline{\Phi}_i$	Mode shape vector no. i.
$\overline{\overline{\Phi}}$	Mode shape matrix.
$\overline{\Psi}_i$	Complex mode shape no. i.
$\overline{\overline{\Psi}}$	Complex mode shape matrix.
ω	Cyclic frequency (rad/Hz).
ω_i	Eigen frequency no. i (rad/sec) (ω_0 for an SDOF system).

Other Symbols

$\Theta^\star$	True value of Θ.
$\hat{\Theta}$	Estimate of Θ.
$\|x\|$	Magnitude of x.
$E[\,]$	Mathematical expectation.
Prob(x)	Probability of x.
Re()	Real part of a number.
Im()	Imaginary part of a number.
i	$\sqrt{-1}$.
a^*	Complex conjugate of a.
$(\,a_i\,)$	Diagonal matrix with element a_i.
$x(t) \equiv x$	In the case of no risk of misinterpretation.
$\dot{x}(t)$	Derivative of $x(t)$.
$\mathbf{N}(\mu, \sigma)$	Normal distribution with mean μ and standard deviation σ.
$\chi^2(n)$	Chi-square distribution with n degrees of freedom.

FRACTURE AND DYNAMICS PAPERS

PAPER NO. 1: J. D. Sørensen & Rune Brincker: *Simulation of Stochastic Loads for Fatigue Experiments.* ISSN 0902-7513 R8717.

PAPER NO. 2: R. Brincker & J. D. Sørensen: *High-Speed Stochastic Fatigue Testing.* ISSN 0902-7513 R8809.

PAPER NO. 3: J. D. Sørensen: *PSSGP: Program for Simulation of Stationary Gaussian Processes.* ISSN 0902-7513 R8810.

PAPER NO. 4: Jakob Laigaard Jensen: *Dynamic Analysis of a Monopile Model.* ISSN 0902-7513 R8824.

PAPER NO. 5: Rune Brincker & Henrik Dahl: *On the Fictitious Crack Model of Concrete Fracture.* ISSN 0902-7513 R8830.

PAPER NO. 6: Lars Pilegaard Hansen: *Udmattelsesforsøg med St. 50-2, serie 1 - 2 - 3 - 4.* ISSN 0902-7513 R8813.

PAPER NO. 7: Lise Gansted: *Fatigue of Steel: State-of-the-Art Report.* ISSN 0902-7513 R8826.

PAPER NO. 8: P. H. Kirkegaard, I. Enevoldsen, J. D. Sørensen, R. Brincker: *Reliability Analysis of a Mono-Tower Platform.* ISSN 0902-7513 R8839.

PAPER NO. 9: P. H. Kirkegaard, J. D. Sørensen, R. Brincker: *Fatigue Analysis of a Mono-Tower Platform.* ISSN 0902-7513 R8840.

PAPER NO. 10: Jakob Laigaard Jensen: *System Identification1: ARMA Models.* ISSN 0902-7513 R8908.

PAPER NO. 11: Henrik Dahl & Rune Brincker: *Fracture Energy of High-Strength Concrete in Compression.* ISSN 0902-7513 R8919.

PAPER NO. 12: Lise Gansted, Rune Brincker & Lars Pilegaard Hansen: *Numerical Cumulative Damage: The FM-Model.* ISSN 0902-7513 R8920.

PAPER NO. 13: Lise Gansted: *Fatigue of Steel: Deterministic Loading on CT-Specimens.*

PAPER NO. 14: Jakob Laigaard Jensen, Rune Brincker & Anders Rytter: *Identification of Light Damping in Structures.* ISSN 0902-7513 R8928.

PAPER NO. 15: Anders Rytter, Jakob Laigaard Jensen & Lars Pilegaard Hansen: *System Identification from Output Measurements.* ISSN 0902-7513 R8929.

FRACTURE AND DYNAMICS PAPERS

PAPER NO. 16: Jens Peder Ulfkjær: *Brud i beton - State-of-the-Art. 1. del, brudforløb og brudmodeller.* ISSN 0902-7513 R9001.

PAPER NO. 17: Jakob Laigaard Jensen: *Full-Scale Measurements of Offshore Platforms.* ISSN 0902-7513 R9002.

PAPER NO. 18: Jakob Laigaard Jensen, Rune Brincker & Anders Rytter: *Uncertainty of Modal Parameters Estimated by ARMA Models.* ISSN 0902-7513 R9006.

PAPER NO. 19: Rune Brincker: *Crack Tip Parameters for Growing Cracks in Linear Viscoelastic Materials.* ISSN 0902-7513 R9007.

PAPER NO. 20: Rune Brincker, Jakob L. Jensen & Steen Krenk: *Spectral Estimation by the Random Dec Technique.* ISSN 0902-7513 R9008.

PAPER NO. 21: P. H. Kirkegaard, J. D. Sørensen & Rune Brincker: *Optimization of Measurements on Dynamically Sensitive Structures Using a Reliability Approach.* ISSN 0902-7513 R9009.

PAPER NO. 22: Jakob Laigaard Jensen: *System Identification of Offshore Platforms.* ISSN 0902-7513 R9011.

Department of Building Technology and Structural Engineering
The University of Aalborg, Sohngaardsholmsvej 57, DK 9000 Aalborg
Telephone: 45 98 14 23 33 Telefax: 45 98 14 82 43